Sequence stratigraphic analysis of the Duvernay Formation, Kaybob area, Alberta, Canada

by

Daniel J. Shaw

A thesis submitted in partial fulfillment of the requirements for the degree of

Master of Science

Department of Earth and Atmospheric Sciences

University of Alberta

Abstract

The Upper Devonian Duvernay Formation is an important hydrocarbon source rock in the Western Canada Sedimentary Basin and has been a significant unconventional oil, gas liquids, and gas reservoir since 2011. Heterogeneity in this and other shale reservoirs is important in predicting rock properties (such as TOC, porosity, permeability, and brittleness) within self-sourced reservoirs to identify target intervals. These properties can change with systems tracts and position within a basin at several scales and can be predicted by sequence stratigraphic models. In this study, we characterize the lithofacies of the Duvernay Formation and develop a sequence stratigraphic model for the formation in the Kaybob Area of Alberta. We also identify a set of features characteristic of mudstone sequence boundaries, describe how they vary stratigraphically and geographically, and interpret processes responsible for their formation.

Five lithofacies were identified in 11 Duvernay cores from the Kaybob area of Alberta, characterized by composition, grain size, sedimentary structures, bioturbation, and cement. Lithofacies were deposited by a combination of suspension settling, sediment-gravity flows, and bottom currents under anoxic to fully oxygenated bottom water conditions. Lithofacies distribution was strongly affected by proximity to sediment sources, bottom topography, and sea level cyclicity. Relatively coarse-grained, carbonate-rich, bioturbated, and organic-poor facies are common close to large carbonate platforms and reefs; silt- and sand-rich facies deposited by bottom currents and sediment gravity flows are common on the slopes of large carbonate platforms; hemipelagic deposited, fine grained, biosiliceous, organic-rich facies are common in distal areas of the basin. Transgressive deposits are characterized by increasingly fine-grained, biosiliceous, organic-rich facies; highstand deposits by increasingly coarse-grained, carbonate-rich, bioturbated, organic-poor facies; lowstand deposits by detrital clay-rich, bioturbated facies.

Sequence stratigraphic surfaces were identified in the 11 cores and correlated across a network of approximately 600 wireline wells in the Kaybob area to develop a sequence stratigraphic model. Three 3rd order depositional sequences and 4th order depositional sequences are identified within the Duvernay. Two types of 3rd order sequence boundaries are identified, their expression dependent on their position within a 2nd order depositional sequence that encompassed the Duvernay. In the 2nd order transgression, sequence boundaries are expressed as scoured surfaces with coarse overlying lags that represent a period of sediment starvation and reworking during lowstand conditions and early transgression. In the 2nd order highstand, sequence boundaries are expressed as soft sediment-deformed surfaces overlain by coarse beds that represent a period of forced regression, with the sequence boundary located at the top. Surfaces become gradational and overlying lags or forced regressive deposits thin basinward.

The high-density data set in our relatively small study area enables us to map 3rd and 4th order sequence stratigraphic surfaces across the study area with a high degree of certainty. We were also able to interpret major sources of sediment and determine geographic extent of topographical features during different stages of Duvernay Formation deposition from geographic distribution of facies and variations in systems tract isopachs. Our interpretation of sequence boundaries produced during a 2nd order TST are consistent with several previous studies that interpreted sequence boundaries in mudstones as combined sequence boundaries and transgressive surfaces overlain by winnowed lags. Our interpretation of sequence boundaries produced during a 2nd order HST differs from previous studies in that we propose the coarse sand beds at sequence boundaries were deposited during forced regression, with the sequence boundary located at its top.

Preface

The works presented in this thesis are part of an ongoing research program by our SURGe research group (Studies in Unconventional Reservoir Geology) that examines the sedimentology, stratigraphy, geochemistry, geomechanics, and petrophysics of organic-rich Devonian shales in Western Canada. This study examines the sedimentology and sequence stratigraphy of the Duvernay Formation in the Kaybob area of Alberta and builds upon a basin-scale study of the Duvernay by Knapp (2016) (Knapp et al., 2017; Knapp et al., 2019).

This thesis is divided into two chapters. In chapter 1, I develop a sequence stratigraphic analysis of the Duvernay formation in the Kaybob area of Alberta. Lithofacies are identified and used to interpret depositional environments, depositional processes, and bottom water oxygenation. Stacking patterns in lithofacies, geochemistry, and petrophysical logs are used to determine sea level change during deposition of the formation. Examination of drill core took place at the AER Core Research Center and Core Labs in Calgary. Thin sections of important features, fabrics, contacts, and representative lithofacies were taken from cores for petrographic analysis. Major, minor, trace element and TOC data was collected from one core and used in conjunction with data from Knapp et al., 2017 and Harris et al., 2018. Sequence stratigraphic surfaces are correlated from core to logs and mapped across a network of wireline logs in Petrel software. Chapter 1 will be submitted to Sedimentary Geology as Shaw, D.J. and Harris, N.B. “Lithofacies and sequence stratigraphic analysis of the Duvernay Formation in the Kaybob Area, Alberta, Canada”.

In chapter 2 we characterize the sequence boundaries of the sequence stratigraphic model presented in chapter 1. We describe how the surfaces and overlying beds change stratigraphically and geographically and we interpret these features to identify processes responsible for their formation. Chapter 2 will be submitted to the GSA Bulletin or Marine and Petroleum Geology as Shaw, D.J. and

Harris, N.B. “The expression of sequence boundaries in cores from the Duvernay Formation mudstone, Kaybob Area, Alberta, Canada”.

Acknowledgements

Thank you to Murphy Oil Corporation for providing funding and support for this research project. Thank you to a number of individuals who I had technical discussions with throughout the course of this project, helping me develop my interpretations: Dr. Noga Vaisblat, Haolin Zhou, Dr. Chris Schneider, Dr. John Weissenberger, Dr. George Pemberton, Dr. Murray Gingras, Cole Ross, Sara Biddle, and of course my supervisor, Dr. Nick Harris. Lastly, thank you to my family and friends who have provided me with unwavering support.

Table of Contents

Chapter 1 : Lithofacies and sequence stratigraphic analysis of the Duvernay Formation in the Kaybob area, Alberta, Canada

1.1 INTRODUCTION

Sedimentological studies in the last 30 years have identified a wide range of depositional processes, environments, and oxygen conditions related to deposition of mudstones. Evidence, including sedimentary structures indicating deposition by sediment gravity flows (Shanmugam, 2000; Martín-Chivelet et al., 2008; Schieber and Southard 2009; Macquaker et al., 2010a; Rebesco et al., 2014; Knapp et al., 2017), bottom currents (Shanmugam, 2000; Konitzer et al., 2014; Lazar et al., 2015; Knapp et al., 2017; Boulesteix et al., 2019), and storm and wave reworking (Schieber, 1999), has forced a reassessment of older models that interpreted mudstone as the product of simple suspension settling. The presence of trace fossils (Bromley and Ekdale, 1984; Knapp et al., 2017; Pratt and Kimmig, 2019), benthic fossils (Schieber, 2009), and redox proxies (S/Fe) (Dong et al., 2017; Harris et al., 2018) demonstrate that organic-rich mudstones were not deposited in conditions of persistent bottom water anoxia.

An understanding of mudstone heterogeneity is important to predicting rock properties within these self-sourced reservoirs, such as TOC, porosity and permeability, and brittleness that are important for locating target intervals for hydrocarbon exploration (Dong et al., 2017; Knapp et al., 2017; Harris et al., 2018; Dong et al., 2019). Mudstone rock properties can change predictably with respect to sequence stratigraphic systems tract and position within a basin at several scales, either as a direct result of sea level variation (TOC) or indirectly as a function of changes in sediment composition or fabric (petrophysical and geomechanical properties; e.g.: Wignall and Maynard, 1993; Ver Straeten et al., 2011; Dong et al., 2018; Harris et al., 2011; Harris et al., 2018; Knapp et al., 2019). These rock properties

can therefore be predicted by sequence stratigraphic models. But where stratigraphic surfaces are subtle and deposition is dominated by sediment gravity flows and other mass transport processes and where sediment is reworked by bottom currents, the practical interpretation of sequence stratigraphic surfaces and systems tracts in mudstones has proven to be difficult (Catuneanu et al., 2011; Knapp et al, 2019).

Most past studies on mudstones have focused on interpreting transgressive-regressive (T-R) cycles (eg: Harris et al., 2011; Ver Straeton et al., 2011; Abouelresh and Slatt, 2012; Dong, 2016; Shaw et al., 2017). Some studies, however, focused on identifying sequence boundaries and systems tracts in their approach to sequence stratigraphy in mudstones (eg: Wignall and Maynard, 1993; Schieber, 1998a; Williams et al., 2001; Schieber and Riciputi, 2004; Hammes and Frebourg, 2012; Bond et al., 2013; Knapp, 2016; Wong et al., 2016; Ayranci et al., 2018; Harris et al., 2018; Knapp et al., 2019), describing a more complete history of sea level and accommodation change.

The Upper Devonian (Frasnian) Duvernay Formation mudstone is a prolific source rock in the Western Canada Sedimentary Basin, believed to have sourced most of the Upper Devonian conventional hydrocarbon reservoirs in Alberta (Allan and Creaney, 1991). It has become a significant unconventional reservoir starting in 2011 (Preston et al., 2016), with development focused on thick, organic-rich, biosiliceous mudstones in the West Shale Basin (Potma et al., 2001) (Fig. 1.1, 1.2). Our study area, the roughly 14,000 km^2 Kaybob area of west-central Alberta (Fig. 1.1), has approximately 2,000 wells that penetrate the Duvernay Formation, approximately 70 of which are cored through at least part of the Duvernay. The Kaybob area is capable of producing dry gas, wet gas, and oil within different parts of the area, related to thermal maturity that ranges from immature in the northeast to dry gas in the southwest, generally trending with burial depth (Preston et al., 2016).

In this study, we characterize the lithofacies of the Duvernay Formation and develop a high resolution depositional and sequence stratigraphic model for the formation, expanding on an earlier regional study by Knapp et al. (2017). The presence of reefs and basinal areas within the study area enables us to analyze facies and architecture transitions from proximal to distal areas. An unusually high-density data set, based on a large number of wells in the relatively small Kaybob area including several with long cores, makes it possible to map facies distributions and heterogeneities at high resolution, including 2nd and 3rd order sequence stratigraphic surfaces. We also map 4th order depositional sequences to better understand basin infilling patterns and sequence stratigraphic architecture.

1.2 GEOLOGIC SETTING

The Duvernay Formation was deposited during the Late Devonian (Frasnian) Period, at a time of greenhouse climate (Read 1995; Lehrmann and Goldhammer, 1999) and high global sea level (Johnson et al., 1985), when a large epicontinental sea covered much of western Canada. The Duvernay is approximately time-equivalent to all or parts of other black shales across North America such as the Muskwa Formation (Horn River Basin), New Albany Shale (Illinois Basin), Woodford Shale (Permian Basin), Chattanooga, and Rhinestreet (Appalachian Basin) (Campbell, 1946; Schieber, 1998a; Lash and Blood, 2004; Ferri et al., 2011; Harris et al., 2018). The Duvernay Formation was deposited in the Alberta basin, part of the Western Canada Sedimentary Basin, on the passive western margin of North America (Weissenberger, 1994). During this time, the area was dominated by carbonate platforms and reefs (Fig. 1.1), with basinal shales deposited in the inter-reef areas. Marine shales were also deposited to the northeast in British Columbia and Northwest Territories, and dolomites and evaporites were deposited to the southeast in Saskatchewan and Manitoba (Switzer et al., 1994; Weissenberger, 1994). The Kaybob

Area (Fig. 1.1) is located in the central part of the West Shale Basin between the Sturgeon Lake reef to the north and the Simonette, Bigstone, and Windfall Leduc reefs to the south (Fig. 1.1).

The Duvernay Formation is the basinal shale equivalent of Middle Leduc Formation pinnacle reef buildups and carbonate platforms (Switzer et al., 1994) (Fig. 1.2). As the carbonate banks and reefs grew, organic-rich Duvernay mudstones were deposited in the semi-starved basin (Mountjoy, 1980; Oliver and Cowper, 1963). Siliciclastics were sourced from the ancestral Canadian Shield to the east and Peace River Arch to the northwest during the Frasnian (Wong et al., 2016). Longshore currents distributed sediment in a clockwise direction within the basin, driven by dominant winds from the present northeast and influenced by bottom topography (Andrichuk, 1958A; McCrossan, 1961; Mountjoy, 1980; Stoakes, 1980; Potma et al., 2001; Harris et al., 2018). At the same time, upwelling along the western edge of North America drove deep, nutrient-rich water into and across the basin in a southeast direction (Golonka et al., 1994; Harris et al., 2018).

Major tectonic features that influenced Duvernay deposition include the Peace River-Athabasca Arch, West Alberta Ridge, Rimbey Arc, and Meadow Lake Escarpment (Fig. 1.1). The Peace River Arch was a landmass located to the northwest of the Alberta basin, fringed by Leduc reefs (Dix, 1990). The West Alberta Ridge was a site of major Leduc Formation reef development along the western edge of the basin (Switzer et al., 1994). The Rimbey Arc, a northeast to southwest trending paleobathymetric high was also a site of Leduc reef growth (Rimbey-Meadowbrook reef chain) that divided the Alberta Basin into the East and West Shale Basins during the Frasnian (Switzer et al., 1994; Rokosh et al., 2012; Preston et al., 2016). The Meadow Lake Escarpment is a pre-Devonian structural and erosional feature overlain by the Killiam Barrier Reef during the Frasnian (Oldale and Munday, 1994). It formed the eastern edge of the East Shale Basin and marked the easternmost extent of Duvernay deposition (Switzer et al., 1994).

In this study we apply sequence hierarchy developed by Wong et al. (2016) for carbonates of the Alberta Basin in which depositional cycles of approximately 1.2 My duration are interpreted as 3rd order cycles. The Duvernay Formation was deposited during the late transgression to early highstand of a 2nd order depositional sequence that spanned the Late Givetian to the Frasnian (Fig. 1.2) (Weissenberger et al., 1994; Potma et al., 2001; Wong et al., 2016). It is part of the Woodbend Group (Fig. 1.2) and conformably overlies the upper Majeau Lake Formation shale (Lower Leduc equivalent) across the East and West Shale Basins, except in the southernmost areas of both basins where non-deposition of the Majeau Lake resulted in deposition of the Duvernay directly on the Cooking Lake carbonates (Switzer et al., 1994). The Duvernay is conformably overlain by the Lower Ireton Formation (Upper Leduc equivalent) throughout most of the basin (Switzer et al., 1994). The Duvernay Formation was informally divided into 3 members by Andrichuck (1961), terminology that is still applied by oil and gas companies: a lower shale, middle carbonate, and upper shale. The Duvernay Formation is composed of siliceous to calcareous, organic-rich shale, locally interrupted by limestones (Switzer et al., 1994; Knapp et al., 2017).

Duvernay sediments of the East Shale Basin are significantly more carbonate-rich than those of the West Shale Basin (Harris et al., 2018). In the West Shale Basin, the Duvernay becomes less calcareous to the west (Rokosh et al., 2012; Preston et al., 2016). Duvernay thickness is typically 70 m but can range from 2 to 99 m (Preston et al., 2016; Knapp et al., 2017; Knapp et al., 2019). It is typically thickest near Leduc reefs and within embayments, where it contains more reef-derived sediment, and thins basinward (Switzer et al., 1994). According to Wong et al. (2016), the Duvernay occurs within Conodont Montagne Noire Zones 6 through 11 (*of* Klapper, 1989), representing deposition over a timespan of roughly 3 – 4 million years. Subsidence within the basin was slow during deposition of the Cooking Lake Formation, increased dramatically during Duvernay deposition, then slowed again during middle to upper Ireton deposition (McCrossan, 1961; Wonfor and Andrichuk, 1953) (Fig. 1.2).

Woodbend Group strata in Alberta dip to the southwest (~44° and increase in dip to the west due to Laramide Orogeny downwarping) (Switzer et al., 1994; Preston et al., 2016).

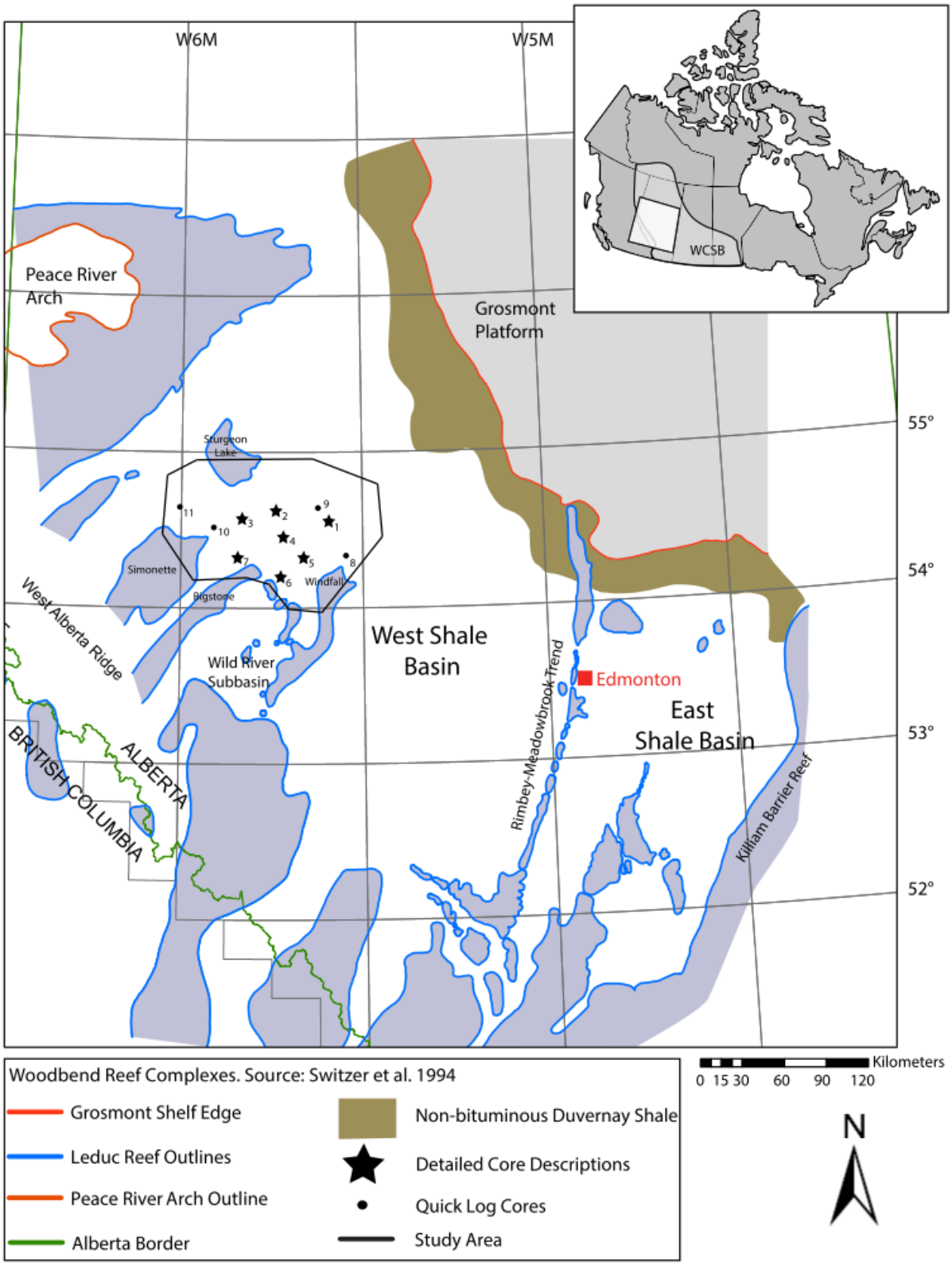

Figure 1.1: Paleogeography of the Alberta Basin in the Late Devonian. Kaybob Area outlined in black. (Modified *from* Knapp et al., 2017)

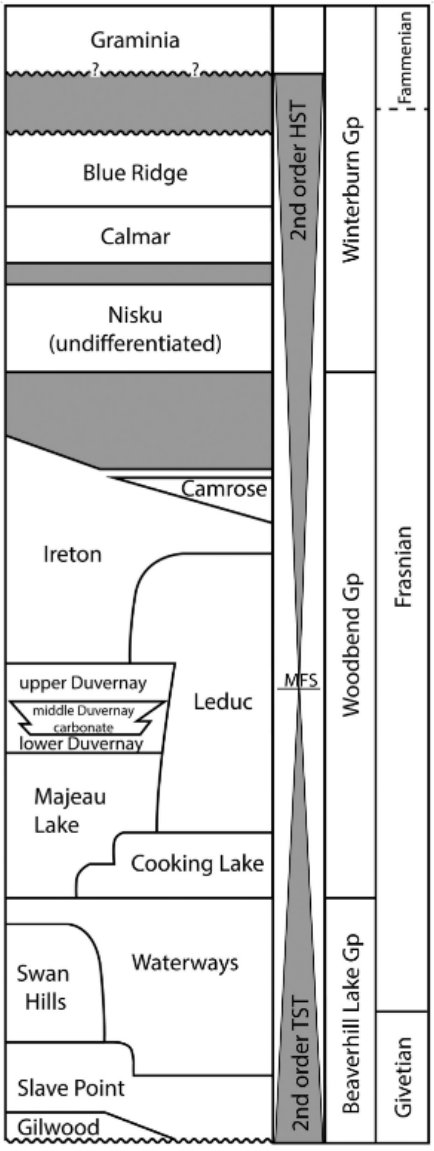

Figure 1.2: Upper Devonian (Frasnian) stratigraphy, Alberta Basin. (*from* Knapp et al., 2019)

1.3 METHODS

Seven long, slabbed drill cores were examined and described in detail, and an additional four cores were briefly logged (Fig. 1.1; Table 1.1). Cores were chosen based on recovery, quality, length of Duvernay Formation penetration, and geographic location within the Kaybob area. Length of cores range from 54-79 m and the length of the Duvernay Formation within the cores range from 47-68 m (total logged core: 445 m; total logged Duvernay core: 366 m). Core descriptions (1:10 scale) recorded macroscopic features including sedimentary structures, fabrics, colour, trace and body fossils, mineralogy, cement type and abundance, pyrite abundance and form, and the abundance and fill of natural fractures. Relative abundance of calcium carbonate was estimated visually using 10% hydrochloric acid.

We prepared 176 extra thin (20 µm) thin sections of important features, fabrics, contacts, and representative lithofacies from the 7 cores. Thin sections were taken normal to bedding and half of each thin section was stained for calcite and ferrous iron. Thin sections made for this study are available at the Alberta Energy Regulator Core Research Center in Calgary. Thin sections were scanned using a Nikon Super Coolscan 5000 ED scanner to observe cm- to mm-scale features. A Zeiss Axio Scope A1 petrographic microscope and camera are used to observe mm- to µm-scale features. Twenty-one samples taken from core 3 were sent for LECO TOC, Rock-Eval-2 and maturity testing as well as XRF Whole Rock & ICP-MS trace elements analysis. Additional geochemical analyses from core 4 were available (previously published in Harris et al., 2018).

Lithofacies were identified from the sedimentological analysis of the cores and thin sections, based on unique combinations of lithology and sedimentary and biogenic structures. Core descriptions were correlated to petrophysical well logs. Sequence stratigraphic surfaces are identified using core descriptions by facies transitions, log signatures, geochemical data, and petrophysics data. Stratigraphic and sequence stratigraphic surfaces are correlated across the Kaybob area using petrophysical well logs

in Petrel software to produce regional cross sections and map sequence stratigraphic surfaces and systems tracts.

Table 1.1: Name, location, and length of Duvernay cores.

Map #	Well name	UWI	Detailed core log	Thin section samples	Geochem samples	Length of Duvernay (m)
1	ATH HZ TWOCK	100/04-21-064-16W5/00	Y	Y	N	46.76
2	ATH HZ KAYBOB	100/04-32-064-20W5/00	Y	Y	N	46.48
3	SCL HZ 102 McKinley	100/04-19-064-22W5/00	Y	Y	Y	48.26
4	SCL HZ KAYBOB	100/02-22-063-20W5/00	Y	Y	Y	52.85
5	TQN FOXCK	103/16-25-061-19W5/00	Y	Y	N	55
6	ROGCI HZ KAYBOBS	100/06-16-060-20W5/00	Y	Y	N	67.82
7	ATH HZ SAXON	100/01-28-061-23W5/00	Y	Y	N	48.7
8	Bounty Wind	100/11-34-061-15W5/00	N	N	N	45.1
9	APL(98) Kaybob	100/14-09-065-17W5/00	N	N	N	18
10	Murphy Simon	100/01-12-064-25W5/00	N	N	N	54
11	CVE HZ KARR	102/09-25-065-27W5/00	N	N	N	28.7

1.4 RESULTS

1.4.1 Lithofacies descriptions

Five lithofacies (Table 1.2) are identified in Duvernay core in the Kaybob area, defined by composition, grain size, sedimentary structures, bioturbation, and cement. Lithofacies are described here in order of highest to lowest average TOC.

LF1: Planar-laminated silt and clay-bearing mudstone

Lithofacies 1 is comprised of dark grey, siliceous-calcareous, faintly planar laminated mudstone (Fig. 1.3a). LF1 is composed of clay and silt-sized detrital grains (calcite, quartz, feldspar, mica, and dolomite), and organic matter (OM). Body fossils are rare in LF1 but include styliolinid tests, brachiopod/ostracod fragments, radiolarians, ammonoid anaptychi, and very rare conodont elements. Clay minerals are in low abundance and typically occur in 100-200 µm long by ~30 µm thick aggregates. OM appears disseminated through the matrix and in thin (typically ~5x50 µm) stringers. The average TOC for LF1 is 2.73 wt.%. Laminae are typically ~300-500 µm thick, continuous and planar-parallel, defined by alternating OM- and pyrite-rich laminae (darker) and clay-rich laminae (lighter) (Fig. 1.3b). Contacts between laminae are diffuse, possibly gradational, and irregular. Sparse to non-existent bioturbation is represented by a low diversity assemblage of burrows, generally horizontal to subhorizontal, mud-infilled (rare silt-infilled), and <1 mm diameter. Burrow types include *Planolites*, *Chondrites*, *Zoophycos*, and *Helminthopsis*.

A variant of LF1 (referred to as LF1A) is defined by presence of discontinuous laminae of pyritized silt and fossil fragments (Fig. 1.3c, 1.3d). Laminae are typically up to 1mm thick and a few mm to several cm long. Contacts are sharp or gradational with planar or slightly wavy bases and slightly wavy top contacts. A second variant of LF1 is LF1B, which contains continuous to discontinuous grain-

supported coarse silt to fine sand laminae, is present throughout lithofacies 1 (Fig. 1.3e, 1.3f). These laminae are typically ~1 mm thick and composed of variable amounts of carbonate and siliceous detrital grains and fossil fragments. Laminae are massive (sharp contacts), normally graded (sharp bases, gradational tops), or inversely graded (gradational bases, sharp tops). Laminae locally display wavy contacts, pinching/swelling, convergence/divergence, current ripples, low angle cross laminae, and silt lenses.

Rare grain-supported beds, up to 4 cm thick, of coarse silt to fine sand carbonate and siliceous detrital grains, fossil fragments, and mud rip-up clasts occur locally in LF1. Some coarse beds (Fig. 1.4a) have erosive bases, gradational tops, normal grading, mud rip-up clasts, fossil fragments, and occasional up to 2 mm thick silt-infilled burrows. Other beds (Fig. 1.4b) display sharp (non-erosive to wavy) bases, sharp tops, normal or no grading, low angle cross laminae, planar laminae, and up to 1mm thick mud drapes. Beds are typically moderately bioturbated but are commonly more bioturbated towards their tops.

LF2: Wavy-laminated sand, silt, and clay-bearing mudstone

Lithofacies 2 consists of medium to light grey silt-sand grains interlaminated with dark-grey mud, the latter similar to lithofacies 1 (Fig. 1.5a). Coarser sediments in LF2 are composed of variable amounts of fine silt to very fine sand sized carbonate and siliceous detrital grains, fossil fragments (brachiopods/ostracods, styliolinid tests, rare conodont elements), minor pyrite, mica, and local phosphate grains (Fig. 1.5b-e). The average TOC for LF2 is 2.64 wt.%. Grain-supported laminae are typically 1-5 mm thick, wavy and continuous to discontinuous, and locally planar (Fig. 1.5a-e). Laminae are massive (with sharp contacts) (Fig. 1.5e), normally graded (sharp bases, gradational tops) (Fig. 1.5a, c, e), or inverse graded (gradational bases, sharp tops) (Fig. 1.5a, e). Laminae commonly display pinching

and swelling, convergence/divergence, and current ripples (Fig. 1.5a-e). Dolomite or calcite cements are common (Fig. 1.5e). Bioturbation, including *Planolites,* is typically very sparse to sparse with low diversity. Mud-infilled burrows are typically sub-mm diameter and horizontal to subvertical. Silt-infilled burrows are typically horizontal to subhorizontal, up to 3mm in diameter, and locally pyritized.

LF3: Bioturbated silt and clay-bearing mudstone

Lithofacies 3 is composed of brown to medium dark to dark grey, moderately to intensely bioturbated mudstone (Fig. 1.6a-c). It contains variable amounts of carbonate and siliceous detrital grains, fossil fragments (brachiopod/ostracod shells, bivalves, styliolinid and tentaculitid tests, rare arthropod fragments (Fig. 1.6e), gastropods, crinoid fragments, radiolarians, and stromatoporoid fragments), clay minerals, minor mica, pyrite, and very rare phosphatic grains (Fig. 6c). In-situ benthic macrofossils (such as bivalves, gastropods, possible agglutinated benthic foraminifera) are generally very rare in the Duvernay in the study area but occur most frequently in LF3 in isolated horizons (Fig. 1.6d). LF3 has abundant clay-sized detrital quartz, carbonate, and clay minerals and common clay aggregates of typically ~20x300 µm. Organic matter is disseminated throughout the matrix, commonly forming stringers typically ~5x50 µm. The average TOC for LF3 is 2.44 wt.%. LF3 is massive to faintly or distinctly planar laminated (typically 600-800 µm); laminae are discontinuous to continuous and locally wispy. Laminae are defined by alternating OM- and pyrite-rich laminae (darker) and clay-rich laminae (lighter), with diffuse to gradational contacts. Local continuous to discontinuous grain-supported laminae of coarse silt to fine sand size (up to 4 mm thick) display rare normal grading (sharp bases, gradational tops), inverse grading (gradational bases, sharp tops), wavy contacts, and current ripples. Bioturbation in LF3 is typically moderate to intense with low diversity. Burrows are horizontal to subvertical, typically up to 1 mm diameter, dominantly mud-infilled and more rarely silt-infilled, and often fully pyritized or

rimmed by pyrite (Fig. 1.6a-b). Burrows include *Planolites*, *Zoophycos*, *Palaeophycus*, *Spirophyton*, *Chondrites*, *Helminthopsis,* and *Navichnia*.

Rare thick grain-supported laminae up to 8 mm thick occur locally in LF3 in the upper part of the Lower Duvernay Member in the central to eastern part of the study area (cores 1 and 4). They contain coarse silt to fine sand carbonate and siliceous detrital grains, fossil fragments, and mud rip-up clasts and are commonly pyritized. Some coarse laminae have erosive bases, are normal graded (massive and coarser near base) and thinly planar laminated (Fig. 1.7a-b). Other thick grain-supported laminae are similar in nature to the two types noted in LF1 (Fig. 1.7c, 1.7d).

LF4: Fossiliferous wackestone

Lithofacies 4 consists of medium grey, massive to faintly planar laminated silt and sand grains in a matrix of argillaceous to calcareous mud (Fig. 1.8a-c). LF4 is composed of variable amounts of carbonate and siliceous detrital grains, fossil fragments (styliolinid tests, ostracod/brachiopod shells, rare conodont elements), and minor pyrite and mica. The average TOC for LF4 is 2.33 wt.%. LF4 is massive to faintly or distinctly planar to slightly wavy or wispy laminated (typically 0.5 – 1 mm thick). Normal grading with sharp bases and gradational tops is locally visible within planar laminae, and laminae are locally pyritized. LF4 is typically moderately to intensely bioturbated with a low ichnodiversity. Burrows are typically up to 1 mm diameter (up to 8 mm long), horizontal to subvertical, mud and silt-infilled and are often partially pyritized. Bioturbation in this facies is often cryptic but includes *Helminthoposis* and *Planolites*.

LF5: Nodular Wackestone

Lithofacies 5 is composed of medium light grey wackestone nodules in a matrix of medium to medium dark grey argillaceous to calcareous mud (Fig. 1.9a-c). Nodules are tabular (2-90 mm thick) to round (2-50 mm thick). Wackestone nodules consist of silt- to fine sand-sized detrital calcite and sparse fossil fragments (brachiopod/ostracod shells, styliolinid tests) (Fig. 1.9d) with minor detrital silicate grains. The average TOC for LF5 is 0.58 wt.%. Nodules are typically massive and less commonly display faint 1-5 mm thick, continuous to discontinuousplanar laminae. Very rarely laminae may be normal and inverse graded. Very rare possible dewatering structures occur locally (Fig. 1.9b). Pyrite nodules up to 8 mm in diameter are relatively abundant throughout LF5.

Nodules occur in a matrix of uncemented argillaceous to calcareous mudstone, similar to LF3, where the ductile matrix mudstone is deformed around nodules. The mudstone matrix is typically massive to discontinuous planar- laminated (<1-5 mm thick). Bioturbation in LF5 is typically moderate to intense with traces that are typically larger, more vertical, and more diverse than other facies (Fig. 1.9e-f). Burrows are mud- or silt-infilled, typically up to 6 mm in diameter (up to 60 mm long) and often pyrite-infilled or rimmed. Burrow types include *Planolites, Zoophycos*, *Nereites*, *Arenicolites*, *Teichichnus*, *Diplocraterion*, and *Navichnia*.

Table 1.2: Lithofacies characteristics.

	LF1	LF2	LF3	LF4	LF5
Name	Planar-laminated silt and clay-bearing mudstone	Wavy-laminated sand, silt, and clay-bearing mudstone	Bioturbated silt and clay-bearing mudstone	Fossiliferous wackestone	Nodular wackestone
Colour	Dark grey	Medium to light grey laminae in dark grey matrix	Medium dark to dark grey	Medium grey	Medium light grey nodules in medium grey matrix
Bedding	Planar laminae	Wavy, lenticular, planar laminae	Massive, wispy/discontinuous, planar laminae	Planar, wavy/wispy laminae	Nodular, planar bedded
Other Sed. Structures	Normal grading, inverse grading, wavy laminae, pinching/swelling, convergence/divergence, current ripples, low angle cross laminae, silt lenses	Normal grading, Inverse grading is also present, pinching/swelling, convergence/divergence, current ripples	Normal grading, inverse grading, wavy laminae, current ripples	Normal grading	(Rare) Normal grading, inverse grading
Grain Size	Silt and clay-bearing mudstone	Sand, silt, and clay-bearing mudstone	Silt and clay-bearing mudstone	Wackestone	Wackestone
Cement	Calcite, pyrite	Dolomite, calcite	Calcite, pyrite	Calcite	Calcite, pyrite
Bioturbation Index	0-1	0-2	2-4	2-4	3-4
Common Taxa	Styliolinids, brachiopods, ostracods, ammonoid anaptychi, very rare conodont jaw elements and radiolarians	Brachiopods, ostracods, styliolinid tests, rare conodont elements	Brachiopods, bivalves, ostracods, styliolinids, tentaculitids, rare arthropod fragments, gastropods, crinoid fragments, radiolarians, possible stromatoporoids, possible agglutinated benthic foraminifera	Styliolinids, ostracods, brachiopods, rare conodont elements	Brachiopods, ostracods, styliolinids
Average TOC	2.73	2.64	2.44	2.33	0.58

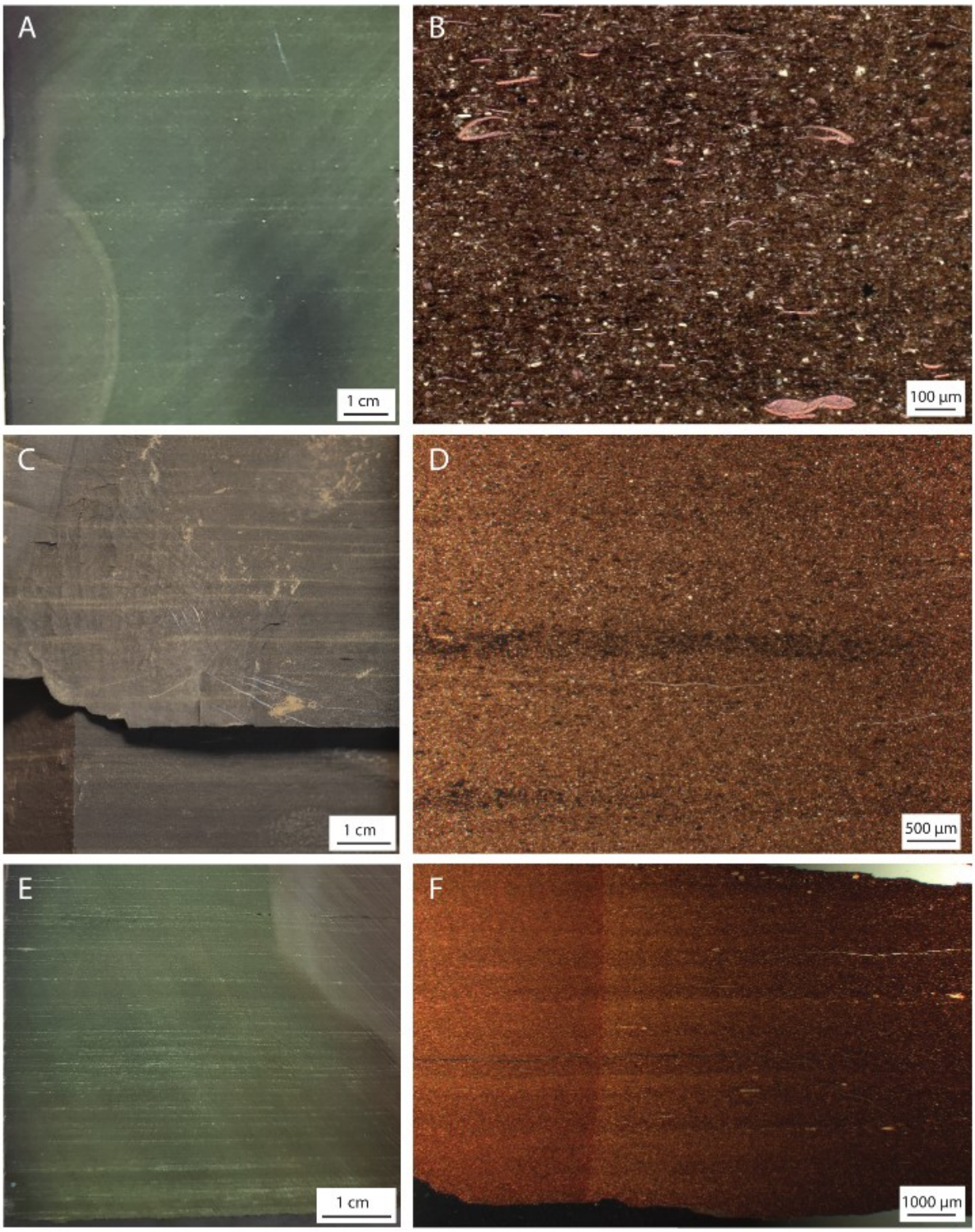

Figure 1.3: LF1: A) Planar laminated mud (3075.07 m, core 4) B) Planar laminated mud thin section; OM- and pyrite-rich and OM- and pyrite poor laminae (PPL) (2825.15, core 1) C) Discontinuous pyrite laminae (3109.7 m, core 5) D) Discontinuous pyrite laminae thin section (PPL) (3325.12 m, core 3) E) Grain-

supported silt laminae in planar laminated mud (~3077.9 m, core 4) F) Grain-supported silt laminae in planar laminated mud, thin section (PPL) (3331.05 m, core 3).

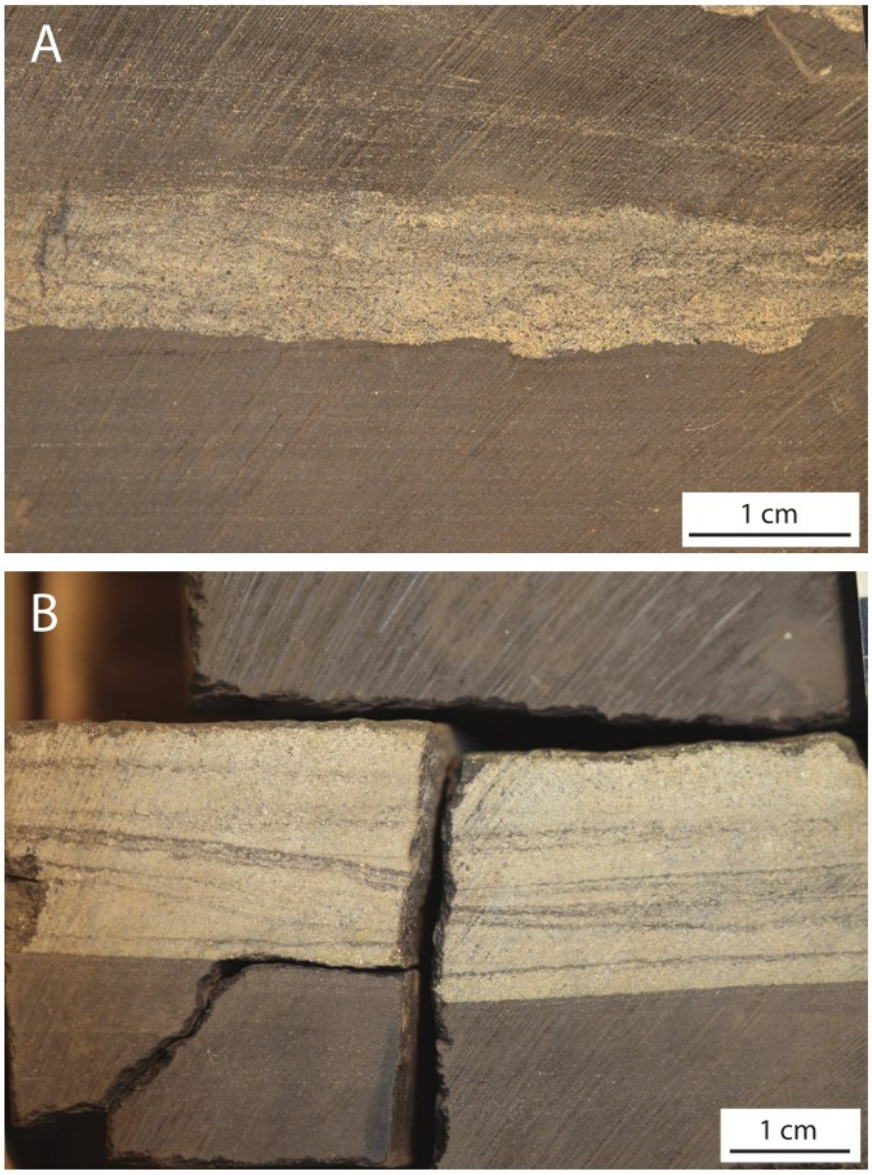

Figure 1.4: LF1: Rare, thick, grain supported beds. A) Turbidite (3403.5 m, core 6) B) Contourite (alternatively a turbidite) (3388.95 m, core 6).

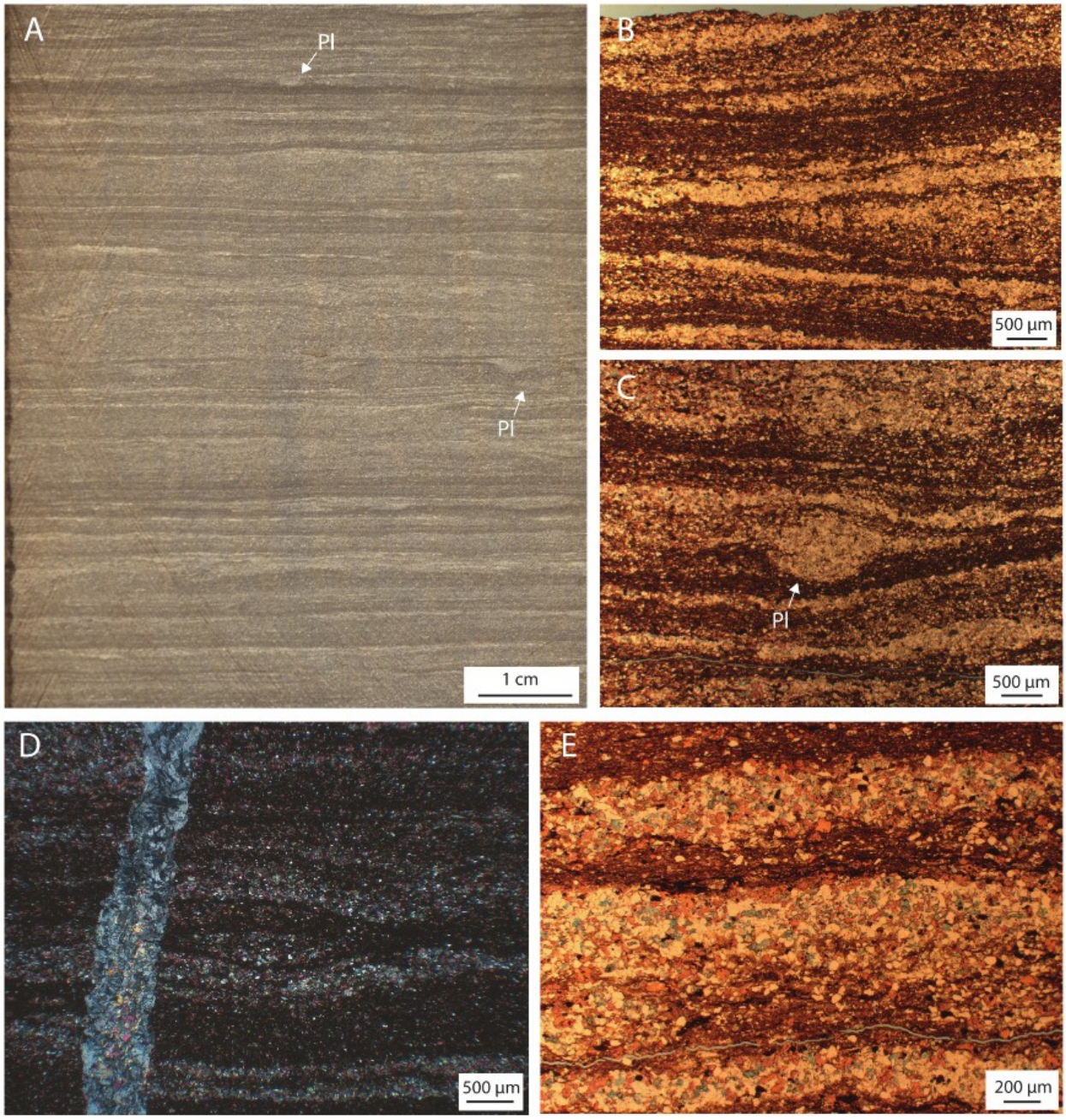

Figure 1.5: LF2: A) Wavy, planar, and nodular laminae, current ripples (3356.40 m, core 6) B) Wavy, pinching/swelling, converging/diverging, continuous and discontinuous laminae (PPL) (2799.86 m, core 1) C) Wavy and pinching and swelling laminae (PPL) (2799.86 m, core 1) D) Wavy and nodular laminae, divergent/convergent laminae (XPL) (3077.22 m, core 4) E) Silt laminae composition, normal grading, inverse grading (PPL) (2799.86 m, core 1). Pl = *Planolites.*

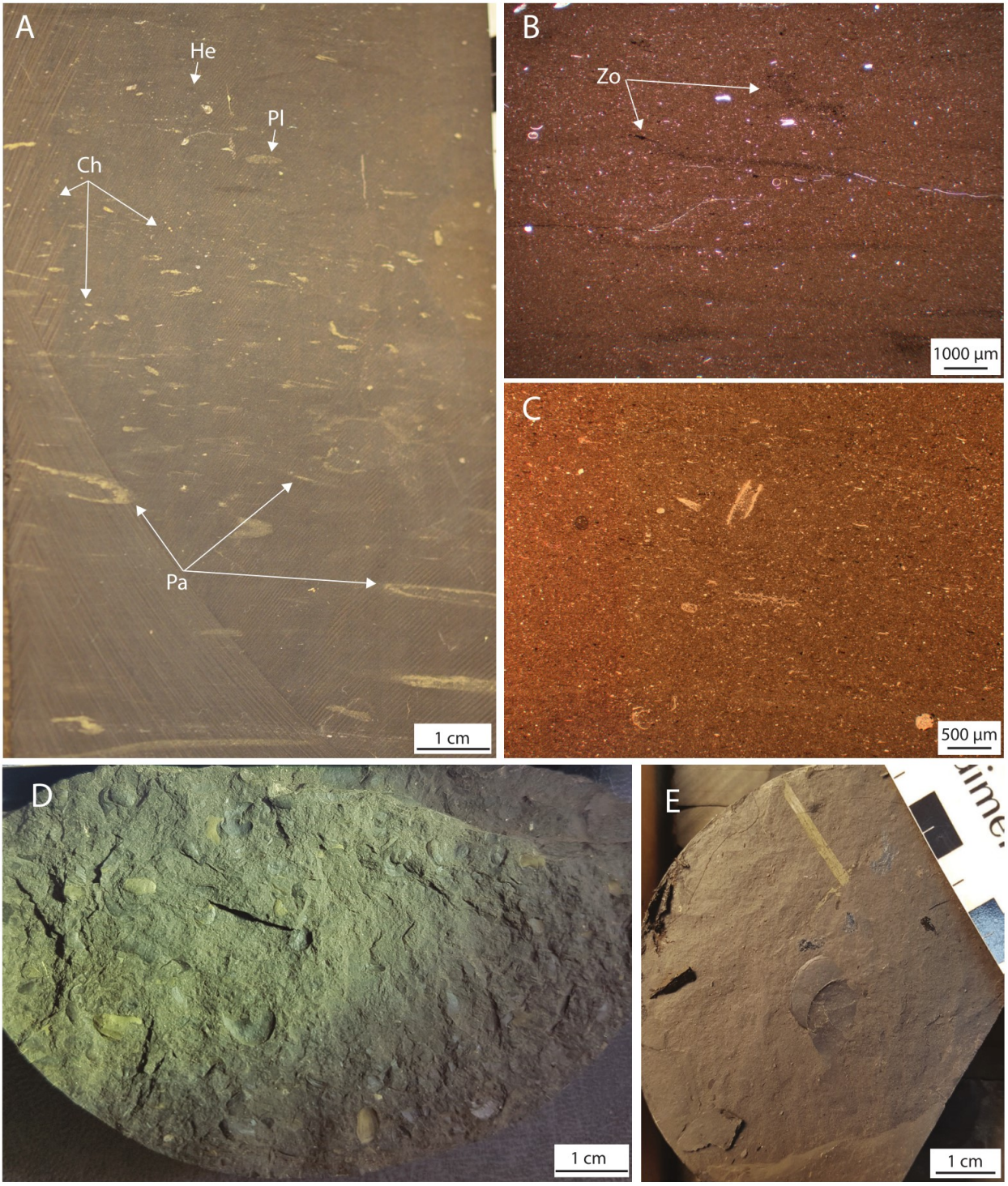

Figure 1.6: LF3: A) intensely burrowed (mud infilled, pyritized) section of LF4 (3372.15 m, core 6) B) Pyritized, mud-infilled burrows (3113.3 m, core 4) C) Matrix composition of LF4 with fossil fragments (styliolnids, tentaculitid, ostracod/brachiopod shell fragments) (2821.17, core 1) D) Bivalves and pyritized bivalves; also fragments; possible gastropods (3106.38 m, core 4) E) Possible arthropod fragments (2cm), 3mm brachiopod (2823.35 m, core 1). Pl = *Planolites*, Ch = *Chondrites*, Pa = *Palaeophycus*, Zo = *Zoophycos*; He = *Helminthopsis*.

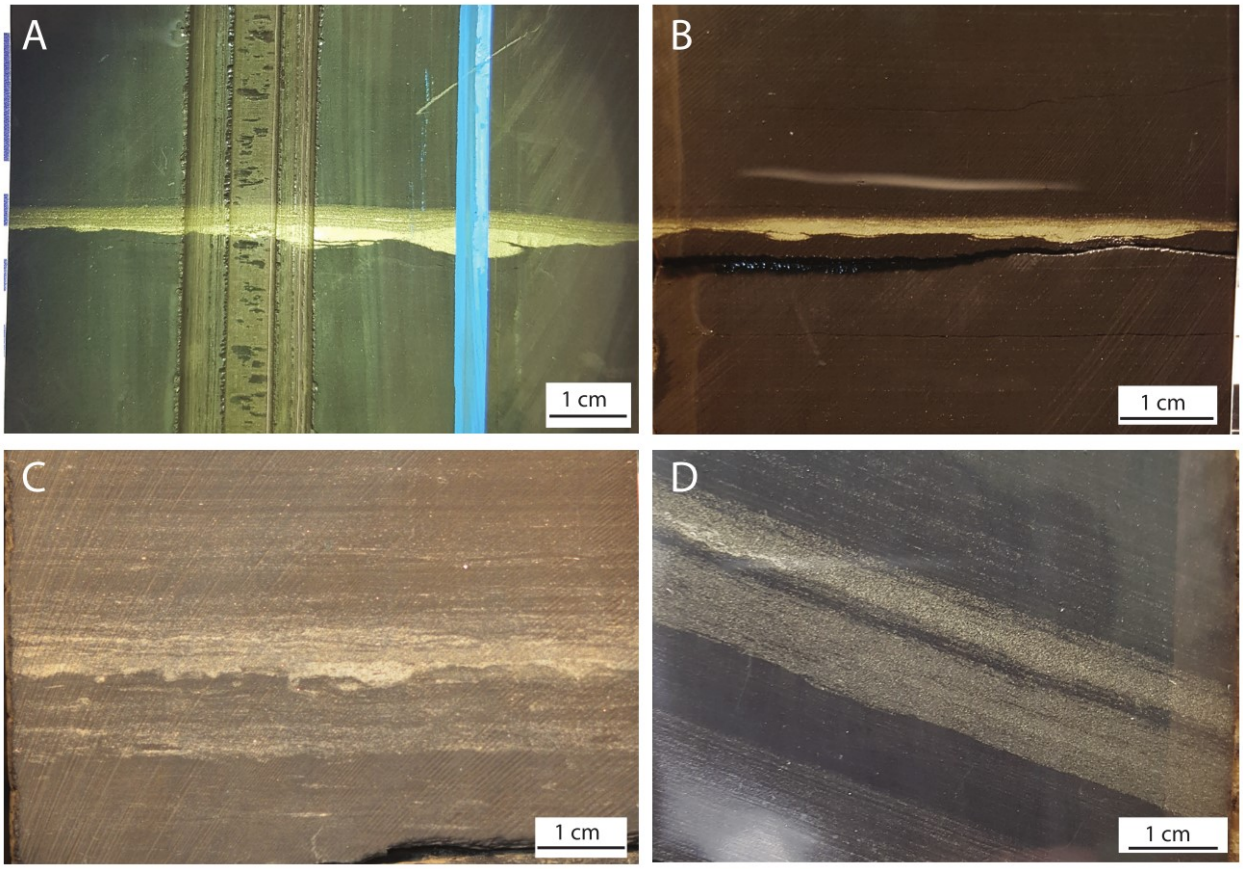

Figure 1.7: LF3: A) Wave enhanced sediment-gravity-flow bed (3-5mm thick) very thinly laminated, erosive base, flame structures (3121.13 m, core 4) B) Wave enhanced sediment-gravity-flow bed (2819.43 m, core 1) C) Turbidite (3368.08, core 6) D) Contourite (3328.71 m, core 3).

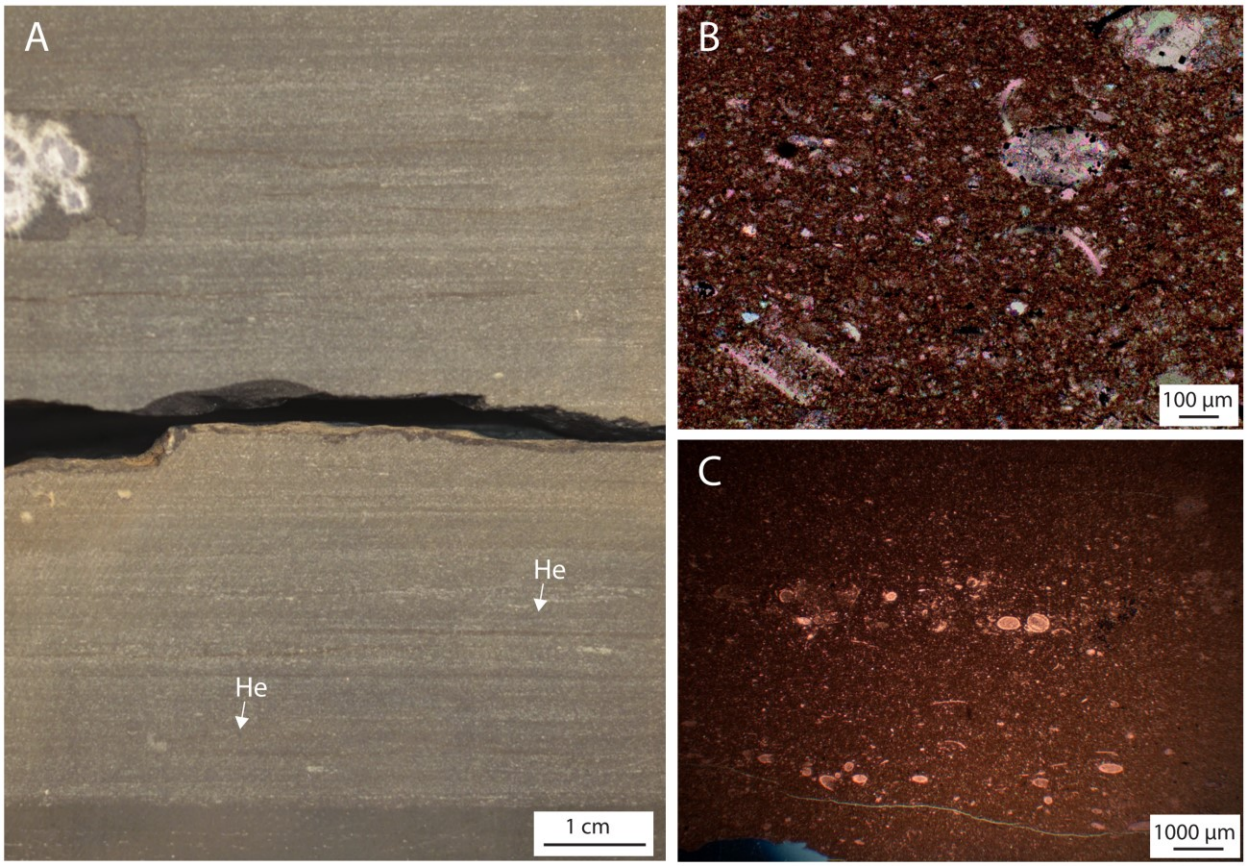

Figure 1.8: LF4: A) Core scale example of LF3 (3099.6 m, core 5) B) Example of faint silt laminae (3122.5 m, core 4) C) Composition of LF3 (3122.5 m, core 4). He = *Helminthopsis*.

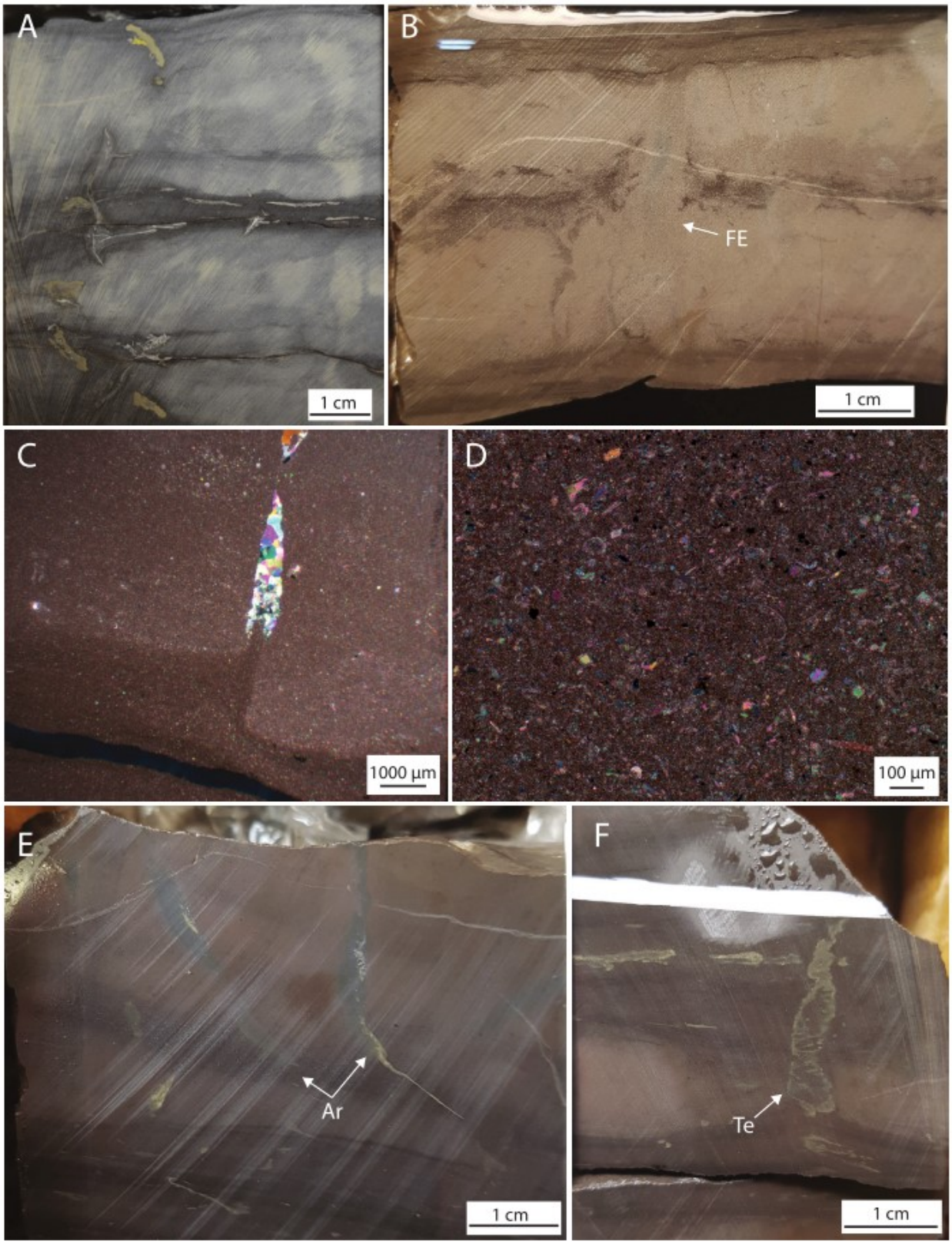
A
1 cm
B
FE
1 cm
C
1000 µm
D
100 µm
E
Ar
1 cm
F
Te
1 cm

Figure 1.9: LF5: A) Wackestone nodules in argillaceous to calcareous mud, pyrite nodules (3133.8 m, core 5) B) Fluid escape structure (2808 m, core 1). C) Wackestone nodule with calcite infilled fracture in thin section (XPL) (3114.5 m, core 4) D) Close up of wackestone nodule composition and massive texture (XPL) (3114.5 m, core 4) E) *Arenicolites* (2x30 mm), slightly pyritized (3339.85 m, core 3) F) *Teichichnus* (pyritized) (3338.75 m, core 3). FE = fluid escape structure, Ar = *Arenicolites*, Te = *Teichichnus*.

1.4.2 Stacking Patterns and Sequence Stratigraphy

3rd Order Depositional Sequences

Facies stacking patterns were used to identify three large stratigraphic units (Depositional Sequence (DS) 1-3), separated by boundaries SB0 through SB3 (Fig. 1.10-1.12). Surfaces were identified in core (Fig. 1.13), correlated to wireline logs, and mapped across the study area to understand stratigraphic architecture and to interpret sequence stratigraphic relationships.

DS1 ranges in thickness from ~32 m to the northeast part of the study area and pinches out against reefs (Fig. 1.14a). SB0 is located at the base of DS1 (Fig. 10-12) at the contact between the underlying argillaceous Majeau Lake Formation (clay-rich, OM-poor, more fissile, with larger and more abundant burrows and in-situ benthic macrofauna) and overlying more siliceous Duvernay. The SB0 contact is expressed as an erosive surface with passively infilled burrows into underlying mud and an overlying silt/sand bed up to 18 mm thick (Fig. 1.13). SB0 is typically recognized on wireline logs as an abrupt increase in resistivity related to high OM content. DS2 ranges in thickness from ~38 m in the far south part of the study area, thins to the northeast and pinches out against reefs (Fig. 1.15a). SB1 is located at the base of DS2 (Fig. 1.10-1.12) between the underlying middle Duvernay member (carbonate-rich mud (LF3) and wackestone (LF5)) and overlying upper Duvernay member (siliceous to argillaceous mud). SB1 is represented by an erosive surface overlain by a layer of silt and sand grains up to 9 mm thick (Fig. 13). SB1 is typically defined on wireline logs as a drop in resistivity and a significant spike in gamma related to decreased carbonate content and increased OM content. DS3 ranges in thickness from ~36 m in the south part of the study area, thins to the northeast toward the Grosmont

Platform and pinches out against reefs (Fig. 1.16a). SB2 is located at the base of DS3 (Fig. 1.10-1.12), within the upper Duvernay member and is typically represented by a soft sediment-deformed surface overlain by an up to 55 mm thick silt and sand bed in proximal areas that becomes gradational basinward (Fig. 1.13). SB2 is typically defined on wireline logs as the beginning of a significant drop in resistivity. SB3 is located at the top of DS3 (Fig. 1.10-1.12), at the contact between the Duvernay and overlying, detrital clay and dolomite-rich, organic-lean, Ireton Formation. SB3 is represented by a soft sediment-deformed surface, overlain by a silt and sand bed up to 17 mm thick that becomes conformable basinward (Fig. 1.13). SB3 is locally overlain by up to 77 cm of sediment transitional between Duvernay and Ireton in the west part of the study area. SB3 is typically defined on wireline logs as a drop in resistivity related to a decrease in OM content. DS1 and DS2 can each be divided into 2 distinct subunits and DS3 can be divided into 3 subunits. These subunits have distinctive internal lithofacies stacking patterns.

TSTs

The lowermost sections of DS1, DS2, and middle section of DS3 (Fig. 1.10-1.12; Fig 1.14b, 1.15b, 1.16c) are predominantly composed of planar laminated mudstone (LF1). Detrital silt and sand grains typically decrease in abundance and sediment typically becomes more biosiliceous stratigraphically upward (consistent with proxies presented in Harris et al. (2018)) with better developed planar laminae (increased continuity and sharpness, decreased thickness). Burrows and fossil fragments typically become more sparse upwards. TOC overall generally increases towards the top of these sections, and redox proxies (S/Fe) suggest more reducing conditions stratigraphically upward (Harris et al., 2018).

In DS2 and DS3, LF3 bioturbated pyritic mudstone (and local LF5 nodular wackestones and LF4 fossiliferous wackestones) transition upwards to LF1 planar laminated mudstone. In DS3, in the central

to northeast part of the study area, LF2 sandy and silty mudstones transition to LF3 and then to LF1 (and LF1B) upward. The lower sections of DS1 and DS2, and middle section of DS3 are quite uniform in thickness across the study area, locally thickening close to reefs (Fig. 1.14b, 1.15b, 1.16c).

HSTs

The upper sections of DS1, DS2, and DS3 (Fig. 1.10-12; Fig. 1.14c, 1.15c, 1.16d) display increases upward in grain size, carbonate content (consistent with proxies presented in Harris et al. (2018)), thickness of laminae (decrease in continuity, sharpness), fossil fragments, and burrows (size, abundance, verticality, diversity), and a decrease in TOC (Harris et al., 2018). Redox proxies suggest more oxidizing conditions upward (Harris et al., 2018).

In the upper section of DS1, facies typically show a gradual transition stratigraphically upward from LF1 planar laminated mudstone to LF3 bioturbated mudstone (and LF4 fossiliferous wackestone locally in the south-central part of study area), to LF5 nodular wackestones. The upper section of DS1 thins from northeast to southwest in the study area, thinning drastically where there is little to no deposition of the middle Duvernay member (Fig. 1.14c). The upper sections of DS2 and DS3 are typically comprised of LF1 planar laminated mudstones (and locally LF3 bioturbated mudstones) transitioning upward to LF2 and LF1B sandy and silty mudstones. In the northeast part of the study area, there is an abrupt transition to LF2 and LF1B that are present to the top of DS2 and DS3. In the south and west parts of the study area, DS2 grades upwards from LF1 to LF3. In DS3, in the south and west parts of the study area, LF3 is most abundant, with LF5 nodular wackestones commonly interbedded with LF3 stratigraphically upward. The upper sections of DS2 and DS3 thicken from northeast to southwest in the study area (Fig. 1.15c, 1.16d).

LST

In the lower section of DS3 (Fig. 1.10-12; Fig. 1.16b), LF3 bioturbated mudstone is the dominant lithofacies. Across SB2 there is an abrupt drop in carbonate sediment, carbonate cement, and grain size. Throughout the lower section of DS3, silt and sand grains are typically sparse and clay content is high (consistent with proxies presented in Harris et al. (2018)). Bioturbation is abundant and burrows are relatively large throughout. Redox proxies suggest oxidizing conditions (Harris et al., 2018). Near reefs in the southwest part of the study area, LF5 nodular wackestones are observed near the base and top of the section. In the far southeast part of the study area, LF2 sandy and silty mudstone is observed throughout the section. The lower section of DS3 thins away from reefs in the study area (Fig. 1.16b)

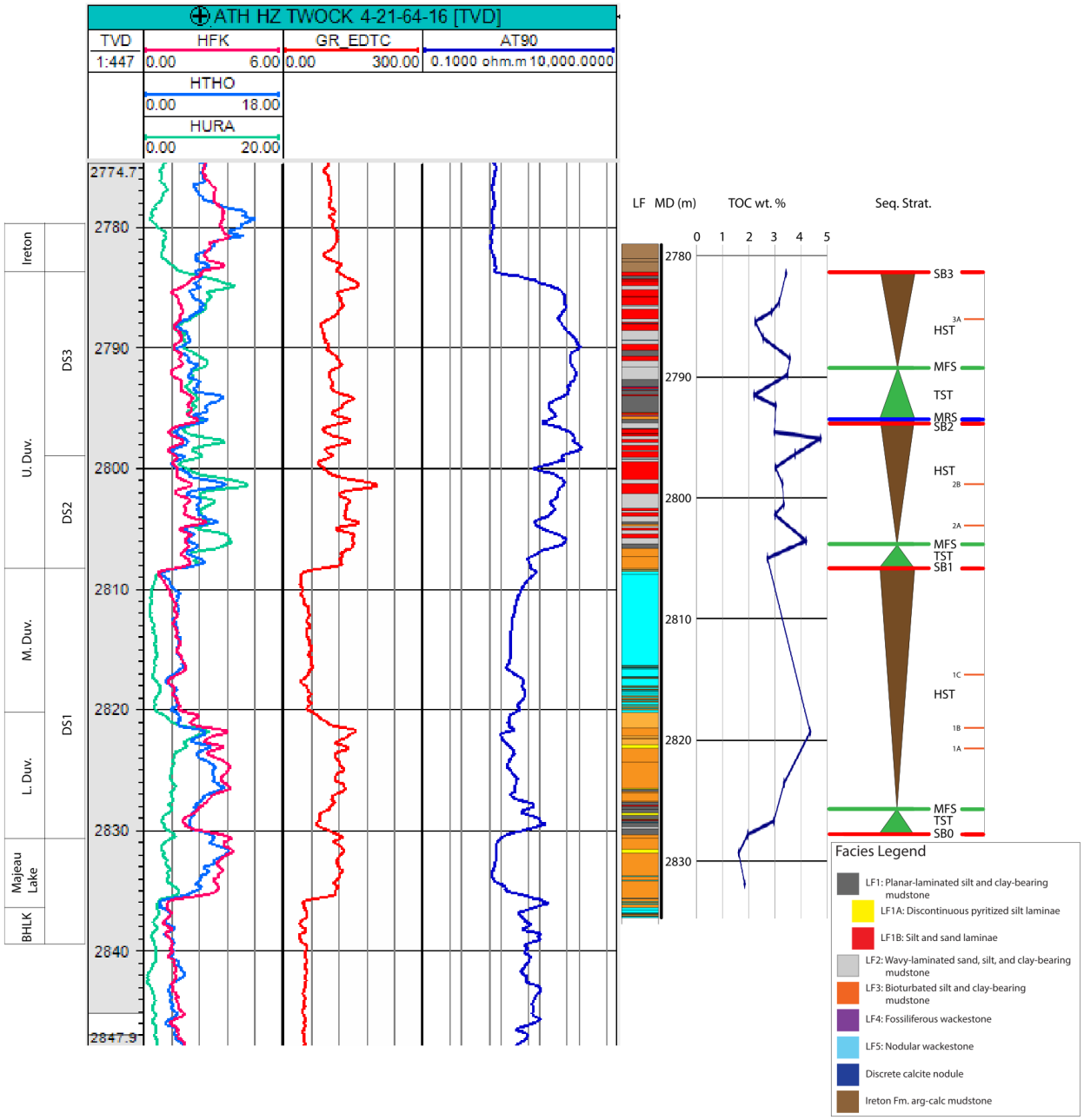

Figure 1.10: Spectral gamma, gamma, neutron porosity, density, PE, deep resistivity log, lithofacies interpretation and sequence stratigraphic interpretation of core 1. (TOC log by Slumberger for Athabasca Oil Corporation, accessed through the Alberta Energy Regulator).

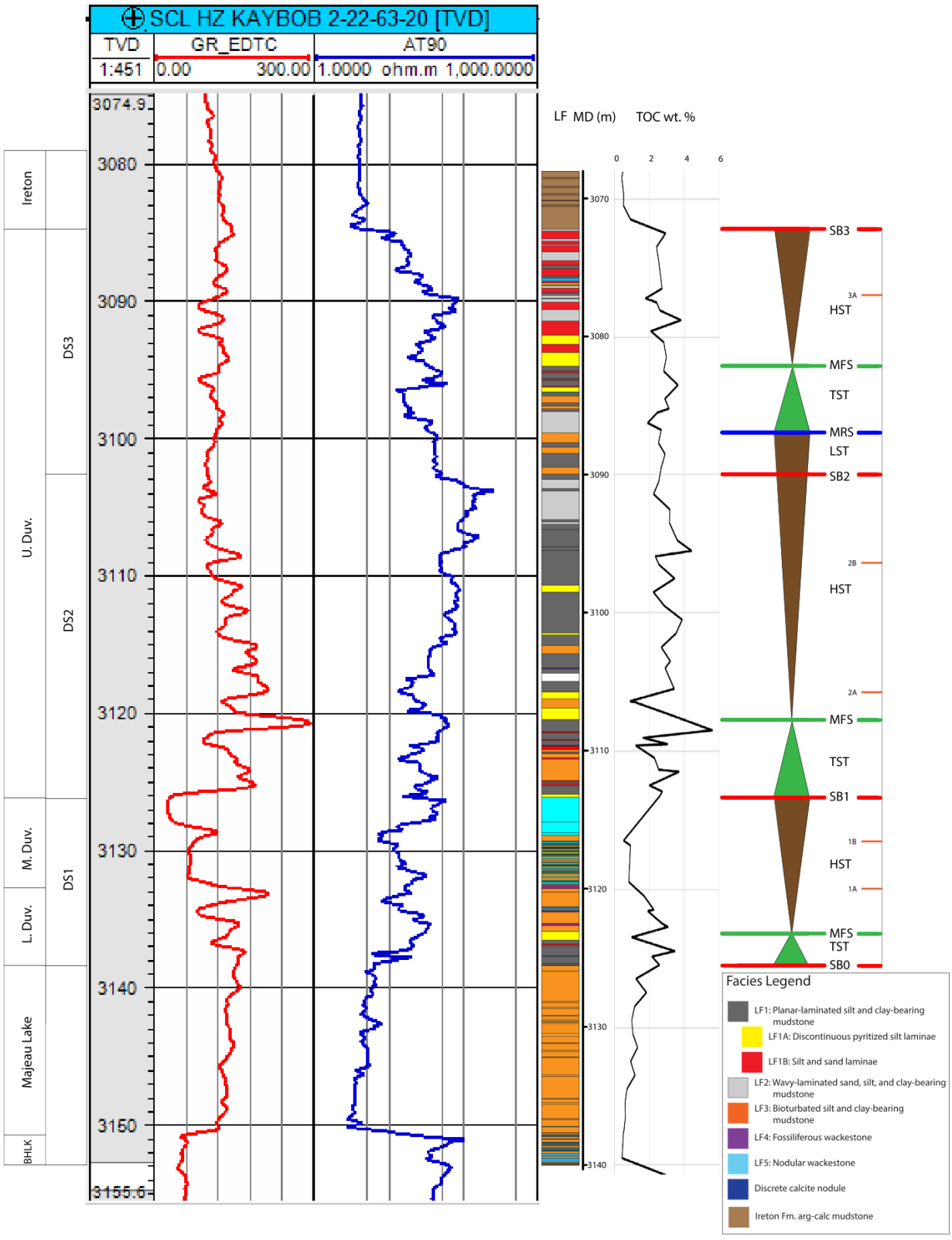

Figure 1.11: Spectral gamma, gamma, neutron porosity, density, PE, deep resistivity log, lithofacies interpretation and sequence stratigraphic interpretation of core 4. (TOC *from* Knapp et al., 2017).

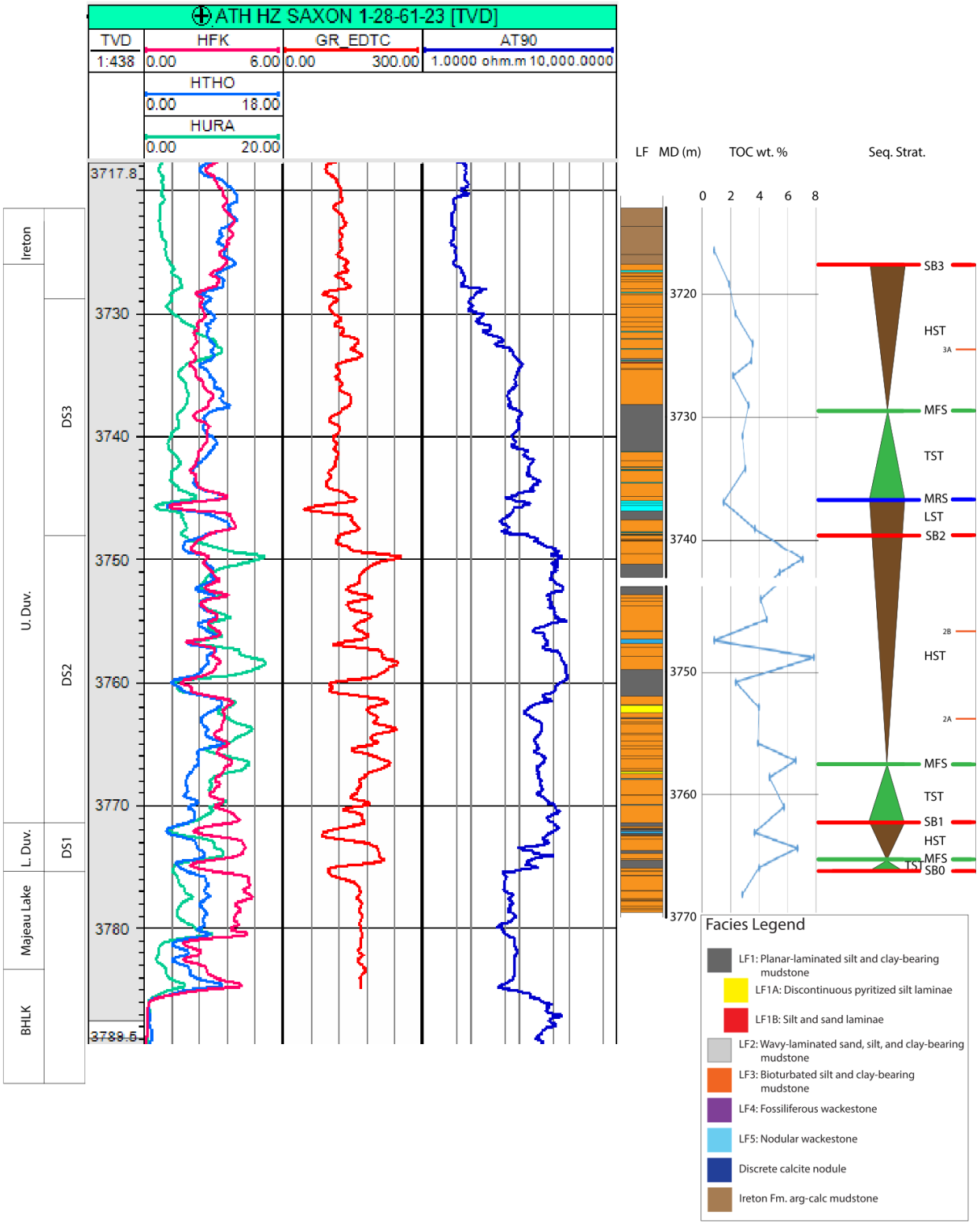

Figure 1.12: Spectral gamma, gamma, neutron porosity, density, PE, deep resistivity log, lithofacies interpretation and sequence stratigraphic interpretation of core 7. (TOC log by Slumberger for Athabasca Oil Corporation, accessed through the Alberta Energy Regulator).

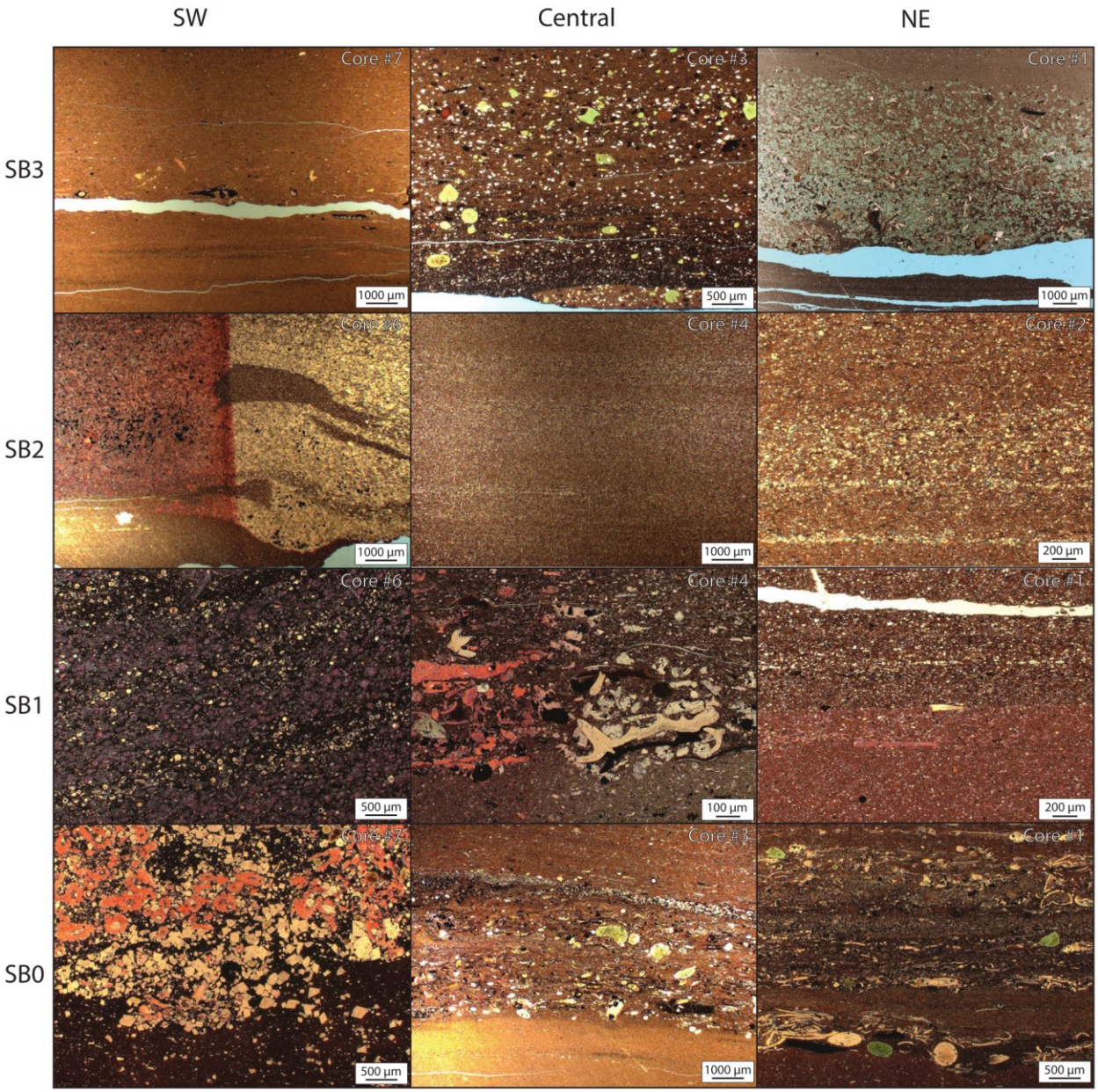

Figure 1.13: Examples of 3rd order sequence boundaries and associated coarse beds from the southwest, central, and northeast parts of the study area.

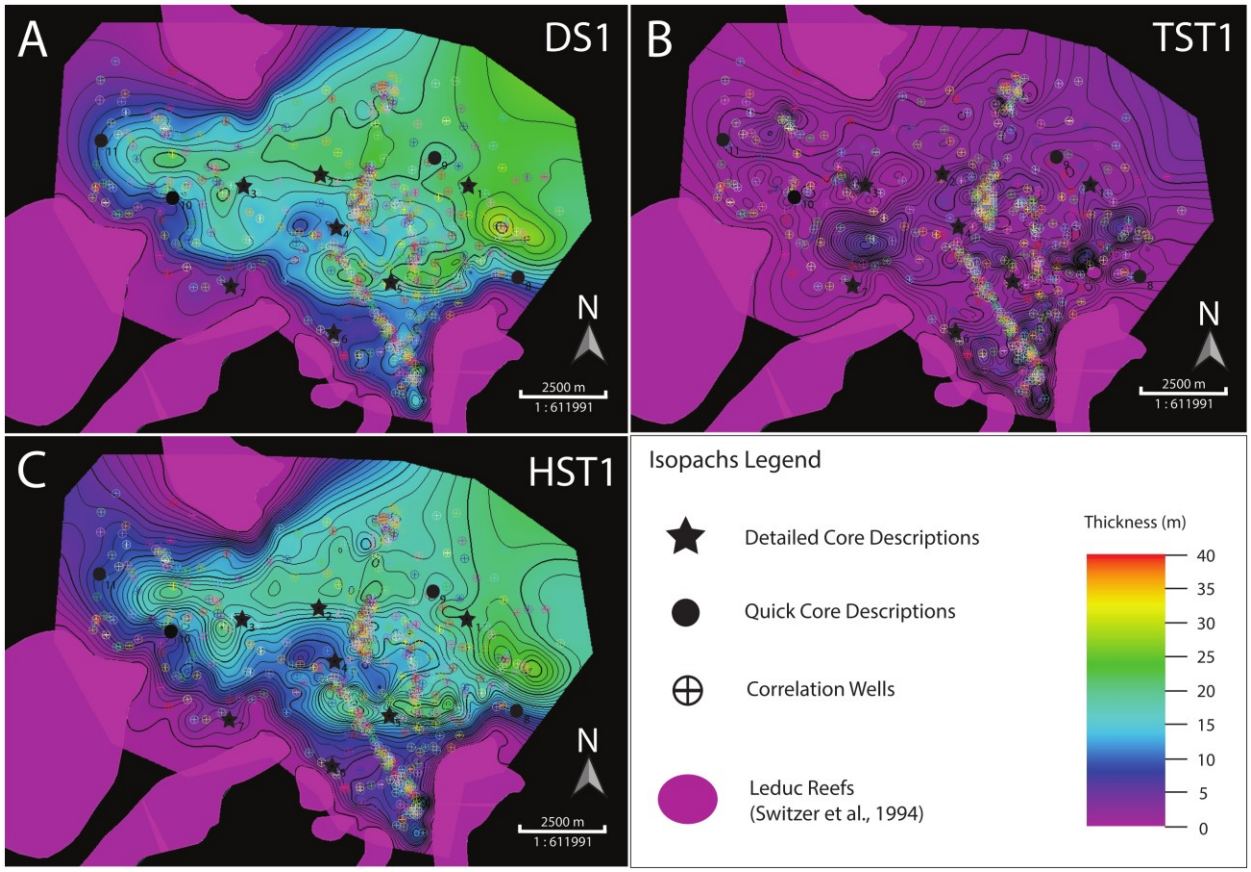

Figure 1.14: Duvernay DS1 isopach maps A) DS1 B) DS1 TST C) DS1 HST.

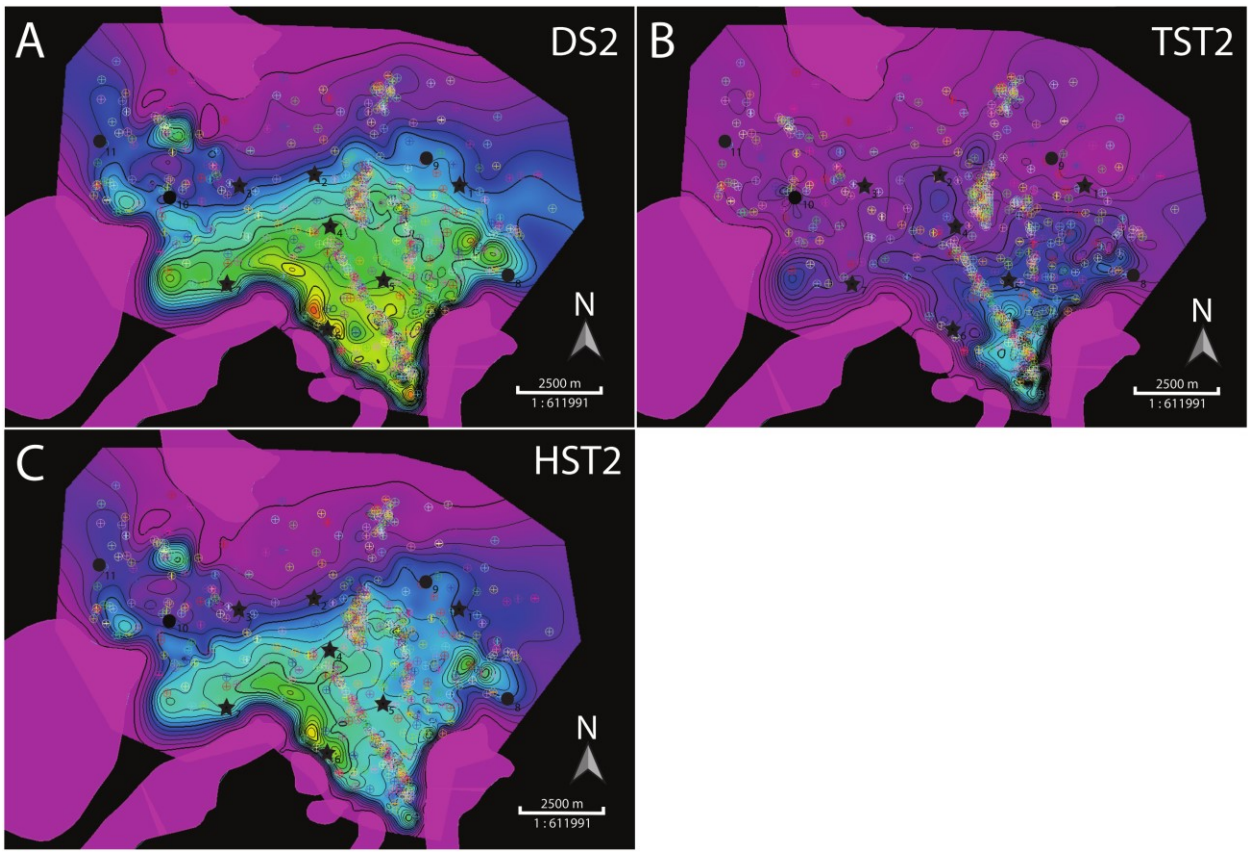

Figure 1.15: Duvernay DS2 isopach maps A) DS2 B) DS2 TST C) DS2 HST.

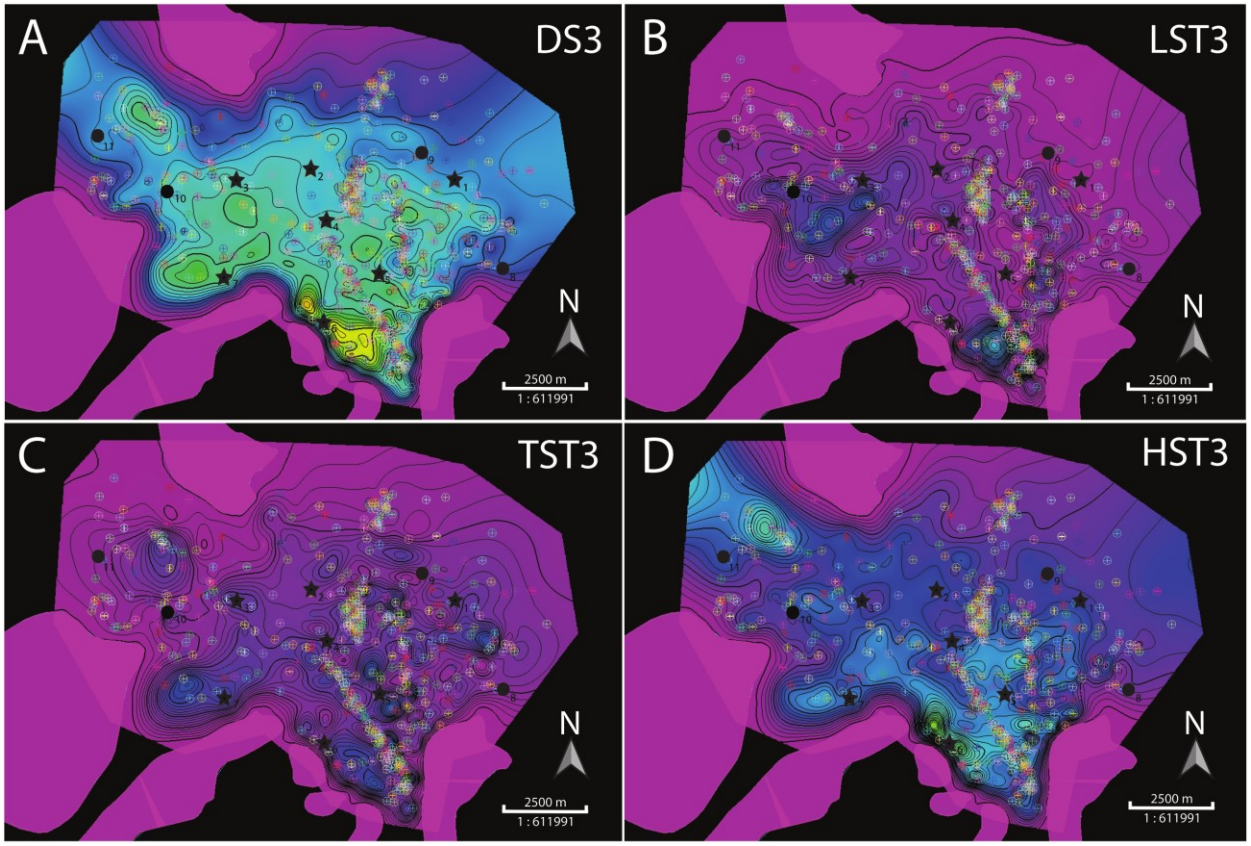

Figure 1.16: Duvernay DS3 isopach maps A) DS3 B) DS3 LST C) DS3 TST D) DS3 HST.

4th Order Depositional Sequences

Within the upper sections of DS1, DS2, and DS3, we identify a total of 9 high frequency depositional sequences, approximately 2 – 7 m thick (locally 1.3 – 10.2 m), which represent the finest cyclicity observed on well logs (Fig. 1.10-1.12) and are recognized by upward increasing resistivity and decreasing gamma (Fig. 1.10-1.12). High frequency sequences display consistent internal stratigraphic trends including: upward increasing grain size, increasing carbonate sediment and cement, increasing laminae thickness, decreasing continuity and sharpness, increasing bioturbation (burrow size, abundance and verticality), increasing fossil fragment abundance (and very rare local in-situ benthic macrofossils), and decreasing TOC. The bottom section of high frequency sequences in DS2 and DS3

locally display internal stacking patterns of upward decreasing grain size, carbonate sediment, and bioturbation and increasing TOC. Redox proxies within high frequency sequences (presented by Harris et al. (2018)) typically suggest less reducing conditions upwards through the sequences with the overlying sequence.

Contacts between high frequency sequences are typically represented by transitions to finer grained, siliceous lithofacies. Contacts may be sharp to gradational and we commonly identify soft sediment deformation, calcite-cemented horizons, and mm-scale silt and sand lag deposits (locally comprised of resistive grains) (Fig. 1.17a-d). Redox proxies (Harris et al., 2018) indicate more reducing conditions just above contacts. Contacts in DS1 are typically sharp while contacts in DS2 and DS3 are commonly gradational. Across contacts, logs display a spike in gamma and a drop in resistivity (Fig. 1.10-1.12).

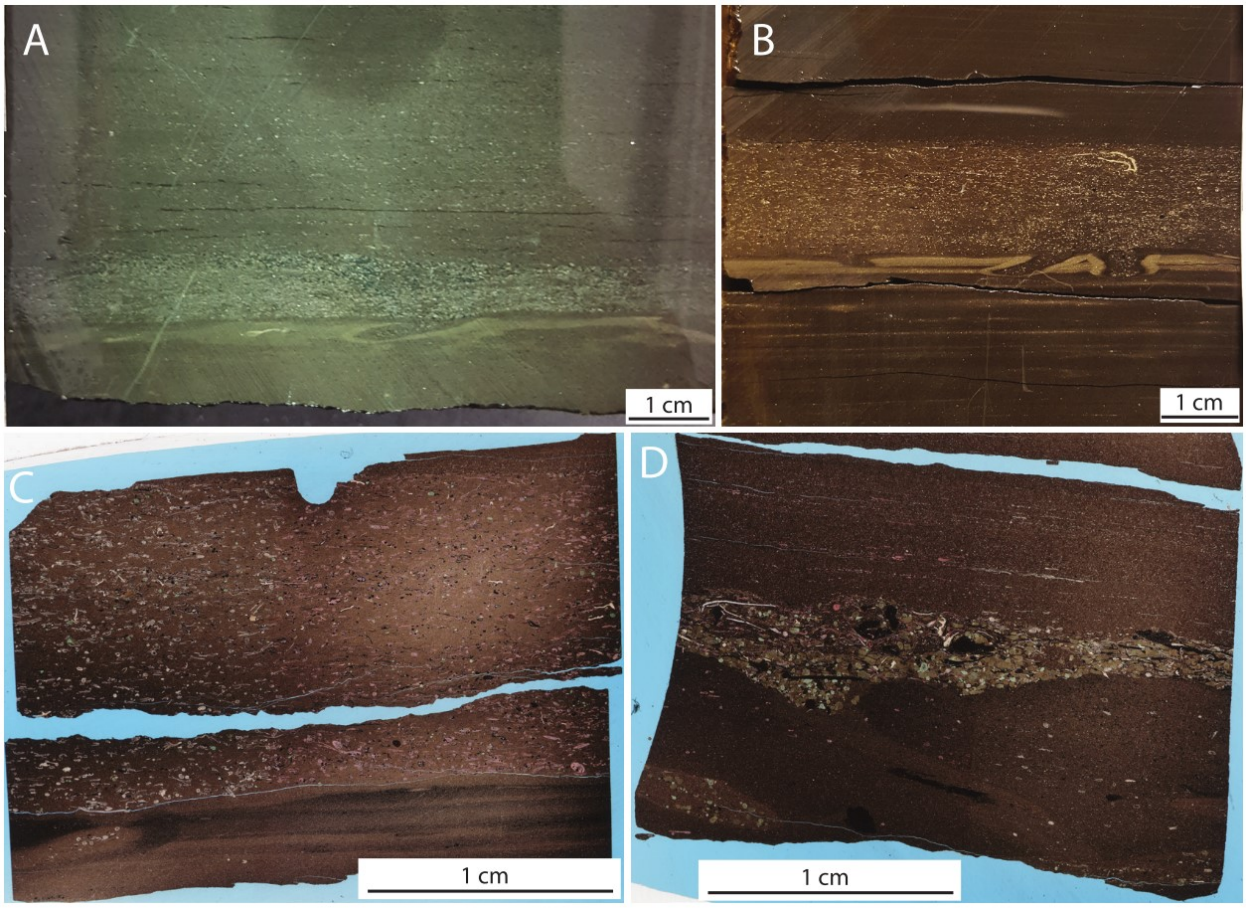

Figure 1.17: Examples of 4th order sequence boundary expressions (P1A) A) soft sediment deformed surface with overlying coarse phosphatic lag (3121.74 m, core 4) B) soft sediment deformed surface with overlying coarse phosphatic lag (2820.44 m, core 1) C) soft sediment deformed surface with overlying glauconitic and phosphatic lag (2820.44 m, core 1) D) soft sediment deformed surface with overlying glauconitic and phosphatic lag (3346.87 m, core 3).

1.5 DISCUSSION

1.5.1 Lithofacies interpretations

LF1: Planar-laminated silt and clay-bearing mudstone

The mud-supported fabric and nature of clay and OM aggregates suggest that lithofacies 1 was primarily deposited by hemipelagic suspension settling. Organic matter aggregates are interpreted as marine snow based on their random distribution throughout the matrix, compacted wispy shape, and diffuse outlines (Macquaker et al., 2010b; Knapp et al., 2017). Marine snow is formed by collisions between particles or by aggregation by organisms (eg: zooplankton grazing), which can accelerate sinking of OM through the water column and plays a significant role in its accumulation and preservation (Kiørboe, 2001; Macquaker et al., 2010b). The interlaminated OM- and pyrite-rich laminae and clay-rich laminae may have been produced by very small scale cyclicity in primary productivity in the water column or variable redox conditions. Clay aggregates in LF1 were interpreted by Knapp et al. (2017) to be deposited by suspension settling from the water column as well, rather than erosion and transport, based on a morphology similar to that of OM aggregates (ovoid shape, whispy/diffuse edges). The common presence of calcite nodules suggests breaks in sedimentation and is consistent with a low energy, low sediment accumulation environment (Boulesteix et al., 2019). The absence or low abundance of burrows, their small diameter (diminution), and low diversity and horizontal nature (low depth of penetration) in LF1 suggest that bottom waters were anoxic to dysoxic (Bromley and Ekdale, 1984; Savrda et al., 1984; Ekdale and Mason, 1988; Gingras et al., 2011). Variable abundance of burrows may be due to episodic sedimentation or variable redox conditions (Gingras et al., 2011).

Secondary processes affecting deposition of LF1 were turbidity currents (depositing turbidites) (Shanmugam, 2000; Konitzer et al., 2014; Lazar et al., 2015; Knapp et al., 2017, Boulesteix et al., 2019) and bottom currents (depositing contourites) (Shanmugam, 2000; Martín-Chivelet et al., 2008; Schieber

and Southard 2009; Rebesco et al., 2014; Knapp et al., 2017; Yawar and Schieber, 2017), suggested by numerous features of grain-supported laminae and thin beds that comprise a small portion of LF1. The local discontinuous laminae comprised of pyritized silt and fossil fragments (LF1A), also described in the Devonian Woodford Shale (Permian Basin) by Hemmesch et al. (2014) and Muskwa Formation (Horn River Basin) by Ayranci et al. (2018), were also likely produced by bottom currents. Bottom currents under low sediment supply may produce migrating barchanoid ripples that can appear as thin discontinuous silt laminae in mud (Yawar and Schieber, 2017). Knapp et al. (2017) interpreted the pyritization of the laminae as the result of slightly increased clay mineral abundance, providing a source of iron. Bottom currents probably reworked sediment that was originally deposited by turbidity currents and other downslope processes (Rebesco et al., 2008; Mulder et al., 2009). LF1A and LF1B are likely transitional between LF1 and LF2.

LF2: Wavy-laminated sand, silt, and clay-bearing mudstone

Numerous thin bedded to laminated coarse silt to fine sand grain layers and sedimentary structures within layers (see LF1) suggest that the dominant processes during deposition of LF2 were bottom water currents (Shanmugam, 2000; Martín-Chivelet et al., 2008; Schieber and Southard 2009; Rebesco et al., 2014) and turbidity currents (Shanmugam, 2000; Konitzer et al., 2014; Lazar et al., 2015; Knapp et al., 2017; Boulesteix et al., 2019). Common soft sediment deformation at the bases of grain-supported laminae suggests high sediment accumulation rates over water-rich muds (Ulmer-Scholle et al., 2014; Boulesteix et al., 2019) or erosion in unlithified sediments (Schieber, 1998a). LF2 is likely the result of downslope deposition of coarser sediment by turbidity currents and reworking of those deposits by bottom currents (Rebesco et al., 2008; Mulder et al., 2009). The absence or low abundance, small diameter, horizontal nature, and low diversity of burrows in LF2 suggest that bottom waters were

anoxic to dysoxic (Bromley and Ekdale, 1984; Savrda et al., 1984; Ekdale and Mason, 1988; Gingras et al., 2011).

LF3: Bioturbated silt and clay-bearing mudstone

The mud-supported fabric and nature of clay and OM aggregates suggest that LF3 was primarily deposited by hemipelagic suspension settling, similar to LF1 (Macquaker et al., 2010b; Knapp et al., 2017). Faint planar laminae may have been produced by very small scale cyclicity in primary productivity in the water column or variable redox conditions. The typically diminutive, low diversity, horizontal to subhorizontal nature of burrows, moderate to intense bioturbation, and rare local in situ benthic macrofossils collectively suggest that bottom waters were dysoxic during deposition of LF3 (Ekdale and Mason, 1988; Gingras et al., 2011). Variable abundance and size of burrows suggests episodic sedimentation or variable redox conditions (Gingras et al., 2011). Rare agglutinated benthic foraminifera would have survived short periods of anoxia (months), but not sustained anoxia (Schieber, 2009), suggesting low dissolved oxygen.

The abundance of pyrite nodules associated with moderate to intense bioturbation suggest a genetic association. Schieber (2002) suggested that pyrite preferentially grows in the mucus matrix left behind by organisms moving through an unconsolidated sediment, where the mucus acts as an initial food source and remains anoxic longer than surrounding sediment for sulfate-reducing anaerobes to thrive. Relatively abundant terrigenous clay in this facies provided a source of reactive iron. The greater abundance of clay in LF3 may also explain the relatively high TOC, despite the moderate to intense bioturbation. Kennedy et al. (2002) and Lalonde et al. (2012) suggested that clay minerals can preserve OM due to their large surface area.

Uncommon thin, grain-supported laminae were likely deposited by bottom currents (Shanmugam, 2000; Martín-Chivelet et al., 2008; Schieber and Southard 2009; Rebesco et al., 2014) and turbidity currents (Shanmugam, 2000; Konitzer et al., 2014; Lazar et al., 2015; Knapp et al., 2017, Boulesteix et al., 2019). Rare thick grain-supported laminae are interpreted as wave-enhanced sediment-gravity-flow beds (WESGF) (Macquaker et al., 2010a; Lazar et al., 2015) (Fig. 1.7a-b), turbidites (Shanmugam, 2000; Konitzer et al., 2014; Lazar et al., 2015; Knapp et al., 2017, Boulesteix et al., 2019) (Fig. 1.7c), and contourites (Shanmugam, 2000; Martín-Chivelet et al., 2008; Schieber and Southard 2009; Rebesco et al., 2014; Knapp et al., 2017) (Fig. 1.7d). WESGFs are produced by storm waves that suspend fine-grained sediment to produce a high-density fluid that flows downslope (Macquaker et al., 2010a; Lazar et al., 2015), capable of moving downslope on gradients as low as 0.5m km^{-1}. Their presence suggests deposition took place on a low gradient slope (Friedrichs and Wright, 2004; Macquaker et al., 2010a).

LF4: Fossiliferous wackestone

LF4 contains features suggesting deposition by turbidity currents, including planar laminae, sharp (possibly erosive) bases, normal grading, sharp to gradational top contacts, and a coarse fossiliferous component (Shanmugam, 2000; Konitzer et al., 2014; Lazar et al., 2015; Knapp et al., 2017; Boulesteix et al., 2019). Knapp et al. (2017) proposed that the high bioclastic content of LF4 is likely due to grain size sorting occurring within turbidity currents. Following Knapp et al. (2017), we suggest that the moderately to intensely bioturbated beds of LF4 are likely due to temporary oxygenation of bottom waters by the downslope advection of oxygenated near-surface water incorporated into sediment gravity flows.

LF5: Nodular Wackestone

We interpret that bottom water conditions during deposition of LF5 were dysoxic to fully oxygenated, based on the moderate to intense bioturbation, moderate diversity, horizontal to vertical nature of burrows, and presence of small and large diameter burrows (Ekdale and Mason, 1988; Gingras et al., 2011). Variable abundance and size of burrows suggests episodic sedimentation or variable redox conditions (Gingras et al., 2011). As in LF3, the form of many pyrite nodules suggests that their formation was related to bioturbation (see LF3; Schieber, 2002).

Sedimentary features in the wackestone in LF5 indicate deposition by turbidity currents, including parallel laminae, sharp (possibly erosive) bottom contacts of laminae and beds, locally gradational top contacts, normal grading, and coarser fossil fragments than surrounding beds (Shanmugam, 2000; Konitzer et al., 2014; Lazar et al., 2015; Knapp et al., 2017, Boulesteix et al., 2019). Fluid-escape structures are consistent with this interpretation, as they commonly form in rapidly deposited silt and sand, aided by normally graded layers in which permeability decreases upward (Lowe and LoPiccolo, 1974; Lowe, 1975; Stromberg and Bluck, 1998; Moretti et al., 2001). Cementation, recrystallization, and bioturbation may have destroyed much of the physical sedimentary structures within silt/sand beds. The nodular form of the wackestone and deformation of mud matrix around them suggests early cementation causing the differential compaction in the water-rich mud (Ulmer-Scholle et al., 2014).

1.5.2 Sequence Stratigraphy

Three scales of cyclicity are identified within the Duvernay Formation: one 2nd order depositional sequence, three 3rd order depositional sequences, and 4th order depositional sequences. These are characterized by systematic core and wireline log patterns: lithology (grain size, composition);

sedimentary structures; facies stacking patterns and abrupt transitions; trace fossil abundance, size and form; presence of benthic macrofossils; geochemistry, including TOC. We follow the definition of a sequence by Catuneanu et al. (2009) as "a succession of strata deposited during a full cycle of change in accommodation or sediment supply". We also follow the four-systems tract model of Hunt and Tucker (1992). Our interpretation expands on the basin scale sequence stratigraphic interpretation of the Duvernay Formation by Knapp et al. (2017; 2019).

3rd Order Depositional Sequences

Depositional sequences 1-3 are interpreted to represent 3rd order depositional sequences, based on a Duvernay depositional timespan of approximately 3 – 4 My and following the cycle hierarchy of Wong et al. (2016). We recognize two distinct intervals within DS1 and DS2 that we interpret as transgressive systems tracts (TSTs) overlain by highstand systems tracts (HSTs). DS3 comprises three distinct intervals that we interpret as a lowstand systems tract (LST) overlain by a TST and HST. TSTs are characterized by an upward trend from typically LF3 bioturbated mudstone to LF1 planar laminated mudstones; HSTs are characterized by an upward trend from LF1 to LF3 and LF4 fossiliferous wackestones, to LF5 nodular wackestones in DS1 and LF2 sandy and silty mudstones in DS2 and DS3; LSTs are dominated by deposition of LF3. Patterns of basin infilling in DS1, DS2 and DS3 are consistent with models of Knapp et al., (2017), in which DS1 corresponds to the platform construction phase of Grosmont Platform development (Fig. 1.18a), and DS2 and DS3 correspond to the early flooded platform phase of deposition (Fig. 1.18b). During the platform construction phase, sediments sourced from the Grosmont Platform prograded perpendicular to the platform (southwest), while during the flooded platform phase of deposition, Grosmont Platform-sourced sediments prograded more strongly

to the southeast (parallel to the platform), possibly due to intensification of platform-parallel currents during the 2nd order HST (Knapp et al., 2017, Knapp et al., 2019).

TSTs

The lower sections of DS1 and DS2 are interpreted to be TSTs due to the abrupt landward shift of facies across SB0 and SB1 from the underlying organic-lean, argillaceous Majeau Lake Formation and LF5 or LF3, respectively, to LF1 or LF3 transitioning to LF1. Similarly, the middle section of DS3 is interpreted as a TST due to the landward shift of facies at its base, from underlying LF3 (locally LF5) to LF1 (locally LF2) or LF3 transitioning to LF1. The TST sections display decreasing grain size, abundance of carbonate sediment, and bioturbation and increasing TOC stratigraphically upwards, typically LF3 transitioning to LF1. TSTs are capped by a thin interval characterized by a spike in gamma log (high uranium on spectral gamma) and high TOC, interpreted as a MFS (Fig. 1.10-1.12).

During a transgression, the increase in accommodation causes shorelines, shelves, and reefs to aggrade and retrograde (backstep), as a result of which the supply of coarse carbonate sediment and clay to the basin decreases (Catuneanu et al., 2011; Wong et al., 2016; Liu et al., 2019). During transgressions in the Frasnian, the Alberta Basin became increasingly sediment starved and enriched in biogenic (radiolarian) silica (Wong et al., 2016). Deposition of OM and biogenic silica in the Duvernay is interpreted by Harris et al. (2018) to increase throughout TSTs due to rising sea levels which allowed for nutrient-rich, deep ocean water to penetrate the Alberta Basin, fueling enhanced bioproductivity. Increasing anoxia is interpreted to be a result of decomposition of OM exceeding supply of oxygen to bottom waters (Harris et al., 2018). Hemipelagic sedimentation and sediment starvation lead to the development of a condensed section, which extends from the upper TST to early HST. The MFS is placed within the condensed section and marks the end of transgression and beginning of highstand normal

regression (Wignall and Maynard, 1993; Pemberton and MacEachern, 1995; Catuneanu et al., 2011; Hammes and Frebourg, 2012). The DS2 MFS coincides with the 2nd order maximum flooding surface of Wong et al, (2016) and marks the greatest depositional extent of distal, oxygen-restricted facies across the basin (Knapp et al., 2017; Knapp et al., 2019) (Fig. 1.2). Fairly uniform TST isopachs (Fig. 1.14b, 1.15b, 1.16c) may be due to dominance of hemipelagic suspension settling. Local thickening of isopachs close to reefs may be due to shedding of material from reefs early in transgression.

HSTs

The upper sections of DS1, DS2, and DS3 are interpreted as HSTs, based on gradually upward increasing grain size, carbonate content, bioturbation, and overall decreasing TOC. The absence of abrupt proximal shifts in facies or regionally mappable erosional surfaces between this section and the underlying TST indicates this regressive sequence is not a lowstand systems tract.

Increasing carbonate content and grain size upward through the HSTs likely represents shedding of reefs and platforms during highstand normal regression, as it is the time of greatest carbonate sediment accumulation in the basin (Schlager et al., 1994; Hammes and Frebourg, 2012). The transition to more abundant and diverse, larger and more vertical burrows upward describes the transition from greater relative SL rise and resulting oxygen-poor, mud-dominated settings to slower relative SL rise, more oxygenated settings, and more arenaceous substrates (Pemberton and MacEachern, 1995). Deposition of OM is interpreted to decrease throughout HSTs with increasing clastic dilution and decreasing nutrient flux after transgression (Creaney and Passey, 1993; Harris et al., 2018; Liu et al., 2019).

Thinning of the DS1 HST from the northeast to the southwest in the study area (Fig. 1.14c) is likely due to growth of the Grosmont Platform slope into the basin (Knapp et al., 2017) (Fig. 1.18a). This

interpretation is supported by progradation of carbonate-rich facies (LF5) from the northeast to southwest in the study area throughout the DS1 HST (Knapp et al., 2019). Grosmont Platform slope growth during DS1 is also supported by the presence of WESGF deposits, deposited ahead of (stratigraphically lower than) the prograding carbonates, which suggest deposition on a low gradient slope (Friedrichs and Wright, 2004; Macquaker et al., 2010a). Reefs in the basin were steep sided (>10°), while platforms had low gradient slopes (<1°), which may have allowed for development of WESGFs (Stoakes, 1980; Wong et al., 2016).

The DS2 and DS3 HSTs thicken from the northeast to southwest in the study area (Fig. 1.15c, 1.16D). Thinning of the isopachs to the northeast may be the result of reworking by bottom currents travelling along bathymetric contours on the Grosmont slope and sediment bypass by turbidity currents downslope (Fig. 1.18b) (Andrichuk, 1958A; McCrossan, 1961; Mountjoy, 1980; Stoakes, 1980; Potma et al., 2001; Knapp et al., 2019). This interpretation is supported by the dominance of LF2 and LF1B in the northeast section of the study area in DS2 and DS3. Thickening of isopachs to the southwest in the study area was probably enhanced by shedding of carbonate material from reefs, supported by the presence of LF5 nodular wackestone in the upper part of the DS3 HST in cores located close to reefs (eg: core #6, 7). Smaller, less diverse, and less abundant burrows in the HST of DS2 compared to DS1 and DS3, along with redox proxies, suggest more persistent reducing conditions, consistent with the interpretation that DS2 was deposited at the time of highest relative sea level (Knapp et al., 2017; Harris et al., 2018; Knapp et al., 2019).

LSTs

The lower section of DS3 is interpreted as an LST, based on an abrupt basinward shift in facies across SB2 (a regionally mappable erosional surface), high clay content (in contrast to the basal sections

of DS1 and DS2), low carbonate content, low abundance of silt and sand grains, low TOC, and high bioturbation. The top of the LST in DS3 is interpreted as a MRS, which marks the transition from lowstand normal regression to transgression (Helland-Hansen and Martinsen, 1996; Catuneanu et al., 2011). The MRS in DS3 is commonly indicated by an increase in resistivity (Fig. 1.10-1.12).

During lowstand normal regressions, subaerial exposure of platform and reef tops commonly causes carbonate production to shut down (Catuneanu, 2006; Catuneanu et al., 2011; Wong et al., 2016) reducing carbonate sediment delivery and typically increasing detrital siliciclastic sediment to the basin (Schlager et al., 1994; Catuneanu, 2006; Hammes and Frebourg, 2012). Increased bioturbation and decreased TOC through the LST (Fig. 10-12) are interpreted to result from the inability of deep nutrient-rich ocean water to penetrate the basin during low relative sea level, decreasing bioproductivity and resulting in increased bottom water oxygenation (Harris et al., 2018). LF5 nodular wackestone present in the LST of cores near the reefs in the study area is likely carbonate sediment shed from reefs and transported to the basin by sediment gravity flows or mass wasting processes (Handford and Loucks, 1993). Thinning of the LST isopach away from reefs (Fig. 1.16b) may be explained by greater accumulation of sediment closer to degrading reef margins and possibly by greater compaction of more clay-rich sediments farther from reefs.

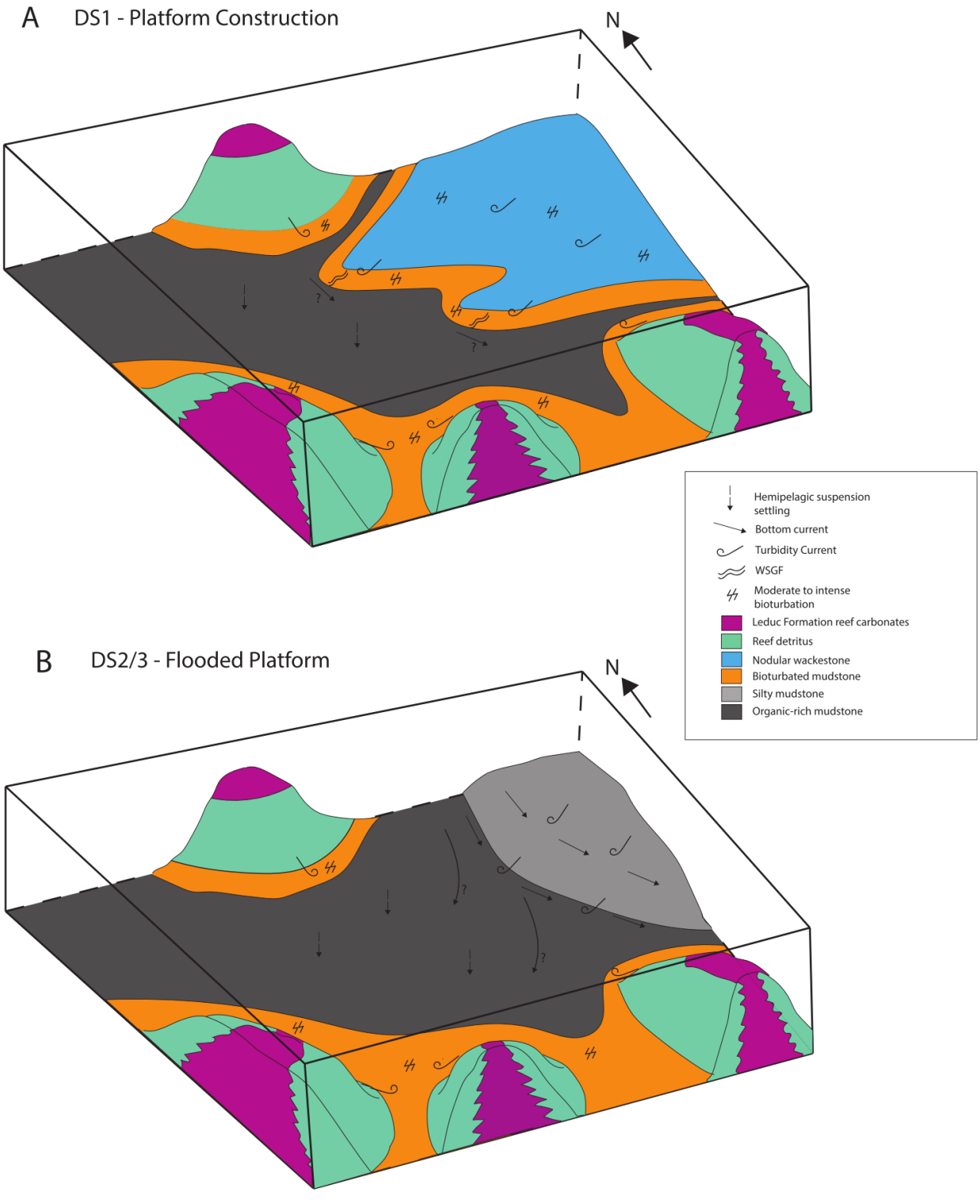

Figure 1.18: Depositional model for the Duvernay Formation in the Kaybob Area during A) Grosmont Platform construction stage and B) Flooded Grosmont Platform stage (*after* Knapp et al., 2017).

4th Order Depositional Sequences

Within high frequency depositional sequences, upward stratigraphic trends of increasing grain size, increasing carbonate sediment and cement, laminae thickness, increasing bioturbation, increasing fossil fragment abundance, including in-situ benthic macrofossils, and decreasing TOC and reducing conditions likely represent regression. Knapp et al. (2017) proposed that intervals of similar thickness and internal stacking patterns indicate deposition during regression and represent parasequences. We interpret these units as 4th order depositional sequences, as they represent full cycles of accommodation change, incorporating positive and negative accommodation of sediments (Catuneanu et al., 2011). We suggest that the regressive intervals of these units represent highstand normal regression, as these are times of greatest carbonate sediment accumulation in the basin (Schlager et al., 1994; Hammes and Frebourg, 2012). Local thin intervals above sequence contacts in DS2 and DS3 displaying decreasing grain size, abundance of carbonate sediment and bioturbation and increasing TOC stratigraphically upwards are interpreted as transgressive intervals and represent part of a TST.

Contacts between 4th order sequences (Fig. 1.17) may represent pauses in sedimentation during forced regression, lowstand conditions, and transgression. Both exposure of platform and reef tops from relative sea level fall or increased accommodation from relative sea level rise may cause sediment starvation in the basin (Catuneanu, 2006; Catuneanu et al., 2011). Soft sediment deformed surfaces and lags of resistive grains at contacts suggest erosion and reworking during sediment starvation (Glenn and Arthur, 1990; Bohacs and Schwalbach, 1992; Cattaneo and Steel, 2003; Wignall and Maynard, 1993; Schieber, 1998a; Scasso and Castro, 1999; Abouelresh and Slatt, 2012; Li and Schieber, 2015). Cemented horizons at contacts also suggest a pause in sedimentation and support the interpretation of sediment starvation (Macquaker et al., 2007). We suggest that contacts between 4th order sequences represent the amalgamation of the basal surface of forced regression (BSFR), SB, LST, MRS, and possibly MFS. The change from typically sharp 4th order sequence boundaries in DS1 to typically gradational boundaries in

DS2 and DS3 (and local overlying transgressive intervals) may be related to the transition from 2nd order transgression to 2nd order highstand. Knapp et al. (2019) noted a similar change in the nature of 4th order contacts and suggested that greater sediment starvation at flooding surfaces during 2nd order transgression formed sharp hiatal surfaces prone to cementation. Increased clastic sedimentation rates during the 2nd order highstand inhibited the development of sharp, cemented, hiatal surfaces.

1.5.3 An appreciation of the significance of data density

Many past studies on mudstones have applied well or outcrop data sets with over 10 km spacing between data points (eg: Schieber, 1998a; Ver Straeten et al., 2011; Hammes and Frebourg, 2012; Hammes et al., 2013; Aryanci et al., 2018). Studies of this nature assume continuity of mudstone depositional environments and features at km scales. This study uses <4 km core spacing and <1 km wireline spacing of wells to map lithofacies and sequence stratigraphic architecture at high resolution. Our findings suggest that core expression of sequence boundaries and facies composition of systems tracts can change drastically at the spacing of our cores with distance from sediment sources and with bottom topography. Similarly, the wireline expression of 3rd and 4th order sequence stratigraphic surfaces and systems tracts can change significantly at the spacing of our wireline wells. The high-density data set in our study area made it possible to correlate 3rd and 4th order sequence stratigraphic surfaces across the study area with a high degree of certainty. We were also able to interpret major sources of sediment and determine geographic extent of topographical features during different stages of Duvernay Formation deposition from geographic distribution of facies and variations in systems tract isopachs (eg: Grosmont platform slope, Leduc Reefs).

1.6 CONCLUSIONS

The Duvernay Formation, a Frasnian-age organic-rich black shale, was deposited in the Kaybob area in a basinal setting, flanked by carbonate reefs and at the northeastern margin, at the toe of a large carbonate platform. This setting, combined with a high resolution data set including 11 long drill cores, enables us to map and interpret facies distributions as functions of paleogeography and changes in relative sea level and to develop a detailed sequence stratigraphic model that encompasses 2nd to 4th order sea level cycles.

Lithofacies in the Duvernay Formation were deposited by a combination of suspension settling, sediment-gravity flows, and bottom currents under anoxic to fully oxygenated bottom water conditions. Distribution of lithofacies were strongly affected by proximity to sediment sources, bottom topography, and sea level cyclicity. Coarse, carbonate-rich, bioturbated, and organic-poor facies are common close to large carbonate platforms and reefs; bottom current and sediment gravity flow deposited facies are common on the slopes of large carbonate platforms; hemipelagic deposited, fine grained, biosiliceous, organic-rich facies are common in distal areas of the basin. Transgressive deposits are characterized by increasingly fine-grained, biosiliceous, organic-rich facies; highstand deposits by increasingly coarse-grained, carbonate-rich, bioturbated, organic-poor facies; lowstand deposits by detrital clay-rich, bioturbated facies.

A high-density data set of wells and cores make it possible to correlate 3rd and 4th order sequence stratigraphic surfaces across the study area with a high degree of certainty. Major sources of sediment and geographic extent of topographical features during different stages of deposition were also determined with a high degree of certainty due to the high-density data set.

Chapter 2 : The expression of sequence boundaries in cores from the Duvernay Formation mudstone, Kaybob area, Alberta, Canada

2.1 INTRODUCTION

Sequence stratigraphic analysis is applied in hydrocarbon exploration of mudstone formations to predict the occurrence of important rock properties at multiple scales, including total organic carbon (TOC), porosity and permeability, and brittleness. Interpretation of stratigraphic sequences in mudstone is made difficult by the subtle effects of sea level change on distal sediments. In addition, the identification of sequence stratigraphic surfaces is particularly challenging in fine-grained sediments that are deposited by diverse processes including hemipelagic suspension settling, sediment gravity flows and other mass transport processes, and reworked by bottom currents (Catuneanu et al., 2011). As a result, many past studies of mudstone stratigraphy have focused on interpreting transgressive-regressive (T-R) cycles (eg: Ver Straeton et al., 2011; Abouelresh and Slatt, 2012; Hemmesch et al., 2014; Dong, 2016; Shaw et al., 2017). Nonetheless, some studies have applied a surface-based approach to the sequence stratigraphic analysis of mudstones (eg: Wignall and Maynard, 1993; Schieber, 1998a; Williams et al., 2001; Schieber and Riciputi, 2004; Hammes and Frebourg, 2012; Bond et al., 2013; Knapp et al., 2017; Wong et al., 2016; Ayranci et al., 2018; Knapp et al., 2019).

Four surfaces are important in developing sequence stratigraphic interpretations of sedimentary successions: 1) sequence boundaries (SB), 2) maximum regressive surfaces (MRS), 3) maximum flooding surfaces (MFS), 4) and basal surfaces of forced regression (BSFR) (Hunt and Tucker, 1992; Catuneanu et al., 2011). Sequence boundaries are subaerial surfaces of erosion and equivalent basinward submarine erosion surfaces and correlative conformities (CC), formed at the end of forced regression (Hunt and Tucker, 1992; Plint and Nummedal, 2000). In carbonate reefs and shallow water platform deposits, sequence boundaries are typically expressed as subaerially exposed surfaces with paleokarst horizons

(Hunt and Tucker, 1992; Bover-Arnal et al., 2009; Chow and Wendte, 2010; Wong et al., 2016). In deep water deposits, the MRS and MFS are typically cryptic surfaces while the SB and BSFR can have physical expression (Hunt and Tucker, 1992; Ayranci et al., 2018; Knapp et al., 2019).

Previous studies of sequence boundaries in basinal mudstones have focused on the presence of correlative conformities of large lateral extents, erosional surfaces, lag deposits, local boring, and pronounced lateral offsets of facies. However, these studies have primarily been aimed at identifying sequences boundaries rather than considering the suite of processes that formed them, and in fact there is little consensus on the latter subject. Among the processes suggested for the formation of sequence boundaries and overlying coarse deposits in mudstones are erosion and reworking during relative sea level fall (Schieber, 1998a; Schieber, 2004; Ayranci et al., 2018; Knapp et al., 2019), erosion during the subsequent transgressiion (Baird and Brett, 1991), or both (Scasso and Castro, 1999; Macquaker et al., 2007; Hammes and Frebourg, 2012; Li and Schieber, 2015; Knapp et al., 2019).

Our analysis of the Upper Devonian (Frasnian) Duvernay Formation in the Western Canada Sedimentary Basin expands on initial descriptions of sequence boundaries in the Duvernay by Knapp et al. (2019) to consider their characteristics and their spatial and stratigraphic variation in more detail. We map 2nd and 3rd order sequence stratigraphic surfaces at a greater resolution, taking advantage of the large database of wells available in the Kaybob area of west-central Alberta. This area, although relatively small (roughly 14,000 km^2), includes several wells with high quality long cores, and the presence of reefs and basinal areas enables us to analyze changes in the character of surfaces from proximal to distal areas. Our study identifies a set of features characteristic of mudstone sequence boundaries and describes how they vary stratigraphically and geographically, and from these features, we interpret the processes responsible for the formation of these surfaces and overlying beds in the Kaybob area.

2.2 GEOLOGIC SETTING

The Duvernay Formation was deposited during the Late Devonian (Frasnian) Period, at a time of greenhouse climate (Read 1995; Lehrmann and Goldhammer, 1999), high global sea level (Johnson et al., 1985), and major black shale deposition across North America (eg: Muskwa Formation (Horn River Basin), New Albany Shale (Illinois Basin), Woodford Shale (Permian Basin), and the Chattanooga and Rhinestreet shales (Appalachian Basin)) (Campbell, 1946; Schieber, 1998a; Lash and Blood, 2004; Ferri et al., 2011; Hemmesch et al., 2014). The Duvernay Formation was deposited in the Alberta Basin, part of the Western Canada Sedimentary Basin, on the passive western margin of North America (Weissenberger, 1994). A large epicontinental sea covered much of what is now western Canada and the area was dominated by carbonate platforms and reefs (Fig. 2.1). Basinal shales were deposited in the inter-reef areas in Alberta, marine shales were deposited to the northeast in British Columbia and Northwest Territories, and dolomites and evaporites were deposited to the southeast in Saskatchewan and Manitoba (Switzer et al., 1994; Weissenberger, 1994).

The Duvernay Formation is the organic-rich, basinal shale equivalent to the Middle Leduc Formation pinnacle reefs (Switzer et al., 1994; Fig. 2.2), deposited between large bounding carbonate platforms to the northeast and south, and clusters of reefs to the north and west. Rivers from the north transported terrigenous siliciclastics sourced from the ancestral Canadian Shield into the basin (Wong et al., 2016). Currents entered the basin from the present-day northeast and distributed sediment in a clockwise direction within the basin (Andrichuk, 1958A; McCrossan, 1961; Mountjoy, 1980; Stoakes, 1980; Potma et al., 2001; Harris et al., 2018). Upwelling along the western edge of North America drove deep, nutrient-rich water into and across the basin in a southeast direction (Golonka et al., 1994; Harris et al., 2018).

Major structural features of the Frasnian Alberta Basin included the Peace River-Athabasca Arch, West Alberta Ridge, Rimbey Arc, and Meadow Lake Escarpment (Fig. 2.1). The Peace River Arch was an exposed landmass fringed by Leduc reefs to the northwest of the Alberta basin (Dix, 1990). The West Alberta Ridge was a site of major Leduc Formation reef development along the western edge of the basin (Switzer et al., 1994). The Rimbey-Meadowbrook Trend was a northeast to southwest oriented paleobathymetric high and a site of Leduc reef growth. During the Frasnian, it divided the Alberta Basin into the East and West Shale Basins (Switzer et al., 1994; Rokosh et al., 2012). The Meadow Lake Escarpment is a pre-Devonian structural feature, represented by the margin of Killiam Barrier Reef during the Frasnian (Oldale and Munday, 1994), that formed the eastern edge of the East Shale Basin and the easternmost extent of Duvernay deposition (Switzer et al., 1994). Subsidence within the basin was slow during Cooking Lake Formation deposition, increased dramatically during Duvernay deposition, then slowed during middle to upper Ireton deposition (McCrossan, 1961; Wonfor and Andrichuk, 1953) (Fig. 2.2). In Alberta, Woodbend Group strata dip to the southwest and increase in dip to the west due to Laramide Orogeny downwarping (Switzer et al., 1994; Hauk et al., 2009; Preston et al., 2016).

The Duvernay Formation was deposited during the late transgression to early highstand of a 2nd order depositional sequence that spanned the Late Givetian to the Frasnian (Fig. 2.2) (Potma et al., 2001; Wong et al., 2016). The Duvernay occurs within Conodont Montagne Noire Zones 6 through 11 *of* Klapper (1988) (Wong et al. 2016), which indicates deposition during a timespan of approximately 3 – 4 million years. The Duvernay is part of the Woodbend Group (Fig. 2.2) and conformably overlies the upper Majeau Lake Formation shale (Lower Leduc-equivalent), except in the southernmost areas of the East and West Shale Basins where the Duvernay was deposited directly on Cooking Lake carbonates (Switzer et al., 1994). The lower Ireton Formation (Upper Leduc equivalent) conformably overlies the Duvernay throughout most of the basin (Switzer et al., 1994). The thickness of the Duvernay is typically 70 m but ranges from 2 to 99 m (Preston et al., 2016; Knapp et al., 2017; Knapp et al., 2019), typically

thickest near Leduc reefs and within embayments, where it contains more reef-derived material, and thinner basinward (Switzer et al., 1994). Andrichuck (1961) informally divided the Duvernay Formation into a lower shale, middle carbonate, and upper shale members, terminology that is still applied by oil and gas companies. The Duvernay Formation is composed of siliceous to calcareous, organic-rich shale, and limestone (Switzer et al., 1994; Knapp et al., 2017). Duvernay sediments of the West Shale Basin are significantly more siliceous than those of the East Shale Basin (Harris et al., 2018) and become less calcareous to the west (Rokosh et al., 2012; Preston et al., 2016).

The Kaybob Area (Fig. 2.1) is located centrally within the West Shale Basin, between the Sturgeon Lake reef to the north and the Simonette, Bigstone, and Windfall reefs to the south (Fig. 2.1). Present day burial depths to the top of the Duvernay Formation increase from northeast to southwest, and thermal maturity shows a corresponding increase from immature to dry gas window (Preston et al., 2016).

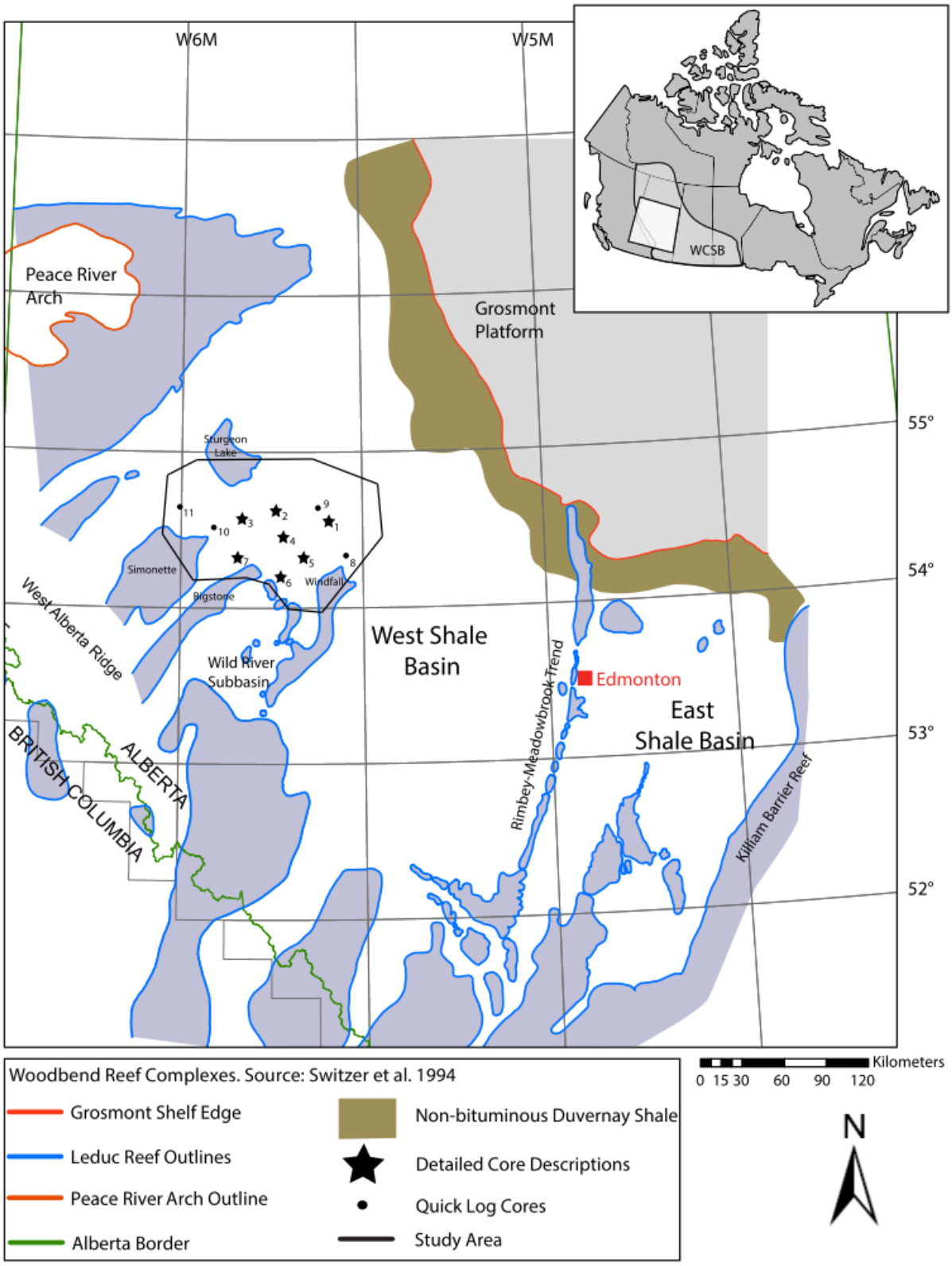

Figure 2.1: Paleogeography of the Alberta Basin in the Late Devonian. Kaybob Area outlined in black. (Modified *from* Knapp et al., 2017)

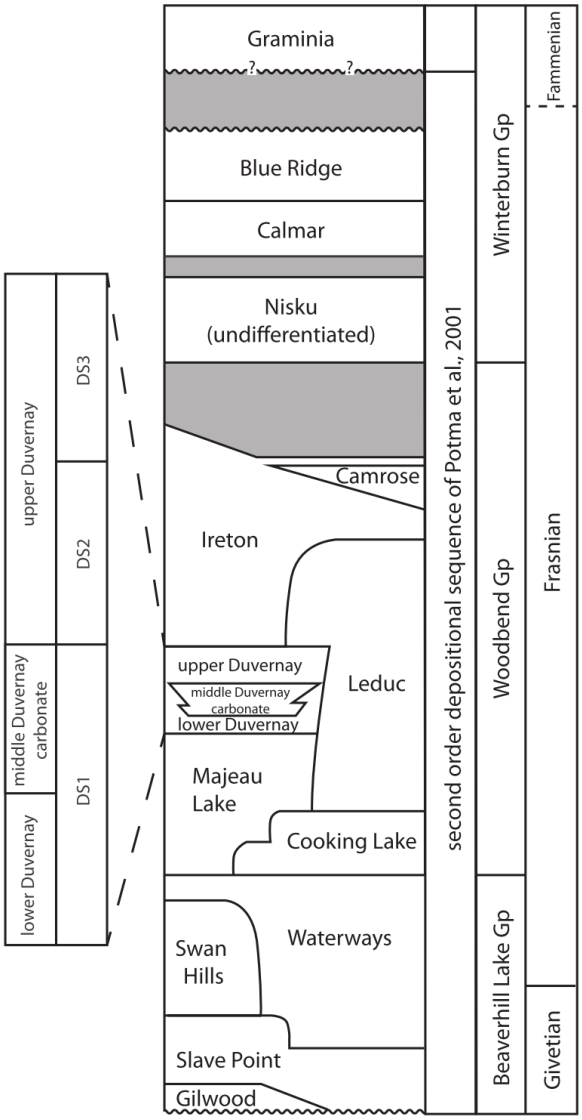

Figure 2.2: Fig. 2. Upper Devonian (Frasnian) stratigraphy, Alberta Basin. (*from* Knapp et al., 2017)

2.3 METHODS

Long, slabbed drill cores from seven wells were examined and described in detail; cores from an additional four wells were logged in less detail (Fig. 2.1; Table 2.1). Cores were chosen for recovery, quality, length of Duvernay penetration, and geographic location in the Kaybob area. Cores range from 54 to 79 m in length, and the length of the Duvernay portion of the cores ranges from 47 to 68 m (total logged core: 445 m; total logged Duvernay core: 366 m). Macroscopic features were recorded during core logging at a 1:10 scale, including sedimentary structures, fabrics, colour, trace and body fossils, mineralogy, cement type and abundance, pyrite abundance and form, and the abundance and fill of natural fractures. Calcium carbonate abundance was estimated using 10% hydrochloric acid.

A total of 176 extra thin (20 µm), bed-normal thin sections of important features, fabrics, contacts, and representative lithofacies were taken from the 11 cores. Half of each thin section was stained for calcite and iron-rich carbonate. Thin sections made for this study are available at the Alberta Energy Regulator Core Research Center in Calgary. Centimeter to mm scale features were observed in thin section using a Nikon Super Coolscan 5000 ED scanner. Millimeter to µm scale features were observed using a Zeiss Axio Scope A1 petrographic microscope and camera.

Lithofacies were identified based on the sedimentological analysis of the cores and thin sections. Core descriptions were correlated to petrophysical well logs. Sequence stratigraphic surfaces were identified by abrupt facies transitions in core and log signatures and compared to transitions in geochemical data. Stratigraphic and sequence stratigraphic surfaces were correlated across petrophysical well logs in the Kaybob area using Petrel software to produce cross sections and a regional map of the formation (Fig. 2.3).

Table 2.1: Name, location, and length of Duvernay cores.

Map #	Well name	UWI	Detailed core log	Thin section samples	Geochem samples	Length of Duvernay (m)
1	ATH HZ TWOCK	100/04-21-064-16W5/00	Y	Y	N	46.76
2	ATH HZ KAYBOB	100/04-32-064-20W5/00	Y	Y	N	46.48
3	SCL HZ 102 McKinley	100/04-19-064-22W5/00	Y	Y	Y	48.26
4	SCL HZ KAYBOB	100/02-22-063-20W5/00	Y	Y	Y	52.85
5	TQN FOXCK	103/16-25-061-19W5/00	Y	Y	N	55
6	ROGCI HZ KAYBOBS	100/06-16-060-20W5/00	Y	Y	N	67.82
7	ATH HZ SAXON	100/01-28-061-23W5/00	Y	Y	N	48.7
8	Bounty Wind	100/11-34-061-15W5/00	N	Y	N	45.1
9	APL(98) Kaybob	100/14-09-065-17W5/00	N	Y	N	18
10	Murphy Simon	100/01-12-064-25W5/00	N	Y	N	54
11	CVE HZ KARR	102/09-25-065-27W5/00	N	Y	N	28.7

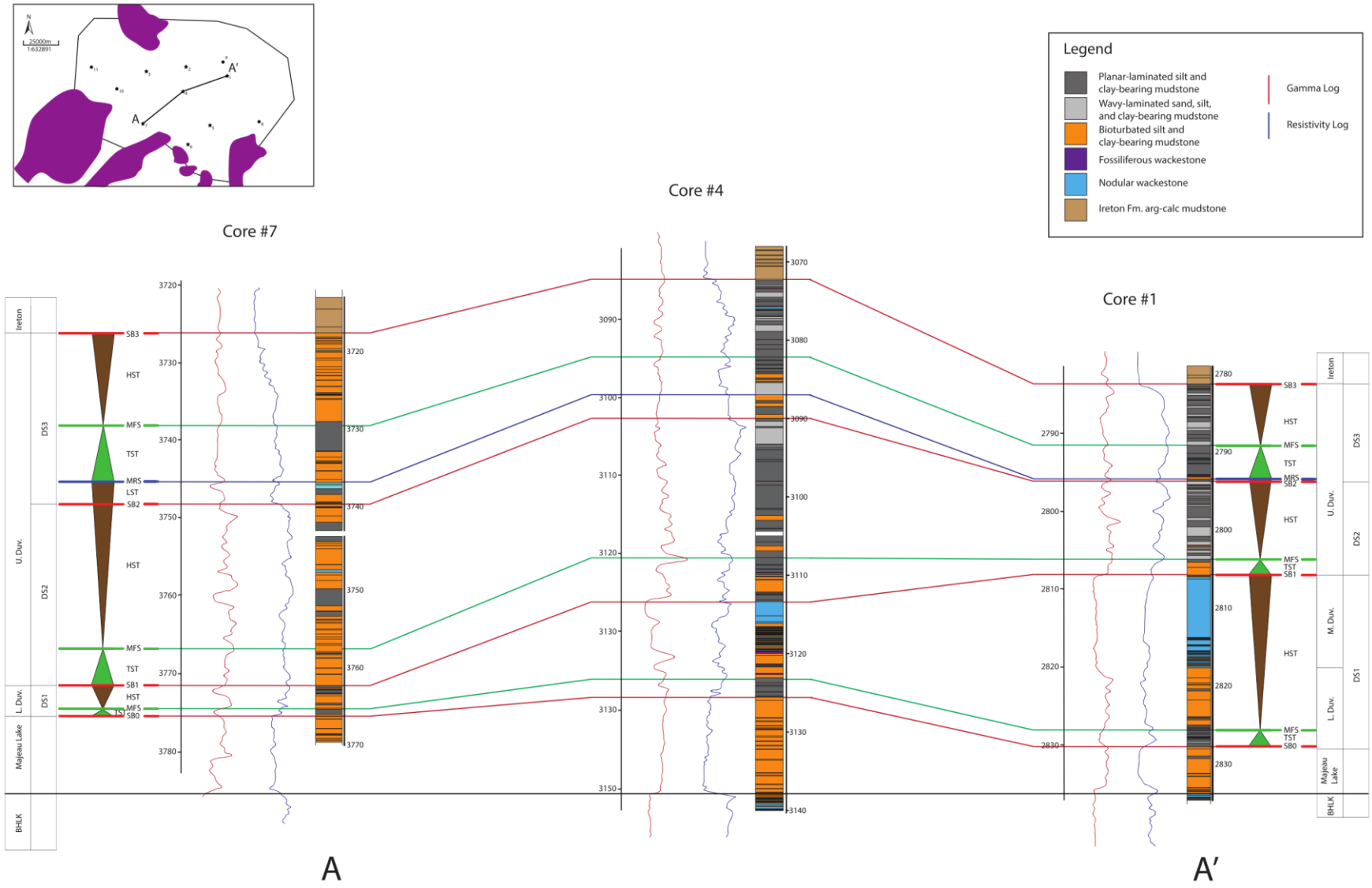
Legend
Planar-laminated silt and clay-bearing mudstone
Wavy-laminated sand, silt, and clay-bearing mudstone
Bioturbated silt and clay-bearing mudstone
Fossiliferous wackestone
Nodular wackestone
Ireton Fm. arg-calc mudstone
Gamma Log
Resistivity Log
Core #7
Core #4
Core #1
A
A′
Ireton
U. Duv.
L. Duv.
Majeau Lake
BHLK
DS3
DS2
DS1
M. Duv.
SB3
MFS
TST
MRS
LST
SB2
HST
SB1
SB0

Figure 2.3: Cross section of study area.

2.4 REVIEW OF LITHOFACIES AND SEQUENCE STRATIGRAPHY

We briefly review lithofacies and stratigraphic sequences present in the Duvernay Formation in the Kaybob area. These are described and interpreted in more detail in Chapter 1. Five lithofacies (Table 2.2) are recognized in Duvernay core in the Kaybob area, defined by distinctive associations of composition, grain size, sedimentary structures, bioturbation, and cement. Lithofacies are listed in order of highest to lowest average TOC.

Lithofacies 1 (LF1) comprises organic-rich, siliceous-calcareous, faintly planar laminated mudstone (Fig. 2.4a). LF1 is interpreted to have been dominantly deposited by hemipelagic suspension settling, based on the random distribution, compacted wispy shape, and diffuse outlines of organic matter and clay aggregates (Macquaker et al., 2010b; Knapp et al., 2017). The absence or low abundance of small diameter, horizontal and low diversity burrows indicate that bottom waters were anoxic to dysoxic (Bromley and Ekdale, 1984; Savrda et al., 1984; Ekdale and Mason, 1988; Gingras et al., 2011). Occasional grain-supported, planar to wavy, silt and sand laminae display normal grading, inverse grading, and current ripples, suggesting that turbidity currents and bottom currents were secondary processes affecting deposition (Shanmugam, 2000; Martín-Chivelet et al., 2008; Schieber and Southard 2009; Konitzer et al., 2014; Rebesco et al., 2014; Lazar et al., 2015; Knapp et al., 2017; Yawar and Schieber, 2017; Boulesteix et al., 2019).

LF2 consists of silt and sand interlaminated with dark-grey mud, the latter similar to LF1 (Fig. 2.4b). Abundant planar to wavy grain-supported laminae, normal and inverse grading, and current ripples suggest deposition predominantly by turbidity currents and bottom currents. The absence or low abundance, small diameter, horizontal nature, and low diversity of burrows in LF2 indicate that bottom waters were anoxic to dysoxic.

LF3 is composed of siliceous to calcareous, moderately to intensely bioturbated mudstone (Fig. 2.4c). The mud-supported fabric and nature of clay and organic matter aggregates suggest that LF3 was primarily deposited by hemipelagic suspension settling, similar to LF1. The typically small diameter, low diversity, horizontal to subhorizontal nature of burrows and the presence of local *in situ* benthic macrofossils suggest that bottom waters were dysoxic (Ekdale and Mason, 1988; Gingras et al., 2011). Uncommon grain-supported, planar to wavy, silt and sand laminae displaying normal grading, inverse grading, and current ripples suggest that deposition by turbidity currents, bottom currents, and wave-enhanced sediment gravity flows were secondary processes, similar to LF1.

LF4 consists of massive to faintly planar laminated silt and sand grains in a matrix of argillaceous to calcareous mud (Fig. 2.4d). Sharp bases, normal grading, sharp to gradational top contacts, and a coarse fossiliferous component in coarser laminae suggest deposition by turbidity currents (Shanmugam, 2000; Konitzer et al., 2014; Lazar et al., 2015; Knapp et al., 2017; Boulesteix et al., 2019). Moderate to intense bioturbation may be associated with temporary oxygenation of bottom waters by the downslope movement of sediment gravity flows.

LF5 is composed of wackestone nodules in an argillaceous to calcareous mud (Fig. 2.4e). Abundant, large diameter, diverse, and vertical burrows suggest the presence of fully oxygenated bottom waters during deposition (Ekdale and Mason, 1988; Gingras et al., 2011). Parallel laminae, sharp (possibly erosive) bottom contacts of laminae and beds, locally gradational (diffuse) top contacts, normal grading, increasing upward bioturbation, and fluid escape structures are consistent with deposition by turbidity currents (Lowe and LoPiccolo, 1974; Lowe, 1975; Stromberg and Bluck, 1998; Shanmugam, 2000; Moretti et al., 2001; Konitzer et al., 2014; Lazar et al., 2015; Knapp et al., 2017, Boulesteix et al., 2019). This is the dominant facies comprising the middle Duvernay member carbonate.

Facies stacking patterns were used to identify three 3rd order depositional sequences (DS1-3), bounded by 4 sequence boundaries (SB0-3) (Fig. 2.3). We follow the definition of a sequence by Catuneanu et al. (2009) as "a succession of strata deposited during a full cycle of change in accommodation or sediment supply". We also follow the four-systems tract model of Hunt and Tucker (1992), in which a sequence boundary represents the correlative conformity marking the end of forced regression. The 3rd order maximum flooding surface (MFS) in DS2 coincides with the MFS of the 2nd order depositional sequence of Potma et al. (2001). DS1 and DS2 are interpreted to comprise transgressive systems tracts (TSTs) overlain by highstand systems tracts (HSTs). DS3 is interpreted to comprise a lowstand systems tract (LST) overlain by a TST and HST. TSTs are characterized by increasing abundance of LF1 planar laminated mudstones upward; HSTs are characterized by an upward stratigraphic trend from LF1 to LF3 bioturbated mudstones and LF4 fossiliferous wackestones, to LF5 nodular wackestones in DS1 and LF2 sandy and silty mudstones in DS2 and DS3; LSTs are dominated by deposition of LF3. Patterns of basin infilling in DS1 are related to the construction phase of Grosmont Platform deposition (Knapp et al., 2017; Chapter 1 Fig. 1.18A), where platform- sourced sediment built out into the basin. DS2 and DS3 are best explained by the early flooded platform phase of deposition (Chapter 1 Fig. 1.18B), when the basin was dominated by hemipelagic deposition of mud.

Table 2.2: Lithofacies characteristics.

	LF1	LF2	LF3	LF4	LF5
Name	Planar-laminated silt and clay-bearing mudstone	Wavy-laminated sand, silt, and clay-bearing mudstone	Bioturbated silt and clay-bearing mudstone	Fossiliferous wackestone	Nodular wackestone
Colour	Dark grey	Medium to light grey laminae in dark grey matrix	Medium dark to dark grey	Medium grey	Medium light grey nodules in medium grey matrix
Bedding	Planar laminae	Wavy, lenticular, planar laminae	Massive, wispy/discontinuous, planar laminae	Planar, wavy/wispy laminae	Nodular, planar bedded
Other Sed. Structures	Normal grading, inverse grading, wavy laminae, pinching/swelling, convergence/divergence, current ripples, low angle cross laminae, silt lenses	Normal grading, Inverse grading is also present, pinching/swelling, convergence/divergence, current ripples	Normal grading, inverse grading, wavy laminae, current ripples	Normal grading	(Rare) Normal grading, inverse grading
Grain Size	Silt and clay-bearing mudstone	Sand, silt, and clay-bearing mudstone	Silt and clay-bearing mudstone	Wackestone	Wackestone
Cement	Calcite, silica, pyrite	Dolomite, calcite	Calcite, pyrite	Calcite	Calcite, pyrite
Bioturbation Index	0-1	0-2	2-4	2-4	3-4
Common Taxa	Styliolinids, brachiopods, ostracods, ammonoid anaptychi, very rare conodont jaw elements and radiolarians	Brachiopods, ostracods, styliolinid tests, rare conodont elements	Brachiopods, bivalves, ostracods, styliolinids, tentaculitids, rare arthropod fragments, gastropods, crinoid fragments, radiolarians, possible stromatoporoids, possible agglutinated benthic foraminifera	Styliolinids, ostracods, brachiopods, rare conodont elements	Brachiopods, ostracods, styliolinids
Average TOC	2.73	2.64	2.44	2.33	0.58

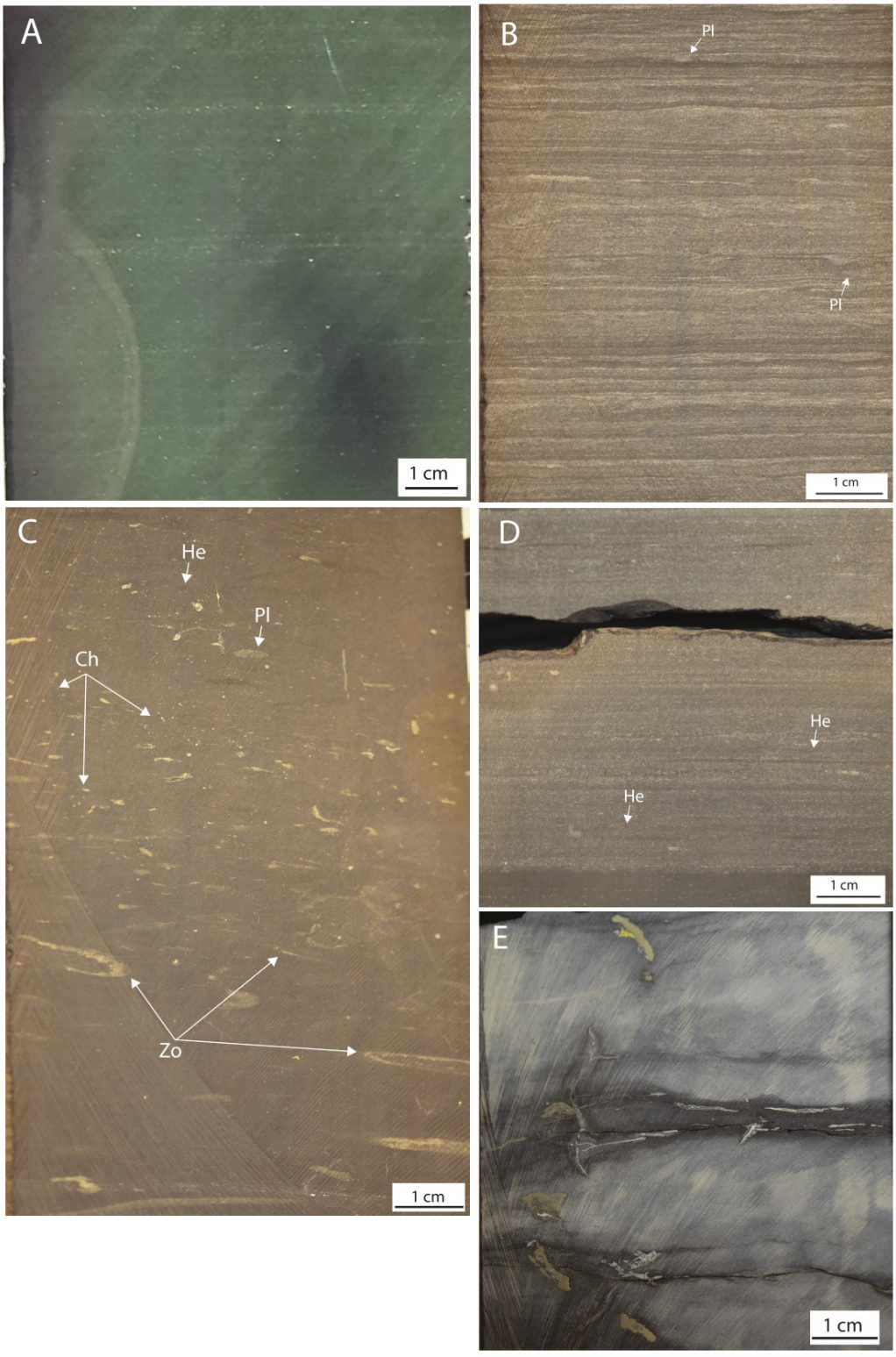

Figure 2.4: Photo plate summary of lithofacies. A) LF1 planar-laminated silt and clay-bearing mudstone. B) LF2 wavy-laminated sand, silt, and clay-bearing mudstone. C) LF3 bioturbated silt and clay-bearing mudstone.

D) LF4 fossiliferous wackestone. E) LF5 nodular wackestone. Pl = *Planolites*, Ch = *Chondrites*, Zo = *Zoophycos*; He = *Helminthopsis*.

2.5 RESULTS

We begin by describing characteristics of sequence boundaries, including evidence for erosion at the boundary, the presence or absence of soft sediment deformation, bioturbation, and the presence and characteristics of an overlying coarse-grained deposit ('lag') (Fig. 2.6-2.9). We then interpret these features to constrain setting and depositional processes. SB0 is located at the base of DS1, at the contact between the underlying argillaceous Majeau Lake Formation and overlying, more siliceous, Duvernay Formation. SB1 separates DS1 and DS2, at the contact between the underlying calcareous middle Duvernay carbonate member and overlying siliceous upper Duvernay member. SB2 is located between DS2 and DS3, within the upper Duvernay member. SB3 is located at the top of DS3, at the contact between the underlying Duvernay and overlying, detrital clay and dolomite-rich, organic-lean, Ireton Formation (Fig. 2.2, 2.3).

2.5.1 Expression of Surfaces

The nature of the sequence boundaries changes systematically stratigraphically and geographically. Across most of the study area, SB0 is expressed as a sharp and erosive surface; SB1 exhibits similar features in the central to northeast part of the study area. Scour is indicated by truncation of underlying laminae at a wavy contact and minimal differential compaction around sand infill of the scour. Up to 3 mm scour relief is observed within the width of the drill core (Fig. 2.5, 2.10a, 2.11, 12). The depth of scour relief typically increases with increasing thickness of the overlying coarse bed (Fig. 2.5, 2.6, 2.7, 2.10a, 2.10b). In the far south and west parts of the study area, SB1 is expressed as gradational and lacks evidence of scour (Fig. 2.5, 2.7, 2.10b). The geographic extent of SB1 expressed

as an erosive surface coincides with the extent of deposition of the middle Duvernay member carbonate (Fig. 2.7, 2.10b).

SB3 exhibits a soft sediment-deformed surface across most of the study area; SB2 exhibits similar features near reefs (Fig. 2.5, 2.8, 2.10c, 2.10d). These features include ball and pillow structures that deform and penetrate as much as 30 mm into the underlying mud laminae (Fig. 2.13, 2.14, 2.15, 2.16). The thickness of the soft sediment-deformed horizon increases with the thickness of the overlying coarse bed (Fig. 2.5, 2.8, 2.9, 2.10c, 2.10d). Locally, close to reefs at SB3 (core #6), some of the deepest penetrating ball structures appear to be sheared, suggesting that sliding or slumping of sediment took place. Elsewhere, SB2 and SB3 surfaces are sharp and planar, specifically at SB2 in the east part of the study area and SB3 in the south-central and southwest parts of the study area (Fig. 2.5, 2.8, 2.9, 2.10c, 2.10d). At these locations, the sequence boundaries are expressed by an abrupt decrease in silt and sand (SB2) or a facies change from the OM-rich and siliceous Duvernay Formation to the detrital clay-rich, organic-lean, Ireton Formation (SB3). Millimeter-scale relief (likely minor soft sediment deformation) and an abrupt change in lithology suggest that erosion took place. At SB2, in the central part of the study area, the surface is gradational and chiefly expressed as a decrease in silt and sand content (Fig. 2.5, 2.8, 2.10c).

2.5.2 Bioturbation

Bioturbation across surfaces and in the overlying coarse beds varies stratigraphically and geographically. At SB0, local ~1.5 mm diameter subhorizontal to subvertical burrows crosscut the surface; these are passively infilled and truncate underlying laminae (Fig. 2.6, 2.11). At SB1, there are no burrows across the surface. At SB2 and SB3, burrows that crosscut the surface are likely concomitantly infilled by overlying coarse material and maximum diameter decreases from SB2 (5 mm) to SB3 (3 mm)

(Fig. 2.14). Burrow diameters typically increase with thickness of the coarse bed overlying the surface (Fig. 2.8, 2.9, 2.10).

In coarse beds at SB0, 2, and 3, horizontal to subvertical, mud and silt-infilled, locally pyritized burrows up to 1 mm thick are present. No obvious burrows are present in the coarse lamina overlying SB1. The diameter of burrows in the coarse bed typically increases with thickness of the coarse bed (Fig. 2.6-2.9, 2.10). Close to reefs (core #7) in the study area at SB2, subvertical, silt-infilled burrows up to 8 mm diameter are locally present (Fig. 2.8, 2.14).

2.5.3 Coarse Bed Thickness and Grain Size

Sequence boundaries in the Duvernay are associated with beds of silt to medium sand, with rare local coarse and very coarse sand-size fossil fragments (Fig. 2.5, 2.6-2.9). The thickness of coarse beds varies stratigraphically, decreasing from SB0 (where the coarse bed ranges from <1 to 18 mm) to SB1 (<1 to 9 mm), increasing to SB2 (<1 to 55 mm), and decreasing again to SB3 (<1 to 12 mm thick) (Fig. 2.6-2.9, 2.10). The thickness of coarse beds also changes geographically. At SB0, the bed is thickest in the northeast and southwest and thins to the central, northwest and southeast parts of the study area (Fig. 2.6, 2.10a). At SB1, the lamina is thickest in the northeast (on the Grosmont Platform slope) and thins to the south and west in the study area (Fig. 2.7, 2.10b). At SB2, the coarse bed thins away from reefs and from the northeast to southwest (Fig. 2.8, 2.10c). At SB3, the bed is thickest in the northeast and northwest and thins to the south and away from reefs in the study area (Fig. 2.9, 2.10d). Where the overlying bed is thin, it is typically also relatively fine grained (Fig. 2.6-2.9).

2.5.4 Sedimentary Structures

Coarse beds at sequence boundaries in the Duvernay are typically massive (Fig. 2.5, 2.6-2.9, 2.11, 2.14, 2.15). Elongate grains are typically aligned parallel to bedding. Top contacts are typically sharp and slightly undulatory, locally giving rise to a pinching and swelling appearance where the beds are relatively thin.

Sedimentary structures within coarse beds vary locally with stratigraphy and geography. Coarse beds overlying SB0 and SB1 are locally normally graded (in far east and west parts of study area at SB0, central in study area at SB1) (Fig. 2.6, 2.7). In the northwest part of the study area, the beds associated with SB0 and SB3 are comprised of 4 and 6 laminae respectively that are ~1-4 mm thick and thin upwards within the bed (Fig. 2.6, 2.9, 2.12, 2.16). At SB0, laminae within the bed are normally graded and display scoured bases. At SB3, the laminae are inversely graded with sharp, slightly wavy contacts, and display soft sediment deformation. Close to reefs in the study area at SB2 (core #6), hummocky cross stratification (HCS) is present within the coarse bed (Fig. 2.8, 2.13).

2.5.5 Coarse Bed Composition

Coarse beds at sequence boundaries in the Duvernay have distinctly different detrital mineral compositions from surrounding mudstone. Beds are composed of variable amounts of calcite and quartz grains, calcareous fossil fragments (styliolinids, tentaculitids, ostracods, brachiopods), phosphatic grains (conodont elements, fish bone fragments, peloids, lingulid brachiopod fragments), dolomite grains, dolomitized calcite grains, and pyrite grains (Fig. 2.10). The beds are locally cemented by pyrite, calcite, and dolomite.

Compositions of the coarse beds change stratigraphically (Fig. 2.10). Mud rip-up clasts are locally present at SB0. Feldspar grains are locally present at SB0 and SB1. Glauconite grains are locally present

at SB0 and SB3. Stromatoporoid fragments are locally present at SB2 and SB3. The composition of coarse beds also changes geographically (Fig. 2.10). Calcite, dolomitized calcite, and dolomite grains typically increase in abundance close to reefs. Quartz, phosphate, pyrite, and feldspar grains are typically most abundant in central parts of the study area. Glauconite grains typically increase in abundance to the northeast toward the Grosmont Platform.

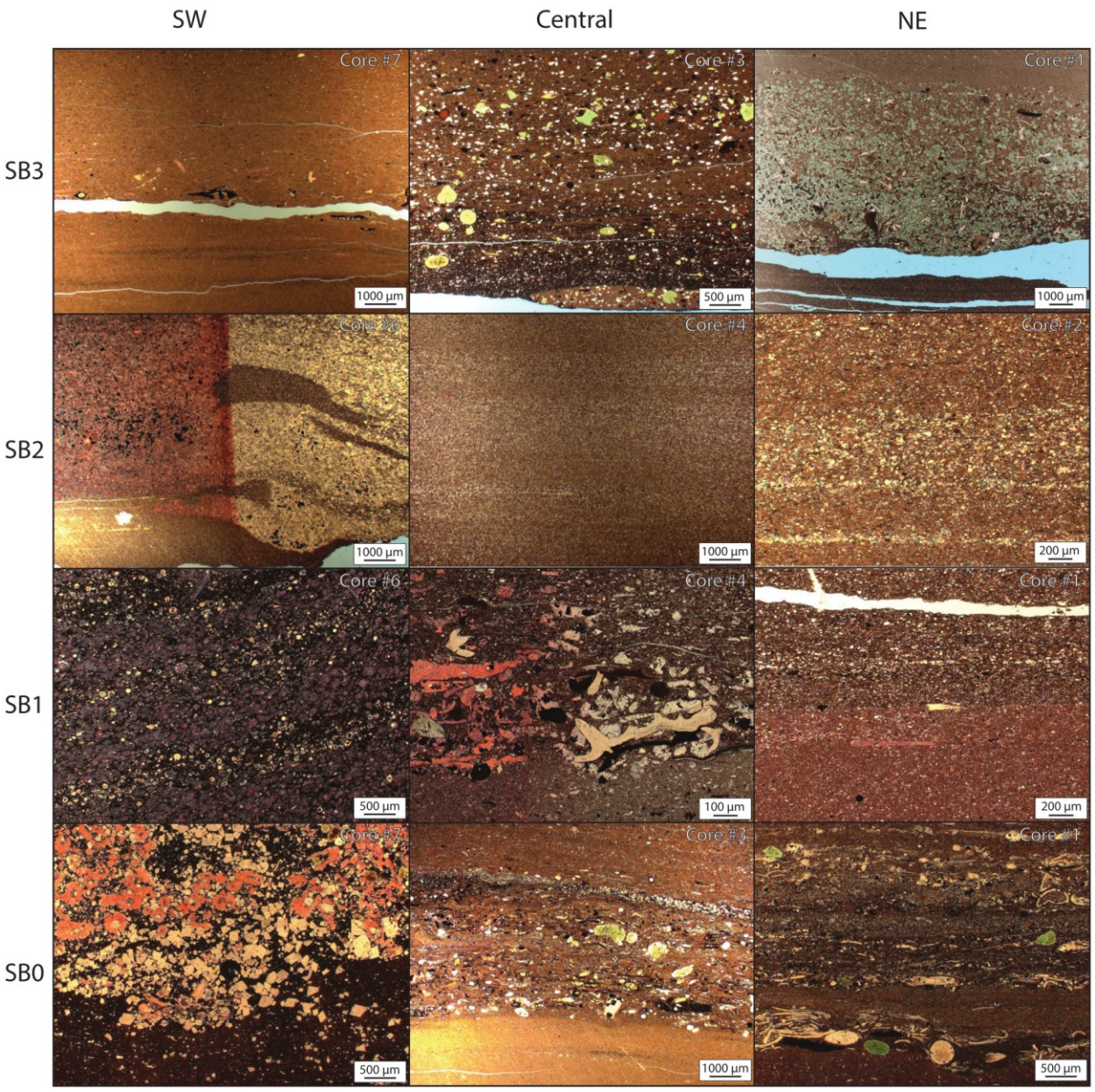

Figure 2.5: Examples of the expression of 3rd order sequence boundaries and associated coarse beds from the southwest, central, and northeast parts of the study area.

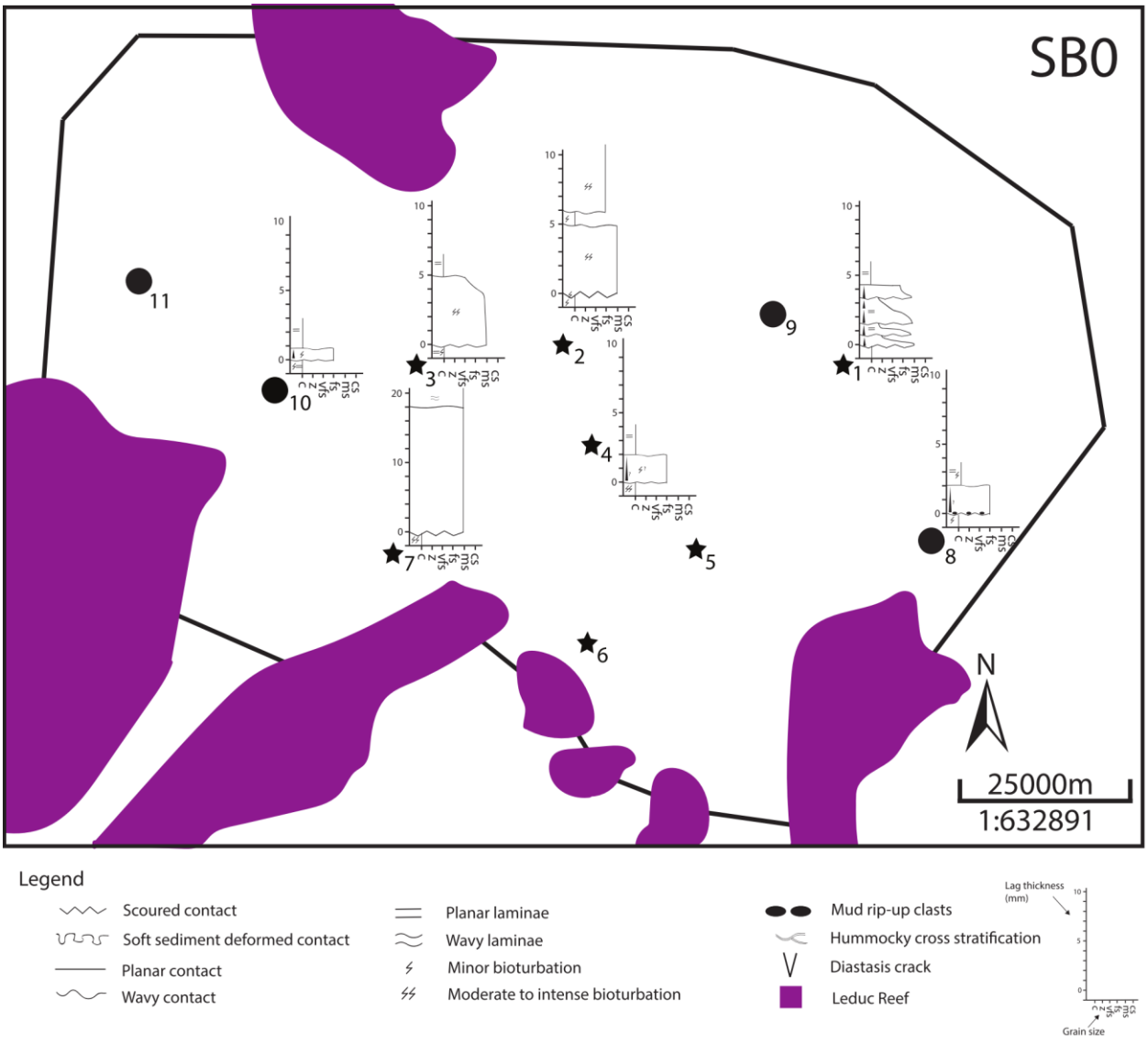

Figure 2.6: Descriptions of SB0 surface and overlying lag.

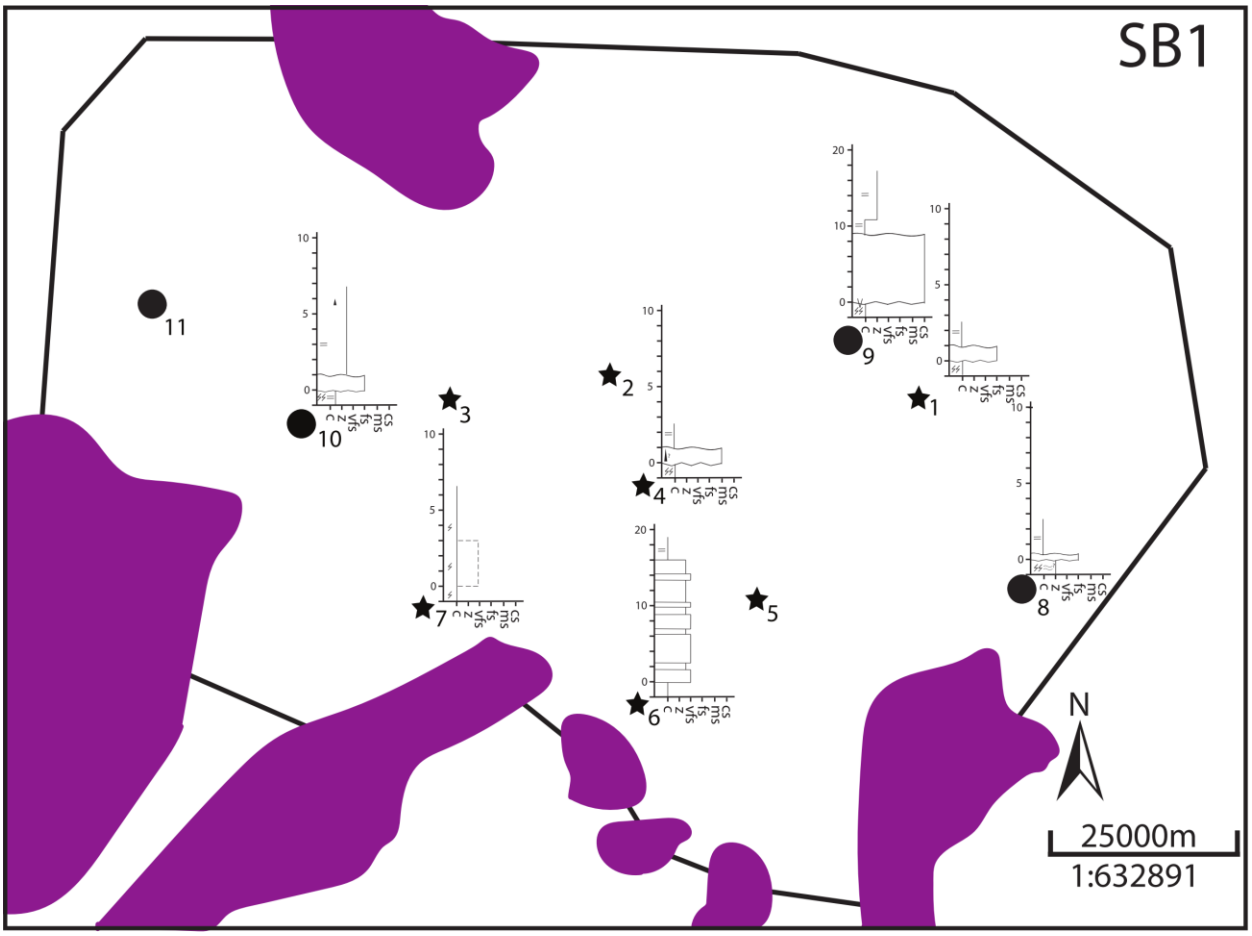

Figure 2.7: Descriptions of SB1 surface and overlying coarse lag.

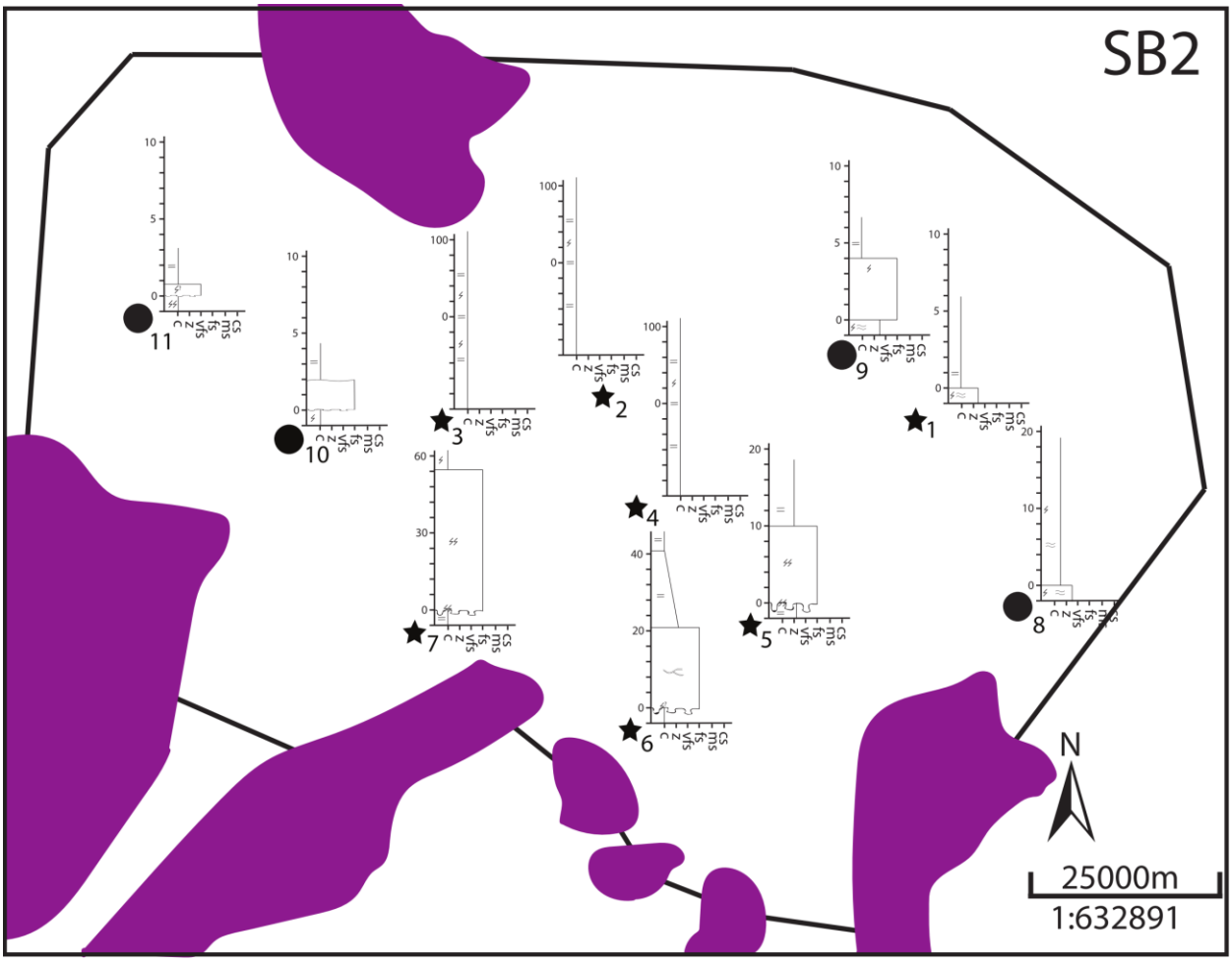

Figure 2.8: Descriptions of the basal surface of forced regression, forced regressive deposit, and SB2.

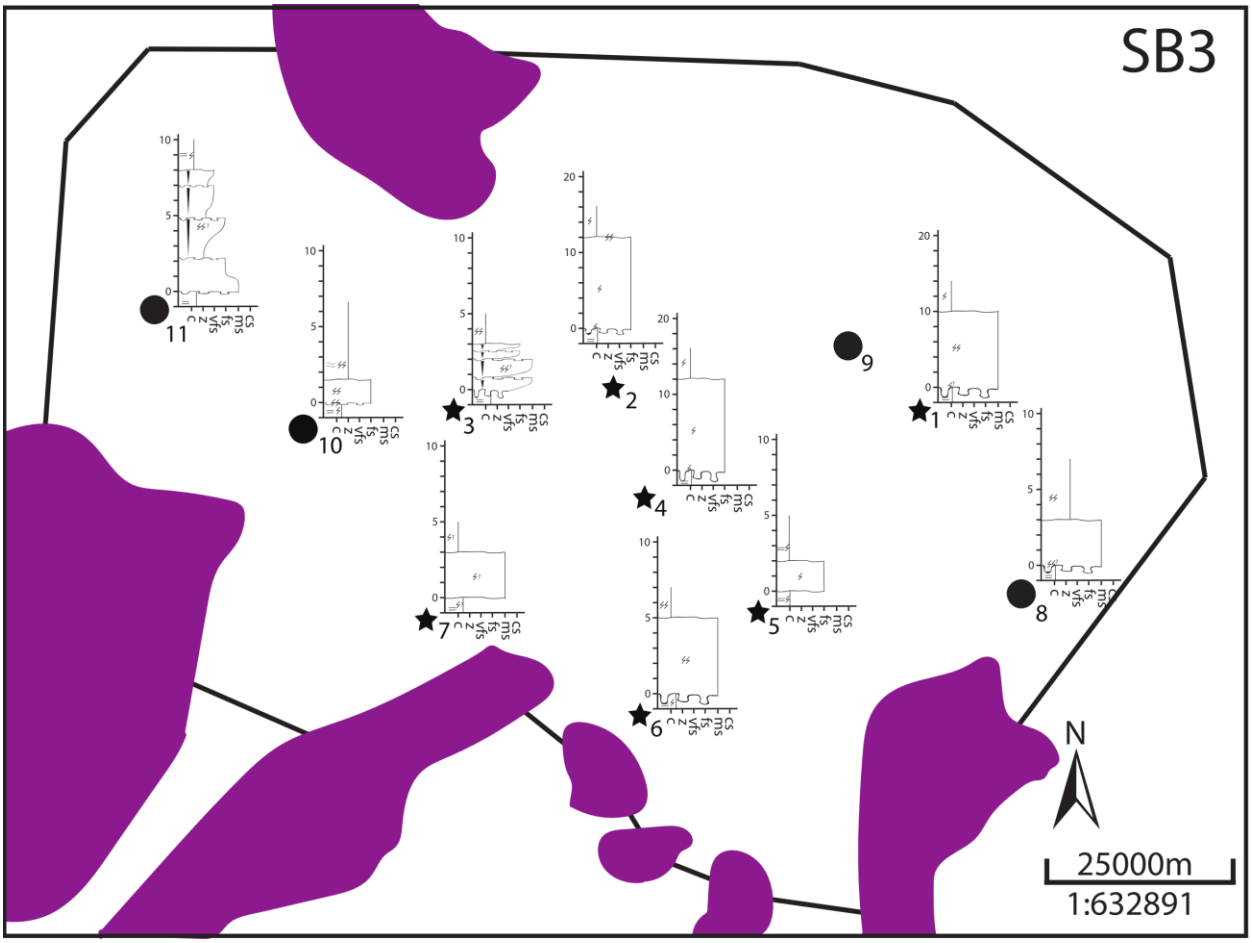

Figure 2.9: Descriptions of the basal surface of forced regression, forced regressive deposit, and SB3.

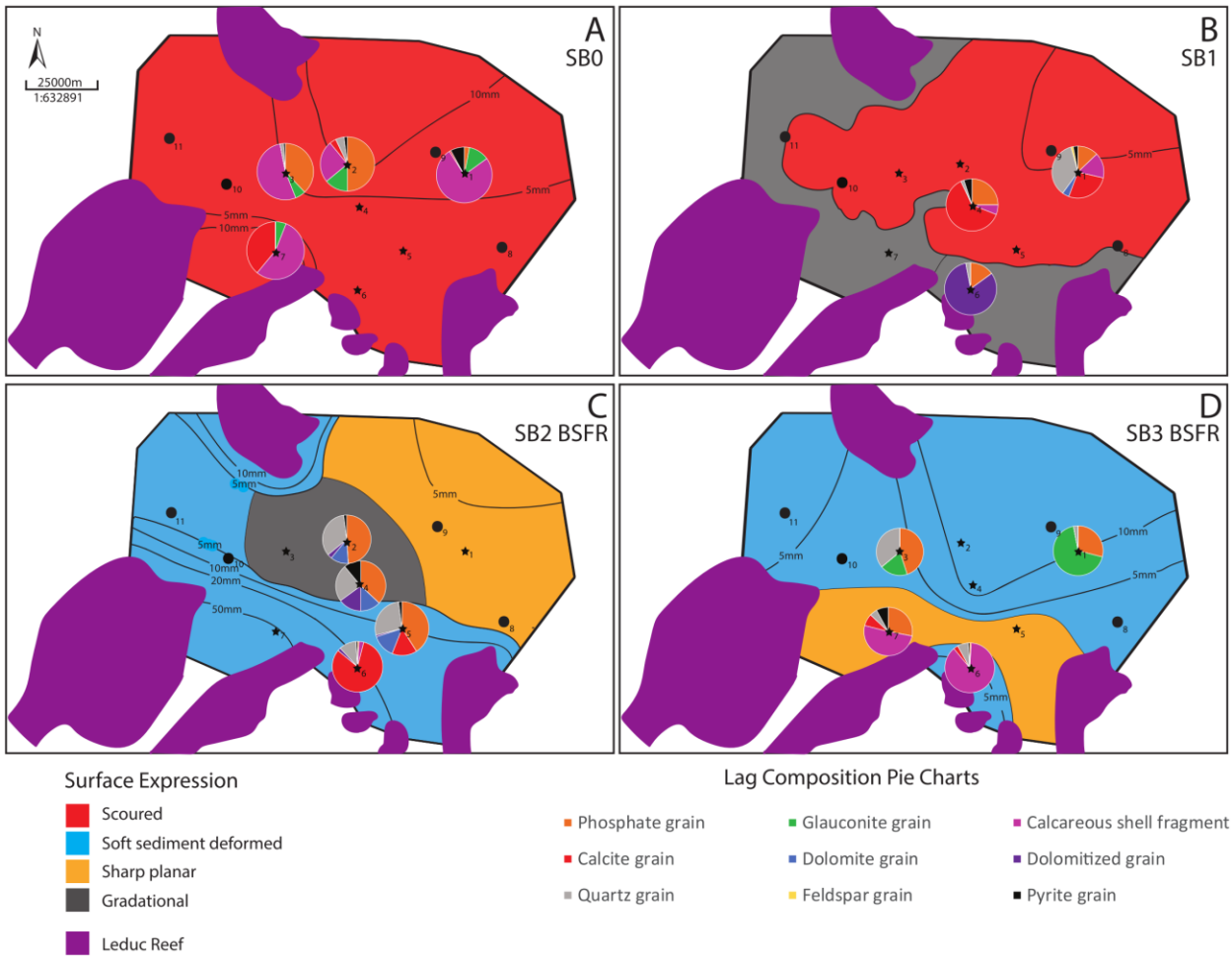

Figure 2.10: Expressions of surfaces and thickness of overlying coarse beds. SB0 and SB1 describe the expression of the sequence boundary and overlying lag. SB2 and SB3 describe the expression of the basal surface of forced regression (BSFR) and overlying bed representing the falling stage systems tract.

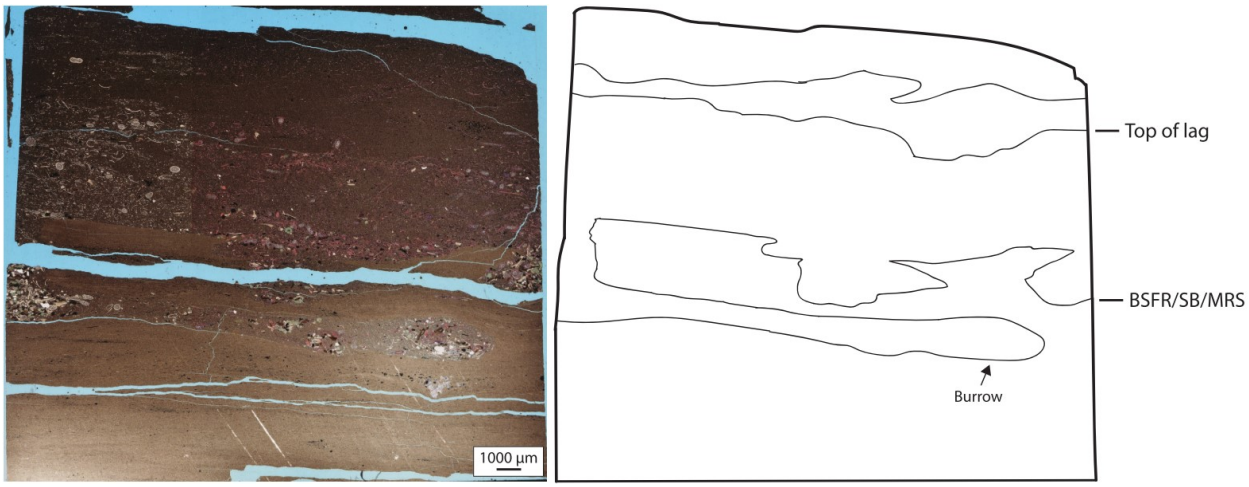

Figure 2.11: Photograph and interpretation of the amalgamated basal surface of forced regression, SB0, and maximum regressive surface and overlying coarse lag at core #2.

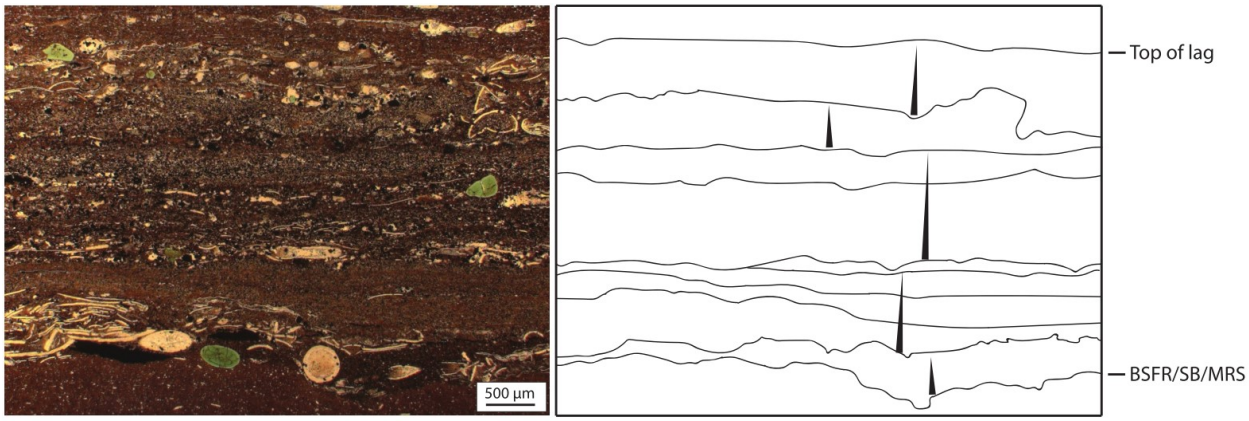

Figure 2.12: Photograph and interpretation of the amalgamated basal surface of forced regression, SB0, and maximum regressive surface and overlying coarse lag at core #1.

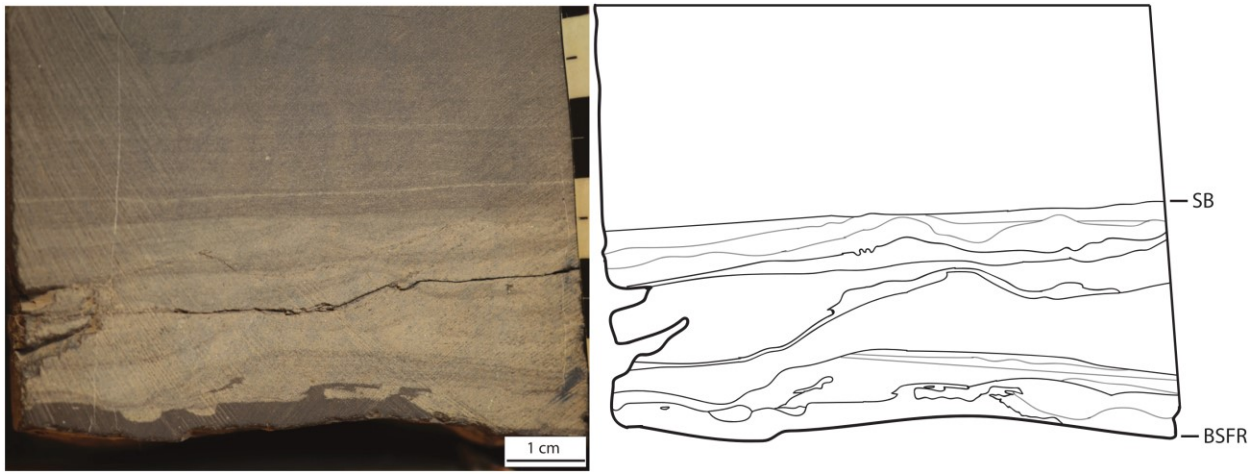

Figure 2.13: Photograph and interpretation of the basal surface of forced regression (BSFR), falling stage systems tract, and SB2 and at core #6.

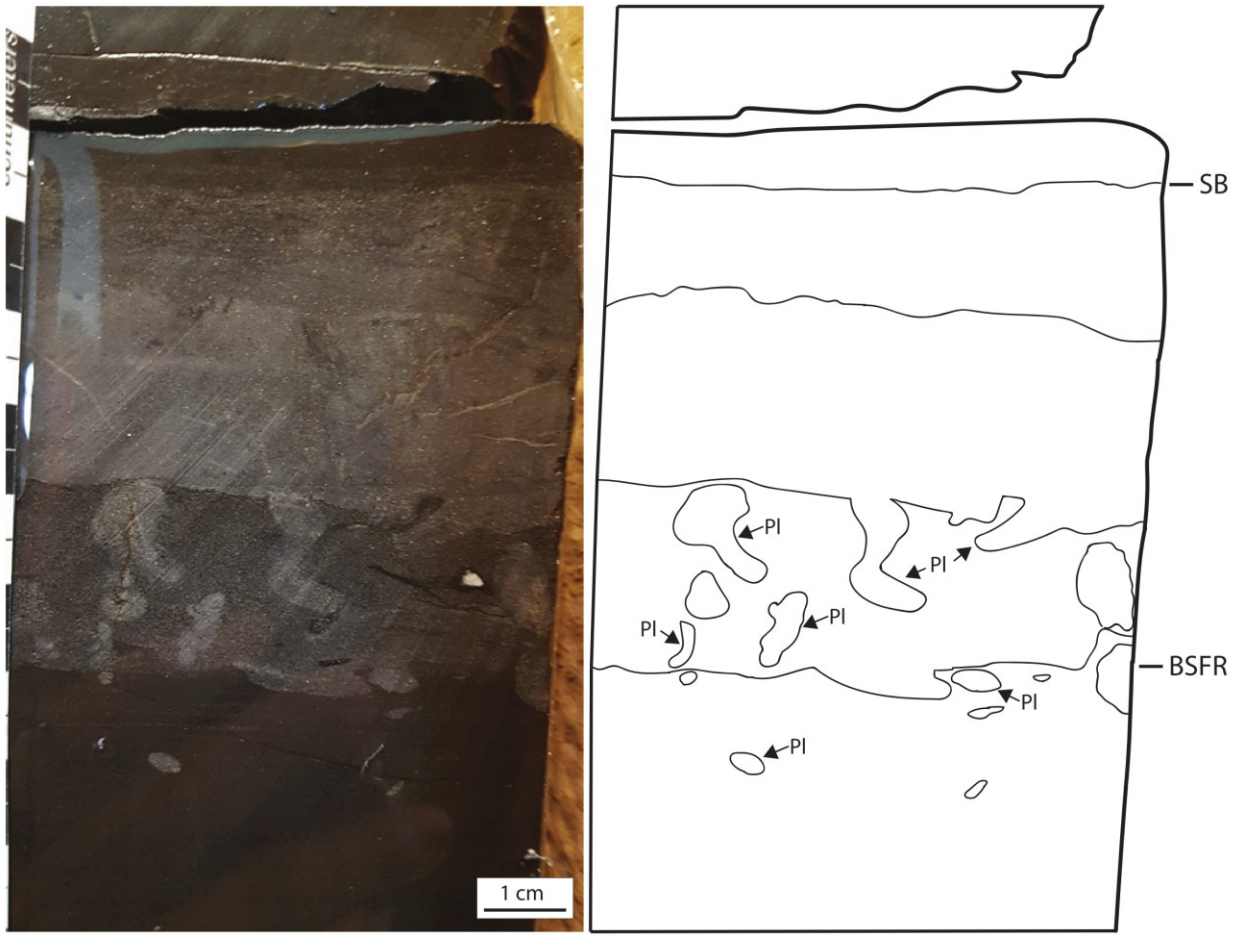

Figure 2.14: Photograph and interpretation of the basal surface of forced regression (BSFR), falling stage systems tract, and SB2 at core #7. Pl = *Planolites*.

Figure 2.15: Photograph and interpretation of the basal surface of forced regression (BSFR), falling stage systems tract, and SB3 at core #1.

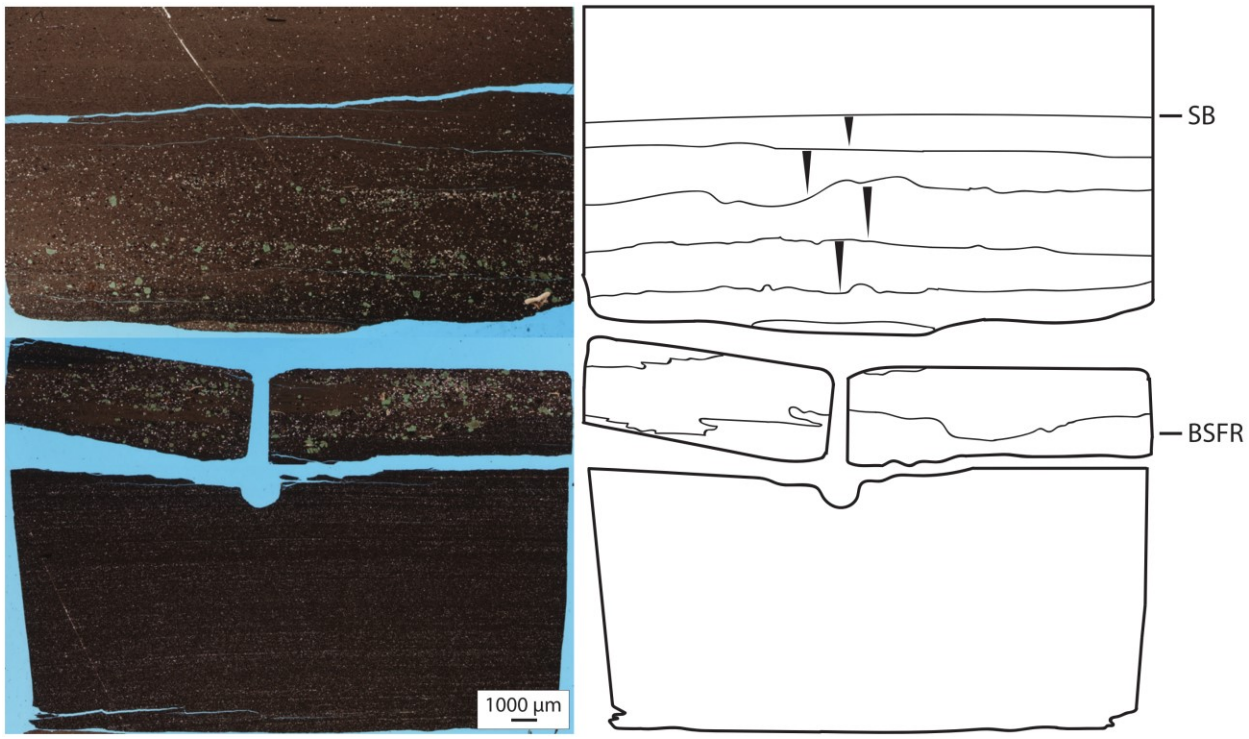

Figure 2.16: Photograph and interpretation of the basal surface of forced regression (BSFR), falling stage systems tract, and SB3 at core #3.

2.6 DISCUSSION

2.6.1 The nature of sequence boundaries in black shale

Previous studies of mudstones have identified sequence boundaries based on patterns in petrophysical well logs (eg: Hammes and Frebourg, 2012; Dong et al., 2017), abrupt facies transitions (eg: Hemmesch et al., 2014; Ayranci et al., 2018), changes in geochemical proxies (eg: Ayranci et al., 2018), and the presence of erosive surfaces of large lateral extent (expressed as sharp, scoured, or soft sediment-deformed) (eg: Schieber, 1998a; Schieber, 2004; Knapp et al., 2019). Surfaces are commonly overlain by lag deposits that may be cemented and often comprised of much coarser and very different detrital mineralogies than the rest of the succession (eg: Macquaker et al., 2007; Li and Schieber, 2015; Knapp et al., 2019). Resistive grains such as phosphate, pyrite, glauconite, quartz, and feldspar are common components of lags above sequence boundaries (Baird and Brett, 1991; Wignall and Maynard, 1993; Schieber, 1998a; Scasso and Castro, 1999; Schieber, 2004; Macquaker et al., 2007; Li and Schieber, 2015; Knapp et al., 2019).

2.6.2 Expression of sequence boundaries in the Duvernay Formation

SB0 and SB1

SB0 and SB1 present evidence for submarine erosion. These surfaces exhibit truncation of underlying laminae, relief on the order of a few mm at the scale of the width of a core, and minor differential compaction around the sand-fill of the scour (Fig. 2.5, 2.11, 2.12). These features suggest that the underlying sediment was firm and had undergone compaction prior to erosion (Schieber, 1998b). In addition, burrows crosscutting the SB0 surface are sharp walled, relatively uncompacted, and passively infilled, suggesting they were formed in a firmground substrate (Pemberton and MacEachern, 1995) (Fig. 2.12). Burrows of this form have been interpreted by Pemberton and MacEachern (1995) and

Cattaneo and Steel (2003) to indicate a depositional hiatus between erosion of underlying sediments and deposition of overlying sediments and can be indicative of burrows across sequence boundaries. No burrows are visible across SB1, but a diastasis crack infilled from above in core #9 is consistent with the interpretation of a disconformity (Cowan and James, 1992). Local small, subhorizontal to subvertical burrows cross-cutting the SB0 surface and small horizontal to subvertical burrows in the overlying coarse bed suggest that bottom waters were likely dysoxic and sedimentation rates were likely low (Ekdale and Mason, 1988; Baird and Brett, 1991; van Buchem et al., 1996; Gingras et al., 2011).

SB2 and SB3

Soft sediment deformed surfaces in mudstone have been proposed as evidence for erosion in unlithified sediments by Schieber (1998), but loading (ball and pillow) structures at SB2 and SB3 provide greater evidence for rapid accumulation of sediment over a weak substrate (Owen, 2003) (Fig. 2.5, 2.13-2.16). Compacted, concomitantly-infilled burrows (Fig. 2.5, 2.13-2.16) and features interpreted as slump structures support the interpretation of formation on an unlithified substrate. These features allow for the possibility of some erosion but without clear evidence for a disconformity at SB2 or SB3. Local large burrows across the SB2 and SB3 surfaces and local large, subvertical burrows throughout overlying coarse beds indicate that bottom waters were likely dysoxic to fully oxygenated and sedimentation rates were likely low (Ekdale and Mason, 1988; Baird and Brett, 1991; van Buchem et al., 1996; Gingras et al., 2011).

2.6.3 Processes that produce overlying beds

SB0 and SB1

The coarse beds overlying the SB0 and SB1 surfaces are interpreted as lag deposits (Fig. 2.5, 2.11, 2.12). Lags are produced by winnowing and have typically been associated with erosive surfaces interpreted as sequence boundaries in black shales (eg: Schieber, 1998a; Schieber and Riciputi, 2004; Knapp et al., 2019).

Structures in lag deposits overlying SB0 and SB1 such as grading provide evidence of hydraulic sorting (Baird and Brett, 1991). Normal grading in lags may have been produced by reworking and winnowing by bottom currents under waning energy conditions (Glenn and Arthur, 1990; Li and Schieber, 2015), with the scoured surfaces forming when the currents were strongest. Where the SB0 lag is composed of multiple normally graded stacked laminae with scour surfaces between (Fig. 2.6, 2.12), we suggest there were multiple events of bottom current reworking and winnowing under waning energy conditions (Baird and Brett, 1991; Schieber and Riciputi, 2004). Massive lags above sequence boundaries in the Duvernay suggest reworking and winnowing by bottom currents under longer duration, moderate energy conditions (Li and Schieber, 2015) (Fig. 2.6, 2.7, 2.11). It is less likely that the massive nature resulted from pervasive bioturbation. Reworking by currents is also consistent with the typically wavy top contact and locally pinching and swelling, discontinuous nature of the lags (Glenn and Arthur, 1990; Baird and Brett, 1991).

Lag deposits at SB0 and SB1 contain high concentrations of physically and chemically stable, and dense clasts such as phosphatic debris, siliceous grains, and detrital pyrite (Fig. 2.10a, b). Their presence, as well as fossil fragments, suggest concentration under sediment-starved conditions by winnowing, erosion, and weathering of previously deposited sediment (Glenn and Arthur, 1990; Bohacs and Schwalbach, 1992; Cattaneo and Steel, 2003; Wignall and Maynard, 1993; Scasso and Castro, 1999;

Abouelresh and Slatt, 2012; Li and Schieber, 2015). Bottom currents likely reworked larger and denser detrital quartz, phosphate, and pyrite grains within lags and winnowed clays, organic matter, and fine silt (Scasso and Castro, 1999; Simandl et al., 2011; Li and Schieber, 2015). The presence of glauconite grains in lags (especially those in association with phosphatic grains, such as at SB0) also suggest deposition by mechanical winnowing and reworking, concentrating large and dense grains (Glenn and Arthur, 1990). Glauconite grains were likely produced in proximal parts of the basin during forced regression and lowstand conditions, due to increased delivery of detrital iron (likely in the form of detrital clay) to the basin, and reworked basinward (Glenn and Arthur, 1990).

SB2 and SB3

Sedimentary structures in coarse beds at SB2 and SB3 provide evidence of hydraulic sorting and reworking by bottom currents and storm waves. Massive beds at SB2 and SB3 (Fig. 2.8, 2.9, 2.14, 2.15) suggest reworking and winnowing by bottom currents under longer term, moderate energy conditions (Li and Schieber, 2015) or bioturbation. Local stacked inversely graded laminae with soft sediment-deformed contacts likely represent multiple reworking events by bottom currents under gradually increasing energy conditions (Glenn and Arthur, 1990; Li and Schieber, 2015) (Fig. 2.9, 2.16). Hummocky cross stratification at SB2 in core #6 (Fig. 2.8, 2.13) represents reworking by storm waves during lowered relative sea level (Schieber, 1998a; Plint and Nummedal, 2000).

Phosphatic debris, silicate grains, detrital pyrite, and fossil fragments in coarse beds at SB2 and SB3 (Fig. 2.10c, d) suggest concentration of large and dense grains under sediment-starved conditions by winnowing and erosion of previously deposited sediment (Glenn and Arthur, 1990; Bohacs and Schwalbach, 1992; Cattaneo and Steel, 2003; Wignall and Maynard, 1993; Scasso and Castro, 1999; Abouelresh and Slatt, 2012; Li and Schieber, 2015). Reworked glauconite grains and the presence of reef

derived carbonate grains and fossil fragments are evidence of basinward transportation of sediment (Glenn and Arthur, 1990).

2.6.4 Stratigraphic and geographic variation

SB0 and SB1

Erosive surfaces in black shales with deep scour and thick sandy overlying lag deposits have been interpreted as being produced in shallower water than surfaces with no evidence of erosion or overlying coarse lags (Schieber, 1998a). This may be due to greater erosion by bottom currents produced by large scale basin circulation as well as storm waves (Baird and Brett, 1991; Schieber, 1994; Plint and Nummedal, 2000; Li and Schieber, 2015). Deeper scour and a thicker overlying lag at SB0 compared to SB1 suggest that water depths may have generally been shallower at SB0, consistent with the interpretation that the SB1 surface occurs later than SB0 in the 2nd order transgression (Knapp et al., 2019; Chapter 1). At SB0 and SB1, the disconformable (scoured) surfaces become conformable (gradational) and the overlying coarse lags thin systematically across the study area (Fig. 2.10a, 2.10b). At SB0, the thickness and grain size of the overlying lag and surface relief are greatest in the northeast and southwest parts of the study area (Fig. 2.6, 2.10a), likely representing shallower, higher energy conditions (Schieber, 1998a). At SB1, the thickness and grain size of the overlying lag and surface relief increase toward the northeast in the study area (Fig. 2.7, 2.10b). This is consistent with the interpretation that during deposition of DS1, Grosmont Platform-sourced sediment built out into the basin, expressed as the middle Duvernay member carbonate (Knapp et al., 2017; Chapter 1). Thus, water depths are interpreted to increase from northeast to southwest in the study area at the time of formation of SB1 which marks the end of the platform construction phase during Duvernay Formation deposition.

SB2 and SB3

Soft sediment deformation and coarse overlying beds are present over a larger area of SB3 than SB2, possibly suggesting that water depths were generally shallower and sedimentation rates were higher, consistent with interpretations that SB3 occurred later in the 2nd order highstand (Harris et al., 2018; Knapp et al., 2019; Paper 1). At SB2, the coarse bed thins, and the bottom contact changes from a soft sediment-deformed surface to a gradational surface basinward of reefs, suggesting that the reefs were the dominant source of sediment with the shallowest water depths (Fig. 2.17). To the northeast in the study area, the surface is sharp and planar, and the sand bed thins from the northeast to southwest (Fig. 2.8, 2.10c); we interpret this as the result of increasing water depth on the previously developed Grosmont Slope and distance from the Grosmont Platform sediment source. At SB3, the sand bed thins and the bottom contact transitions from a soft sediment deformed surface to a sharp planar surface to the south and away from reefs in the study area (Fig. 2.9, 2.10d), likewise as thinning to deeper, lower energy parts of the basin and away from the sediment source. The coarse bed and the soft sediment deformed horizon are thickest in the northeast in the study area, suggesting that the Grosmont Platform was the dominant source of sediment with the shallowest water depths.

2.6.5 Towards a more refined sequence stratigraphic model of black shales

SB0 and SB1

The SB0 and SB1 surfaces are erosive, forming firmgrounds and representing disconformities. The composition and structure of lags suggest they were produced by reworking and winnowing by bottom currents under sediment starved conditions and waning energy conditions. Dysoxic bottom conditions, suggested by burrows, has been linked to times of low relative sea level during Duvernay

deposition (Harris et al., 2018). SB0 and SB1 are also interpreted to be overlain by 3rd order transgressive systems tracts (TSTs) (Knapp et al., 2019; Paper 1). We interpret SB0 and SB1 to be polygenetic/composite surfaces and overlying lags, corresponding to a hiatus equivalent to the basal surface of forced regression, sequence boundary, maximum regressive surface (MRS), and possibly early transgression (Fig. 2.11, 2.12, 2.17).

In a sequence stratigraphic framework, sediment starvation can take place during forced regression, lowstand, and transgression in carbonate systems (Hunt and Tucker, 1992); in this regard, carbonate systems differ from clastic system. In clastic systems, substantial sediment transport to deep parts of the basin can occur during forced regressions and lowstands, whereas in carbonate systems, during falling stage and lowstand conditions, subaerial exposure of platform and reef tops causes the carbonate factory to shut down, reducing carbonate sediment delivery to the basin (Hunt and Tucker, 1992; Catuneanu, 2006; Catuneanu et al., 2011; Wong et al., 2016). During transgression, the increase in accommodation causes shorelines, shelves, and reefs to aggrade and retrograde (backstep) and causes the supply of coarse carbonate sediment and clay to the basin to decrease (Catuneanu et al., 2011; Wong et al., 2016; Liu et al., 2019).

SB2 and SB3

The base of the coarse beds at SB2 and SB3 show evidence of loading of unlithified sediment and no evidence of a disconformity. The composition and structure of sand beds at SB2 and SB3 suggest erosion and reworking by bottom currents, similar to SB0 and SB1, but also basinward transportation of reef- and platform-derived carbonate sediment and clastic material. Evidence of storm wave reworking (Fig. 2.8, 2.13) and fully oxygenated bottom conditions (Fig. 2.8, 2.9, 2.14) in the sand beds suggest shallow relative sea level, possibly on the scale of tens of meters (Schieber, 1994; Harris et al., 2018).

SB2 is interpreted to be overlain by a 3rd order lowstand systems tract (LST), and similarly SB3 is represented by a basinward shift in lithofacies across, also possibly representing lowstand conditions (Knapp et al., 2019; Chapter 1). We suggest that the coarse beds at SB2 and SB3 represent thin falling stage systems tracts (FSSTs). The bottom contacts of the sand beds are interpreted to represent the basal surfaces of forced regression (BSFR), marking the beginning of relative sea level fall (Hunt and Tucker, 1992; Plint and Nummedal, 2000; Bover-Arnal et al., 2009) (Fig. 2.13-2.17). The coarse sand beds are interpreted to be produced during forced regression and the top contacts of the sand beds are interpreted to be sequence boundaries (correlative conformities) and the base of the LST (Hunt and Tucker, 1992; Plint and Nummedal, 2000).

During relative sea level fall, subaerial exposure of platform and reef tops shuts down platform carbonate production. Mechanical and chemical erosion of the exposed platform and reefs and the remains of carbonate-producing communities on the slopes cause the accumulation of allochthonous debris on the toes of slopes (Fig. 2.17) (Bover-Arnal et al., 2009). Siliciclastic sediment can also be transported across a shelf and deposited at the toe of the slope during forced regression (Hunt and Tucker, 1992). Glauconite at SB3 was likely produced in proximal parts of the basin during forced regression from increased delivery of detrital clay to the basin (Glenn and Arthur, 1990). This material is then reworked basinward by bottom currents and storm waves (Bover-Arnal et al., 2009). Thin eroded and winnowed phosphatic beds in other Middle Paleozoic shales deposited in epicontinental seas have also been interpreted as representing the beginning of forced regression (Brett et al., 1996; McLaughlin et al., 2008). The sequence boundary can be expressed as an abrupt decrease in grain size and allochthonous debris at the end of forced regression (Hunt and Tucker, 1992; Bover-Arnal et al., 2009).

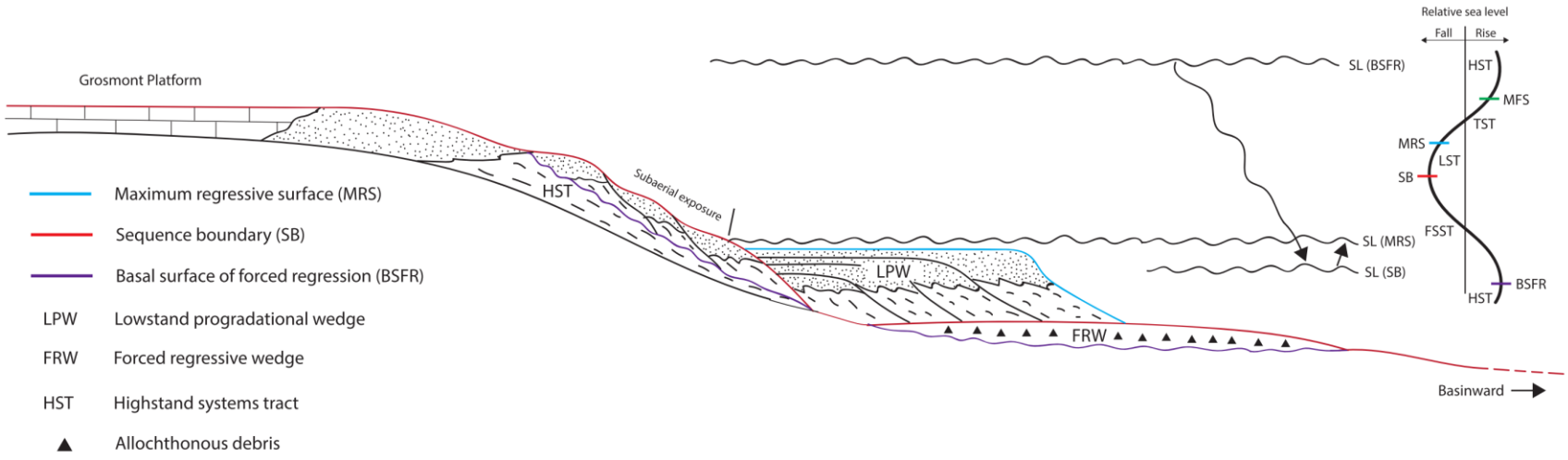
Grosmont Platform
Maximum regressive surface (MRS)
Sequence boundary (SB)
Basal surface of forced regression (BSFR)
LPW Lowstand progradational wedge
FRW Forced regressive wedge
HST Highstand systems tract
Allochthonous debris
HST
Subaerial exposure
LPW
FRW
SL (BSFR)
SL (MRS)
SL (SB)
Basinward
Relative sea level
Fall
Rise
HST
MFS
TST
MRS
LST
SB
FSST
HST
BSFR

Figure 2.17: Sequence stratigraphic model of carbonate platform during forced regression to early transgression. (modified *from* Hunt and Tucker, 1992)

2.6.6 Contributions of this study

Several previous studies have interpreted erosive surfaces in mudstones to represent a combined sequence boundary and transgressive surfaces, which are in turn overlain by a winnowed lag (eg: Scasso and Castro, 1999; Macquaker et al., 2007; Hammes and Frebourg, 2012; Li and Schieber, 2015; Knapp et al., 2019). Our interpretation of stratigraphic surfaces in the 2nd order TST of the Duvernay (SB0 and SB1) is consistent with these models, but our interpretation of surfaces in the 2nd order HST differs in that we propose that the coarse sand beds with soft sediment deformed bases were deposited during forced regression. Our results are consistent with Schieber (1998) in documenting increases in thickness and grain size of overlying lags and erosional relief with decreasing water depth in a basin. We show that coarse beds deposited during forced regressions follow this same pattern with water depth and with distance from a sediment source.

Without the high-density dataset of high-quality cores covering proximal to distal areas in our study area, it would have not been possible to recognize the transition of sequence boundaries from disconformable to conformable surfaces across the 2nd order maximum flooding surface nor identify the thin, coarse beds representing the winnowed lags or forced regressive deposits in these basinal black shales. A strong understanding of the sequence stratigraphic framework of a formation is also necessary to understand the systems tracts overlying sequence boundaries to understand processes involved in their formation.

2.7 CONCLUSIONS

In our study of the Upper Devonian Duvernay Formation, we describe two types of basinal mudstone sequence boundaries and summarize the differences with respect to position within a 2nd order depositional sequence, comparing 3rd order sequence boundaries produced during deposition of a 2nd order TST and those produced during deposition of a 2nd order HST. Multiple 3rd order sequence boundaries are present, two within a 2nd order TST and two within the overlying 2nd order HST.

Sequence boundaries produced during the 2nd order TST are represented by scoured (disconformable) surfaces with coarse overlying lags that represent periods of sediment starvation and reworking during forced regression, lowstand conditions, and early transgression. Bottom currents winnowed fine material, producing an erosive surface and leaving behind a coarse overlying lag of dense and resistive grains. The coarse lag thins, and the surface becomes gradational (conformable) with increasing water depth and decreasing energy conditions.

Sequence boundaries produced during the 2nd order HST are represented by soft sediment-deformed surfaces overlain by coarse beds that represent a period of forced regression. Components of the forced regressive bed were produced by winnowing of fine material by bottom currents and basinward redeposition of reef- and platform-derived carbonate sediments and clastic material. The sequence boundary is located at the top of the coarse beds and mark the end of relative sea level fall. The forced regressive deposit thins, and the surface becomes gradational with increasing water depth and decreasing energy conditions and with increasing distance from the sediment source.

Chapter 3 : Conclusions

This study examines the effects of sequence stratigraphy and paleogeography on mudstone depositional processes and environments. In Chapter 1 we identify lithofacies within the Duvernay Formation and describe a set of processes and environments under which these lithofacies were produced. Facies distributions are examined as a function of paleogeography and relative sea level to develop a sequence stratigraphic model for the Duvernay in the Kaybob area of Alberta that encompasses 2nd, 3rd, and 4th order sea level cycles. In Chapter 2 we describe two types of 3rd order mudstone sequence boundaries and summarize the differences with respect to position within a 2nd order depositional sequence.

3.1 LITHOFACIES DISTRIBUTION FROM PALEOGEOGRAPHY AND SEQUENCE STRATIGRAPHY

Lithofacies in the Duvernay Formation were deposited by a combination of suspension settling, sediment-gravity flows, and bottom currents under anoxic to fully oxygenated bottom water conditions. Coarse, carbonate-rich, bioturbated, and organic poor facies are common close to large carbonate platforms and reefs. Silt- and sand-rich, bottom current and sediment gravity flow deposited facies are common on the slopes of large carbonate platforms. Fine-grained, biosiliceous, organic-rich facies deposited by hemipelagic suspension settling are common in distal areas of the basin. Transgressive deposits are characterized by increasingly fine-grained, biosiliceous, and organic rich lithofacies. Highstand deposits are characterized by increasingly coarse grained, carbonate-rich, bioturbated, and organic-poor facies. Lowstand deposits are characterized by detrital clay-rich and bioturbated facies.

3.2 SEQUENCE BOUNDARY EXPRESSION AND POSITION WITHIN A 2ND ORDER DEPOSITIONAL SEQUENCE

Sequence boundaries produced during a 2nd order transgression are represented by scoured surfaces and coarse overlying lags that represent disconformities equivalent to forced regression, lowstand, and early transgression. Lags were produced when bottom currents eroded and winnowed underlying sediment and left behind coarse, dense, and resistive grains. The surface becomes gradational (conformable) and the overlying lag thins with increasing water depth and decreasing energy conditions.

Sequence boundaries produced during a 2nd order highstand are represented by soft sediment deformed surfaces overlain by coarse beds that represent a period of forced regression. Components of the forced regressive deposit were produced by reworking and winnowing by bottom currents as well as basinward redeposition of reef- and platform-derived carbonate sediments and clastic material. The sequence boundary is placed at the top of the coarse bed to represent the end of relative sea level fall. The forced regressive deposit thins and the surface becomes gradational with increasing water depth and decreasing energy conditions and increasing distance from the sediment source.

References

Abouelresh, M. O., & Slatt, R. M. (2012). Lithofacies and sequence stratigraphy of the Barnett Shale in east-central Fort Worth Basin, TexasGeohorizon. *AAPG bulletin*, *96*(1), 1-22.

Allan, J., & Creaney, S. (1991). Oil families of the Western Canada basin. *Bulletin of Canadian Petroleum Geology*, *39*(2), 107-122.

Andrichuk, J. M. (1958). Stratigraphy and facies analysis of Upper Devonian reefs in Leduc, Stettler, and Redwater areas, Alberta. *AAPG Bulletin*, *42*(1), 1-93.

Andrichuk, J. M. (1961). Stratigraphic evidence for tectonic and current control of Upper Devonian reef sedimentation, Duhamel area, Alberta, Canada. *AAPG Bulletin*, *45*(5), 612-632.

Ayranci, K., Harris, N. B., & Dong, T. (2018). High resolution sequence stratigraphic reconstruction of mud-dominated systems below storm wave base; A case study from the Middle to Upper Devonian Horn River Group, British Columbia, Canada. *Sedimentary geology*, *373*, 239-253. Ayranci, K., Harris, N. B., & Dong, T. (2018). High resolution sequence stratigraphic reconstruction of mud-dominated systems below storm wave base; A case study from the Middle to Upper Devonian Horn River Group, British Columbia, Canada. *Sedimentary geology*, *373*, 239-253.

Baird, G. C., & Brett, C. E. (1991). Submarine erosion on the anoxic sea floor: Stratinomic, palaeoenvironmental, and temporal significance of reworked pyritebone deposits. *Geological Society, London, Special Publications*, *58*(1), 233-257.

Berner, R. A. (1970). Sedimentary pyrite formation. *American journal of science*, *268*(1), 1-23.

Bohacs, K. M., & Schwalbach, J. R. (1992). Chapter II-Sequence Stratigraphy of Fine-Grained Rocks with Special Reference to the Monterey Formation.

Bohacs, K.M., Grabowski Jr., G.J., Carroll, A.R., Mankiewicz, P.J., Miskell-Gerhardt, K.J., Schwalbach, J.R., Wegner, M.B., Simo, J.A., 2005. Production, destruction, and dilution—the many paths to

source-rock development. In: Harris, N.B. (Ed.), The Deposition of Organic-Carbon Rich Sediments: Models, Mechanisms, and Consequences. SEPM Special Publication 82, pp. 61–101.

Bond, D. P., Zatoń, M., Wignall, P. B., & Marynowski, L. (2013). Evidence for shallow-water 'Upper Kellwasser'anoxia in the Frasnian–Famennian reefs of Alberta, Canada. *Lethaia*, *46*(3), 355-368.

Boulesteix, K., Poyatos-Moré, M., Flint, S. S., Taylor, K. G., Hodgson, D. M., & Hasiotis, S. T. (2019). Transport and deposition of mud in deep-water environments: Processes and stratigraphic implications. *Sedimentology*, *66*(7), 2894-2925.

Bover-Arnal, T., Salas, R., Moreno-Bedmar, J. A., & Bitzer, K. (2009). Sequence stratigraphy and architecture of a late Early–Middle Aptian carbonate platform succession from the western Maestrat Basin (Iberian Chain, Spain). *Sedimentary Geology*, *219*(1-4), 280-301.

Brett, C. E., Baird, G. C., & Witzke, B. J. (1996). Middle Devonian sedimentary cycles and sequences in the northern Appalachian Basin. *Special Papers-Geological Society of America*, 213-242.

Bromley, R. G., & Ekdale, A. A. (1984). Chondrites: a trace fossil indicator of anoxia in sediments. *Science*, *224*(4651), 872-874.

Campbell, G. (1946). New Albany Shale. *Geological Society of America Bulletin*, *57*(9), 829-908.

Cattaneo, A., & Steel, R. J. (2003). Transgressive deposits: a review of their variability. *Earth-Science Reviews*, *62*(3-4), 187-228.

Catuneanu, O. (2006). *Principles of sequence stratigraphy*. Elsevier.

Catuneanu, O., Galloway, W. E., Kendall, C. G. S. C., Miall, A. D., Posamentier, H. W., Strasser, A., & Tucker, M. E. (2011). Sequence stratigraphy: methodology and nomenclature. *Newsletters on stratigraphy*, *44*(3), 173-245.

Catuneanu, O. (2020). Sequence stratigraphy of deep-water systems. *Marine and Petroleum Geology*, *114*, 104238.

Chow, N., & Wendte, J. (2011). Palaeosols and palaeokarst beneath subaerial unconformities in an Upper Devonian isolated reef complex (Judy Creek), Swan Hills Formation, west-central Alberta, Canada. *Sedimentology*, *58*(4), 960-993.

Cowan, C. A., & James, N. P. (1992). Diastasis cracks: mechanically generated synaeresis-like cracks in Upper Cambrian shallow water oolite and ribbon carbonates. *Sedimentology*, *39*(6), 1101-1118.

Creaney, S., Passey, Q.R. (1993). Recurring patterns of total organic carbon and source rock quality within a sequence stratigraphic framework. *AAPG Bull*. 77, 386–401.

Dix, G. R. (1990). Stages of platform development in the Upper Devonian (Frasnian) Leduc Formation, Peace River Arch, Alberta. *Bulletin of Canadian Petroleum Geology*, *38*(1), 66-92.

Dong, T. (2016). Geochemical, petrophysical and geomechanical properties of stratigraphic sequences in Horn River Shale, Middle and Upper Devonian, northeastern British Columbia, Canada.

Dong, T., Harris, N. B., Ayranci, K., & Yang, S. (2017). The impact of rock composition on geomechanical properties of a shale formation: Middle and Upper Devonian Horn River Group shale, Northeast British Columbia, Canada. *AAPG Bulletin*, *101*(2), 177-204.

Dong, T., Harris, N. B., Knapp, L. J., McMillan, J. M., & Bish, D. L. (2018). The effect of thermal maturity on geomechanical properties in shale reservoirs: An example from the Upper Devonian Duvernay Formation, Western Canada Sedimentary Basin. *Marine and Petroleum Geology*, *97*, 137-153.

Dong, T., Harris, N. B., McMillan, J. M., Twemlow, C. E., Nassichuk, B. R., & Bish, D. L. (2019). A model for porosity evolution in shale reservoirs: An example from the Upper Devonian Duvernay Formation, Western Canada Sedimentary Basin. *AAPG Bulletin*, *103*(5), 1017-1044.

Ekdale, A. A., & Mason, T. R. (1988). Characteristic trace-fossil associations in oxygen-poor sedimentary environments. *Geology*, *16*(8), 720-723.

Ferri, F., Hickin, A. S., & Huntley, D. H. (2011). Besa River Formation, western Liard Basin, British Columbia (NTS 094N): geochemistry and regional correlations. *Geoscience Reports*, 1-18.

Friedrichs, C. T., & Wright, L. D. (2004). Gravity-driven sediment transport on the continental shelf: implications for equilibrium profiles near river mouths. *Coastal Engineering*, *51*(8-9), 795-811.

Gingras, M. K., MacEachern, J. A., & Dashtgard, S. E. (2011). Process ichnology and the elucidation of physico-chemical stress. *Sedimentary Geology*, *237*(3-4), 115-134.

Glenn, C. R., & Arthur, M. A. (1990). Anatomy and origin of a Cretaceous phosphorite-greensand giant, Egypt. *Sedimentology*, *37*(1), 123-154.

Golonka, J., Ross, M. I., & Scotese, C. R. (1994). Phanerozoic paleogeographic and paleoclimatic modeling maps.

Hammes, U., & Frébourg, G. (2012). Haynesville and Bossier mudrocks: A facies and sequence stratigraphic investigation, East Texas and Louisiana, USA. *Marine and Petroleum Geology*, *31*(1), 8-26.

Handford, C. R., & Loucks, R. G. (1993). Carbonate depositional sequences and systems tracts--responses of carbonate platforms to relative sea-level changes: Chapter 1.

Harris, N. B., Miskimins, J. L., & Mnich, C. A. (2011). Mechanical anisotropy in the Woodford Shale, Permian Basin: Origin, magnitude, and scale. *The Leading Edge*, *30*(3), 284-291.

Harris, N. B., McMillan, J. M., Knapp, L. J., & Mastalerz, M. (2018). Organic matter accumulation in the Upper Devonian Duvernay Formation, Western Canada Sedimentary Basin, from sequence stratigraphic analysis and geochemical proxies. *Sedimentary Geology*, *376*, 185-203.

Helland-Hansen, W., & Martinsen, O. J. (1996). Shoreline trajectories and sequences; description of variable depositional-dip scenarios. *Journal of Sedimentary Research*, *66*(4), 670-688.

Hemmesch, N. T., Harris, N. B., Mnich, C. A., & Selby, D. (2014). A sequence-stratigraphic framework for the upper Devonian Woodford Shale, Permian Basin, west Texas. *AAPG Bulletin*, *98*(1), 23-47.

Hunt, D., & Tucker, M. E. (1992). Stranded parasequences and the forced regressive wedge systems tract: deposition during base-level fall. *Sedimentary Geology*, *81*(1-2), 1-9.

Johnson, J. G., Klapper, G., & Sandberg, C. A. (1985). Devonian eustatic fluctuations in Euramerica. *Geological Society of America Bulletin*, *96*(5), 567-587.

Kennedy, M. J., Pevear, D. R., & Hill, R. J. (2002). Mineral surface control of organic carbon in black shale. *Science*, *295*(5555), 657-660.

Killops, S., Killops, V. (2005). Introduction to Organic Geochemistry. second ed. Blackwell Publishing, Malden, MA, USA (406 pp.).

Kiørboe, T. (2001). Formation and fate of marine snow: small-scale processes with large-scale implications. *Scientia marina*, *65*(S2), 57-71.

Klapper, G. (1988). The Montagne Noire Frasnian (Upper Devonian) conodont succession.

Knapp, L. J., McMillan, J. M., & Harris, N. B. (2017). A depositional model for organic-rich Duvernay Formation mudstones. *Sedimentary Geology*, *347*, 160-182.

Knapp, L. J., Harris, N. B., & McMillan, J. M. (2019). A sequence stratigraphic model for the organic-rich Upper Devonian Duvernay Formation, Alberta, Canada. *Sedimentary Geology*, *387*, 152-181.

Könitzer, S. F., Davies, S. J., Stephenson, M. H., & Leng, M. J. (2014). Depositional controls on mudstone lithofacies in a basinal setting: implications for the delivery of sedimentary organic matter. *Journal of Sedimentary Research*, *84*(3), 198-214.

Lalonde, K., Mucci, A., Ouellet, A., & Gélinas, Y. (2012). Iron promotes the preservation of organic matter in sediments. *Nature*, *483*, 198-200.

Lash, G. G., & Blood, D. R. (2006). The Upper Devonian Rhinestreet black shale of western New York state—Evolution of a hydrocarbon system. In *New York State Geological Association, 78th Annual Meeting Guidebook* (pp. 223-289). University at Buffalo.

Lazar, O. R., Bohacs, K. M., Macquaker, J. H., Schieber, J., & Demko, T. M. (2015). Capturing Key Attributes of Fine-Grained Sedimentary Rocks In Outcrops, Cores, and Thin Sections: Nomenclature and Description GuidelinesMUDSTONES: NOMENCLATURE AND DESCRIPTION GUIDELINES. *Journal of Sedimentary Research*, *85*(3), 230-246.

Lehrmann, D. J., & Goldhammer, R. K. (1999). Secular variation in parasequence and facies stacking patterns of platform carbonates: a guide to application of stacking-patterns analysis in strata of diverse ages and settings.Rebesco, M., & Camerlenghi, A. (Eds.). (2008). *Contourites*. Elsevier.

Li, Y., & Schieber, J. (2015). On the origin of a phosphate enriched interval in the Chattanooga Shale (Upper Devonian) of Tennessee—A combined sedimentologic, petrographic, and geochemical study. *Sedimentary Geology*, *329*, 40-61.

Liu, B., Schieber, J., Mastalerz, M., & Teng, J. (2019). Organic matter content and type variation in the sequence stratigraphic context of the Upper Devonian New Albany Shale, Illinois Basin. *Sedimentary Geology*, *383*, 101-120.

Lowe, D. R., & LoPiccolo, R. D. (1974). The characteristics and origins of dish and pillar structures. *Journal of Sedimentary Research*, *44*(2), 484-501.

Lowe, D. R. (1975). Water escape structures in coarse-grained sediments. *Sedimentology*, *22*(2), 157-204.

Macquaker, J. H., Taylor, K. G., & Gawthorpe, R. L. (2007). High-resolution facies analyses of mudstones: implications for paleoenvironmental and sequence stratigraphic interpretations of offshore ancient mud-dominated successions. *Journal of Sedimentary Research*, *77*(4), 324-339.

Macquaker, J. H., Bentley, S. J., & Bohacs, K. M. (2010) A. Wave-enhanced sediment-gravity flows and mud dispersal across continental shelves: Reappraising sediment transport processes operating in ancient mudstone successions. *Geology*, *38*(10), 947-950.

Macquaker, J. H., Keller, M. A., & Davies, S. J. (2010) B. Algal blooms and “marine snow”: Mechanisms that enhance preservation of organic carbon in ancient fine-grained sediments. *Journal of sedimentary Research*, *80*(11), 934-942.

Martín–Chivelet, J., Fregenal–Martínez, M. A., & Chacón, B. (2008). Traction structures in contourites. *Developments in Sedimentology*, *60*, 157-182.

McCrossan, R. G. (1961). Resistivity mapping and petrophysical study of Upper Devonian inter-reef calcareous shales of central Alberta, Canada. *AAPG Bulletin*, *45*(4), 441-470.

McLaughlin, P. I., Brett, C. E., & Wilson, M. A. (2008). Hierarchy of sedimentary discontinuity surfaces and condensed beds from the middle Paleozoic of eastern North America: implications for cratonic sequence stratigraphy. *Geological Association of Canada Special Paper*, *48*, 175-200.

Moretti, M., Soria, J. M., Alfaro, P., & Walsh, N. (2001). Asymmetrical soft-sediment deformation structures triggered by rapid sedimentation in turbiditic deposits (Late Miocene, Guadix Basin, southern Spain). *Facies*, *44*(1), 283-294.

Mountjoy, E. (1980). Some questions about the development of Upper Devonian carbonate buildups (reefs), Western Canada. *Bulletin of Canadian Petroleum Geology*, *28*(3), 315-344.

Mulder, T., Faugeres, J.-C., Gonthier, E. (2009). Mixed turbidite-contourite systems, in: Rebesco, M., Camerlenghi, A. (Eds.), Contourites. Elsevier, Amsterdam, pp. 435–456, forthcoming.

Oldale, H. S., Munday, R. J., & Ma, K. (1994). Devonian Beaverhill Lake Group of the western Canada sedimentary basin. In *Geological Atlas of the Western Canada Sedimentary Basin* (Vol. 4). Calgary, AB: Canadian Society of Petroleum Geologists and Alberta Research Council.

Oliver, T. A., & Cowper, N. W. (1963). Depositional environments of the Ireton Formation, central Alberta. *Bulletin of Canadian Petroleum Geology*, *11*(2), 183-202.

Owen, G. (2003). Load structures: gravity-driven sediment mobilization in the shallow subsurface. *Geological Society, London, Special Publications*, *216*(1), 21-34.

Patchett, P. J., Embry, A. F., Ross, G. M., Beauchamp, B., Harrison, J. C., Mayr, U., Isachsen, C. E., Rosenberg, E. J. & Spence, G. O. (2004). Sedimentary cover of the Canadian Shield through Mesozoic time reflected by Nd isotopic and geochemical results for the Sverdrup Basin, Arctic Canada. *The Journal of Geology*, *112*(1), 39-57.

Pemberton, S. G., & MacEachern, J. A. (1995). The sequence stratigraphic significance of trace fossils: examples from the Cretaceous foreland basin of Alberta, Canada.

Plint, A. G., & Nummedal, D. (2000). The falling stage systems tract: recognition and importance in sequence stratigraphic analysis. *Geological Society, London, Special Publications*, *172*(1), 1-17.

Potma, K., Weissenberger, J. A., Wong, P. K., & Gilhooly, M. G. (2001). Toward a sequence stratigraphic framework for the Frasnian of the Western Canada Basin. *Bulletin of Canadian Petroleum Geology*, *49*(1), 37-85.

Pratt, B. R., & Kimmig, J. (2019). Extensive bioturbation in a middle Cambrian Burgess Shale–type fossil Lagerstätte in northwestern Canada. *Geology*, *47*(3), 231-234.

Preston, A., Garner, G., Beavis, K., Sadiq, O., & Stricker, S. (2016). *Duvernay Reserves and Resources Report: A Comprehensive Analysis of Alberta's Foremost Liquids-Rich Shale Resource*. Alberta Energy Regulator.

Read, J. F. (1995). Overview of carbonate platform sequences, cycle stratigraphy and reservoirs in greenhouse and icehouse worlds.

Lehrmann, D. J., & Goldhammer, R. K. (1999). Secular variation in parasequence and facies stacking patterns of platform carbonates: a guide to application of stacking-patterns analysis in strata of diverse ages and settings.Rebesco, M., & Camerlenghi, A. (Eds.). (2008). *Contourites*. Elsevier.

Rebesco, M., & Camerlenghi, A. (Eds.). (2008). *Contourites*. Elsevier.

Rebesco, M., Hernández-Molina, F. J., Van Rooij, D., & Wåhlin, A. (2014). Contourites and associated sediments controlled by deep-water circulation processes: state-of-the-art and future considerations. *Marine Geology*, *352*, 111-154.

Richiano, S., Schwarz, E., Veiga, G. D., & Trentini, G. Á. (2019). Non-depositional and erosional “offshore” bioeroded hardgrounds from the Lower Cretaceous of the Neuquén Basin, Argentina: Insights into their sequence-stratigraphic implications and controls. *Marine and Petroleum Geology*, *104*, 1-10.

Rokosh, C. D., Lyster, S., Anderson, S. D. A., Beaton, A. P., Berhane, H., Brazzoni, T., Chen, D., Cheng, Y., Mack, T., Pana, C. & Pawlowicz, J. G. (2012). Summary of Alberta’s shale-and siltstone-

hosted hydrocarbon resource potential. *Energy Resources Conservation Board, ERCB/AGS Open File Report*, *6*, 327.

Savrda, C. E., Bottjer, D. J., & Gorsline, D. S. (1984). Development of a comprehensive oxygen-deficient marine biofacies model: evidence from Santa Monica, San Pedro, and Santa Barbara Basins, California Continental Borderland. *AAPG bulletin*, *68*(9), 1179-1192.

Scasso, R. A., & Castro, L. N. (1999). Cenozoic phosphatic deposits in North Patagonia, Argentina: Phosphogenesis, sequence-stratigraphy and paleoceanography. *Journal of South American Earth Sciences*, *12*(5), 471-487.

Schieber, J. (1994). Evidence for high-energy events and shallow-water deposition in the Chattanooga Shale, Devonian, central Tennessee, USA. *Sedimentary Geology*, *93*(3-4), 193-208.

Schieber, J. (1998a). Developing a sequence stratigraphic framework for the Late Devonian Chattanooga Shale of the southeastern USA: relevance for the Bakken Shale. Williston Basin Symposium.

Schieber, J. (1998b). Sedimentary features indicating erosion, condensation, and hiatuses in the Chattanooga Shale of Central Tennessee: relevance for sedimentary and stratigraphic evolution. In *Shales and mudstones (Volume I, Basin studies, sedimentology, and paleontology)* (pp. 187-215).

Schieber, J. (1999). Distribution and deposition of mudstone facies in the Upper Devonian Sonyea Group of New York. *Journal of Sedimentary Research*, *69*(4), 909-925.

Schieber, J. (2002). The role of an organic slime matrix in the formation of pyritized burrow trails and pyrite concretions. *Palaios*, *17*(1), 104-109.

Schieber, J., & Riciputi, L. (2004). Pyrite ooids in Devonian black shales record intermittent sea-level drop and shallow-water conditions. *Geology*, *32*(4), 305-308.

Schieber, J. (2009). Discovery of agglutinated benthic foraminifera in Devonian black shales and their relevance for the redox state of ancient seas. *Palaeogeography, Palaeoclimatology, Palaeoecology*, *271*(3-4), 292-300.

Schieber, J., & Southard, J. B. (2009). Bedload transport of mud by floccule ripples—Direct observation of ripple migration processes and their implications. *Geology*, *37*(6), 483-486.

Schlager, W., Reijmer, J. J., & Droxler, A. (1994). Highstand shedding of carbonate platforms. *Journal of Sedimentary Research*, *64*(3b), 270-281.

Shanmugam, G. (2000). 50 years of the turbidite paradigm (1950s—1990s): deep-water processes and facies models—a critical perspective. *Marine and petroleum Geology*, *17*(2), 285-342.

Shaw, D. J., Nicolas, M. P. B., & Chow, N. (2017). Stratigraphy and geochemistry of the Cretaceous Boyne Member, Carlile Forma-tion, in the Manitoba Potash Corporation core at 3-29-20-29W1, southwestern Manitoba (parts of NTS 65K1). *Report of Activities*, 173-182.

Simandl, G. J., Paradis, S., & Fajber, R. (2011). Sedimentary phosphate deposits mineral deposit profile F07. *Geological Fieldwork, 6p*.

Stoakes, F. A. (1980). Nature and control of shale basin fill and its effect on reef growth and termination: Upper Devonian Duvernay and Ireton formations of Alberta, Canada. *Bulletin of Canadian Petroleum Geology*, *28*(3), 345-410.

Stromberg, S. G., & Bluck, B. (1998). Turbidite facies, fluid-escape structures and mechanisms of emplacement of the Oligo-Miocene Aljibe Flysch, Gibraltar Arc, Betics, southern Spain. *Sedimentary Geology*, *115*(1-4), 267-288.

Switzer, S. B., Holland, W. G., Christie, D. S., Graf, G. C., Hedinger, A. S., McAuley, R. J., Wierzbicki, R. A., & Packard, J. J. (1994). Devonian Woodbend-Winterburn strata of the Western Canada sedimentary basin. *Geological Atlas of the Western Canada Sedimentary Basin*, 165-202.

Ulmer-Scholle, D. S., Scholle, P. A., Schieber, J., & Raine, R. J. (2014). *A color guide to the petrography of sandstones, siltstones, shales and associated rocks*. American Association of Petroleum Geologists.

van Buchem, F. S., Razin, P., Homewood, P. W., Philip, J. M., Eberli, G. P., Platel, J. P., Roger, J., Eschard, R., Desaubliaux, G. M. J., Boisseau, T., Leduc, J. P., Labourdette, R. & Cantabloube, S.

(1996). High resolution sequence stratigraphy of the Natih Formation (Cenomanian/Turonian) in Northern Oman: distribution of source rocks and reservoir facies. *GeoArabia*, *1*(1), 65-91.

Ver Straeten, C. A., Brett, C. E., & Sageman, B. B. (2011). Mudrock sequence stratigraphy: a multi-proxy (sedimentological, paleobiological and geochemical) approach, Devonian Appalachian Basin. *Palaeogeography, Palaeoclimatology, Palaeoecology*, *304*(1-2), 54-73.

Weissenberger, J. A. (1994). Frasnian reef and basinal strata of West Central Alberta: a combined sedimentological and biostratigraphic analysis. *Bulletin of Canadian Petroleum Geology*, *42*(1), 1-25.

Wignall, P. B., & Maynard, J. R. (1993). The Sequence Stratigraphy of Transgressive Black Shales: Chapter 4.

Williams, C. J., Hesselbo, S. P., Jenkyns, H. C., & Morgans-Bell, H. S. (2001). Quartz silt in mudrocks as a key to sequence stratigraphy (Kimmeridge Clay Formation, Late Jurassic, Wessex Basin, UK). *Terra Nova*, *13*(6), 449-455.

Wonfor, J. S., & Andrichuk, J. M. (1953). Upper Devonian in Stettler area, Alberta, Canada: Alberta Soc. *Petroleum Geologists Jour*, *1*(9), 3-6.

Wong, P. K., Weissenberger, J. A. W., Gilhooly, M. G., Playton, T. E., & Kerans, C. (2016). Revised regional Frasnian sequence stratigraphic framework, Alberta outcrop and subsurface. *New Advances in Devonian Carbonates: Outcrop Analogs, Reservoirs, and Chronostratigraphy*, *49*(1), 37-85.

Yawar, Z., & Schieber, J. (2017). On the origin of silt laminae in laminated shales. *Sedimentary geology*, *360*, 22-34.

APPENDIX A: Thin Section Descriptions

Core 1 - ATH HZ TWOCK

2827.75

- Surface
    - Likely sharp and erosive
        - Some possible truncation of laminae
        - Slightly deformation of underlying laminae (likely from compaction)
        - Slightly wavy surface
- Lag
    - Silt to m sand
    - Likely comprised of multiple lags/event beds
        - Sharp, erosional, wavy bases
        - More gradational tops
        - Fining upwards (to carbonate (and some quartz) fine silt and clay size grains at tops)
        - Likely 3 or 4 events
    - Composition
        - Styliolinid fragments
            - Some of circular ones have silica cement interiors
        - Tentaculitid fragments
        - Likely ostracod/small brachiopod fragments
        - Likely glauconite grains (subangular to subrounded)
        - Sparse phosphatic grains
            - Conodont elements
            - Likely fish bone fragments
            - Structureless peloids
        - Abundant possible pyritized grains or pyrite cement
- Above
    - Likely discontinuous pyrite laminae?
        - Planar laminated more siliceous matrix mud
    - Very rare, very small phosphate peloids throughout
    - One laminae of a couple glauconite grains
- Below
    - Clay rich mud with sparse calcite silt
    - Common small OM stringers
    - Small common pyrite grains

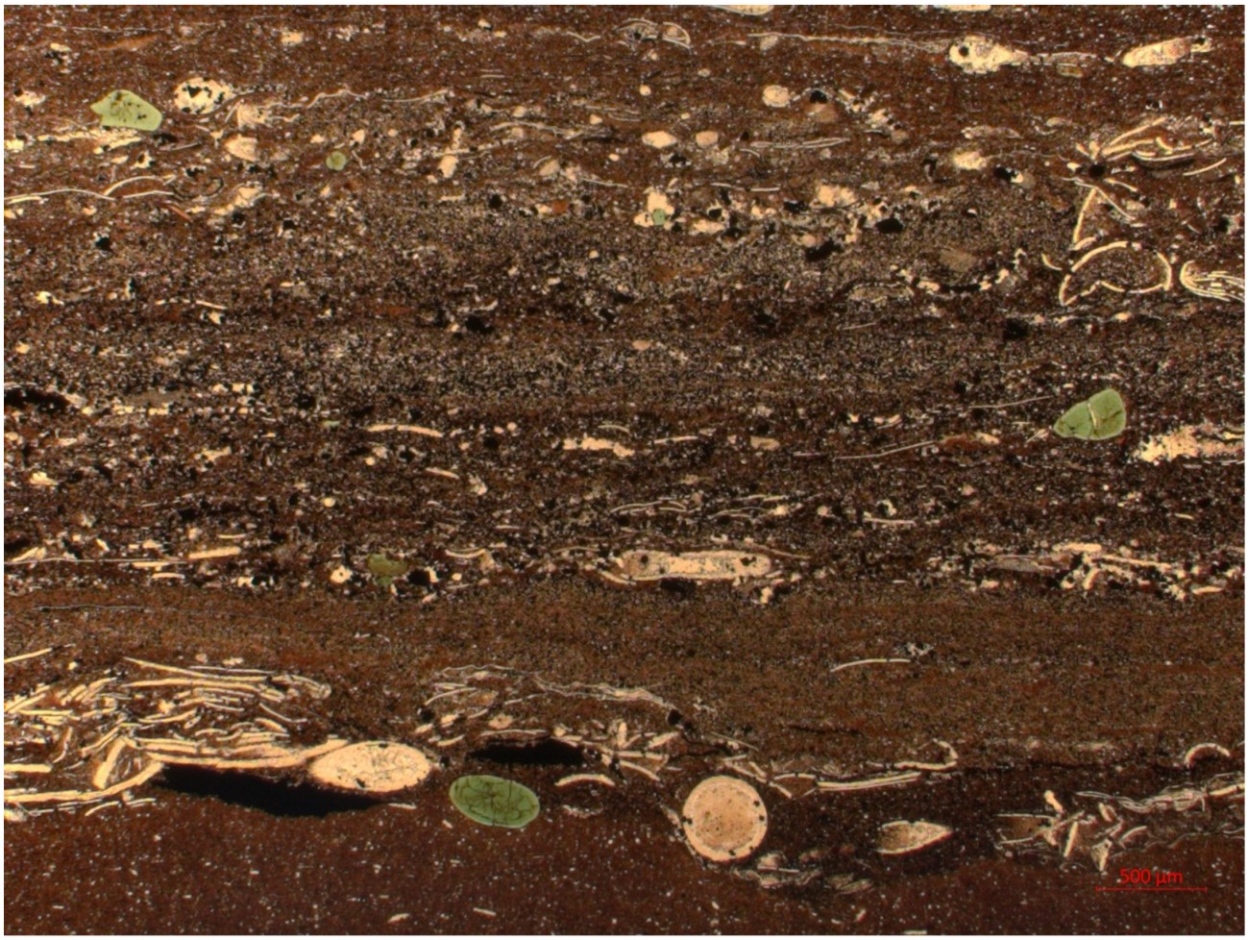

2826.55

- Mud (nearly siltstone) with planar silt laminae
- Silt laminae:
    - Up to 4mm thick
    - Up to m sand sized grains
        - Most of coarse component = coarse silt to vfs round calcite grains
            - Possibly calcitized calcispheres, peloids or pisoids?
        - Styliolinid fragments
            - Largest grains
        - Very sparse possible bivalve/brachiopod fragments
    - Sharp top and bottom contacts
    - Planar (to possibly slightly wavy)
- ~20-30% vfs to m.sand
    - Round calcite grains
        - Calcispheres?
    - Styliolinids
- ~30% m-coarse silt

    - ~65% calcite (lots of fossil fragments)
    - ~3% quartz
    - ~5% pyrite
- ~40% matrix
    - ~35% fine carbonate-silt (carbonate-rich matrix)
    - ~40% clay
    - ~10% OM?
    - ~5% pyrite
- Likely some calcite cement in matrix
- Likely sparse to moderate bioturbation
    - Subhorizontal to subvertical mud infilled burrows

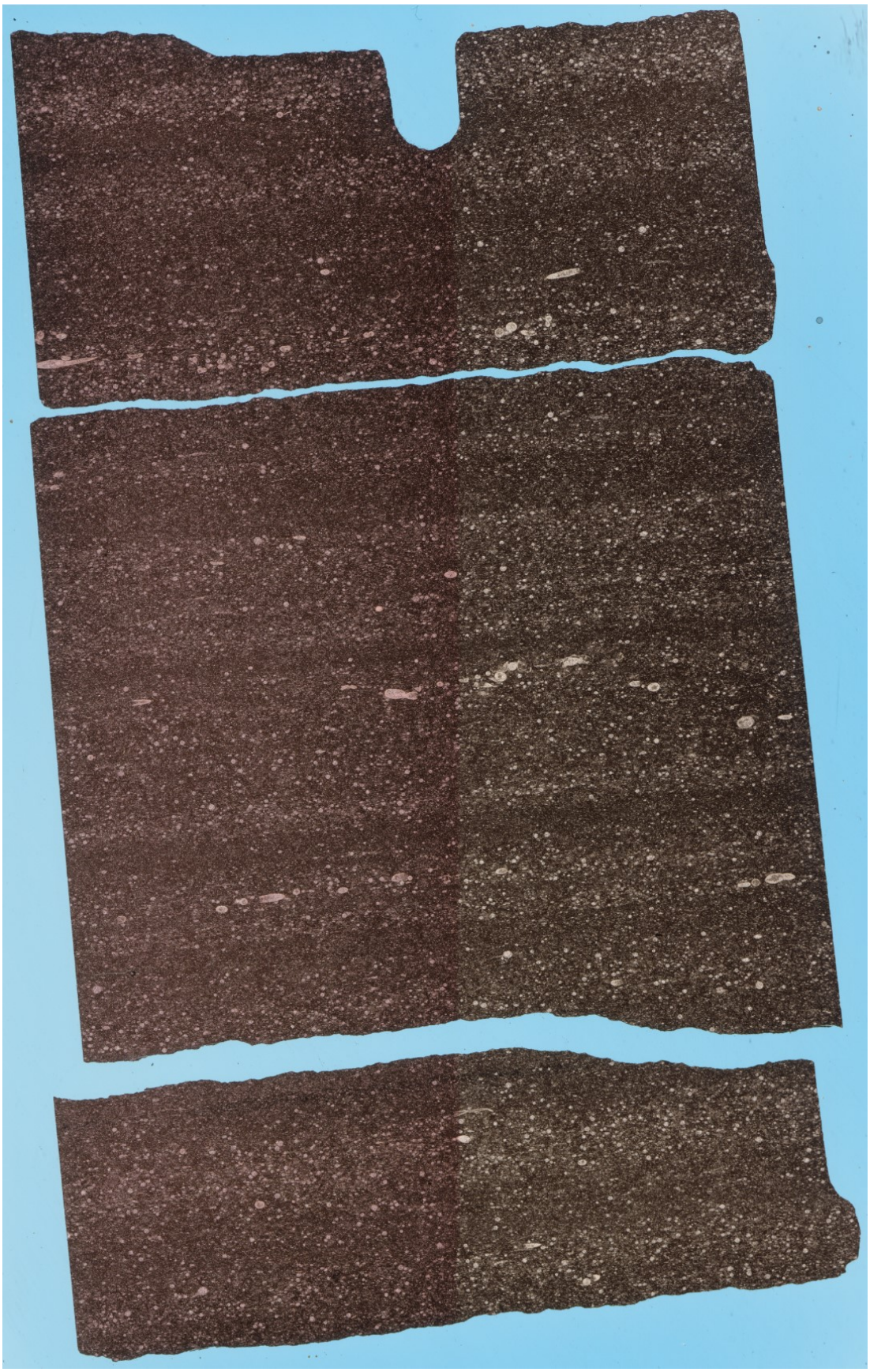

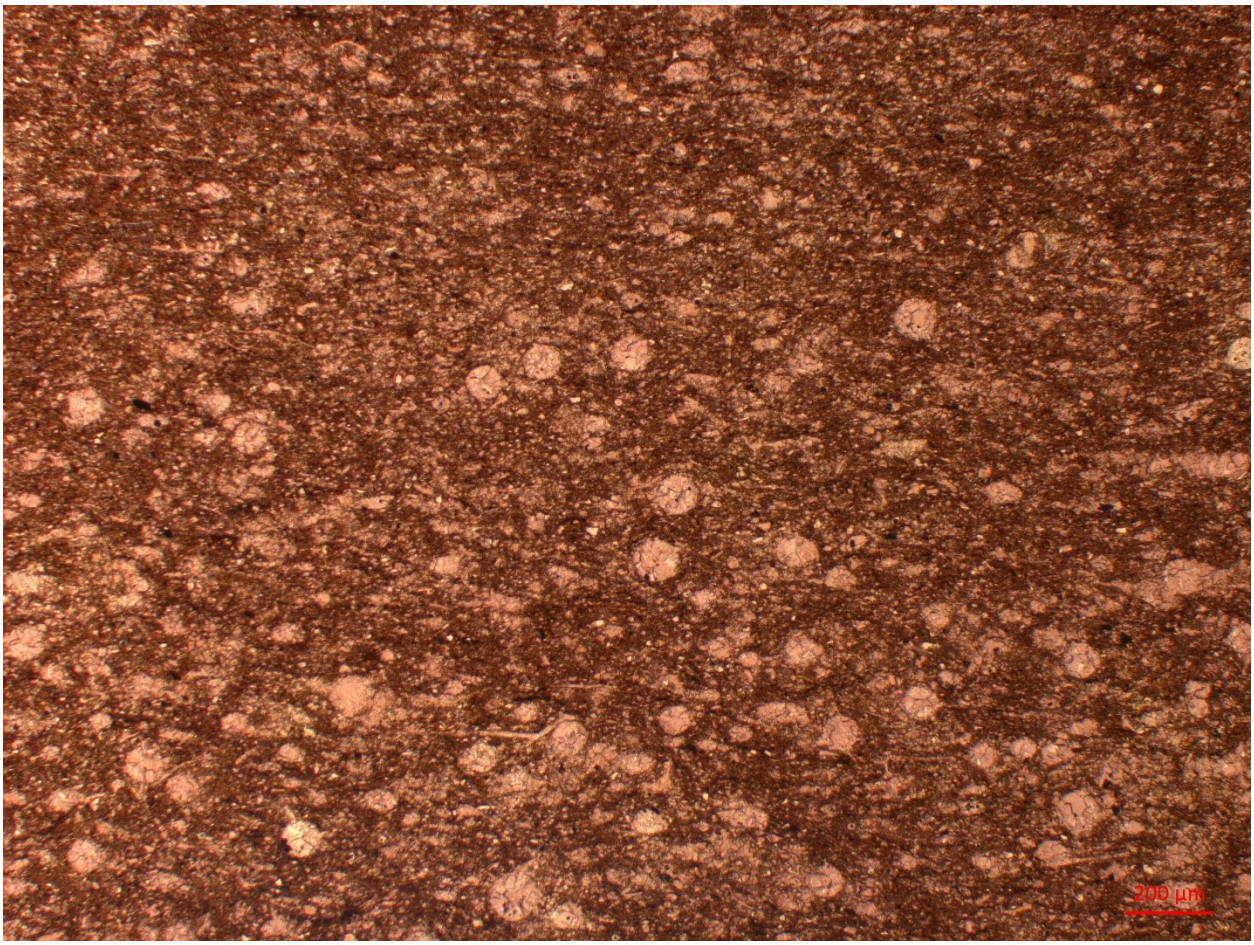

2825.63

- Mud with abundant fine to medium sand sized styliolinid fragments
- ~40% vf-m sand sized styliolinid fragments
    - Possibly some bivalve/brachiopod fragments
    - Oriented roughly bed parallel
    - Roughly organized into laminae
        - Appear planar to slightly wavy
        - Quite sharp contacts
- Appears moderately burrowed
    - Subvertical, mud infilled, pushing aside coarse grains
- Quite massive appearing mud and fine silt matrix

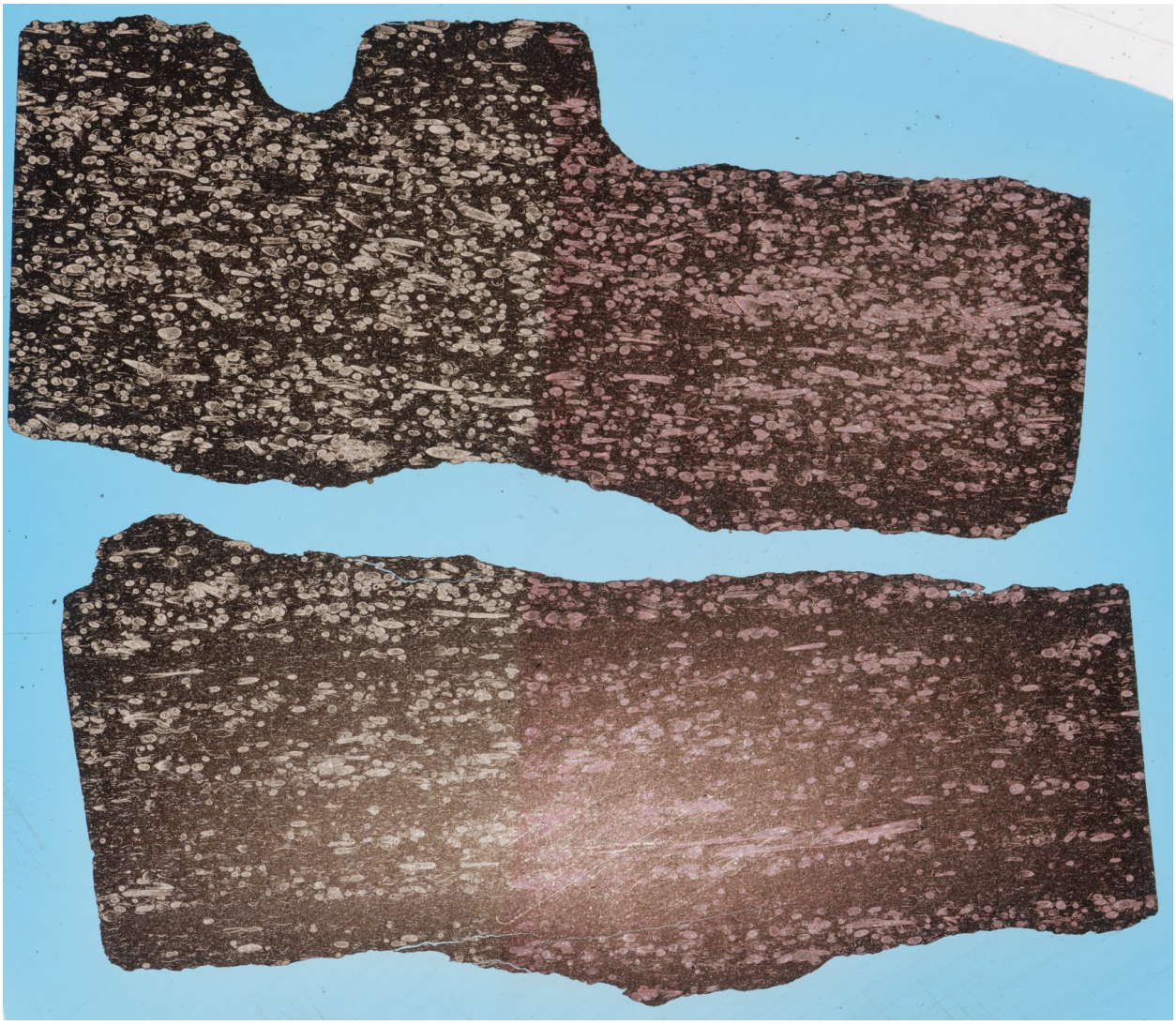

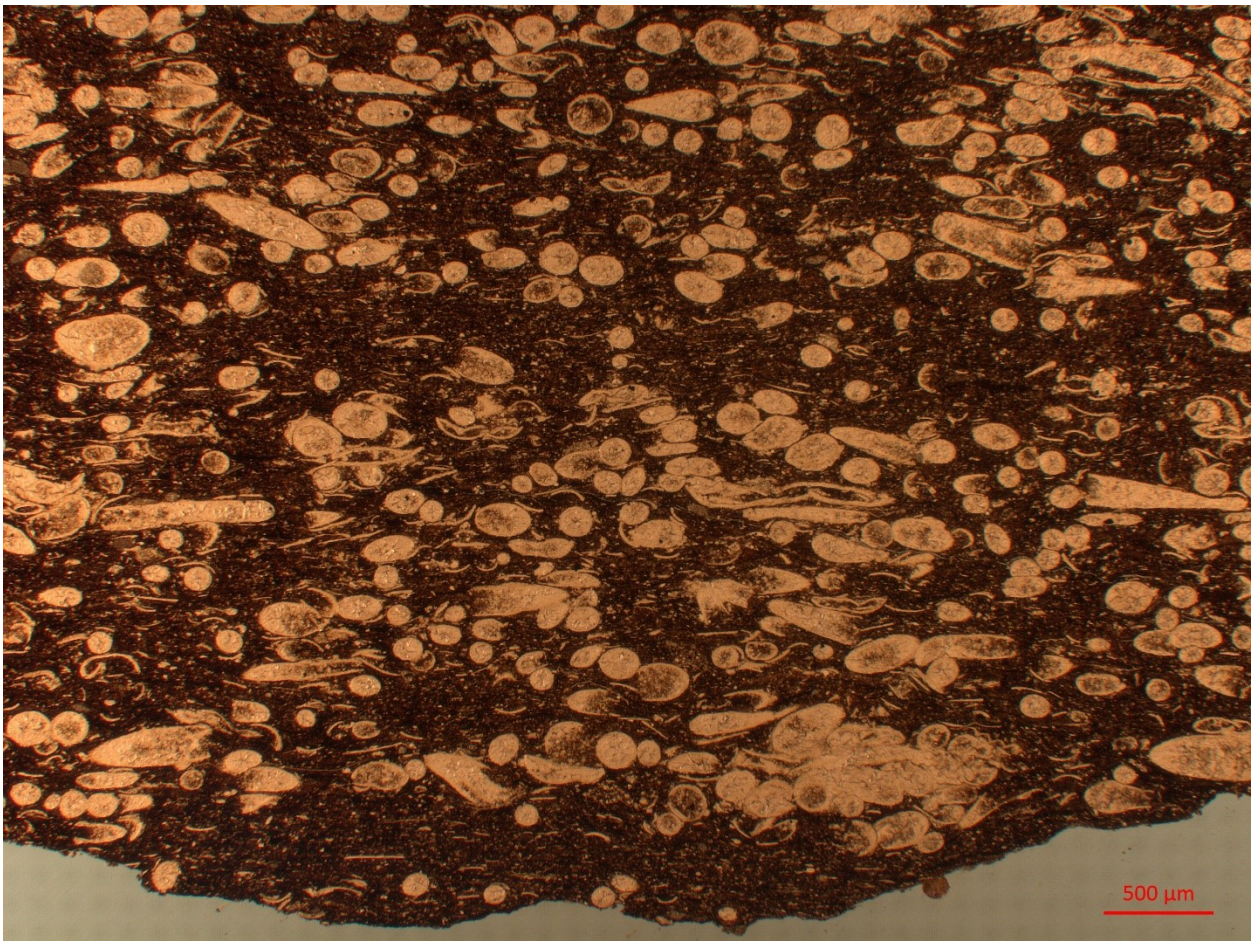

2825.15

- Planar laminae
    - Appears to be more OM- and pyrite-rich and OM- and pyrite-poor laminae
        - ~300 um thick
        - OM content appears to be biggest change in composition
        - Appear fairly continuous and planar
        - Very diffuse, possibly gradational, somewhat irregular boundaries
        - Fossil fragments common in both laminae but larger (more intact) styliolinid (ostracod/calcisphere??) fragments more common in OM-rich laminae
            - Possibly also more fossil fragments in OM-rich laminae but not obvious
            - OM:
                - Mostly disseminated through matrix and very thin small stringers (~5x50 um) long
                - Some stringers up to 20x100 um
        - Possibly more clay-rich in OM-poor laminae (but likely OM just covering clay)
- ~10% coarse silt to fine sand
    - ~65% calcite

        - Mostly styliolinid fragments
        - Some round grains
        - Other small fossil fragments (possibly some ostracod or brachiopod)
    - ~35% quartz
        - Round grains
- Rare phosphatic grains in matrix (f-c silt)

2821.17

- Quite massive appearing mud
    - Possibly some very faint possibly disrupted more organic- and pyrite-rich and organic- and pyrite-poor (more visible at top of thin section)
        - ~600-800 um thick
        - More discontinuous and disrupted
            - Wispy or disrupted?
            - Pinch and swell slightly
        - Diffuse and gradational contacts
        - OM:
            - Lots disseminated through matrix
            - Common stringers up to ~10 x 100 um
                - Typically 5x50um
        - Likely slightly greater concentration of pyrite grains in OM-rich laminae
            - Appears quite related to OM
        - Not that much difference in clay composition between laminae
        - No real obvious difference in grains size or composition otherwise

- ~5% sand sized grains
    - All fossil fragments
        - Styliolinids and tentaculitids
            - Possibly some ostracod and small brachiopod fragments
- ~20% vf-coarse silt
    - ~40% quartz
    - ~40% calcite
    - ~10% mica
    - ~10% pyrite
- ~75% matrix
    - ~85% clay
    - ~10% OM stringers
    - ~5% pyrite
- Likely intensely bioturbated
    - Massive appearance (burrow mottled)
        - No obvious visible burrows
    - Evidence of burrow mottling (possibly cryptic) throughout

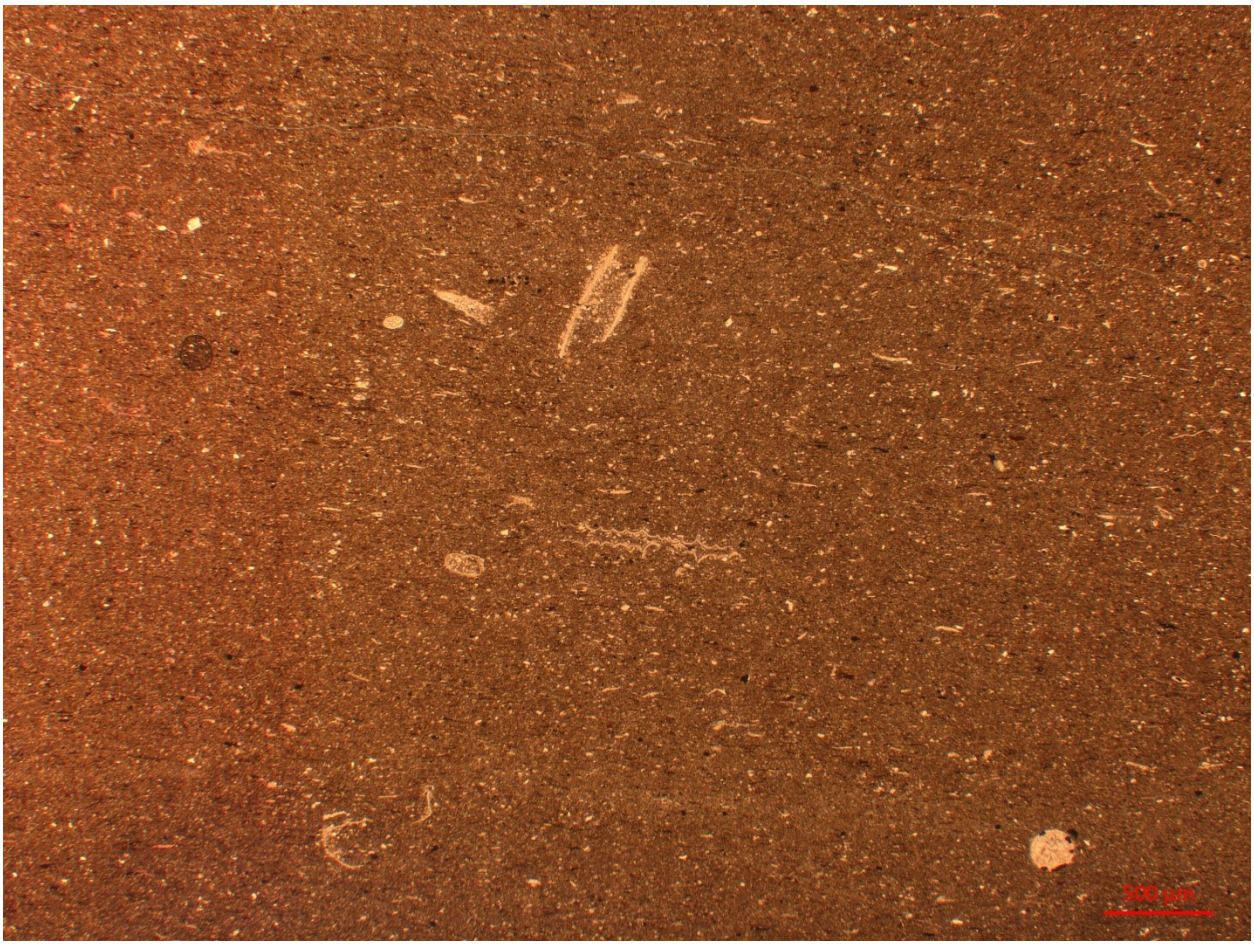

2820.44

- Planar laminated mud overlain by ~14 mm thick lag deposit (or possibly sediment gravity flow?)
- Planar laminated mud:
    - Planar to slightly wavy/undulatory
    - Slightly pinching/swelling to discontinuous
    - Pyrite-rich and pyrite-poor/clay-rich laminae
        - Appears to be basically the same makeup but pyrite-rich laminae has more pyrite (replacing clay?/growing in clay?)
    - Pyrite-rich laminae:
        - ~35% silt:
            - 40% Pyrite
            - 25% Quartz
            - 15% Mica
            - 10% Dolomite
            - 10% Calcite
        - ~65% matrix
            - ~30% pyrite

                - ~40% clay
                - ~15% OM
                - ~15% fine silt
        - Clay-rich laminae:
            - ~25% silt:
                - 30% Quartz
                - 25% Mica
                - 20% Dolomite
                - 15% Pyrite
                - 10% Calcite
            - ~75% matrix
                - ~10% pyrite
                - ~50% clay
                - ~15% OM
                - ~25% fine silt
- Lag deposit:
    - Slightly wavy, likely erosive bottom contact
    - Sharp, planar (to slightly wavy) top contact
    - Quite massive structure throughout
        - Slight bed parallel orientation to large fossil grains
    - ~30% silt/sand grains
        - ~65% fossiliferous
            - Mostly styliolinid fragments
            - Some possible ostracods
            - Tentaculitids
            - Conodonts
            - Some possible brachiopod fragments (maybe bivalve)
        - ~20% pyrite
        - ~10% blue/green mud rip up clasts (glauconite?)
        - ~5% phosphatic grains
    - 70% matrix
        - High clay content
        - Low pyrite/OM
        - ~50% clay
        - ~10% pyrite
        - ~40% fine silt
    - Likely moderately to intensely bioturbated

2819.43

- Faintly (possibly disrupted) planar laminated mudstone
- Faint, possibly disrupted planar laminae
    - More clay-rich and more pyrite/OM-rich laminae
    - Less sharp and planar contacts than siliceous planar laminated mud
    - Clay-rich laminae:
        - ~15-20% silt to vfs
            - ~30% Micas
            - ~30% Quartz
            - ~25% Dolomite
            - ~15% pyrite
            - ~1% phosphatic grains
        - ~60% clay
            - Most appears in Aggregate form
        - ~10% OM?
        - ~10% fine pyrite
    - Pyrite/OM rich laminae

        - 20% silt to vfs
            - ~35% quartz
            - ~25% pyrite
            - ~25% Dolomite
            - ~15% mica
        - ~40% Clay
            - ~25% in clay aggregates
        - ~20% OM
        - ~20% fine pyrite
- Possibly some fossil fragments but not obvious
- Likely moderately to intensely bioturbated
    - Mud infilled
    - More pyritized
    - Subvertical
    - Cross cutting silt laminae

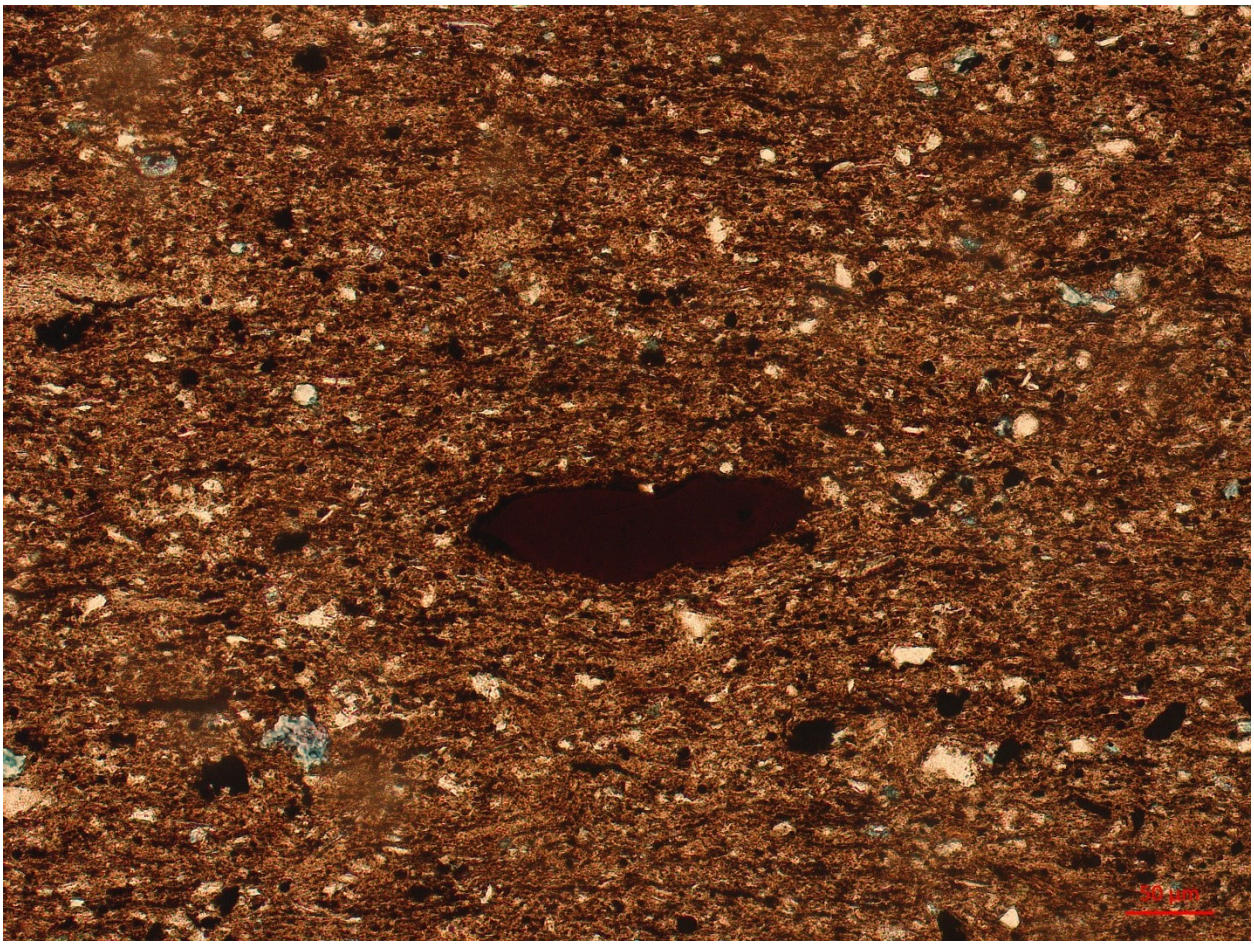

2816.69

- Nodular wackestone
    - Up to vfs
    - ~20% vfs very round calcite grains (possibly calcitized styliolinids or peloids or pisoids)
    - ~40% calcite silt
    - ~40% calcite cement and carbonate mud?
    - ~1% pyrite grains
    - <1% quartz grains
    - Quite massive
        - Likely moderate to intensely bioturbated
    - Sparse visible fossil fragments (brachiopods/ostracods?) but most grains very recrystallized

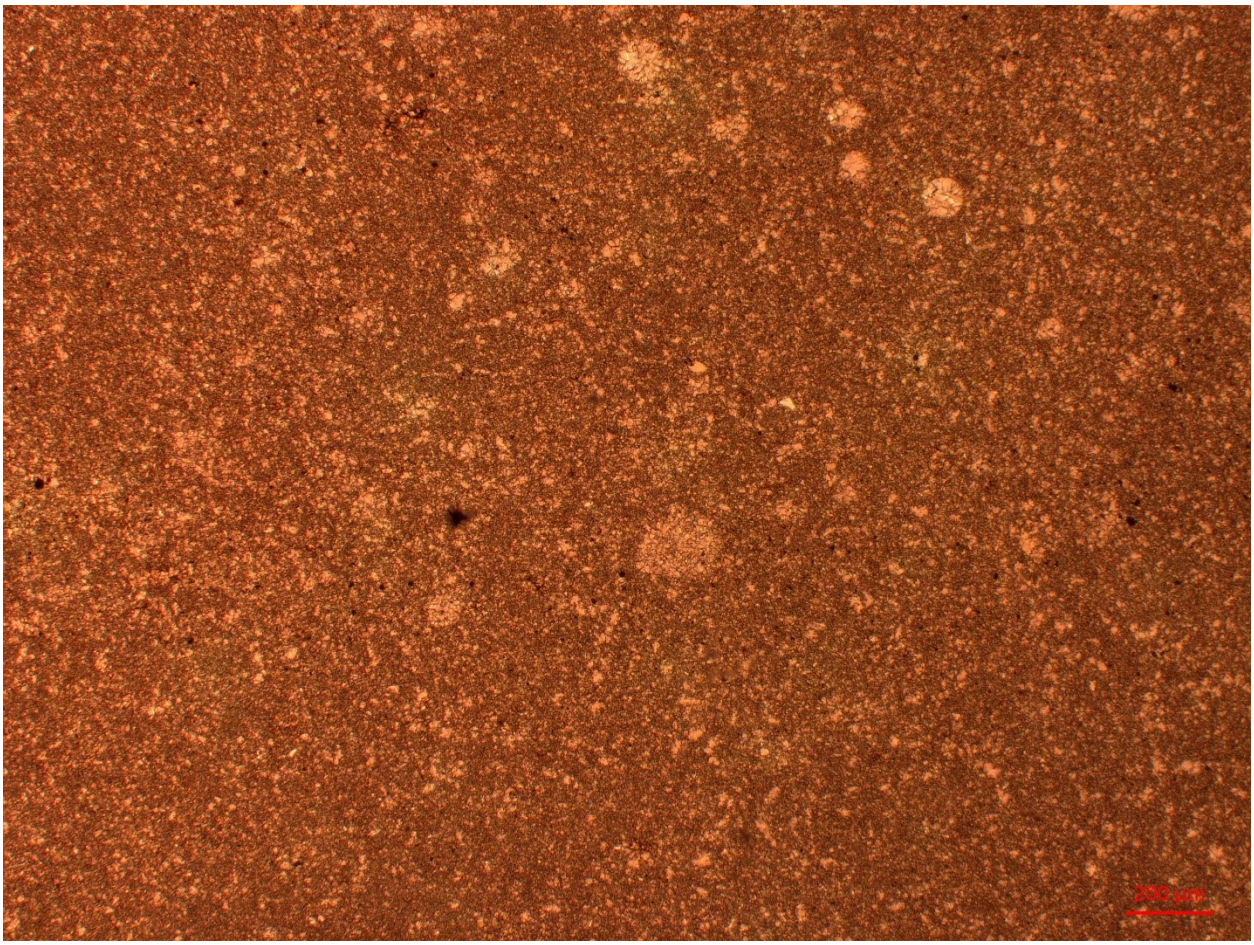

2807.65

- Wackestone nodules in mud matrix
- Matrix = massive to faintly planar laminated mud
    - ~20-30% silt
        - ~90% calcite
            - Predominantly fossil fragments (likely styliolinids, ostracods, brachiopods)
        - ~5% quartz
        - ~5% pyrite
- Wackestone nodules:
    - Up to vfs
    - ~96% calcite
        - ~10-15% fossil fragments
            - Styliolinids
            - Ostracods/brachiopods
        - Up to 20% calcite cement??
    - ~1% quartz

    - ~3% pyrite
    - Grains become coarser and less fossiliferous towards edges of wackestone nodules
- Likely moderately to intensely bioturbated

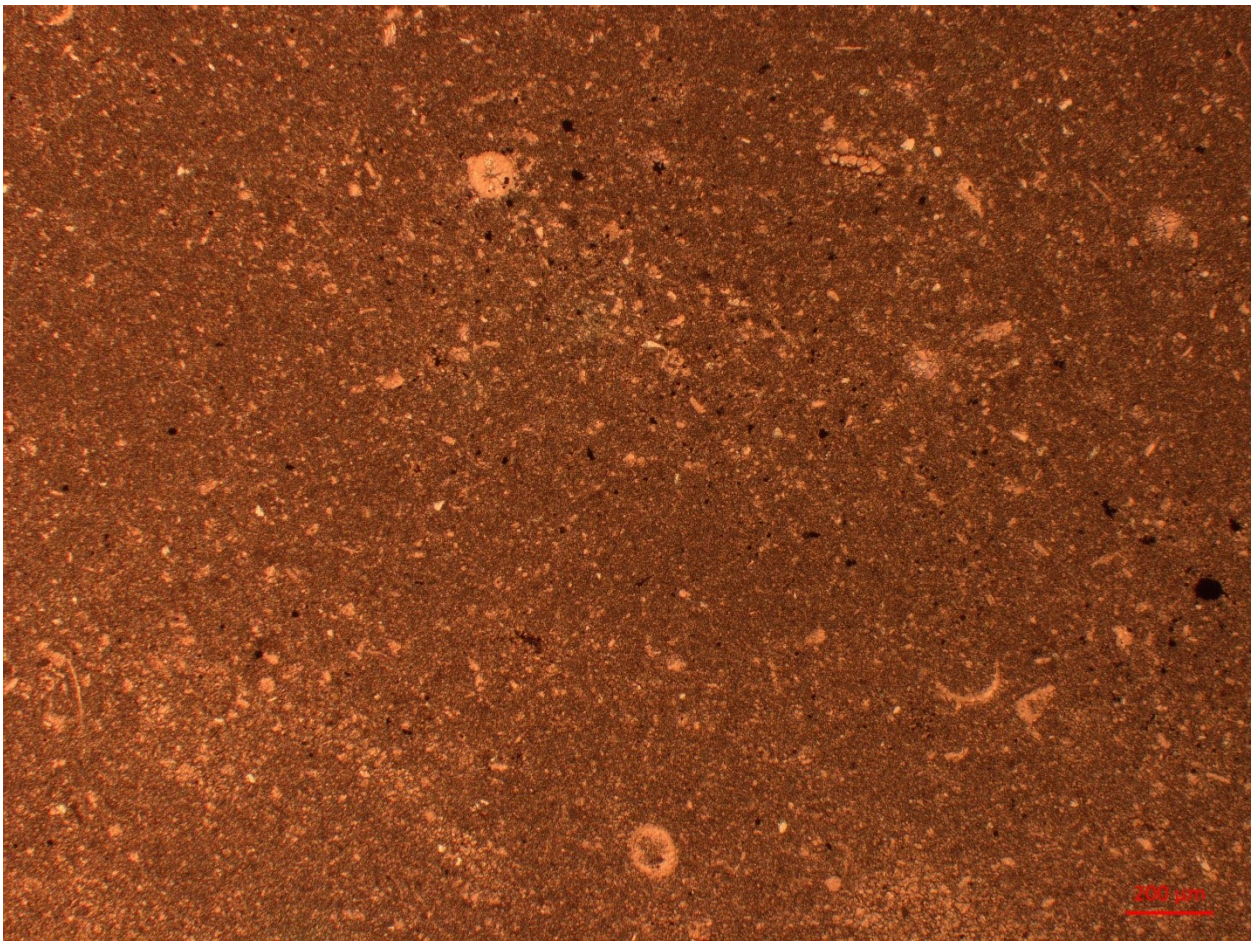

2805.74

- Surface
    - Likely the sharp contact between underlying nodular wackestone and overlying silty planar laminated mud
        - Very sharp surface
            - Likely erosive (some possible scour)
                - Quite massive underlying sediment (hard to tell if crosscutting)
            - Quite planar
    - Possibly bottom of 0.3mm thick ostracod/small brach/styliolinid rich layer at top of nodular wackestone
- Lag
    - Silt - VFS size
    - A few coarse grains distributed along the erosive surface
    - Composition
        - One feldspar grain (twinning)
        - Some very dissolved, pyritized calcite grains
        - Some styliolinid/ostracod/small brachiopod fragments

            - One shell fragment interior has purple stain, likely dolomite replacement
        - Two phosphatic conodont element or skeletal grains
- Above
    - Couple phosphate peloids visible above lag
        - Typically in silt laminae
    - Abundant quartz silt roughly concentrated into laminae
        - Some dolomite grains
    - Abundant OM and pyrite in matrix
    - Lots of clay in matrix too
- Below
    - Very massive carbonate-rich mud
    - Common shell fragments distributed throughout
        - Some rough alignment into lamiane
    - Some fine quartz silt and pyrite grains throughout
    - Little to no OM
    - Rare very small phosphate peloids randomly distributed
    - Likely quite bioturbated
    - Possible large pyritized burrows

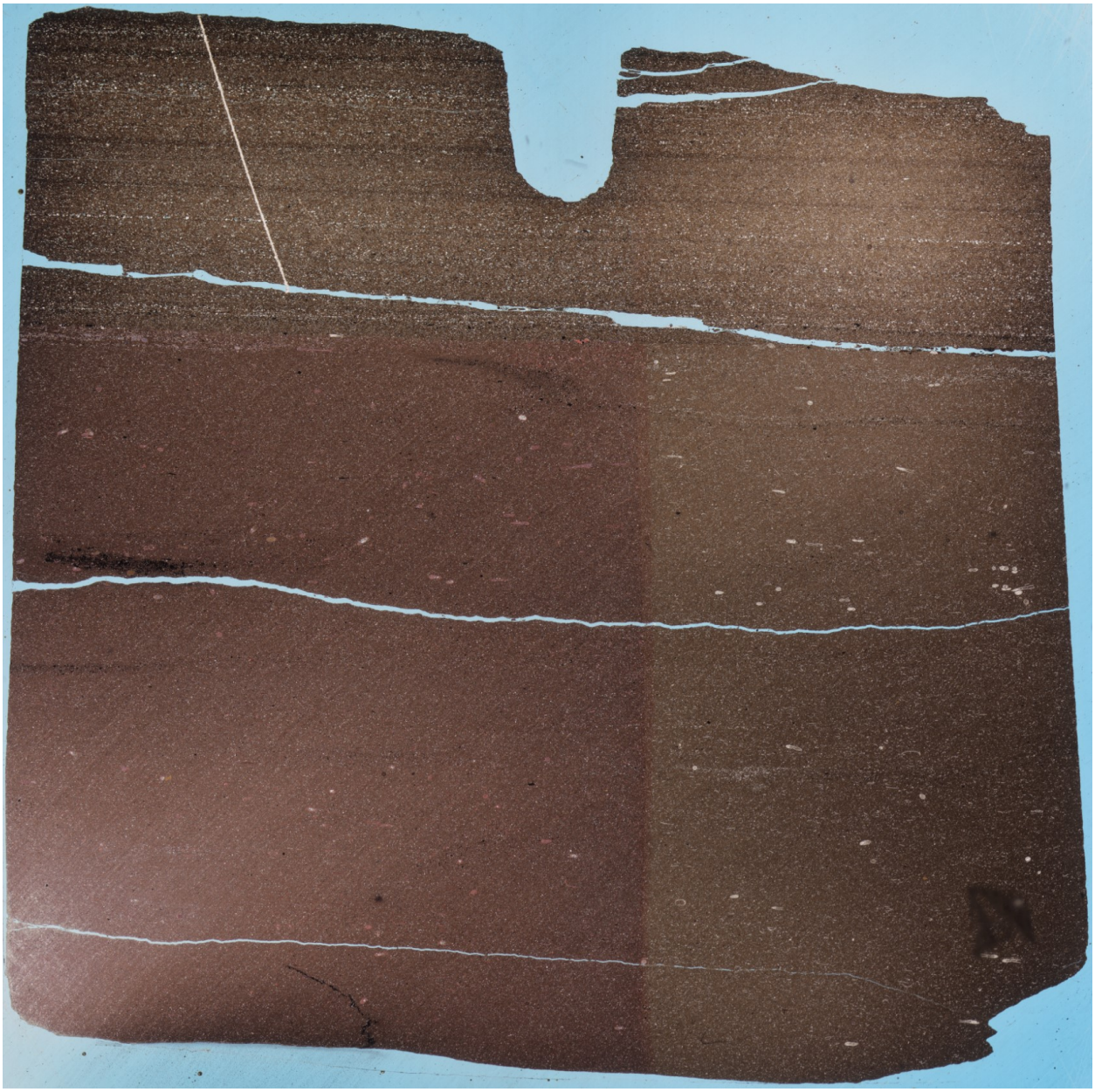

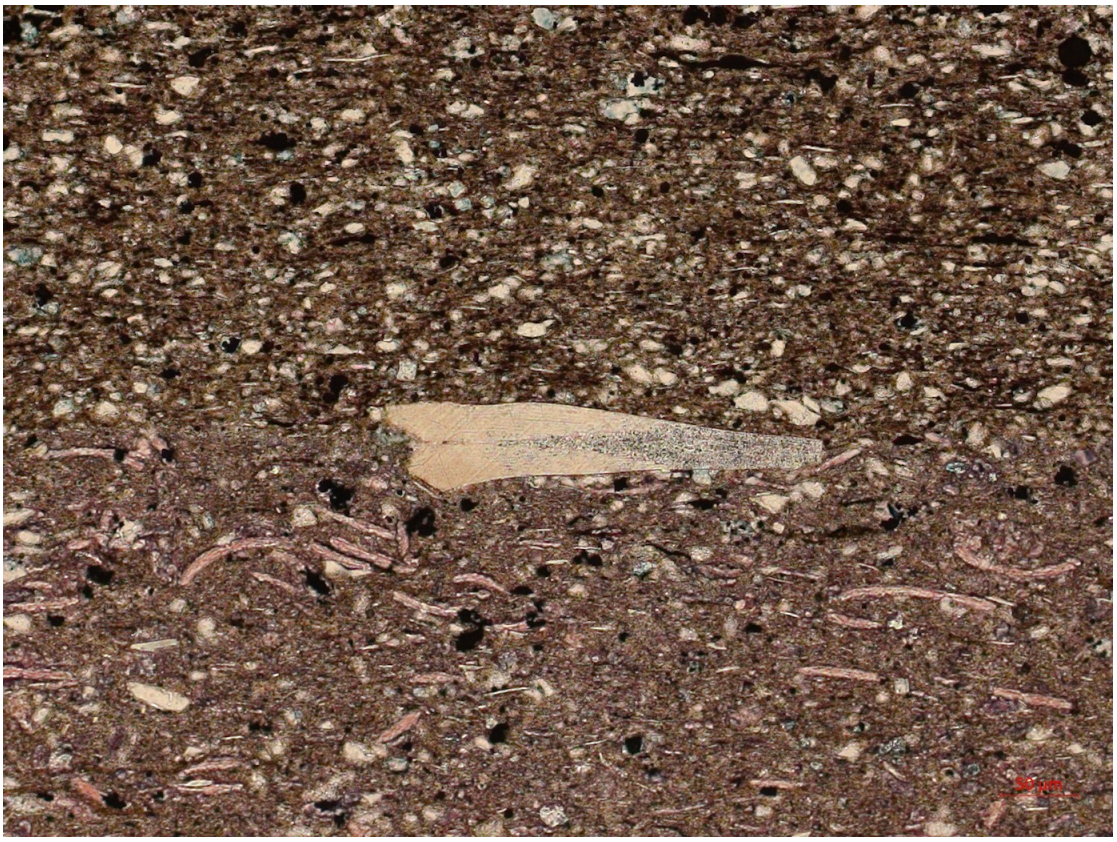

2799.86

- Wavy silt/vfs laminae in mud
    - Up to 1.5 mm thick
    - Some sharp bases and tops; no obvious grading
    - Some sharp bases (possibly erosive) with gradational tops; normal grading
    - Some gradational bases with sharp tops; inverse grading
    - Pinching and swelling laminae
    - Diverging converging laminae
    - Some round silt structures. Possible concretions or burrows
        - Mud deformed around them
    - Makeup:
        - ~35% quartz
        - ~30% calcite
        - ~20% Dolomite
        - ~10% pyrite
        - ~5% phosphate grains
    - Sparse fossil fragments
        - Some conodont elements
        - Some Likely brachiopod and/or ostracod fragments
    - Sparse bioturbation

- Mud infilled, subhorizontal to subvertical
- Zones of possibly up to moderate bioturbation

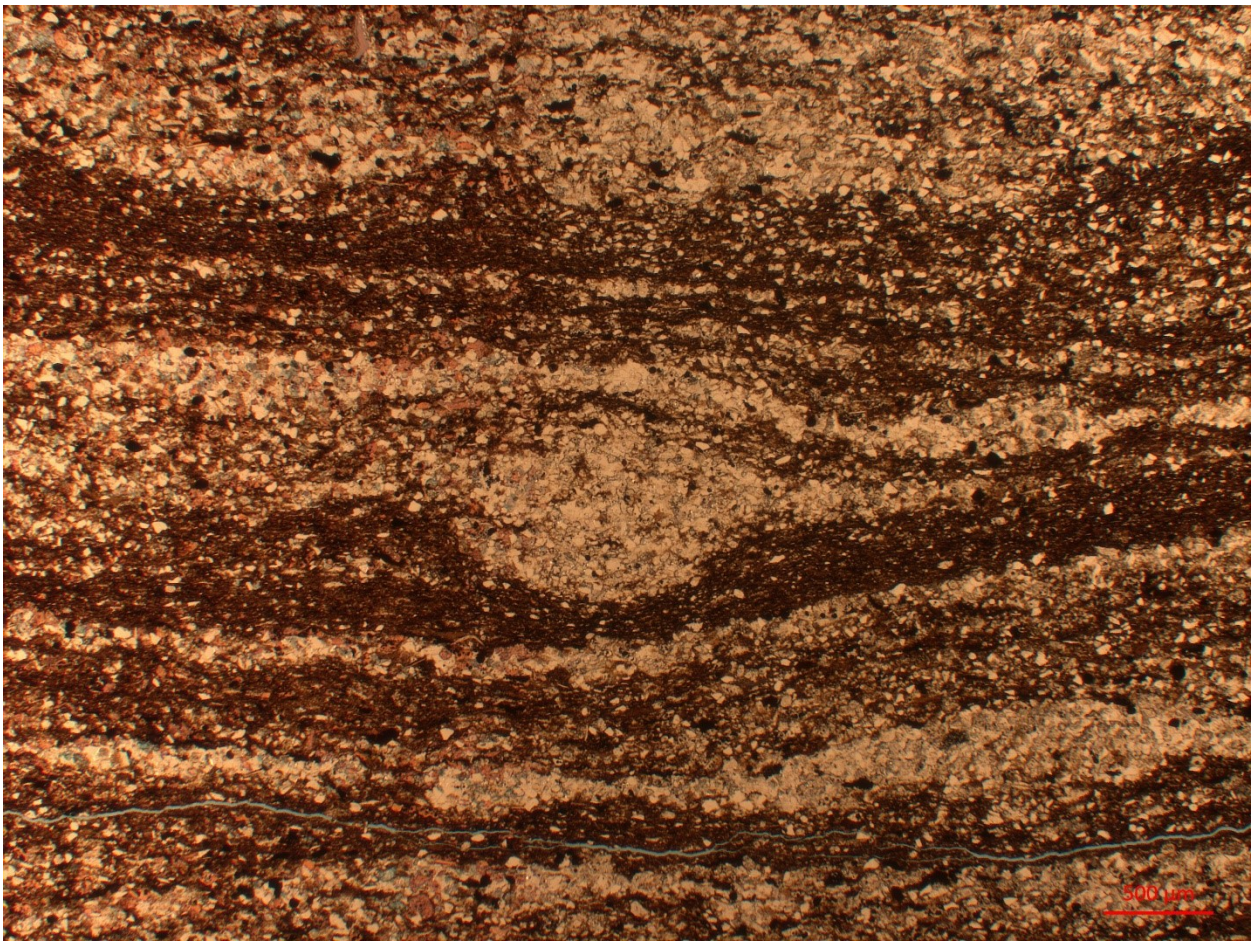

2798.38

- Mud with planar silt/sand laminae
- 100um up to 3mm thick silt/sand laminae
    - Thinner laminae continuous to discontinuous, pinching and swelling
        - Appears sharp bottom and top contacts
            - No obvious grading
    - Thicker laminae continuous and show erosive bottom contact, no obvious grading, sharp planar top contact
        - ~50% silt and sand grains
            - ~50% calcite grains (predominantly styliolinid fragments)
            - ~25% quartz grains (typically finer)
            - ~15% pyrite
            - ~10% phosphate grains (~40% conodont elements)
    - Some thin silt laminae in mud
        - ~40% silt/sand
        - Non-fossiliferous ones in lower part of thin section:
            - ~45% quartz

        - ~35% calcite
        - ~10% phosphate grains
        - ~10% pyrite
    - Fossiliferous ones in upper part of thin section:
        - ~45% styliolinid fragments
        - ~40% quartz
        - 10% pyrite grains
        - ~5% phosphate grains
- ~1% clay aggregates
- Sparse to moderate bioturbation
    - Mud infilled
    - Subvertical

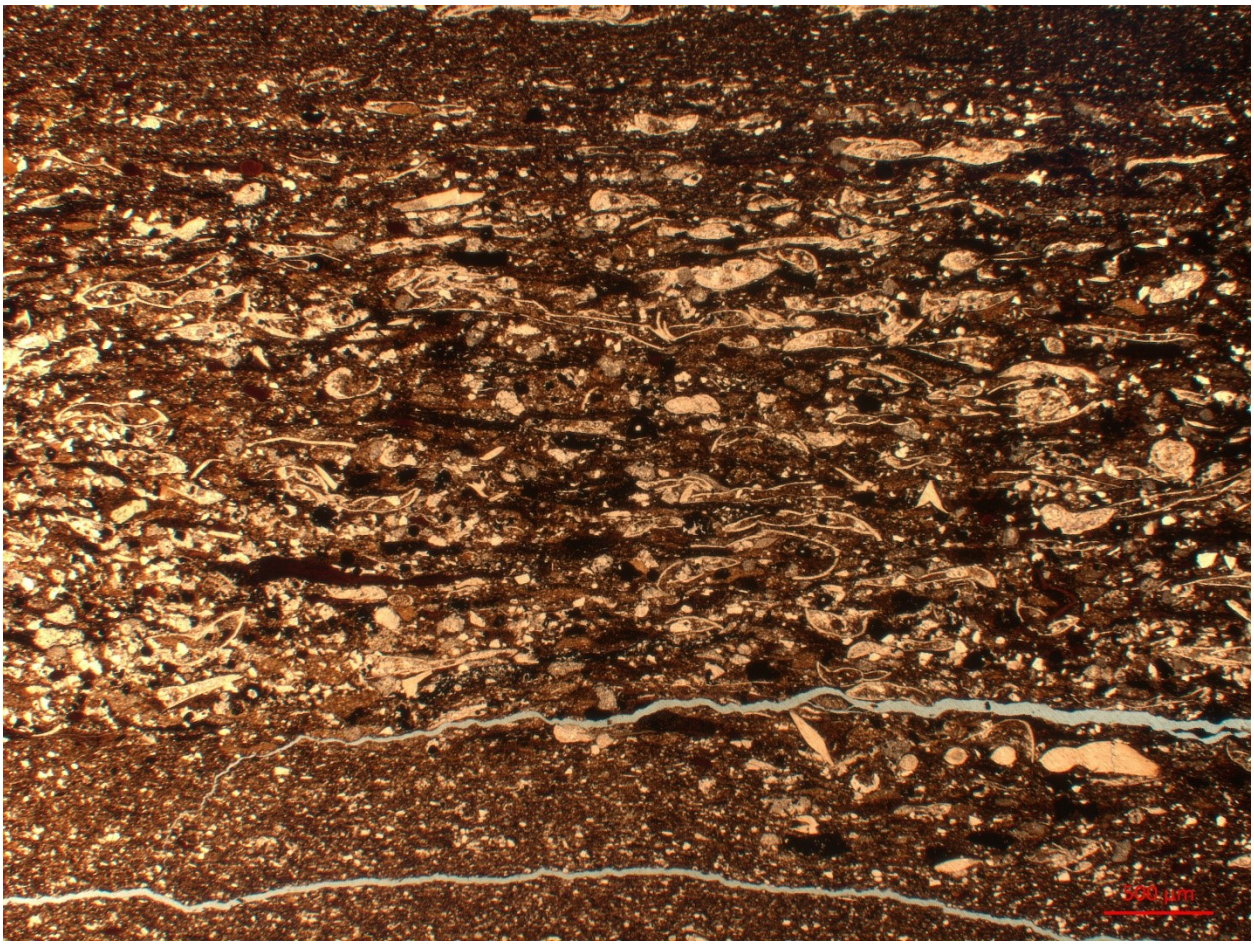

2794.63

- Massive appearing vfs calcite grains making up 28 mm thick layer
    - Faint planar to slightly wavy laminae
        - Some sharp bottoms and tops
        - Some sharp to possibly erosive bottoms and possibly gradational tops
            - Possibly fining up
    - Silt and vfs in laminae composition:
        - ~90% calcite
            - Dominantly very round calcite grains
                - Possibly transported or possibly could be recrystallized styliolinids, peloids, or pisoids?
        - ~7% quartz
            - Small silt grains
        - ~3% dolomite
            - Small silt grains
- ~Moderate bioturbation
    - Mud infilled (moving aside coarse silt grains)

    - Subvertical
    - Bioturbation possibly disrupting/obscuring laminae
- Sparse fossil fragments
    - Quite broken up
    - Likely styliolinids, possibly bivalves/brachiopods
- Planar laminated mud below

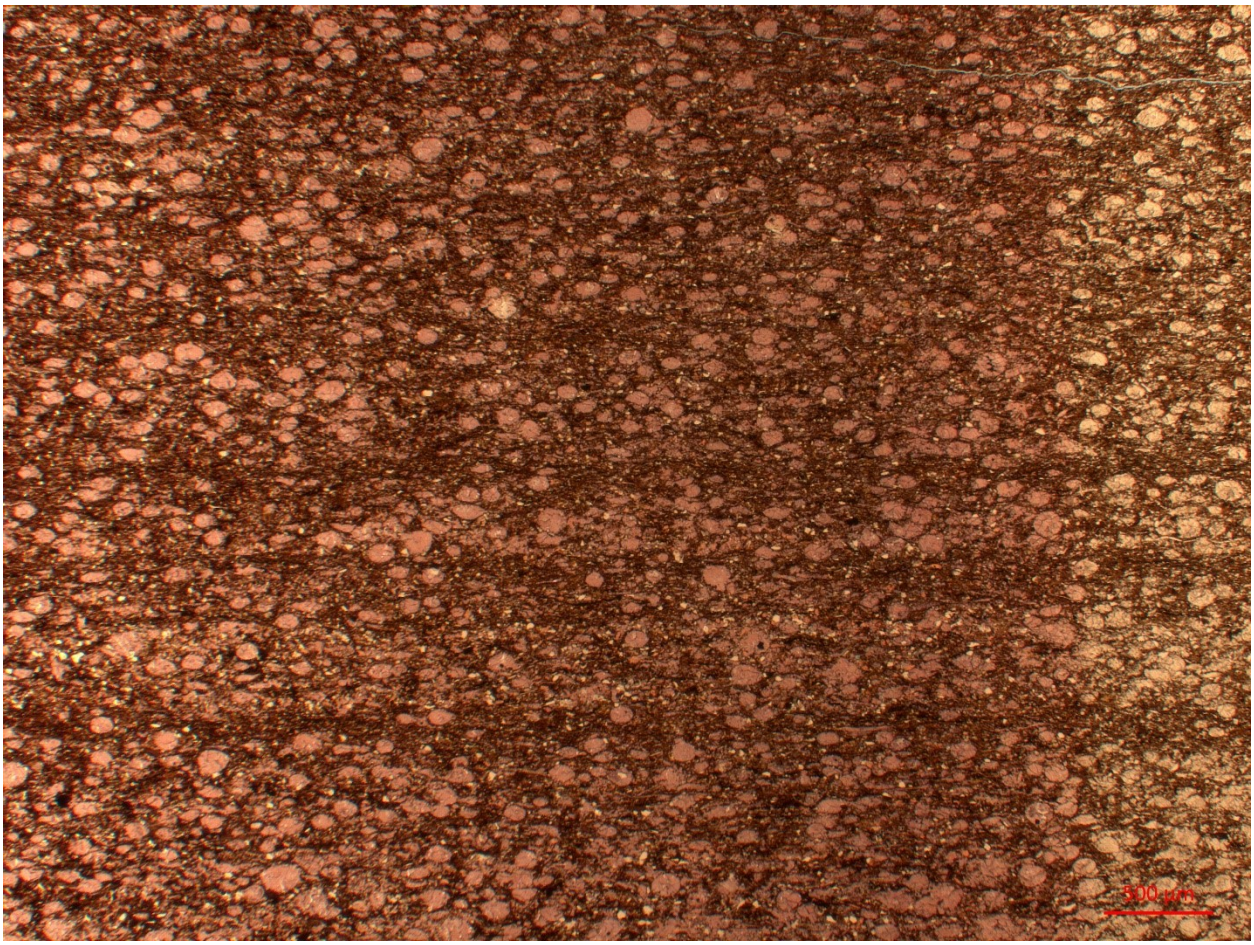

2788.3

- Planar laminated silt in mudstone
- Silt laminae:
    - Planar to slightly wavy
    - Some sharp bottoms and tops
    - Some gradational bottoms and sharp tops
        - Slight inverse grading
    - Some slight pinching and swelling of laminae
    - Composition:
        - Silt to some very fine sand
        - ~38% calcite
            - Some shell fragments
        - ~39% quartz
        - ~3% dolomite
        - ~10% pyrite
- Possibly sparse to moderate bioturbation
- Sparse styliolinids and phosphatic grains

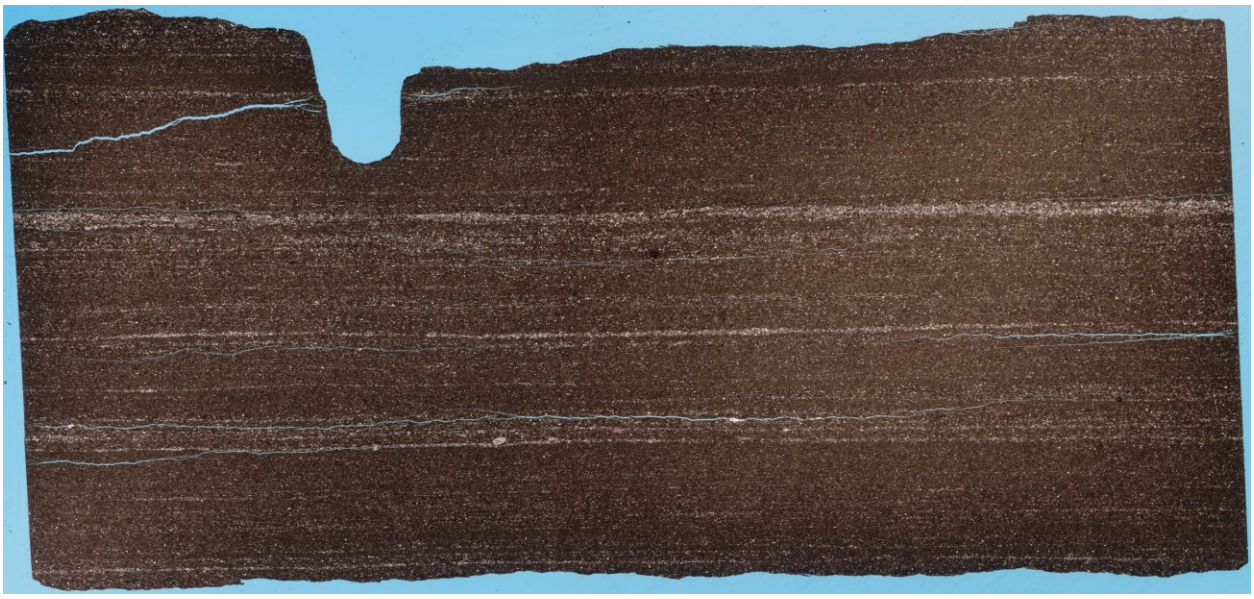

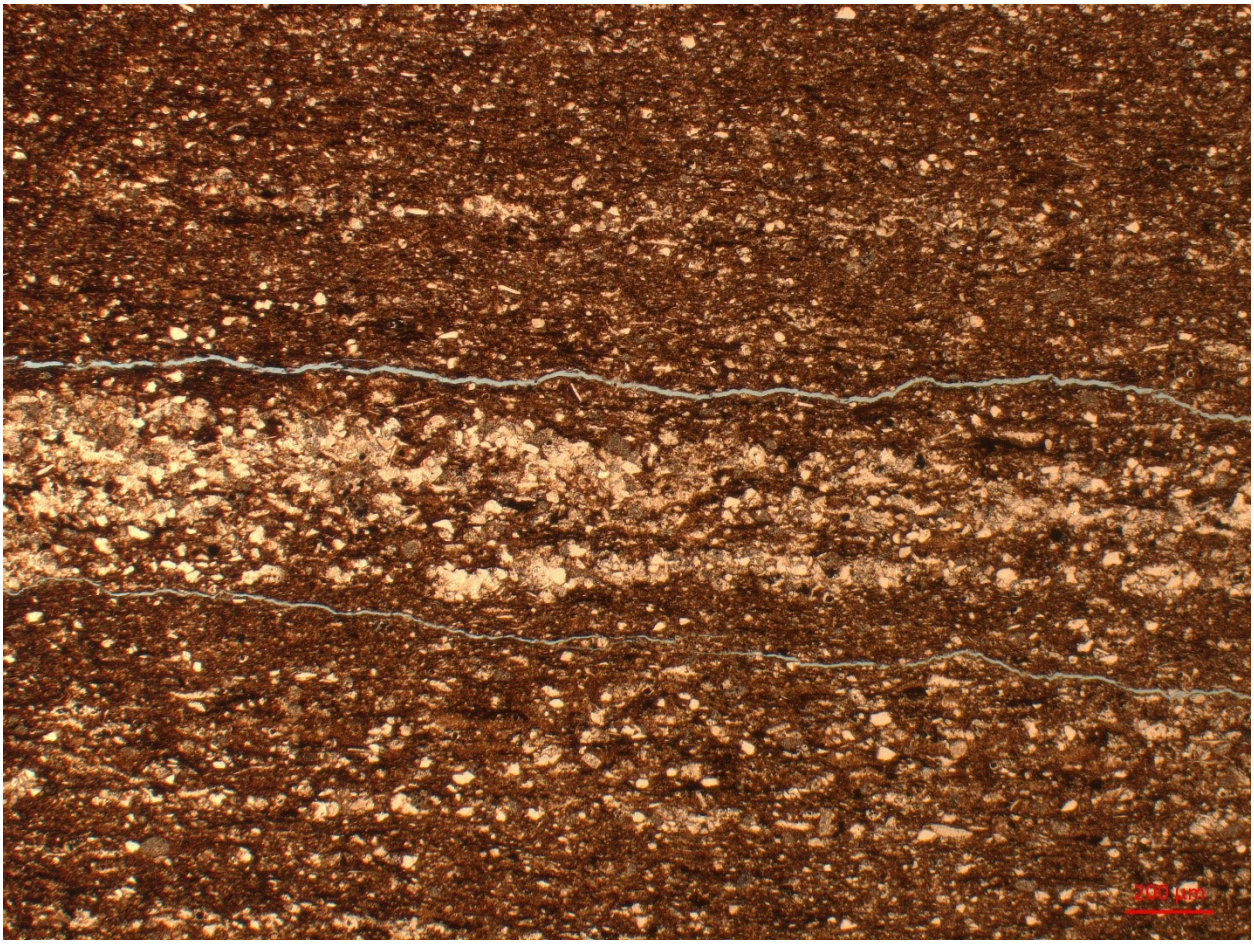

2785.32

- Silt and vfs laminae in mud
    - ~35% of whole rock
    - Some wavy bases and possibly slightly wavy tops (sharp)
    - Some pinching and swelling and divergent/convergent laminae
    - Some wavy sharp bases and gradational tops
    - Some sharp planar bases and gradational tops
    - Some faint gradational bases and sharp planar tops
- Possible sparse to moderate subvertical burrowing (mud infilled)
- Round silt structures along silt laminae
    - Possibly burrows
    - Mud deformed around round silt structure
- Silt in laminae:
    - ~40% calcite grains
    - ~30% Quartz grains
    - ~25% fossil fragments
        - Styliolinids
        - Possible brachiopods/ostracods
    - ~5% dolomite

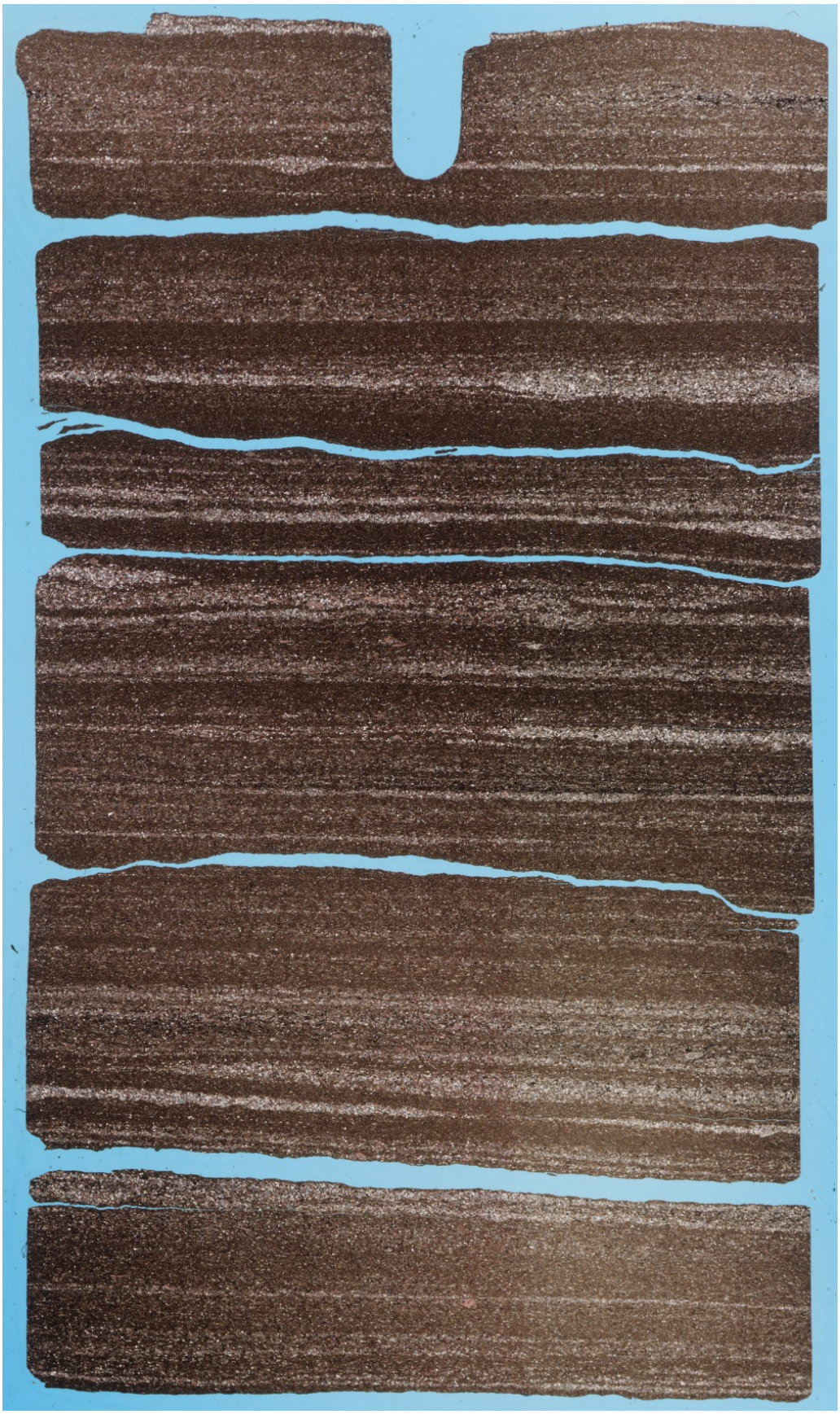

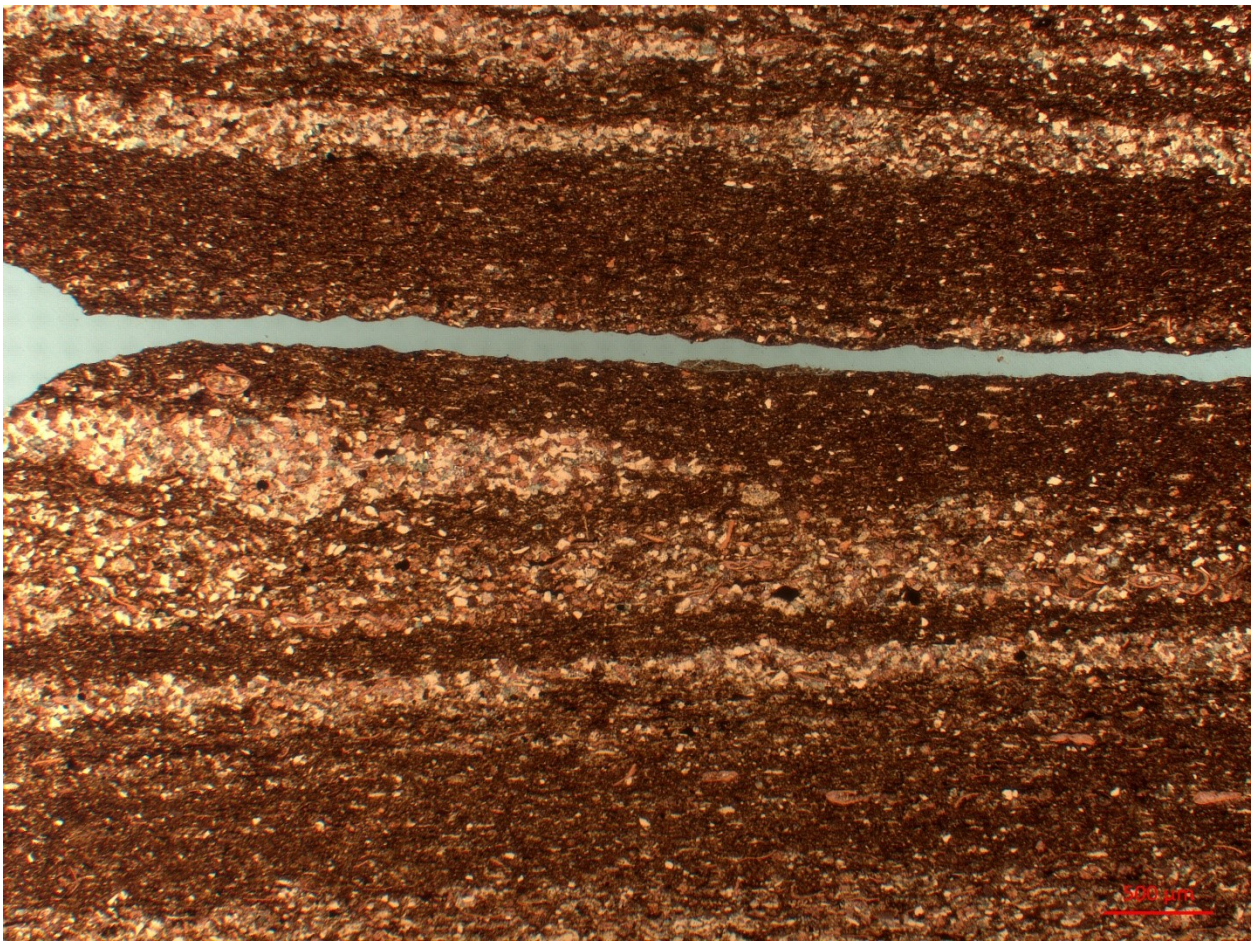

2781.96

- ~40% vfs
  - Very round calcite grains
    - Calcispheres? Styliolinids?
    - Very recrystallized
  - Some elongate shell fragments
- ~30% silt
  - ~70% calcite
  - ~30% quartz
- ~30% clay and fine silt matrix
  - Low OM and pyrite content
  - ~3-5% pyrite
- Faintly visible planar laminae
  - Quite planar but possibly slightly undulatory
  - Some visible sharp bases, normal grading and gradational tops
  - Some pinching/swelling and divergence/convergence of laminae
  - Possibly some inverse grading with gradational base and sharp top

        - But much less obvious
- Sparse possible subhorizontal to subvertical mud infilled burrows

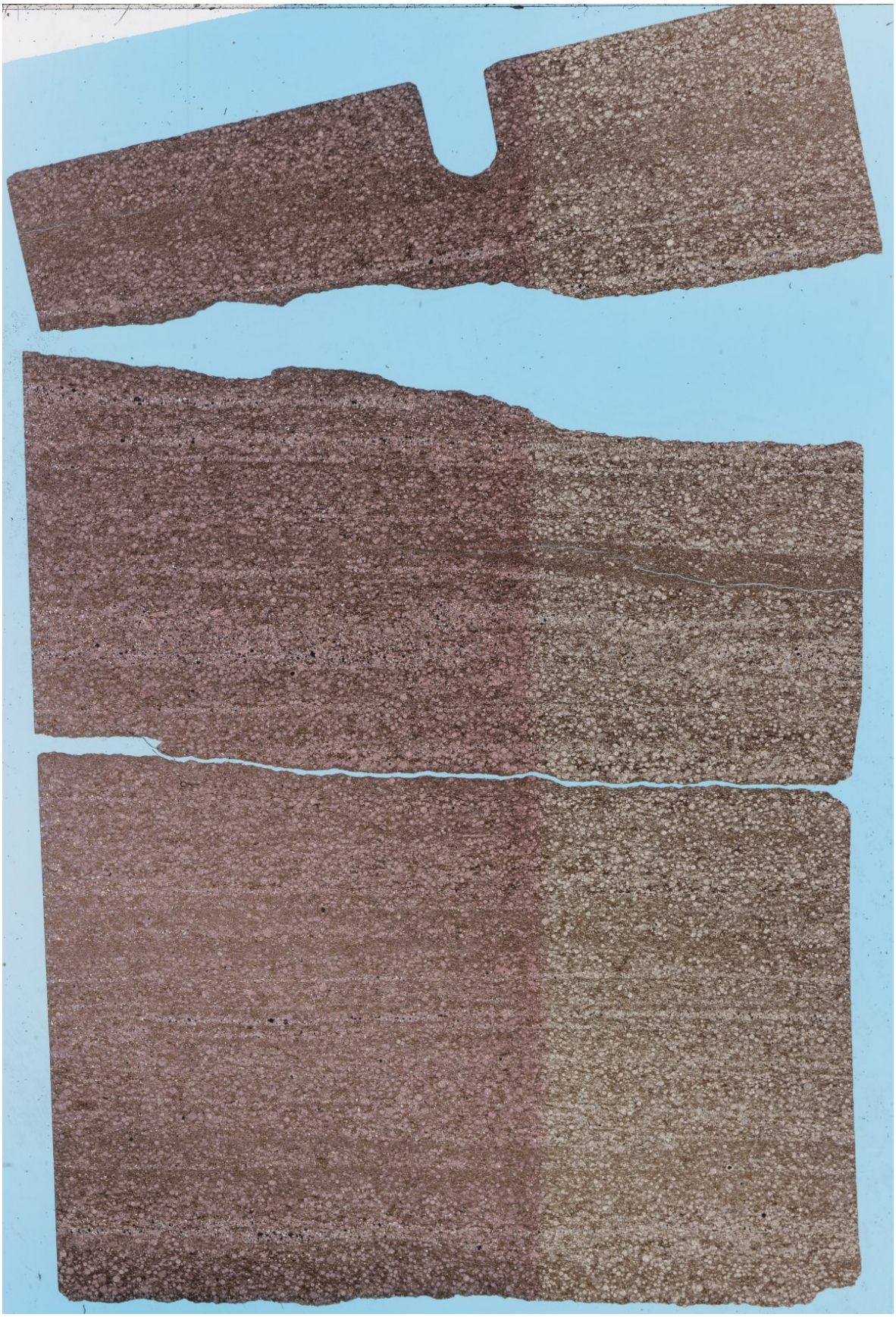

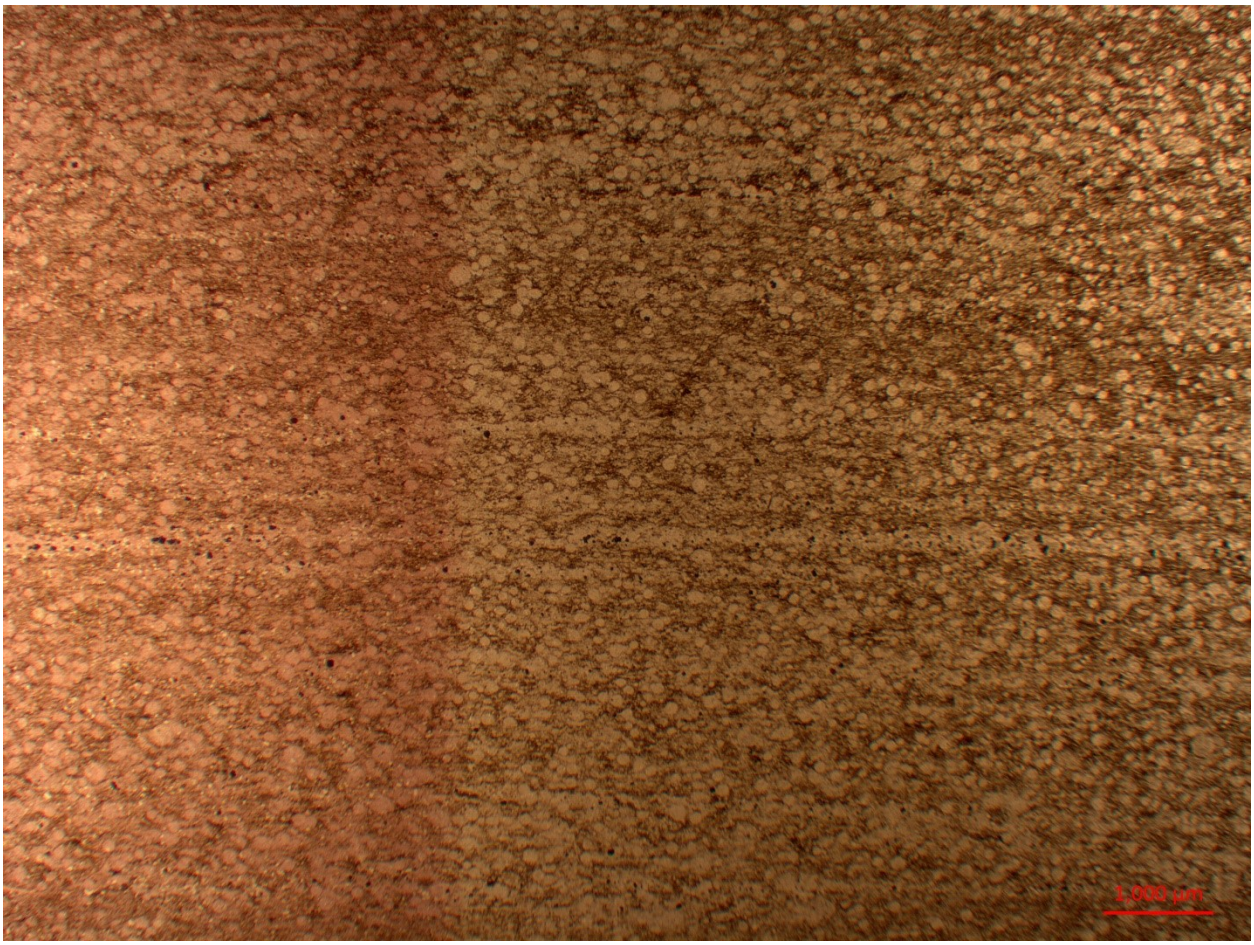

2781.29

- Surface
    - Soft sediment deformed
        - Ball and pillow structure
            - Made up of lag composition
        - Mud laminae deformed below
- Lag
    - 10mm thick
    - Mostly up to M.sand grains
        - A couple coarse sand phosphatic grains
    - Likely fining up throughout (or more coarse grains towards base)
    - Sharp slightly wavy top contact
    - Very massive structure
        - No real orientation of large grains
    - Composition:
        - Abundant glauconite grains
            - Subangular to rounded

        - Abundant phosphatic grains
            - Conodont elements/skeletal fragments
            - Peloids
                - Mostly massive internal, some appear possibly concentric
            - Likely fish bone fragments
                - Spongy interior (often pyritized)
            - Likely lingulid shell fragments
        - Couple possible stromatoporoid fragments
        - Abundant quartz silt
        - Sparse dolomite silt sized grains growing on/replacing other grains
        - Matrix of clay and some pyrite
- Above
    - Clay rich Ireton
    - Planar laminated
    - Rare phosphate peloids and glauconite grains (small) occur along a couple laminae just above lag
    - Quite bioturbated
- Below
    - Silty planar laminated mud
        - Quartz and some dolomite silt concentrated into layers
    - OM and pyrite-rich matrix
    - Rare phosphate peloids

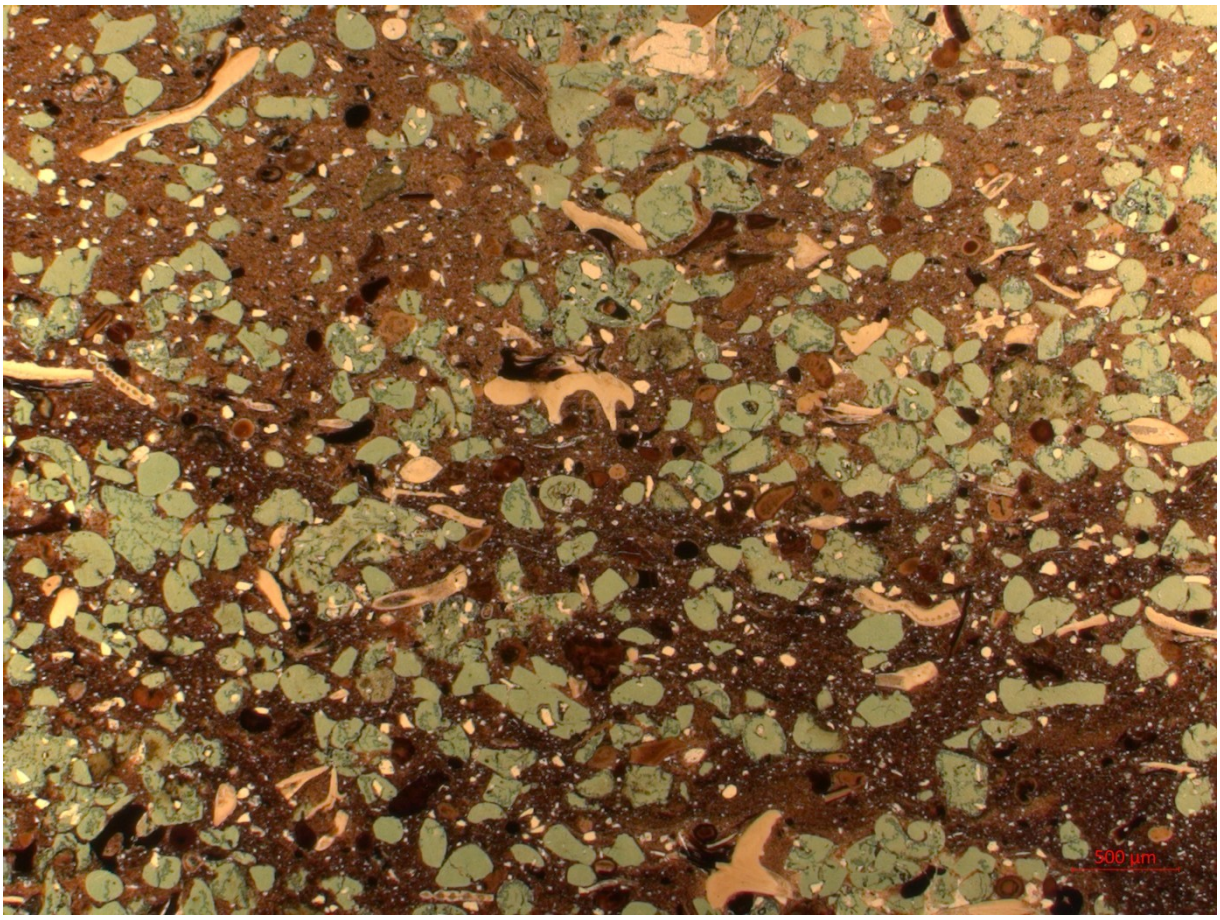

Core 2 – ATH HZ Kaybob

<u>3054.26</u>

- Surface
  - Sharp and erosive
    - Scour surface cross cutting underlying mud laminae
  - Large possible *Thalassinoides* or *Planolites* burrow into underlying mud from surface
    - Crosscuts underlying mud laminae
    - Infilled passively by lag material
- Lag
  - First main lag about 5mm thick
  - Mostly vf to f sand size
    - Some grains up to m-coarse sand
  - Possible glauconite grains
    - Concentrated at base
    - Subrounded

        - Appear partially dissolved
    - Common phosphatic grains
        - Conodont elements
        - Likely fish/bone fragments
            - Definitive shapes
            - Spongy, typically pyritized interiors
            - Some very brown like peloids, some very white like conodont elements
        - Peloids
            - Subrounded
            - Most appear structureless inside (besides some pyritization)
            - Some have possible concentric interior
                - Possibly just pyritization
        - Possible lingulid brachiopod fragments
    - Carbonate fossil fragments
        - Common styliolinid fragments
        - Rare tentatulitid fragments
        - Some possible ostracods/small brachiopod fragments
    - Calcite grains
        - Subrounded
        - Very dissolved looking
    - Quartz grains
        - Subangular to subrounded
    - Possible feldpsar grains
        - Similar to quartz but appear to have some rough crosshatch twinning
        - Possibly just transported quartz?
    - Appears quite bioturbated
        - Likely subhorizontal to subvertical mud infilled burrows
    - Quite massive internal structure
- Above
    - Similar composition to main lag but:
        - Fewer coarse grains
        - Much fewer phosphatic grains and much smaller
        - No possible glauconite grains
    - Multiple possible depositional events above main lag
        - Possibly erosive, slightly wavy bases
        - Some less well developed and smaller overlying silt infilled burrows into underlying mud (possibly firmground)
        - Main components:
            - Styliolinids
            - Possible ostracod/small brachiopod shell frags
            - Much fewer and much smaller phosphatic peloids
                - Some possibly fish bone fragments with pyritized interior (or possibly concentric ooid?)
        - Very bioturbated and massive

            - Likely subhorizontal to subvertical mud infilled burrows
        - Some show slight fining up
        - Typically sharp bases and less sharp tops
- Below
    - Very clay rich mud
        - Very small OM stringers throughout
        - Rare Phosphatic peloids throughout
            - Typically very small
            - Overall smaller than lag
        - Two possible parts of conodont fragments (quite shapeless)
        - Some pyrite and possible pyritized burrows

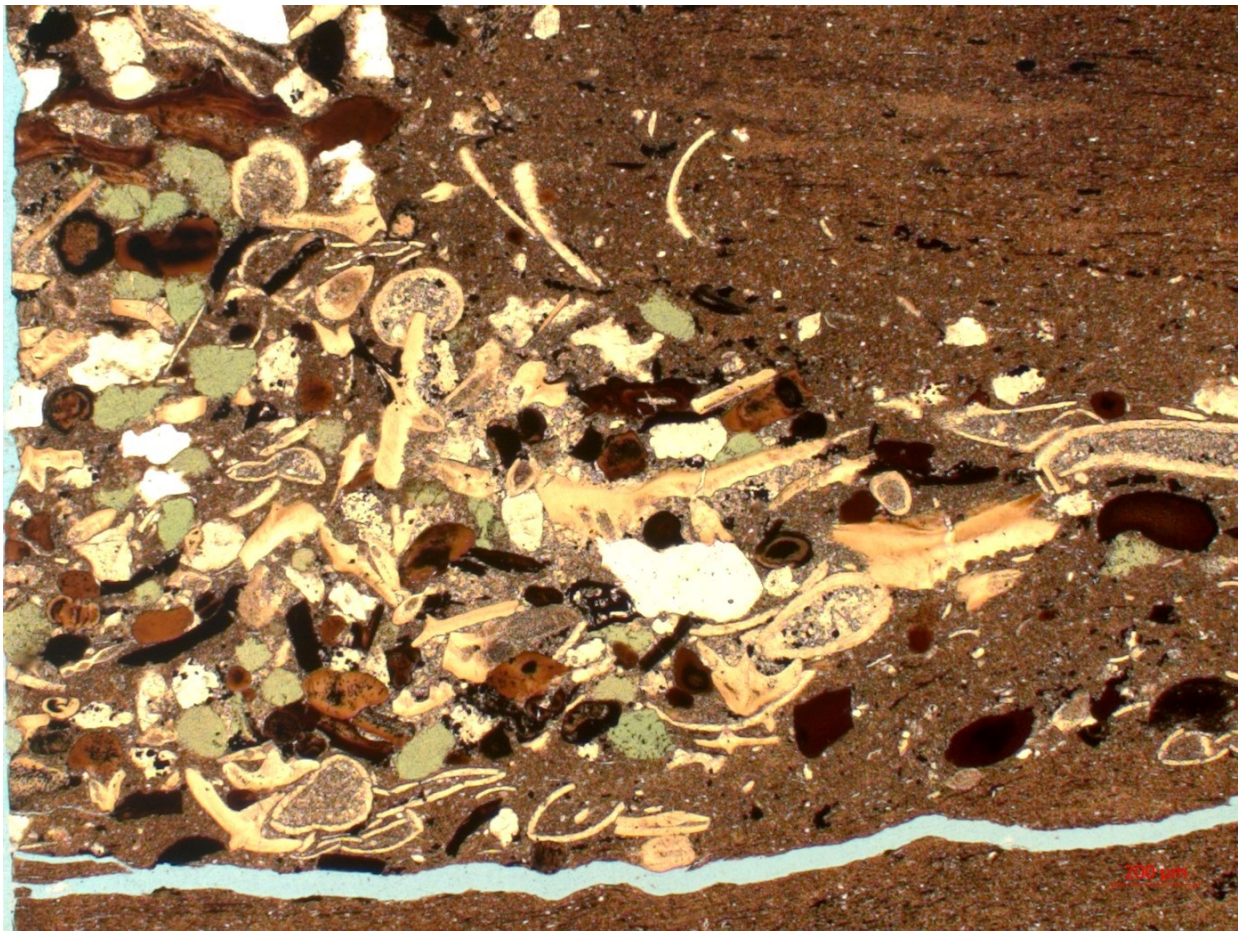

3023.34

- Surface
  - Sharp, possibly planar surface
    - Possibly slightly undulatory
  - Base of most prominent silt laminae in area
- Lag
  - 1mm thick
  - Mostly silt to vfs grains
  - Coarse grains very concentrated at base
    - Also more dolomite cemented at base
  - Composition
    - Abundant quartz grains
    - Abundant likely phosphatic grains
      - Some peloids
      - Common conodont elements/bone fragments
      - Likely lingulid shells
      - Commonly partially dolomitized (quartz grains not dolomitized)

        - Common dolomite grains
        - Some pyrite grains
        - Very clay rich matrix
    - Overall quite massive structure
    - Appears quite burrowed
        - Subhorizontal to subvertical mud infilled burrows
    - Quite sharp planar top contact
- Above
    - Thinner silt laminae than main lag
        - Much less sharp contacts
        - Much fewer phosphatic grains
    - More OM in matrix than below and lag in clay rich matrix
    - Appears very bioturbated like lag
- Below
    - Thinner silt laminae than main lag
        - Much less sharp contacts
        - Much fewer phosphatic grains
    - Less OM in matrix than above and lag in clay rich matrix
        - Very clay rich matrix
    - Appears very bioturbated like lag

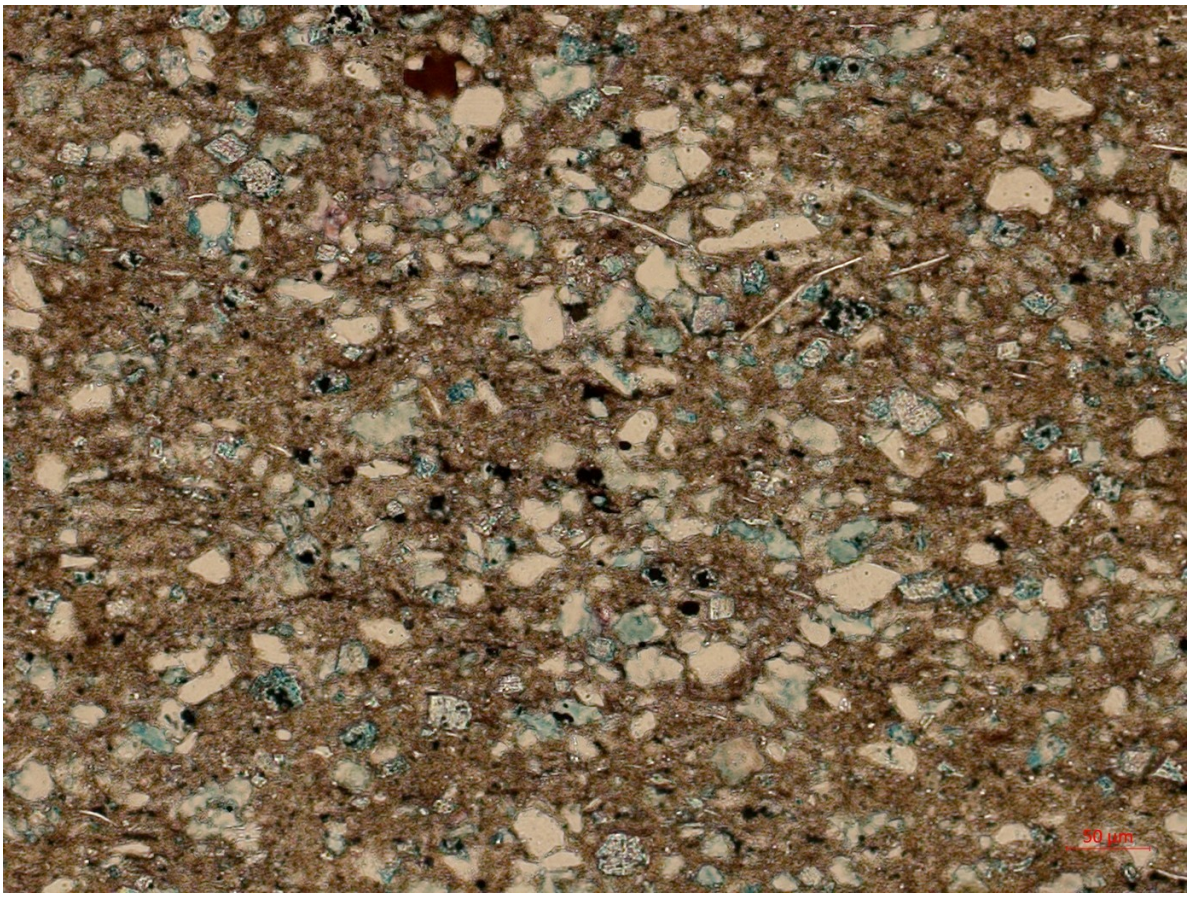

Core 3 - SCL HZ 102 McKinley

3366.15 m

- Sedimentary structures:
    - Planar, continuous laminae
        - Up to ~6mm thick in silty layers
            - Slightly wavy in some areas
        - Up to ~100 um thick in muddy layers
- Texture:
    - Angular to Rounded
    - Moderately sorted (concentrated into silt-rich and mud rich layers)
    - Larger grains aligned to sub-aligned with parallel laminae
- Medium to Coarse Sand: (~15%)
    - Non-Skeletal: (0%)
    - Skeletal: (100%)
        - ~90% Styliolinid fragments
            - Calcite infilled centers that have been dissolved out (jagged edges) and dolomite has been precipitated in its place (crystalline, blocky)

        - ~7% Brachiopod? Fragments
            - One possible (almost) intact cross section
        - ~3% Tentaculitid fragments
            - Also likely dolomite replacement infilled
- V. Fine to Fine Sand: (25%)
    - Non-Skeletal: (5%)
        - Phosphatic grains?
            - Subrounded to rounded
            - Amorphous to rounded
    - Skeletal: (95%)
        - Styliolinid fragments
            - Calcite infilled centers (of round fragments) that have been dissolved out (jagged edges) and dolomite has been precipitated in its place (crystalline, blocky)
- Medium to Coarse Silt: (20%)
    - Non-Skeletal: (60%)
        - ~55% Quartz/feldspar
        - ~30% Quartz grains
        - ~10% Pyrite grains
        - ~5% Dolomite grains
    - Skeletal: (40%)
        - Styliolinid fragments
        - Calcispheres? Possible calcitized radiolarians?
        - Very sparse possible conodont jaw elements
- V. Fine to Fine Silt: (15%)
    - ~30% Quartz/feldspar
    - ~30% Dolomite
    - ~30% Calcite
    - ~10% Pyrite
- Matrix: (25%)

3365.89 m

- Sedimentary Structures:
    - 2 cm thick calcite nodule in middle of thin section
        - Abundant, large fossil fragments up to 9mm long
        - Very recrystallized
            - Fossil fragments and grains have sometimes jagged and irregular grain boundaries
            - Usually have jagged rim of calcite (recrystallized)
        - Carbonate (micrite) rich matrix (recrystallized)
        - Massive internal structure
    - Mud zones have slightly wavy (likely from calcite nodules) planar, continuous laminae
        - Shown by alignment of fossil fragments
        - Up to ~1.5 mm thick
- Texture:
    - Subangular to subrounded
    - Moderately to poorly sorted
- Medium to Coarse Sand: (~15%) (~40% in calcite nodules)
    - Non-Skeletal: (0%)
    - Skeletal: (100%)
        - ~90% Styliolinids
            - Some internal cavities filled with recrystallized dolomite
                - Crystalline with some jagged edges on fossils
        - ~7% Brachiopods?
        - ~3% Crinoids
            - Some internal cavities filled with recrystallized dolomite
        - <1% Phosphatic grains
- V. Fine to Fine Sand: (~20%) (~20% in calcite nodules)
    - Non-Skeletal: (~1%)
        - Pyrite grains
            - Quite round
    - Skeletal: (99%)
        - ~70% Styliolinid fragments
            - Some internal cavities filled with recrystallized dolomite
        - ~20% Brachiopod? Fragments
        - ~10% Crinoid fragments
            - Some internal cavities filled with recrystallized dolomite
- Medium to Coarse Silt: (25%)
    - Non-Skeletal: (60%)
        - ~50% Calcite grains
        - ~30% Pyrite grains
        - ~20% Quartz/Feldspar grains
    - Skeletal: (40%)

        - Likely styliolinid fragments
        - Possibly brachiopod fragments
        - Elongate
- V. Fine to Fine Silt: (20%)
    - ~60% calcite
    - ~25% quartz/feldspar
    - ~15% pyrite
- Matrix: (20%) (~30% calcite (and ~5% replaced with dolomite) cement in calcite nodule)

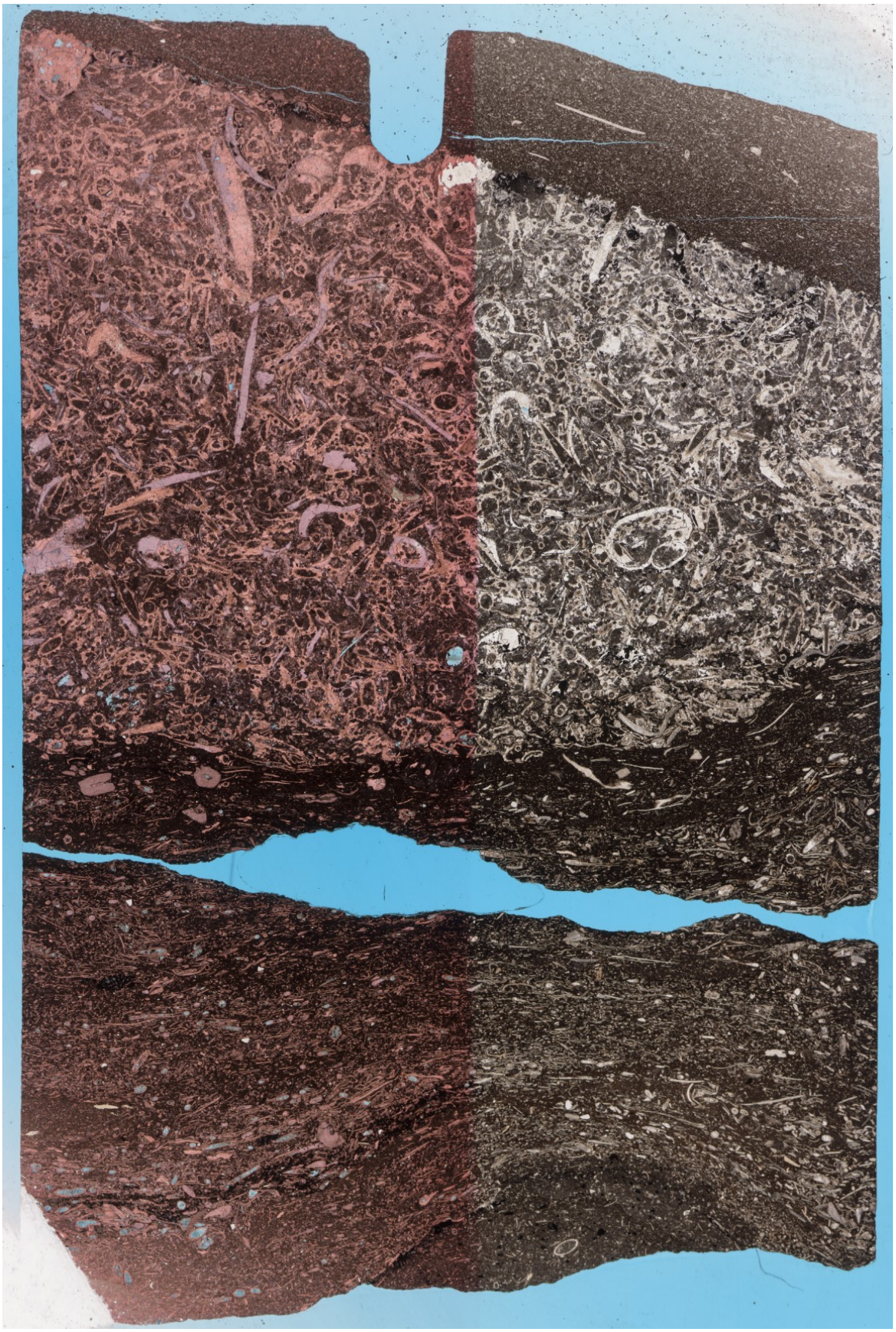

3365.3 m

- Sedimentary structures:
    - Bottom third of thin section is mudstone:
        - Larger grains (fossil fragments) roughly oriented into planar, continuous laminae
            - Up to 1mm thick
    - Top 2/3 of TS is fossiliferous wackestone
        - Very massive structure
        - Quite calcite cemented (instead of mud matrix)
- Texture:
    - Subangular to subrounded
    - Poorly sorted
- Medium to Coarse Sand: (~15%) (~20% in mud section)
    - Non-Skeletal: (0%)
    - Skeletal: (100%)
        - Appears to be almost entirely styliolinid fragments
            - Internal cavities usually filled by crystalline calcite
        - Possibly some calcispheres?
- V. Fine to Fine Sand: (~15%) (~20% in mud section)
    - Non-Skeletal: (0%)
    - Skeletal: (100%)
        - Appears to be almost entirely styliolinid fragments
            - Internal cavities usually filled by crystalline calcite
        - Possibly some calcitized rads
- Medium to Coarse Silt: (~45%) (~25% in mud section)
    - Non-Skeletal: (90%) (30% in mud section)
        - ~95% Calcite grains (subangular, round to rectangular)
            - Some can be seen growing off of fossil fragments in the top 2/3 of TS
            - Possibly suggests that they are crystalline (precipitated)
        - ~5% Pyrite grains (quite amorphous to round)
        - (~60% Calcite grains, ~30% quartz/feldspar grains, ~9% pyrite grains, ~1% phosphatic grains in mud section)
    - Skeletal: (10%) (70% in mud section)
        - Possible Styliolinid fragments (maybe brachiopod fragments)
- V.Fine to Fine Silt: (~10%) (~15% in mud section)
    - ~85% Calcite
    - ~10% Quartz/Feldspar
    - ~5% Pyrite
- Matrix (Und.): (~15%) (~20% in mud section; not cement)
    - Likely mostly calcite cement

3363.78 m

- Sedimentary structures:
    - Bottom ~1/10th of thin section is more mud-rich section
    - Rest of thin section is carbonate-rich (almost all calcite) calcite nodule with very cemented matrix
    - Overall very massive structure (no obvious alignment of large fossil grains)
- Texture:
    - Angular to subrounded grains
    - Poorly sorted
- Medium to Coarse Sand: (~25%)
    - Non-Skeletal: (0%)
    - Skeletal: (100%)
        - Styliolinid fragments
            - Most have up to coarse silt, jagged calcite rims or jagged calcite grains growing off of fossil fragments
                - Suggests recrystallization or precipitation of those minerals
            - Internal cavities filled by likely crystalline calcite
        - Some possible brachiopod fragments and possible calcitized rads
- V. Fine to Fine Sand: (~15%)
    - Non-Skeletal: (0%)
    - Skeletal: (%)
        - Styliolinid fragments
            - Most have up to coarse silt, jagged calcite rims or jagged calcite grains growing off of fossil fragments
                - Suggests recrystallization or precipitation of those minerals
            - Internal cavities filled by likely crystalline calcite
                - Some fossil fragments in muddy section infilled by crystalline dolomite
        - Some possible brachiopod and ostracod fragments
- Medium to Coarse Silt: (~50%)
    - Non-Skeletal: (100%)
        - Crystalline calcite
            - Mostly interlocking grains, likely recrystallized or precipitated
            - (not in muddy section)
        - ~5% Pyrite grains (round, amorphous)
    - Skeletal: (0%)
- V.Fine to Fine Silt: (~5%)
    - 90% Calcite
    - 10% Pyrite
- Matrix (Und.): (~5%)

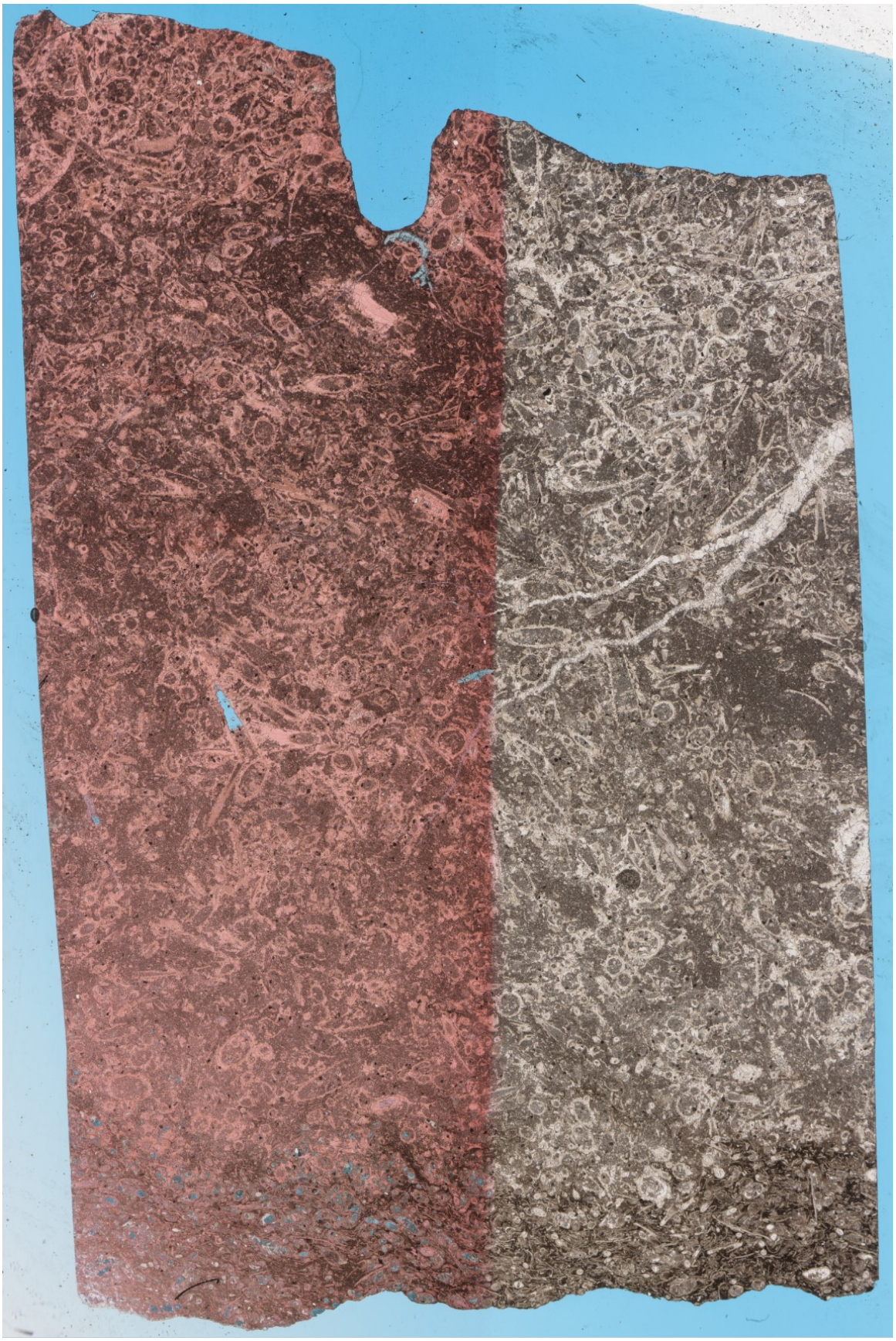

3358.17 m

- Sedimentary structures:
    - 8mm thick fossiliferous lag deposit near bottom of TS
        - Overlying possible erosive, bioturbated surface
            - Sharp, wavy bottom contact
            - Lag deposit material infilled, subvertical to vertical burrows going into underlying mud
        - Underlying mud (bottom 1/8 of TS) is more massive looking, very faintly laminated, mud-dominated mudstone
        - Overlying mud (top 5/8 of TS) is more distinctly planar, continuous laminated mud with more silt-rich (fossil fragments and dolomite grains) and pyrite-rich layers helping to define laminae
            - Some bed parallel pyritized and silt infilled burrows
            - Some fining-up laminae
        - ~25% medium to coarse sand
            - Styliolinid fragments (infilled by crystalline calcite and dolomite, some jagged edges suggesting dissolution and precipitation but mostly straight edges), possible brachiopod fragments
        - ~30% Fine sand
            - Styliolinid fragments, microcrystalline dolomite grains?. phosphatic grains?, pyrite grains?, conodont fragments?
        - ~20% Medium to coarse silt
            - Styliolinid fragments, microcrystalline dolomite grains?. phosphatic grains?, pyrite grains?, conodont fragments?
        - ~15% V fine to fine silt
        - ~10% matrix
        - Quite massive structure (no obvious grain orientation)
        - Slight fining up throughout lag
    - 9mm thick pyrite nodule at bottom of TS
- Texture:
    - Lag deposit = poorly sorted; below mud = well sorted; above mud = well to moderately sorted
    - Subangular to subrounded
- Medium to Coarse Sand: (~1%)
    - Non-Skeletal: (0%)
    - Skeletal: (100%)
        - Styliolinid fragments
- V. Fine to Fine Sand: (~4%)
    - Non-Skeletal: (~40%)
        - ~30% Calcite grains (quite round,
        - ~30% Glauconite?
        - ~20% Phosphate grains (quite round)

        - ~20% Pyrite grains
    - Skeletal: (~60%)
        - Styliolinid fragments
            - Often infilled by crystalline dolomite, sometimes by microcrystalline dolomite?
        - Very sparse Possible calcitized rads
- Medium to Coarse Silt: (~20%)
    - Non-Skeletal: (~60%)
        - ~45% Quartz/feldspar grains
        - ~30% Pyrite grains
        - ~15% Glauconite?
        - ~10 Calcite grains
    - Skeletal: (~40%)
        - Styliolinid fragments
- V.Fine to Fine Silt: (25%)
    - ~45% Quartz/feldspar grains
    - ~30% Pyrite grains
    - ~15% Glauconite?
    - ~10 Calcite grains
- Matrix (Und.): (50%)

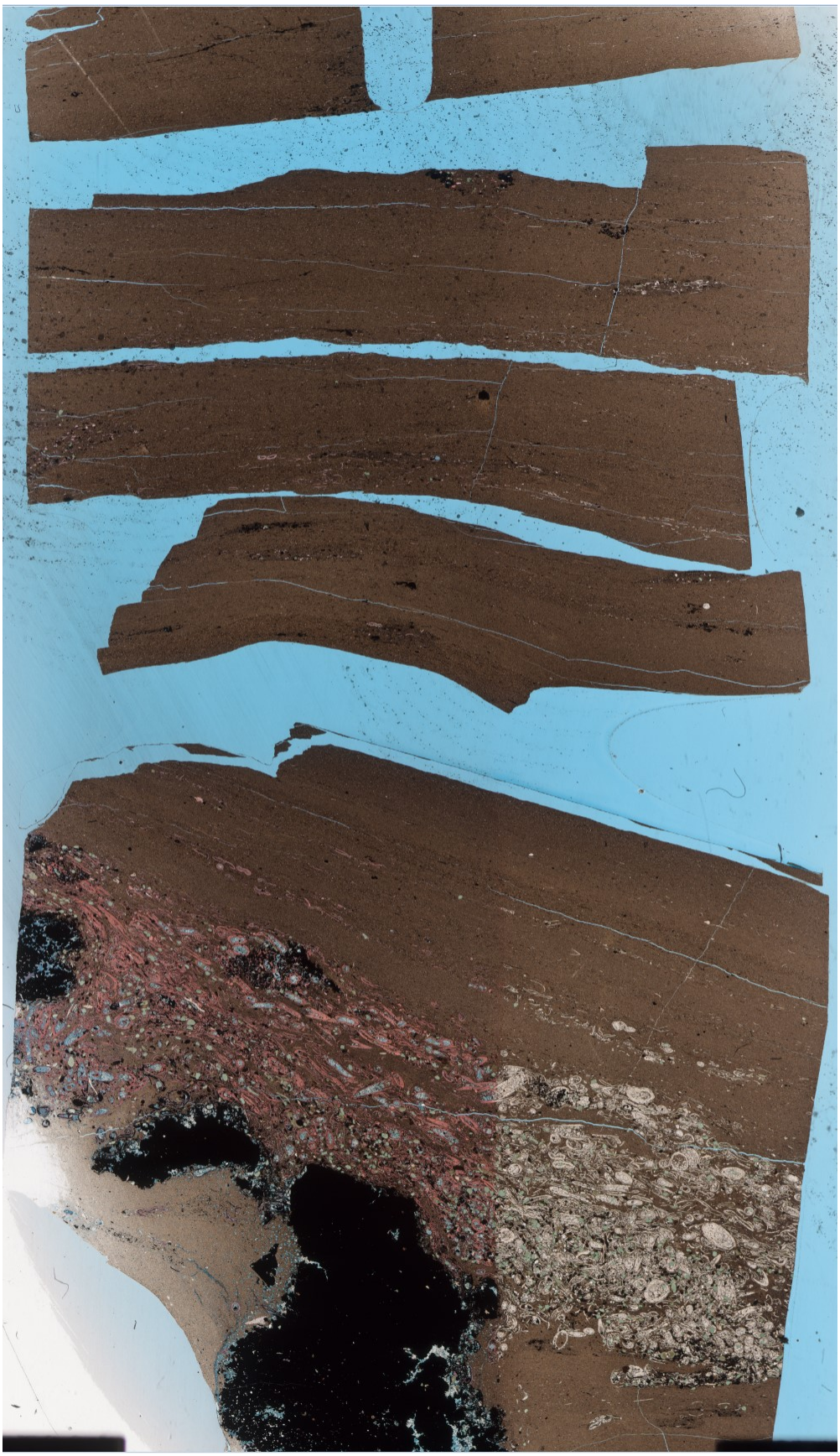

3353.92 m

- Sedimentary Structures:
    - Thin planar laminae throughout TS
        - Defined by up to medium to coarse silt
            - Most likely fossil fragments (styliolinids)
            - Dark (likely pyrite grains) as well
    - Medium to coarse sand sized styliolinid fragments throughout TS and organized into up to 5mm thick layer
        - Single possible medium sand phosphatic clast
        - ~35% styliolinids
        - ~15% pyrite
        - ~20% calcite medium-coarse silt
        - Slightly undulatory base (possibly erosive or soft sed def)
            - Quite planar top
        - Possibly bioturbated (where fossil fragments pushed to sides)
            - Up to 1.5x6 mm
- Texture:
    - Well to possibly moderately sorted
        - Poorly sorted in styliolinid layer
    - Subrounded
- Medium to Coarse Sand: (3%)
    - Non-Skeletal: (0%)
    - Skeletal: (100%)
        - Styliolinid fragments
- V. Fine to Fine Sand: (2%)
    - Non-Skeletal: (0%)
    - Skeletal: (100%)
        - Styliolinid fragments
- Medium to Coarse Silt: (10%)
    - Non-Skeletal: (50%)
        - Pyrite
    - Skeletal: (50%)
        - Styliolinid fragments
- V. Fine to Fine Silt: (20%)
    - 60% quartz/feldspar
    - 30% pyrite
    - 10% calcite
- Matrix: (65%)

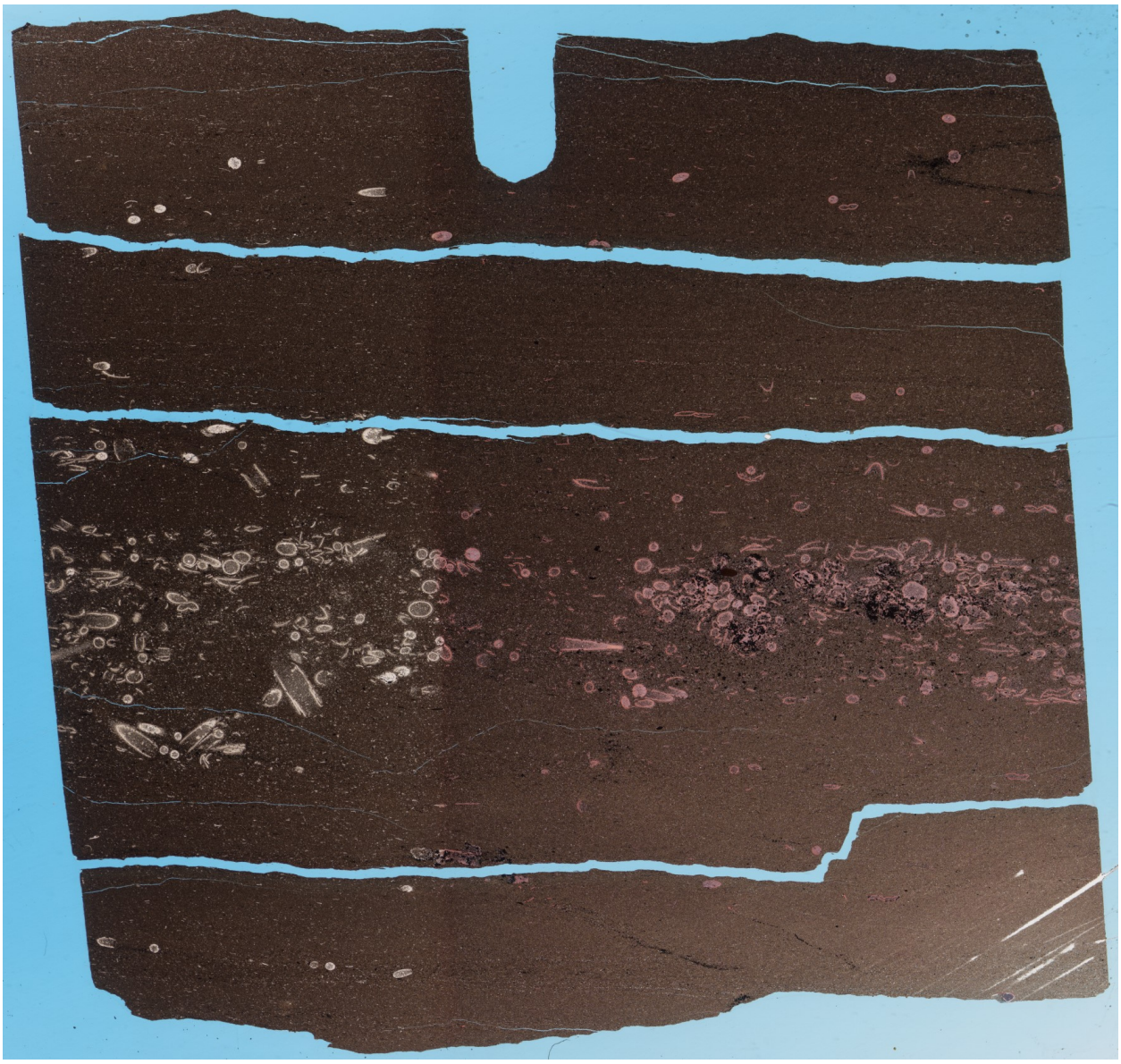

3353.85m

- Laminated mudstone
  - Some faint, slightly pyritized, whispy, fairly continuous laminae
  - A few (up to 500 um by 1mm pyrite nodules)
    - Possibly burrows but less likely
  - Sparse (~3%) styliolinid fragments
    - One visible cluster
- 4 mm thick styliolinid fragment-rich layer
  - Up to medium to coarse sand sized styliolinid fragments
    - Possibly some ostracod/brachiopod fragments as well
    - Clustered in some zones into calcite cemented (and pyrite cemented) nodules?

        - Up to 4mm across
    - Pyritized planar laminated mud at base
    - Quite massive appearance of grain distribution of coarse fossil fragments within layer
    - Fossil-rich layer appears to be broken up possible mud-rich burrows
        - Possibly up to 0.5 mm thick
        - Subhorizontal to subvertical
        - Possibly *Planolites*

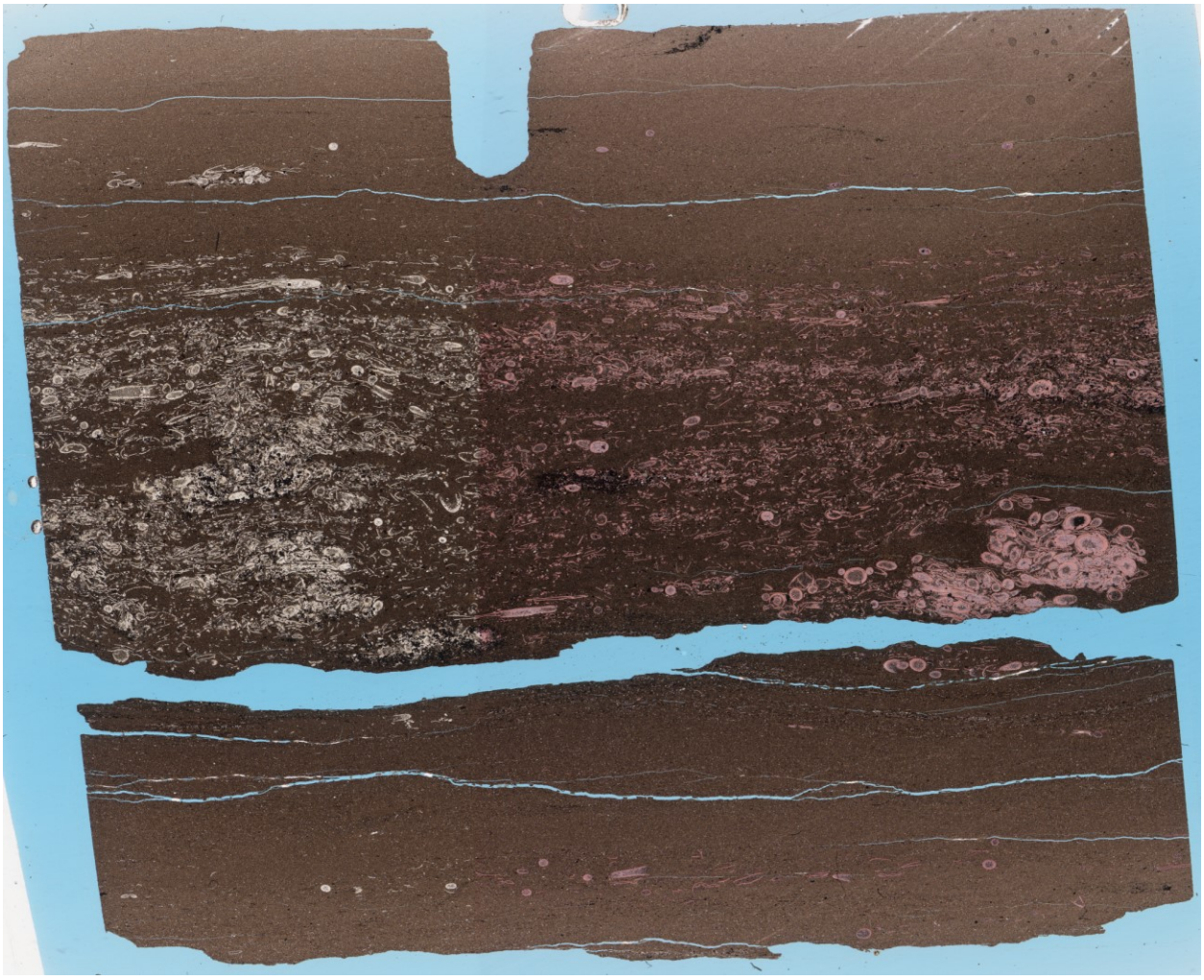

<u>3352.64</u>

- Contact between Majeau and Duvernay
- Above:
    - Slightly coarser mud
    - ~10% coarse silt to very fine sand sized possible calcispheres and calcite grains
    - More abundant pyrite grains and in matrix (~3-5%)
    - More fossiliferous layers (very similar) above one at contact
    - Likely more abundant OM in matrix

- Up to 5mm thick fossiliferous, up to coarse sand lag deposit
    - Sharp base and top
        - Top appears to have ~300 um thick calcite cemented layer
    - 25-30% silt to sand sized fossiliferous grains
        - All partially to fully pyritized
        - ~60% styliolinid fragments
        - ~20% thin shelled ostracods/brachiopods
        - ~10% Tentaculitid fragments
        - ~5% possible radiolarians
        - ~5% phosphatic grains (some possible fish bone fragments)
    - ~5% calcite grains
    - ~10% blue/green round to amorphous glauconite? grains
        - Appear partially dissolved
    - Quite massive appearing organization of grains but overall does have slight planar parallel organization of grains
- Below (Majeau):
    - Planar laminated, slightly pyritized, slightly whispy (possibly discontinuous) mud below (Majeau)
        - Very fine mud
        - More siliceous looking
        - Very little pyrite (~<1%)
    - Very sparse (~2%) possible styliolinid or ostracod fossil fragments
        - Randomly distributed but somewhat clustered
- Surface:
    - Sharp, possibly erosive surface
        - Slightly undulatory
        - Change across from more clay rich Majeau to more OM and pyrite rich and possibly more siliceous matrix Duvernay
- Lag:
    - Silt to medium sand
        - Possible horn coral is coarse sand
    - Clast to matrix supported
    - Matrix appears same as overlying Duvernay
    - Sharp undulatory base
    - Appears to be sharp top
        - Top appears cemented by calcite and pyrite and in some areas maybe silica
        - Some styliolinid fragments at top in some places
    - Composition:
        - Abundant styliolinid fragments
            - Also tentaculitid fragments
            - Likely ostracods/small brachiopod frags
            - Partially to fully pyritized
        - Common glauconite grains?
            - Very round to subangular

                - Appear partially dissolved or broken up (transported?)
            - One possible Large horn coral fossil frag
            - Sparse conodont elements/bone frags
            - Sparse possible phosphatic grains
            - Sparse calcite grains
            - Couple rare possible calcispheres or styliolinid x-sections
        - Rare possible dolomite cement infilling fossil fragments
        - Likely subhorizontal to subvertical mud infilled burrows through lag
        - Quite massive internal structure,
            - Alignment of elongate grains parallel to bedding
            - Possible disturbed internal laminae?
- Above:
    - More OM and pyrite rich Duvernay
- Below:
    - More clay rich and burrowed Majeau
        - OM and pyrite lean

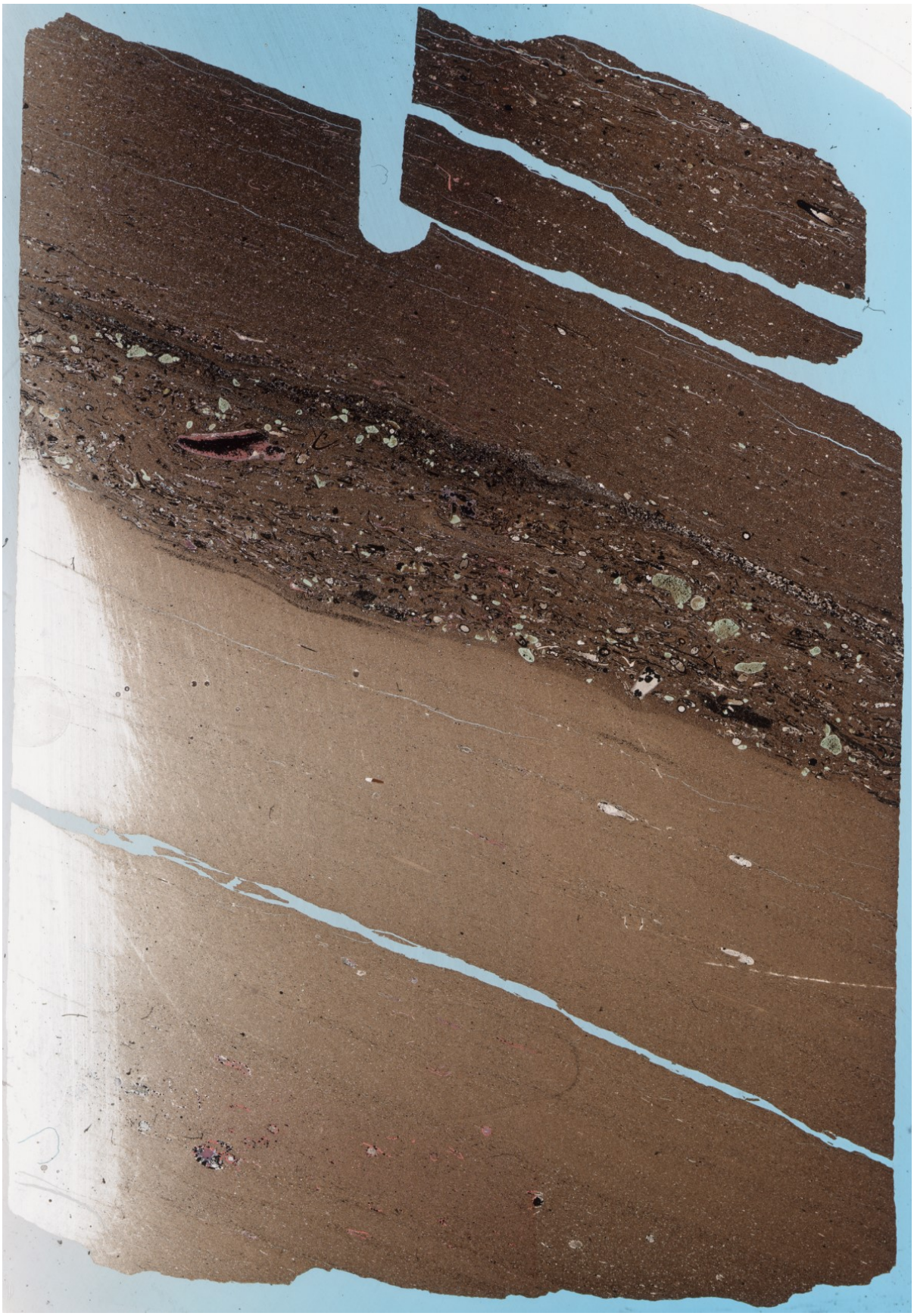

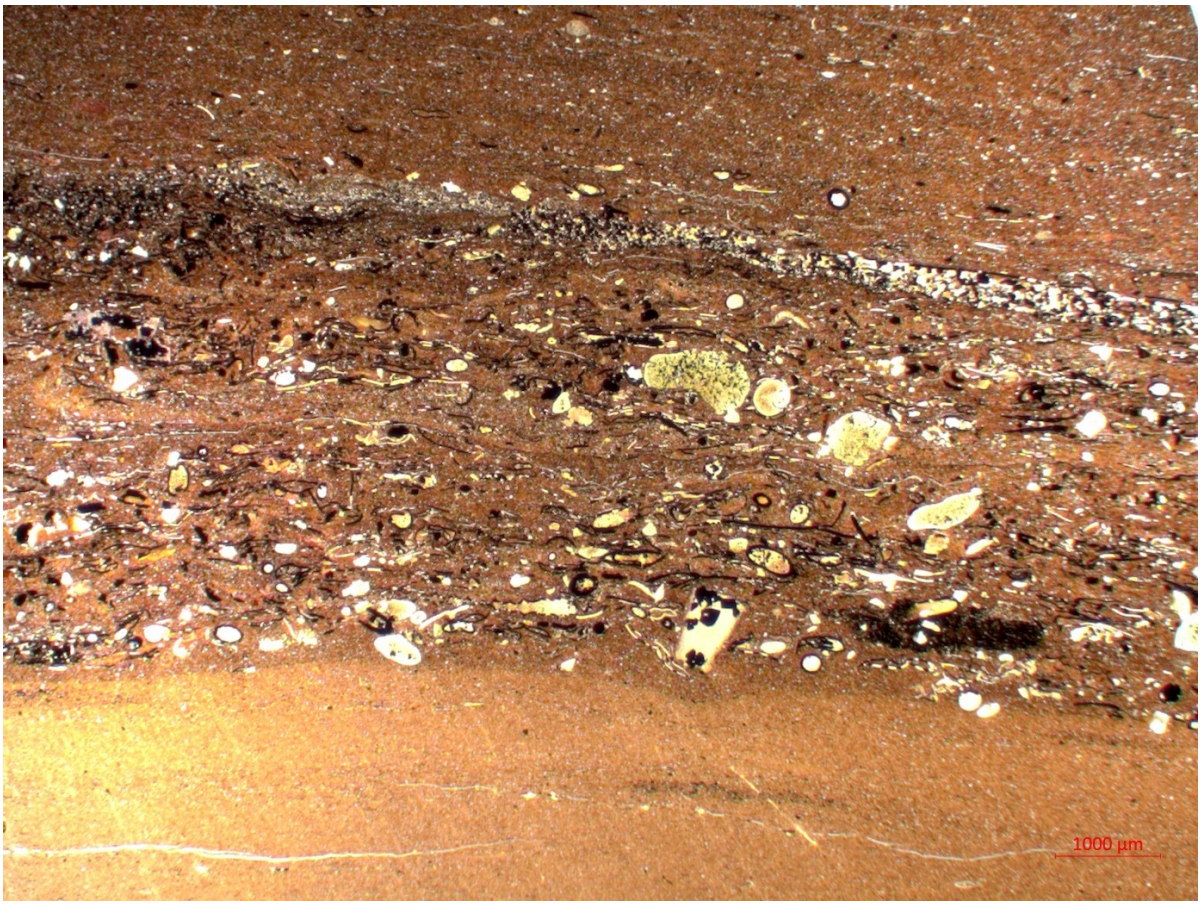

3347.26 A

- Possible contourite
- Sharp planar base and top
- Overall fining upward structure throughout
- Possible planar laminae throughout?
    - Hard to see and burrowed
- Possible burrowing (mud infilled)
    - Subhorizontal toward base
    - Subvertical toward top
    - ~500 um thick
- Near base:
    - ~30-40% fossil fragments
        - Coarse silt to coarse sand sized
        - ~90% Styliolinids
        - ~10% Tentaculitids
        - (Possibly up to 20% rads/calcispheres but more likely small styliolinid cross sections)
        - Almost all partially pyritized

    - ~5-10% (framboidal) pyrite grains
- Near top:
    - ~20% fossil fragments
        - Vf silt to vs sand sized (~10% of that is m sand sized styliolinid fragments
        - Partially pyritized
        - ~5% up to vfs (framboidal pyrite grains)

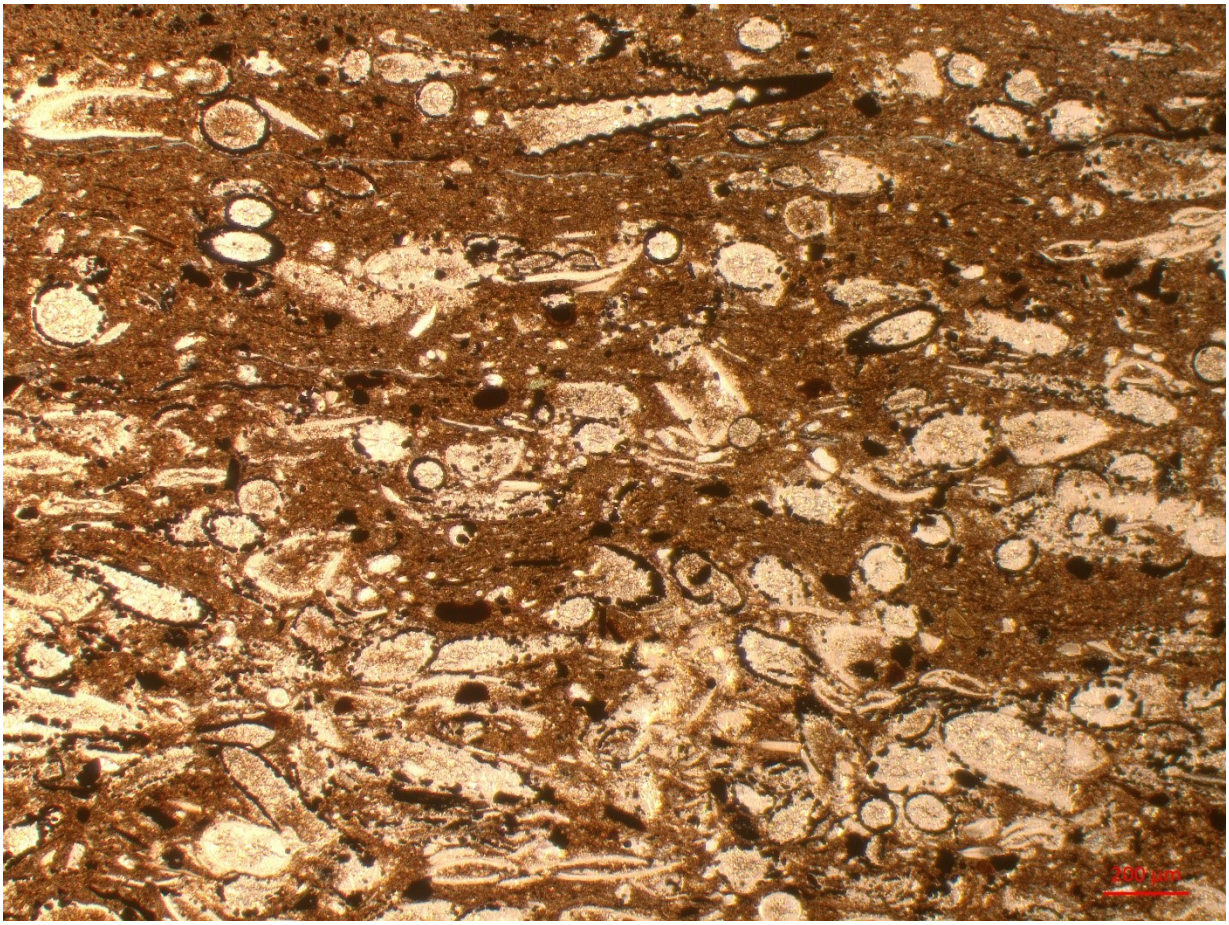

3346.87

- Sharp, possibly erosive contact with overlying up to 3mm thick fossiliferous lag deposit
- Lag:
    - Likely slight fining up texture to lag
    - Sharp, Likely erosive base
    - Sharp, slightly undulatory top
    - ~40-20% glauconite grains moving up in lag (up to nearly 1mm)
    - ~15% styliolinid fragments (most partially pyritized on outside) (up to nearly 1mm long)
    - ~5-10% bivalve/brachiopod fragments (up to 3mm across)
    - ~3% conodont jaw elements (up to 600 um)
    - ~3% phosphatic grains (up to 300 um)
    - ~10% Up to 1.5 mm thick pyrite nodules; some possibly burrows
- Below:
    - More bioturbated mud
    - Appears more massive
    - Possible pyritized burrows
    - More clay-rich burrows
    - Large subhorizontal burrow from base of lag into underyling mud

- Above:
    - Planar laminated mud
    - ~10% thin calcite and quartz silt layers
        - ~20% fossil fragments (Likely styliolinids, tentaculitids, bivalves/brachiopods)
    - ~10-15% of rock very fine fossil fragments (possibly brachiopods, bivalves, styliolinids)
    - Clay aggregates (mud lenses) (up to 1mm long) increasing in abundance towards top of TS
        - Elongate shape
        - Some areas forming ~300 um thick layers
        - ~10-30% (increasing upward)

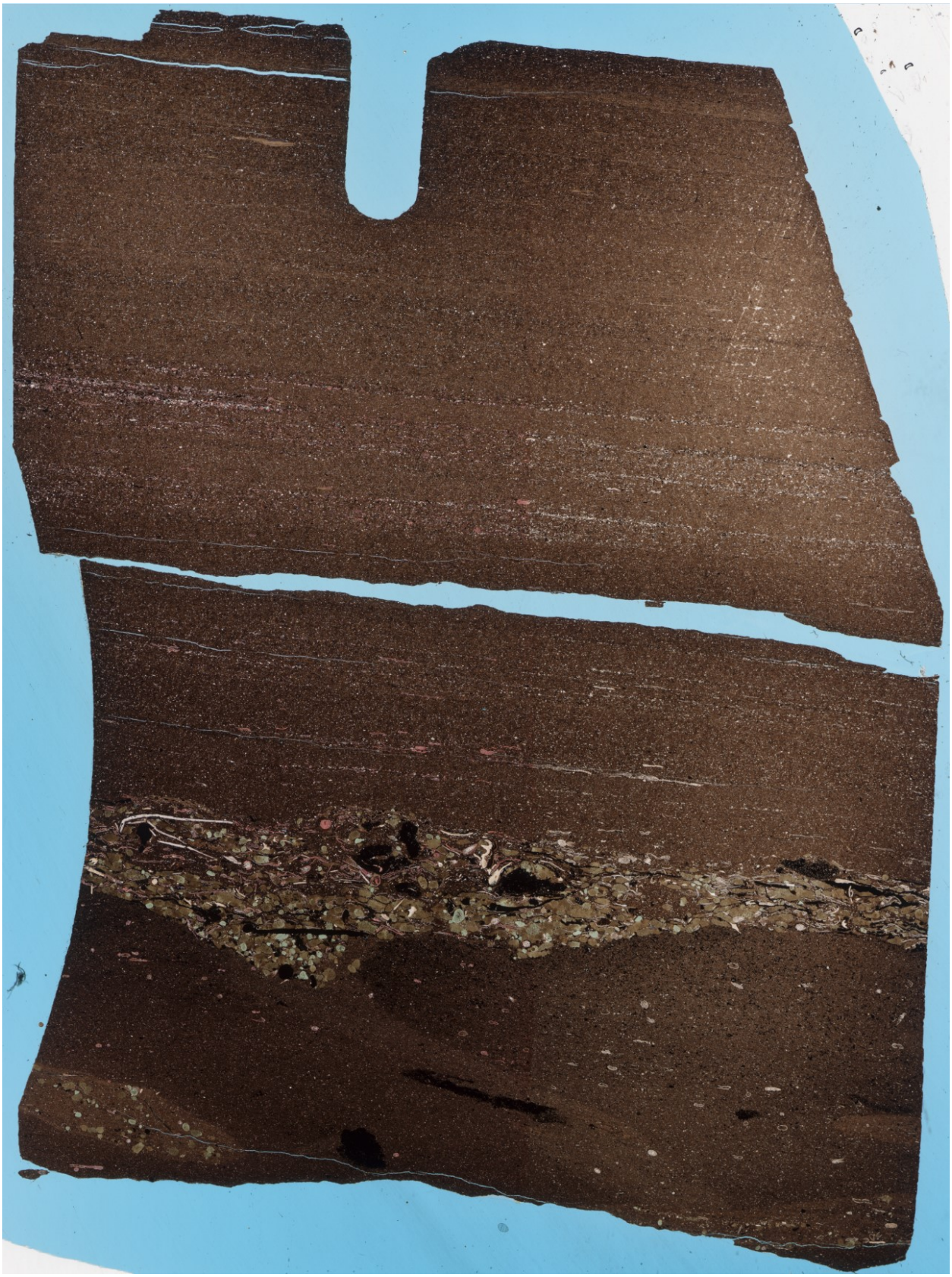

3346.35

- 7mm thick pyrite-rich layer
    - Quite sharp planar base and more gradational planar top
    - Decreasing pyrite content and grain size moving up through layer
    - ~30-15% pyrite (up to ~200 um)
    - ~5% phosphatic grains throughout layer (up to 150 um)
    - ~5% dolomite crystals (up to 150 um)
    - ~15% styliolinid and tentaculitid fossil fragments
    - 5-10% quartz silt
    - Appears to be quite burrow mottled
        - Likely pyrite lining or surrounding burrows
        - Burrows appear more clay infilled with no pyrite
- Above and below layer
    - Burrow mottled, mudstone
    - Planar laminated (disrupted by burrowing)
    - Up to 0.5 mm thick burrows (possibly planolites)
    - ~5% styliolinid and tentaculitid fragments

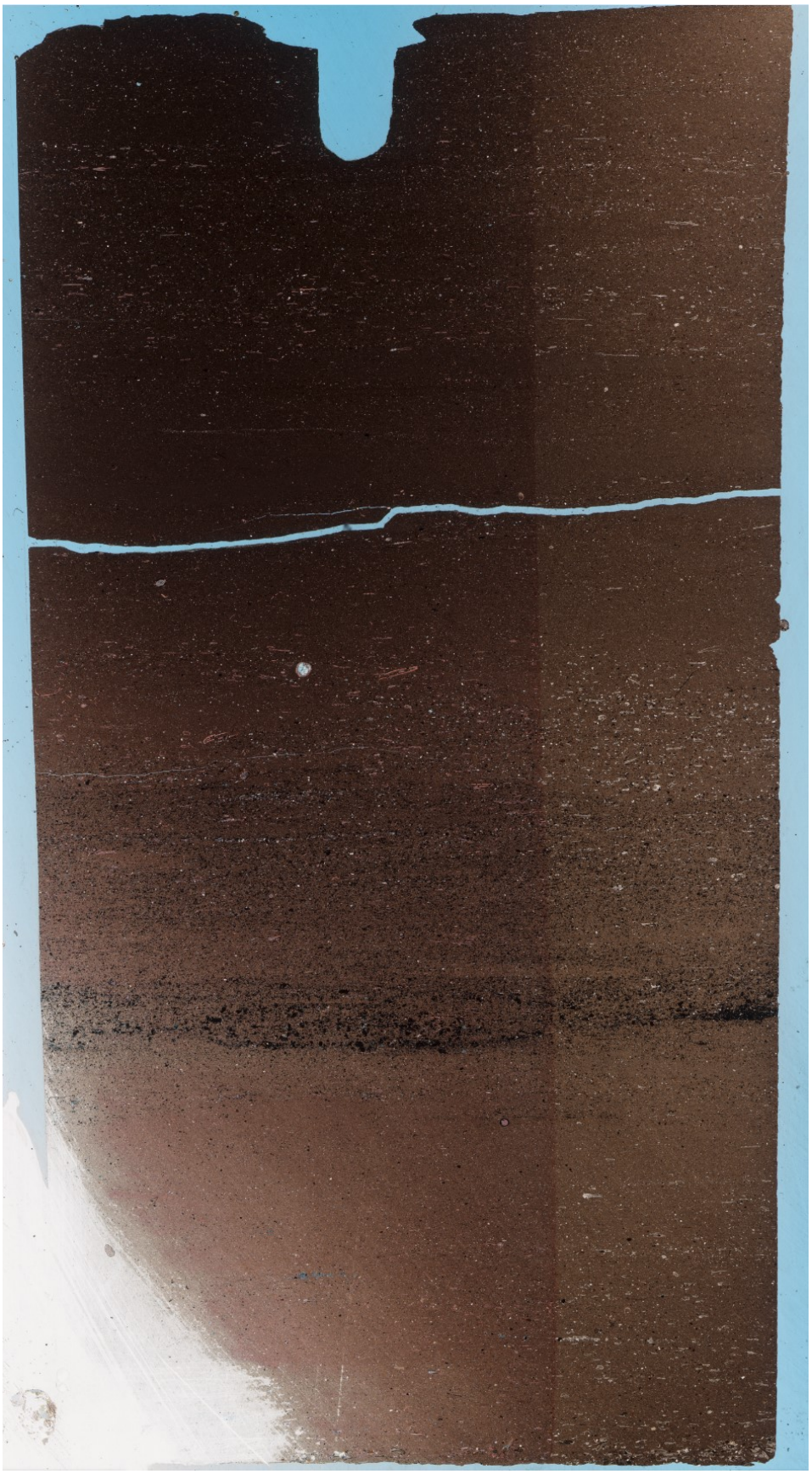

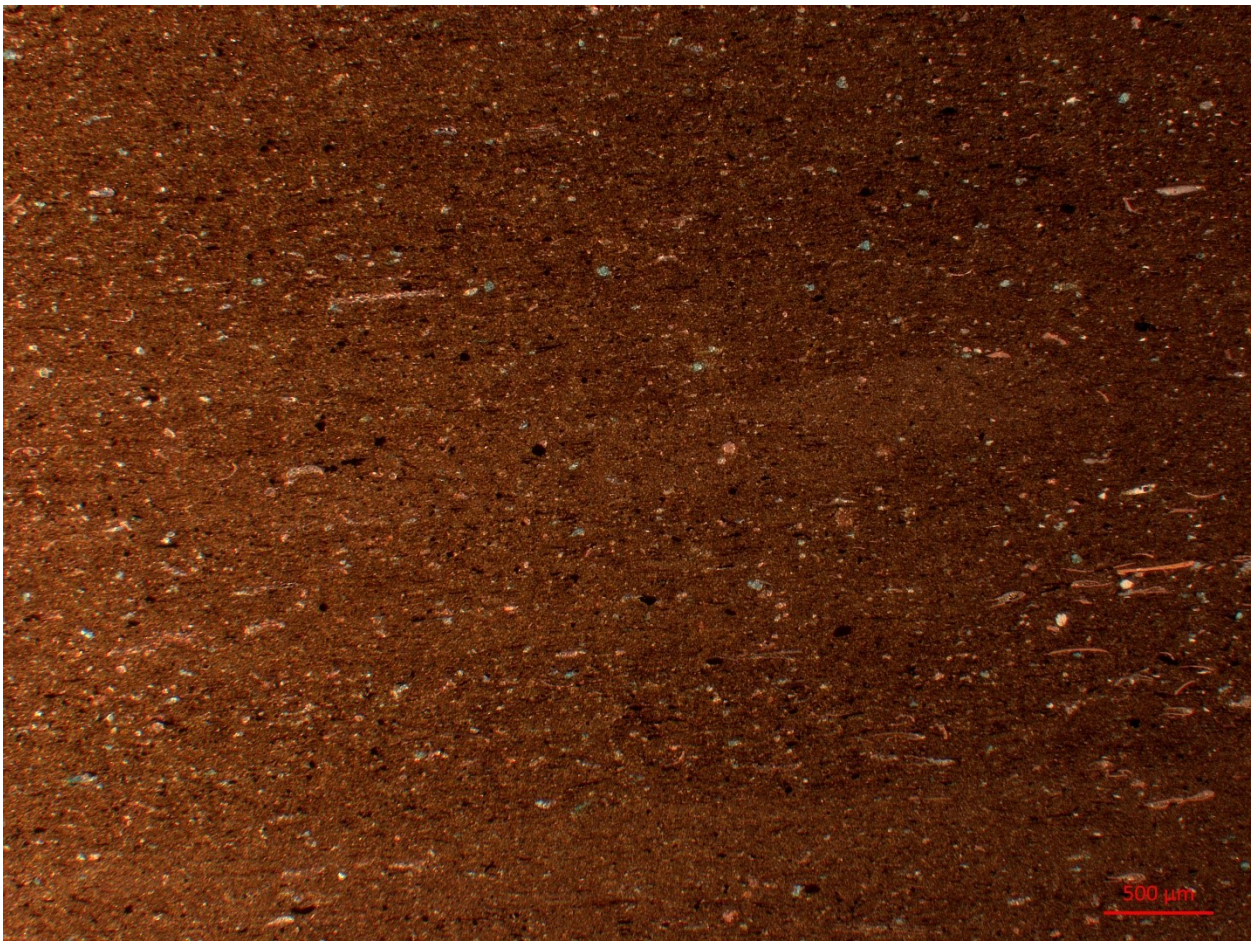

3333.04

- Very Massive appearing mudstone
- Large pyritized burrows (mud infilled)
    - <1mm thick
    - subhorizontal
- One possible pyritized water escape structure or fracture
- ~10% pyrite throughout thin section
- ~3-5% silt to vfs sized styliolinid and possibly tentaculitid fragments and ostracod/brachiopod fragments?
- Possibly 1% calcispheres? (but possibly styliolinids) (maybe radiolarians?)
- <1% silt sized phosphatic grains

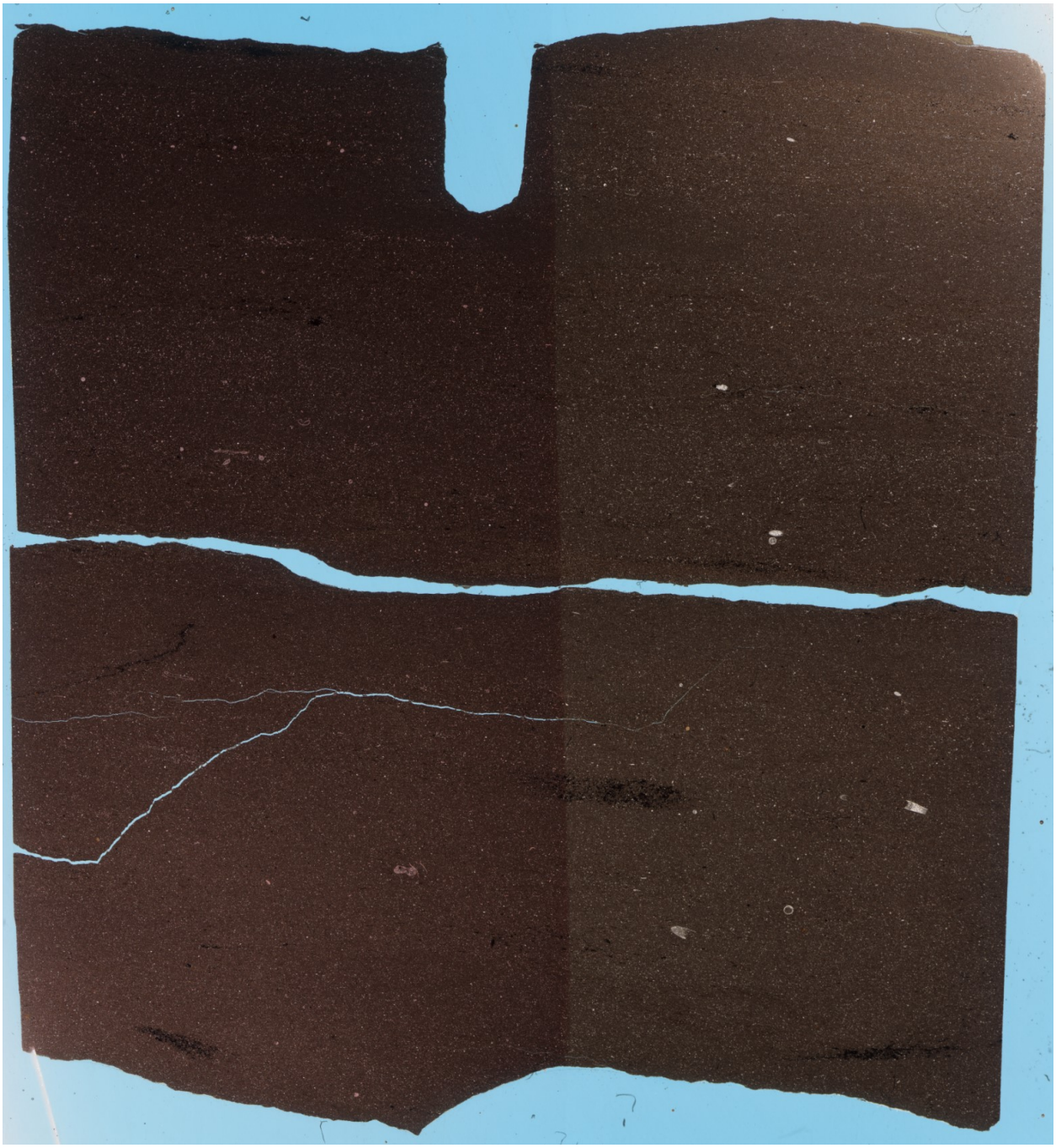

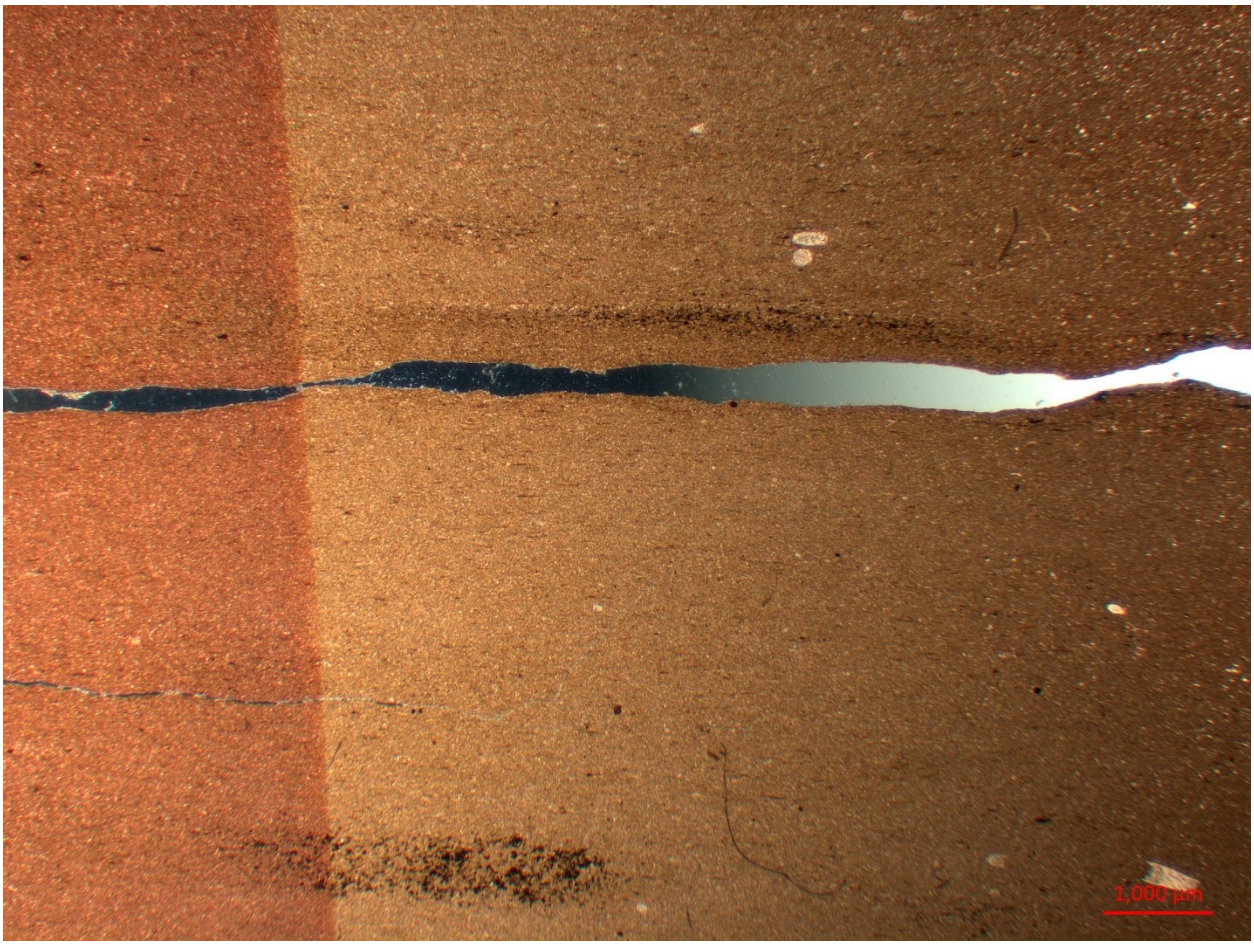

3332.85

- 7 mm thick fossiliferous silt and pyrite grain layer
    - Quite carbonate cemented
    - ~30% silt to m. sand grains
        - 40% styliolinid fragments
        - 30% pyrite grains
        - 3% conodont jaw elements
    - Massive structure
    - Generally random orientation of grains
        - Possibly rough horizontal orientation
    - Possible load casts/water escape/soft sed def structures at base of silt layer
        - Possibly burrow escape structures but no obvious burrowing signs
- Above and below:
    - Planar laminated mud
        - Continuous
        - ~100-500 um thick coarser (up to silt sized) and more organic/clay lean laminae and finer more organic rich laminae

- ~75% carbonate silt (~25% quartz silt)
    - ~30% carbonate silt is very broken up fossil fragments

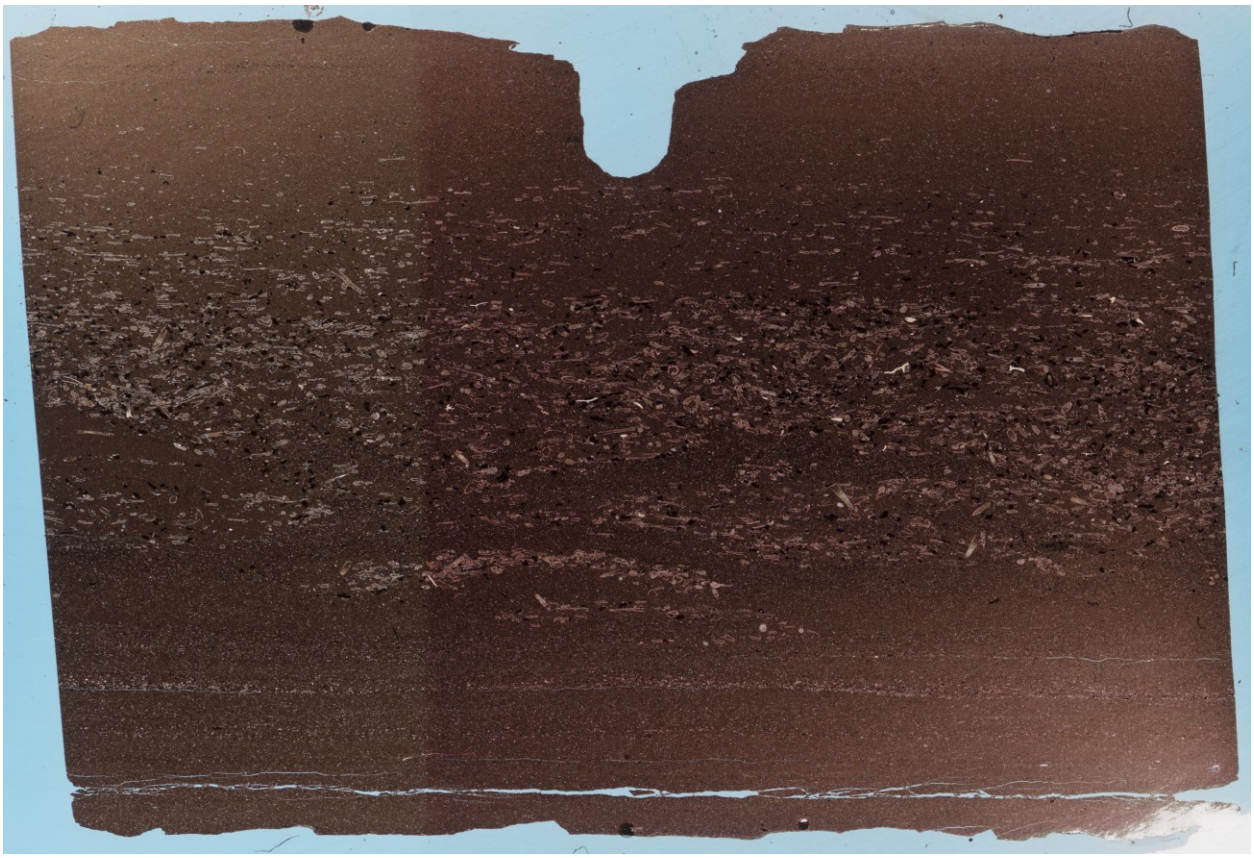

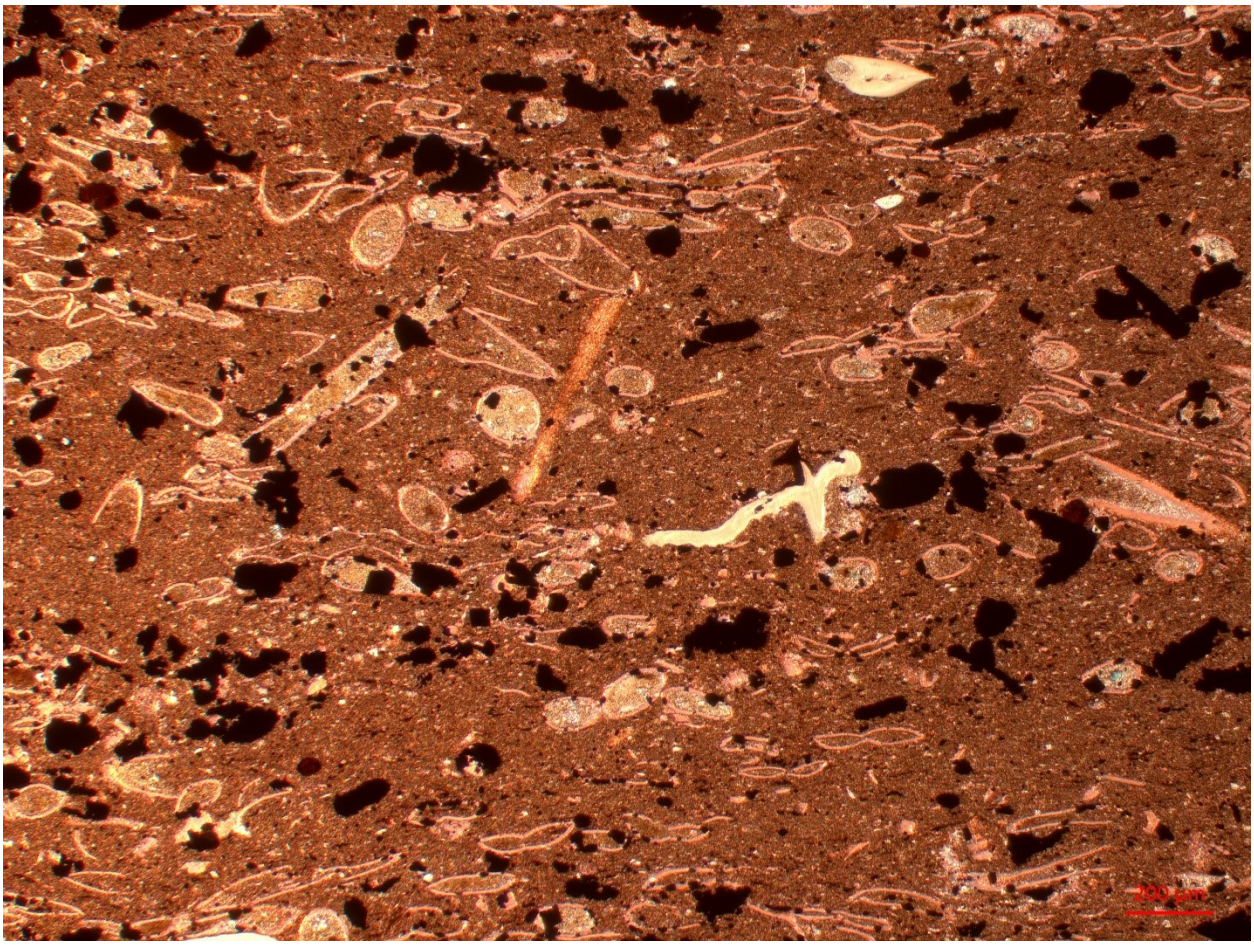

3331.05

- Planar laminated mud
    - ~100-500 um thick coarser (up to silt sized) and more organic/clay lean laminae and finer more organic rich laminae
        - No obvious grading within laminae
        - Pyrite more abundant in finer layers
            - ~5% coarse layers; ~10% fine layers
- Roughly 10% Fossil fragments
    - Up to f. sand sized
    - Fossils
        - 90% styliolinid fragments
        - ~5% conodont elements (phosphatic)
        - ~5% possible radiolarians? (siliceous)
    - Organized into planar continuous to semi-continuous layers up to 2mm thick
        - No obvious grading
        - Sharp bottom and top contacts

- Lenticular silt-rich, fossiliferous layers may represent starved ripples or silt-infilled burrows
- ~10% pyrite grains within layers
    - Some partially replacing fossil fragments

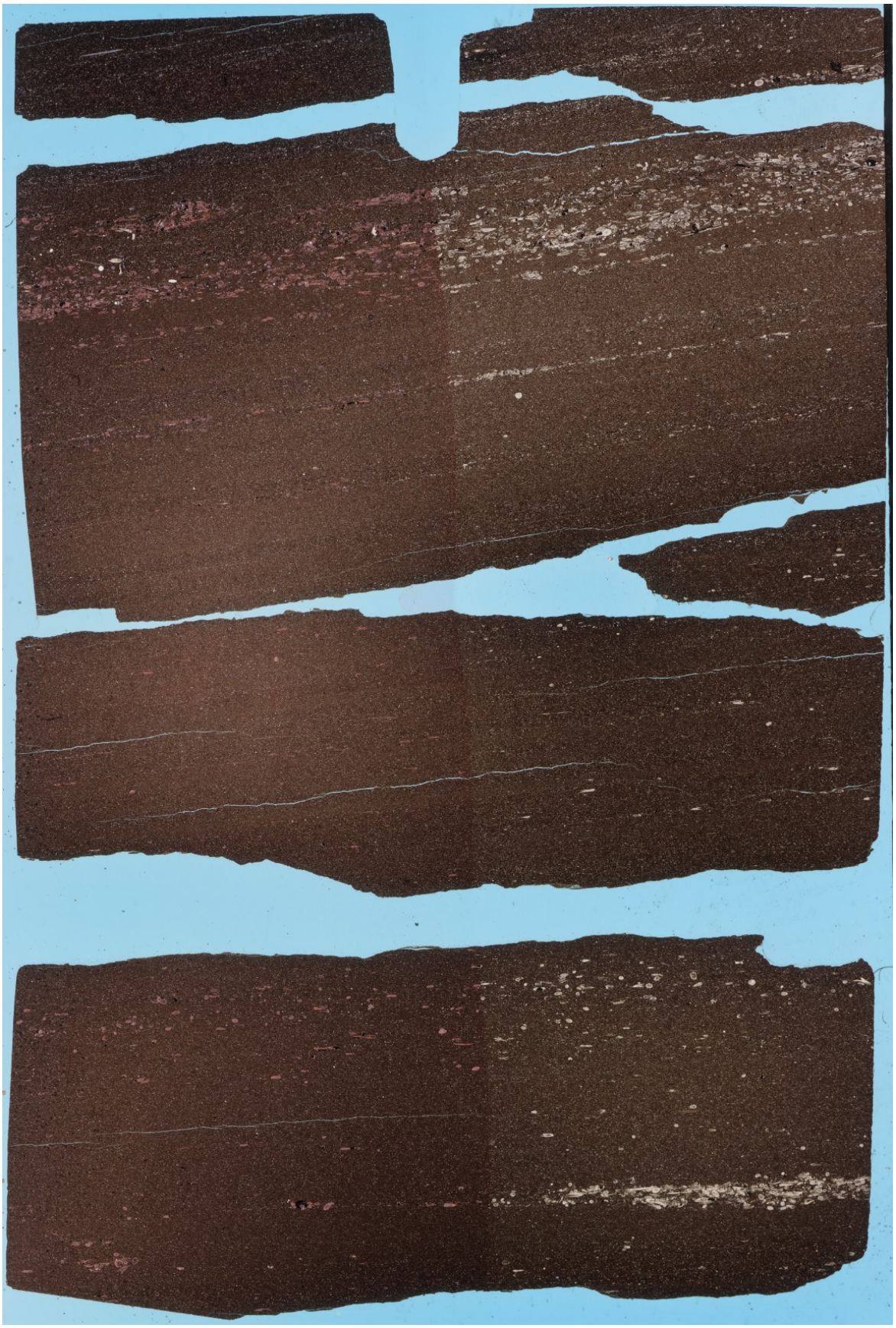

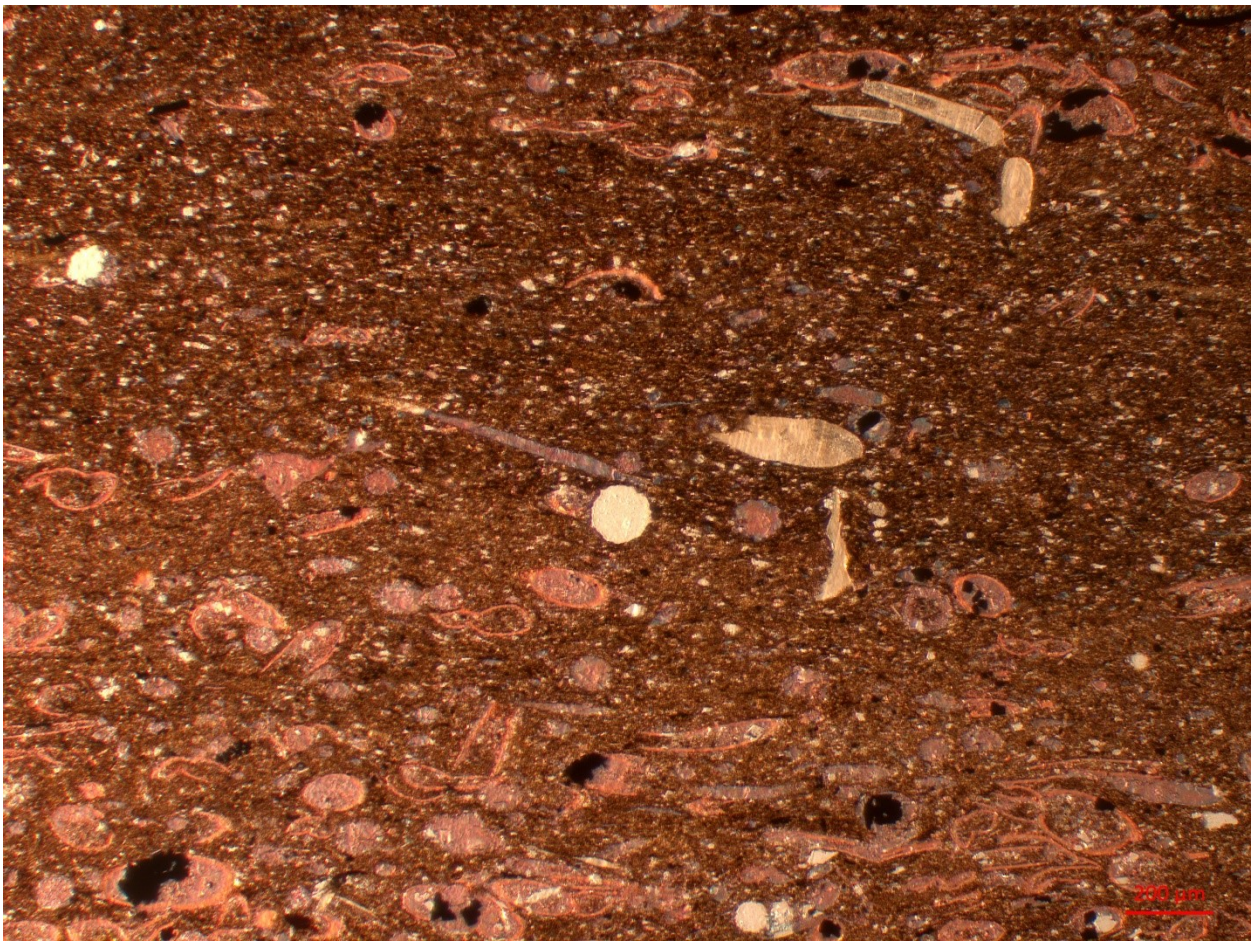

3329.75

- Carbonate silt layers in planar laminated mud
- Planar laminated mud:
    - Planar, continuous laminae
        - ~100 um thick
        - Darker = more clay/OM rich
        - Lighter = slightly coarser, less OM/clay rich
    - ~10-15% Silt to vfs grains
        - ~80% calcite grains
            - ~30% fossil fragments (thin bivalves/brachiopods, styliolinids)
        - ~18% Quartz feldspar grains
        - ~1% dolomite grains
        - ~1% phosphatic grains
    - 1-3% clay aggregates (or mud peloids) (up to 450 um)
    - ~5% pyrite grains
- Silt layers:
    - Up to 5mm thick

- Up to M. sand grains (couple larger fossil fragments)
- Wavy laminae
- Continuous to discontinuous
    - Possibly starved ripples or burrowing
- Sharp bases (possibly erosional)
    - One more gradational base
- Sharp and gradational tops
- Typically:
    - Sharp (to possibly gradational) base – sharp top (contourite?)
    - Erosional sharp base – gradational top (Turbidite?)
- ~70% calcite silt/sand
- ~30% Quartz/feldspar silt/sand
- ~5% pyrite grains
- ~1% phosphatic grains (conodont elements)
- Possible contourite layers typically much less fossil content
    - Up to ~5%
    - Shell fragments
    - Possibly just very recrystallized fossils
    - Round calcite crystals
    - More cemented
- Possible turbidite layers typically higher fossil content
    - ~90% fossils
        - ~90% styliolinids
        - ~5% brachiopod/bivalve shells
        - ~5% conodonts
    - Possible large subhorizontal mud filled burrows visible in silty layers

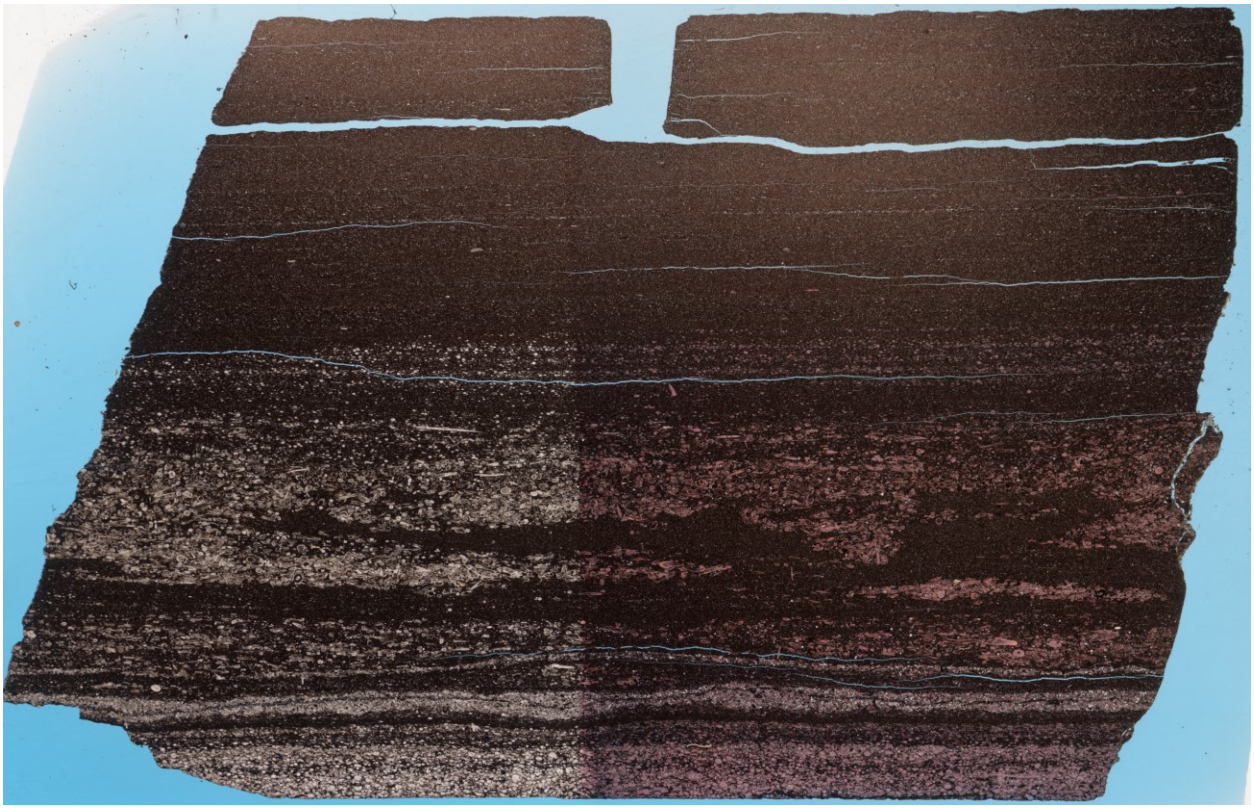

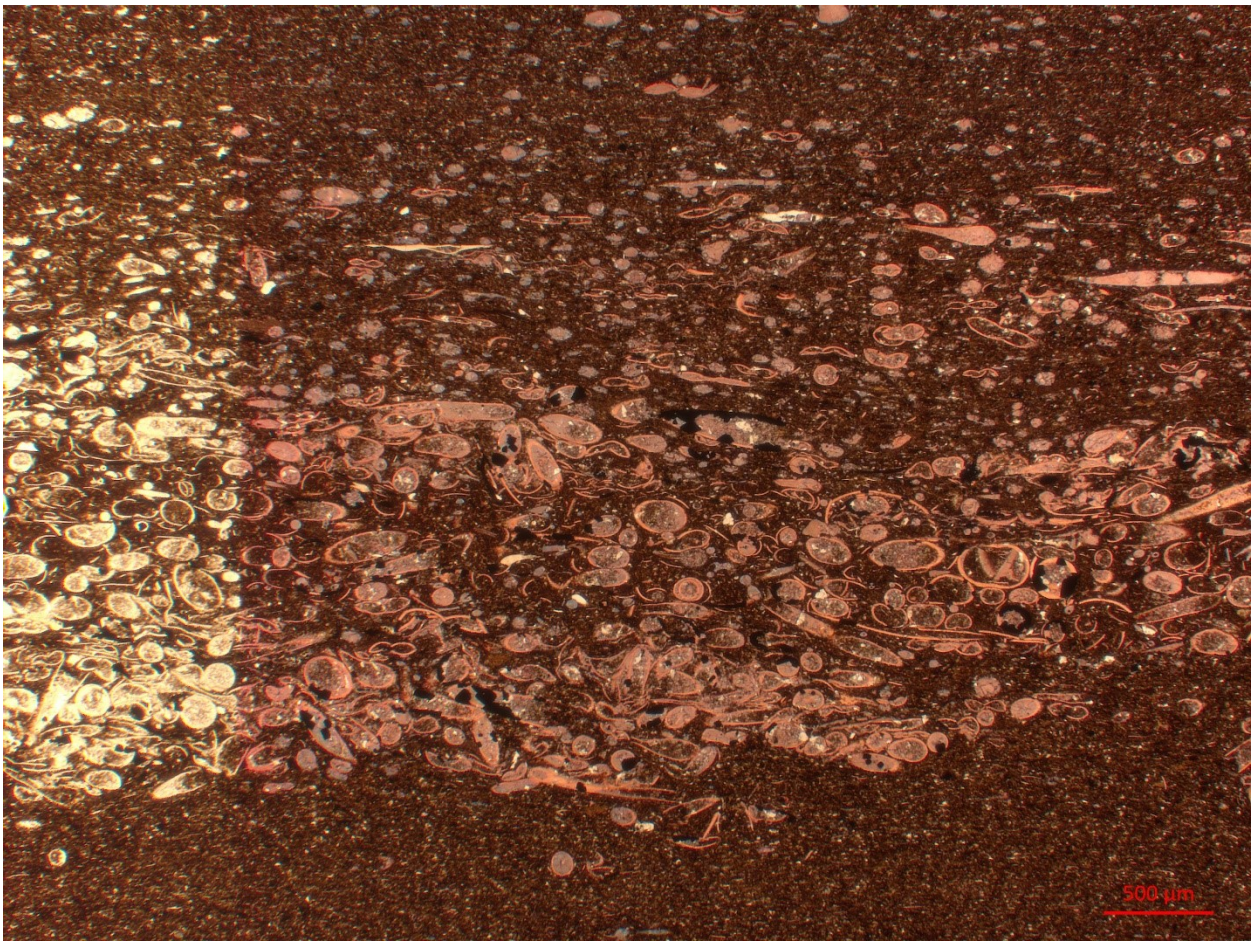

3328.7

- Pyritized vfs layer at top of thin section:
  - Appears moderately to intensely bioturbated
    - Subhorizontal to subvertical burrows
    - Mud infilled (pushing aside silt/sand grains)
  - Most of matrix made up of lenticular shaped clay aggregates
    - ~50% appear very pyritized or are possibly just elongate pyrite nodules
    - Likely current rip-up clasts
  - Base of pyritized zone irregular and likely burrowed and possibly erosive
    - Pyritized burrows (subhorizontal to subvertical) penetrating into underlying unit
  - ~3% fossil fragments
    - Up to f. sand sized bivalves?/brachiopods? fragments, conodont elements, styliolinid fragments
- Slightly wavy continuous silt and vfs laminae in mud:
  - Up to ~0.6 mm thick
  - Silt laminae thicken into silt nodules (bedload transport)
  - Silt laminae diverge and converge slightly

        - Suggests bedload by bottom currents (Contour currents)
    - Silt in laminae:
        - ~80% quartz
        - ~20% calcite
    - ~3% clay aggregates/mud rip up clasts in matrix
    - ~10% pyrite in matrix
    - ~35% clay matrix
    - Moderate bioturbation
        - More bioturbation toward top of silt laminae unit (subvertical to subhorizontal)

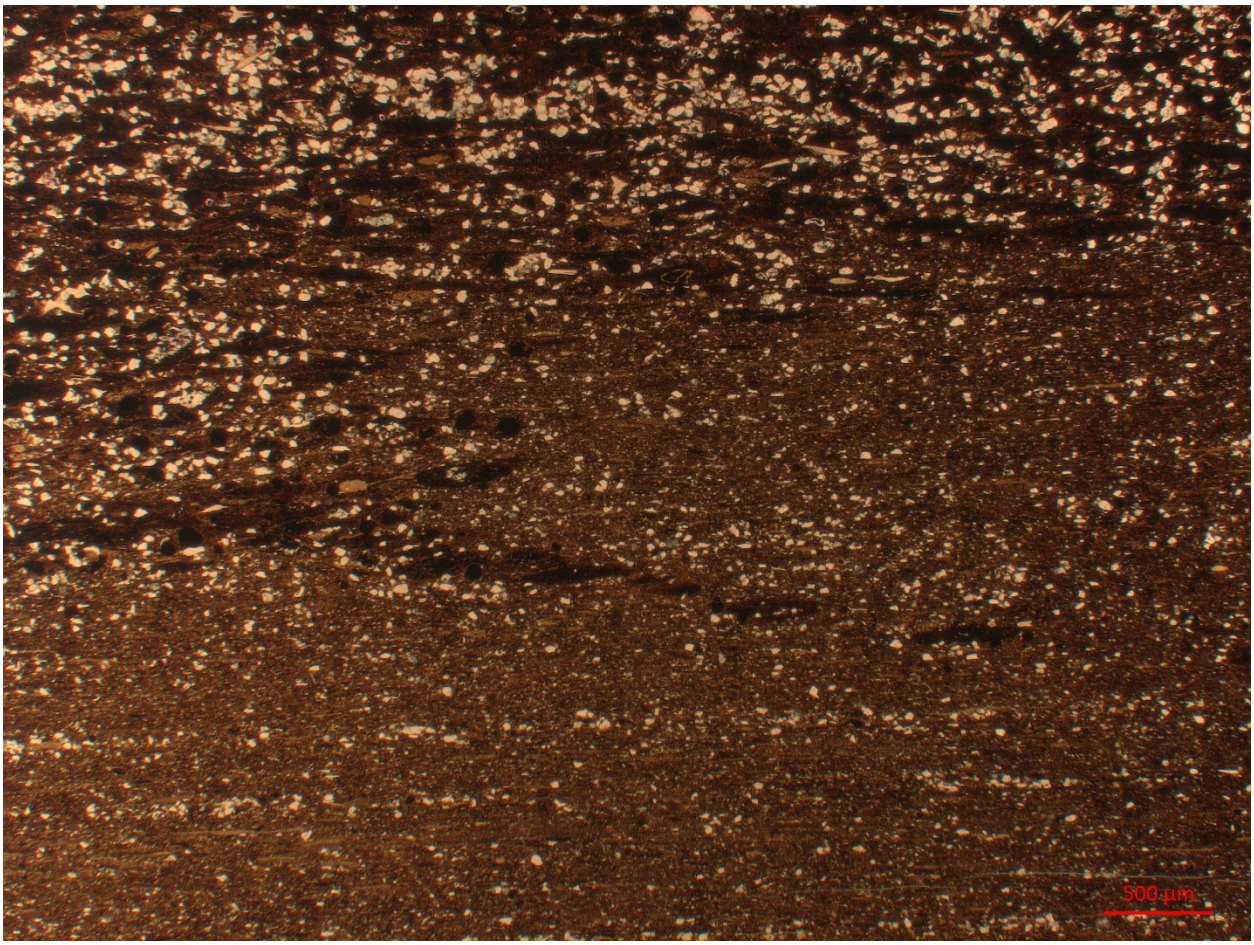

3325.12

- Discontinuous pyritized laminae
    - Slightly wavy
    - Slightly gradational upper and lower boundaries
    - Pinch and swell a bit
    - Converge and diverge slightly
    - Appear possibly more continuous viewed in XPL but pyrite less continuous and obvious in PPL
        - Possibly due to more carbonate silt in pyrite laminae and more clay in others
- ~15% silt throughout
    - ~90% calcite silt
        - ~20% fossil fragments (likely brachiopods/ostracods/styliolinid shell fragments)
    - ~10% quartz silt
- ~15% pyrite
- <1% clay aggregates/ mud rip-up clast
- <1% conodont elements
- Clay matrix

- Likely sparse to moderate bioturbation
    - Subvertical to subhorizontal mud infilled disrupting laminae
    - Thin, small (up to ~125 um)

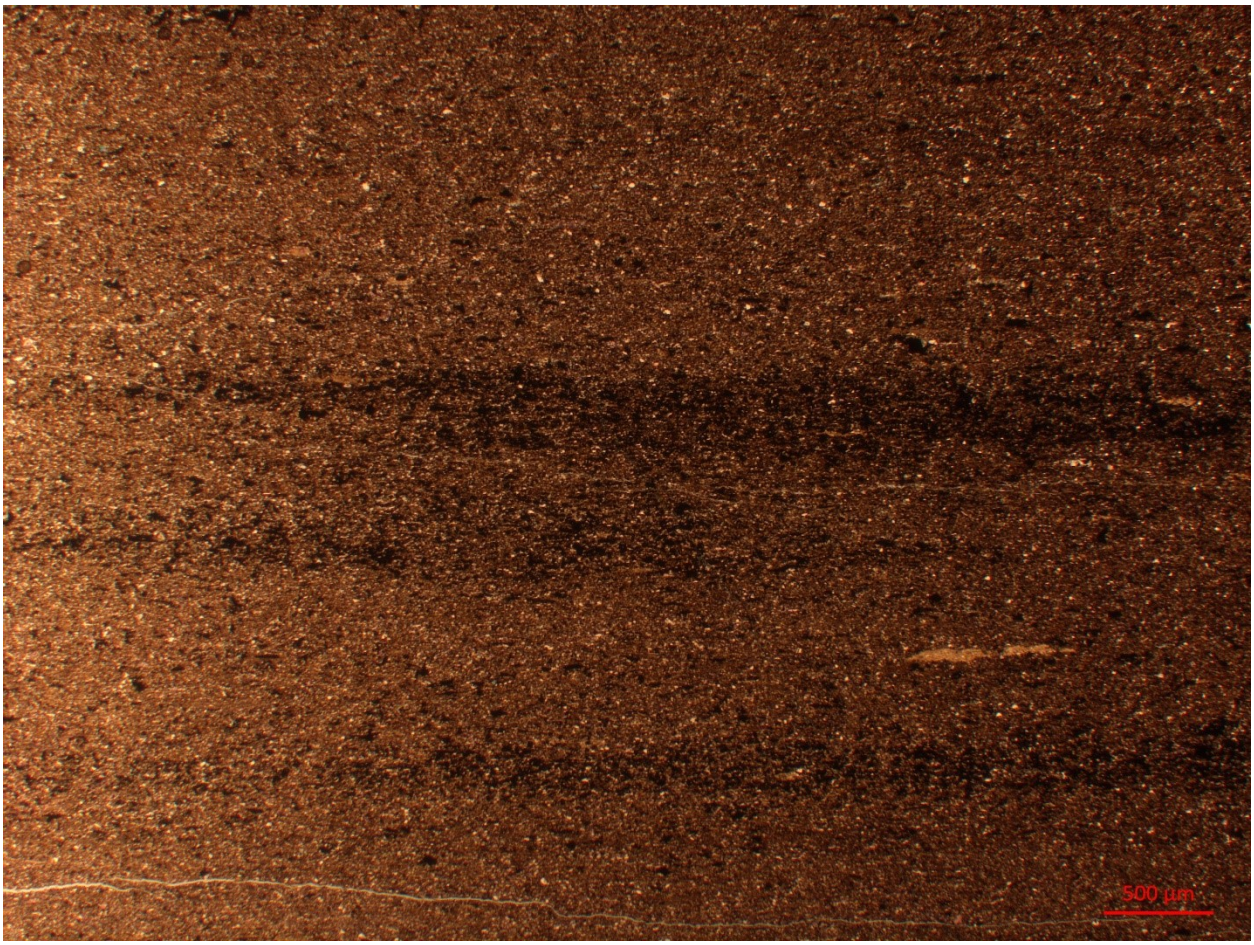

3316.97

- Quite massive appearing mudstone
  - No obvious laminae (possibly disrupted)
- 2 visible large possible pyritized burrows
  - Horizontal
  - Up to 0.5 mm thick
  - Infilled by pyrite grains (not pyritized fossil fragments and silt grains like in the discontinuous pyrite laminae facies)
  - Appear to be slightly richer in clay than surrounding rock
- ~30-35% silt
  - ~42% quartz
  - ~42% calcite
  - ~15% pyrite
    - ~50% likely pyritized fossil fragments (brachiopod/bivalve/styliolinid shell fragments?)
  - ~1% dolomite?
- ~1-3% clay aggregates/mud clasts

    - Elongate bed parallel
- Clay rich matrix
- One visible m. sand calcite grain
- Likely moderately to intensely background bioturbated
    - Hard to see
    - Lots of small possible subvertical to subhorizontal burrows
        - Mud infilled
    - Completely disrupted laminae

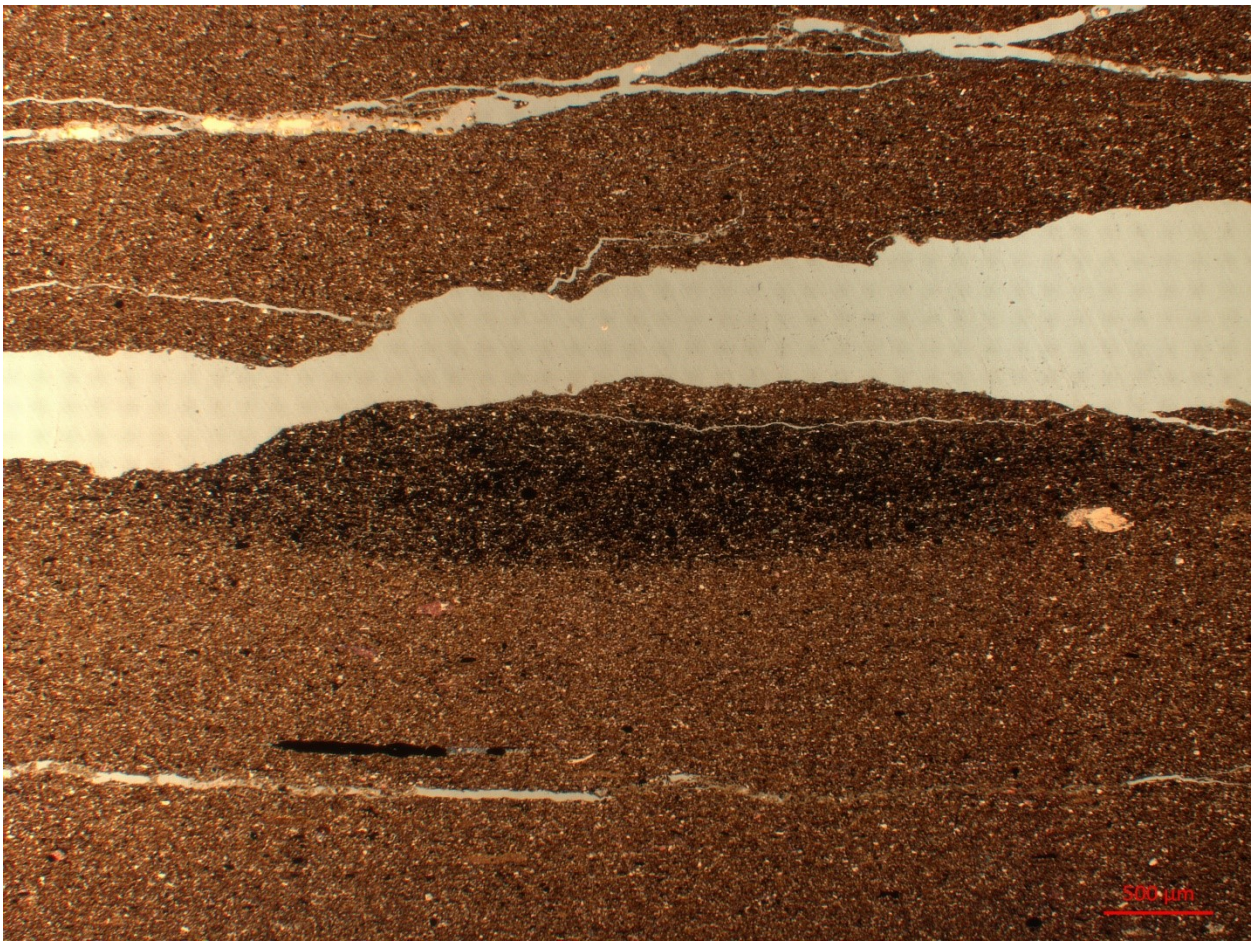

3304.37

- *(Bottom half and top half of thin section are mixed up)*
- Above contact (Ireton):
    - Carbonate (likely dolomite) cemented, clay rich mud
    - ~10-15% silt and vfs
        - ~35% dolomite
            - Sparse possible shell fragments
        - ~25% quartz
        - ~15% pyrite
        - ~20% phosphatic grains
            - Some conodont elements
        - ~5% glauconite grains (closer to surface)
    - ~3-5% clay aggregates/mud rip up clasts
    - Abundant very thin, wispy OM aggregates
    - Sparse very faint possible planar laminae but appears quite disrupted or cemented
- Contact and lag:
    - Undulatory, erosive appearing surface

- Lag:
    - Matrix appears somewhat transitional between Duvernay and Ireton
        - Possibly disrupted laminae or large lenses (rip-up clasts?) of Ireton-like dolomitized clay in Duvernay-like OM/pyrite-rich mud
            - Possibly up to 1.5x7 mm
        - Slightly undulatory laminae
    - Elongate silt and sand sized grains aligned semi-bed parallel
        - Likely deposited by high energy
    - ~25-30% silt to vfs grains
        - ~25% glauconite grains
        - ~10% conodont elements
        - ~10% phosphatic grains
        - ~20% pyrite grains
        - ~17% quartz grains (silt)
        - ~17% Dolomite grains (Silt) (birefringent but not stained)
- Residual lag deposits above surface and main lag?:
    - Up to 0.5 mm thick
    - Appear slightly undulatory
    - Inverse grading
    - Gradational bases, sharp tops
    - Similar fossil, silt and sand component to main lag

- Below contact (Duvernay):
    - Planar laminated mud with thin silt laminae
        - Thin silt laminae
            - Up to ~200 um thick
            - Slightly wavy
            - Normal (sharp base, gradational tops) and inverse grading (gradational bases, sharp tops)
            - Slight pinching and swelling
            - Slight divergence and convergence of laminae
            - (likely contourites)
    - ~30% silt and vfs
        - ~65% calcite
        - ~25% quartz
        - ~10% pyrite
    - ~1% clay aggregates/mud clasts
    - Likely sparse to moderate bioturbation
        - Subvertical, mud infilled
        - More bioturbation where less silt laminae
- Surface:
    - Likely soft sediment deformed
        - Likely ball structures in underlying Duvernay mud
            - Elongate, squished
            - Made up of overlying material including lag material

                - Up to ~4mm thick
                - Quite diffuse, possibly interfingering boundaries
                - (could it be a raft or rip up clast?)
            - Somewhat diffuse surface
                - Rough interfingering look to overlying and underlying mud
                    - Similar look to clay aggregates
                - Possibly no definitive contact anymore from soft sed def
- Lag:
    - Appear to have multiple (3-4 visible) lag deposits above surface?
        - Coarse grains appear to increase towards tops
            - Inverse graded
            - Sharp tops, more gradational bottoms
        - Structure of lags appears quite disturbed by abundant subvertical mud infilled burrows
    - Elongate grains oriented roughly parallel to bedding
    - Composition:
        - Abundant quartz silt to fs
        - Abundant glauconite grains (very high birefringence)
        - Common dolomite and calcite z-fs
        - Common conodont/skeletal elements
        - Common possible phosphatic grains
        - Clay rich matrix
            - Some ~10x100 um OM stringers (partially pyritized) and pyrite grains
                - Continue through Ireton
- Above:
    - Very clay rich Ireton
    - Likely quite bioturbated
        - Appears to be abundant very discrete subvertical mud infilled burrows
        - More visible in more silt rich zones
    - Sparse silt throughout
        - Appears to be very similar composition to lag deposits
- Below:
    - Planar laminated Duvernay mud
        - Appears quite continuous
    - Silt concentrated along laminae
        - Abundant calcite and quartz silt
            - ~65% calcite, 35% quartz?
            - Subangular to subrounded
    - More OM and pyrite rich
    - More siliceous
    - Appears slightly clay rich for Duvernay

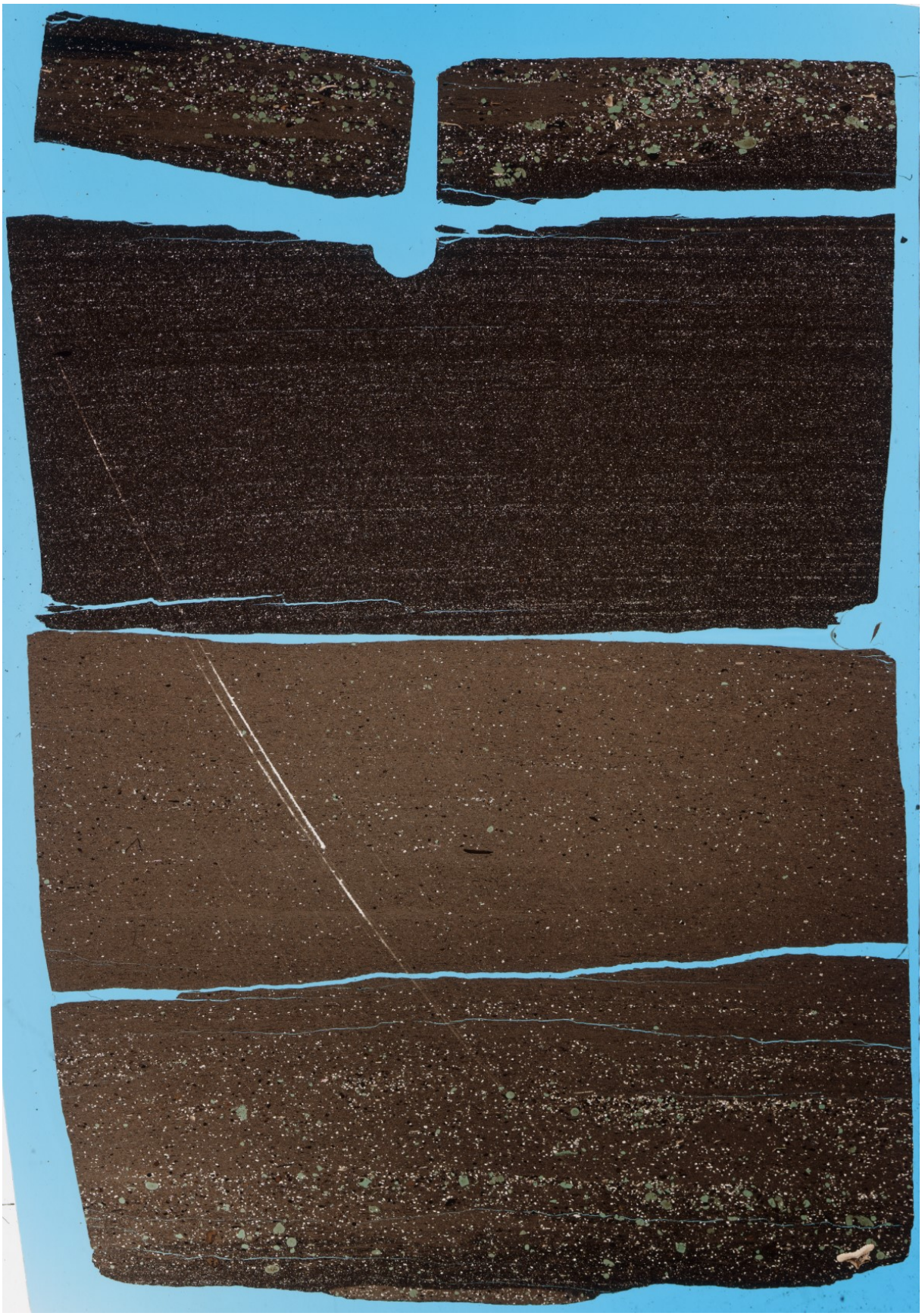

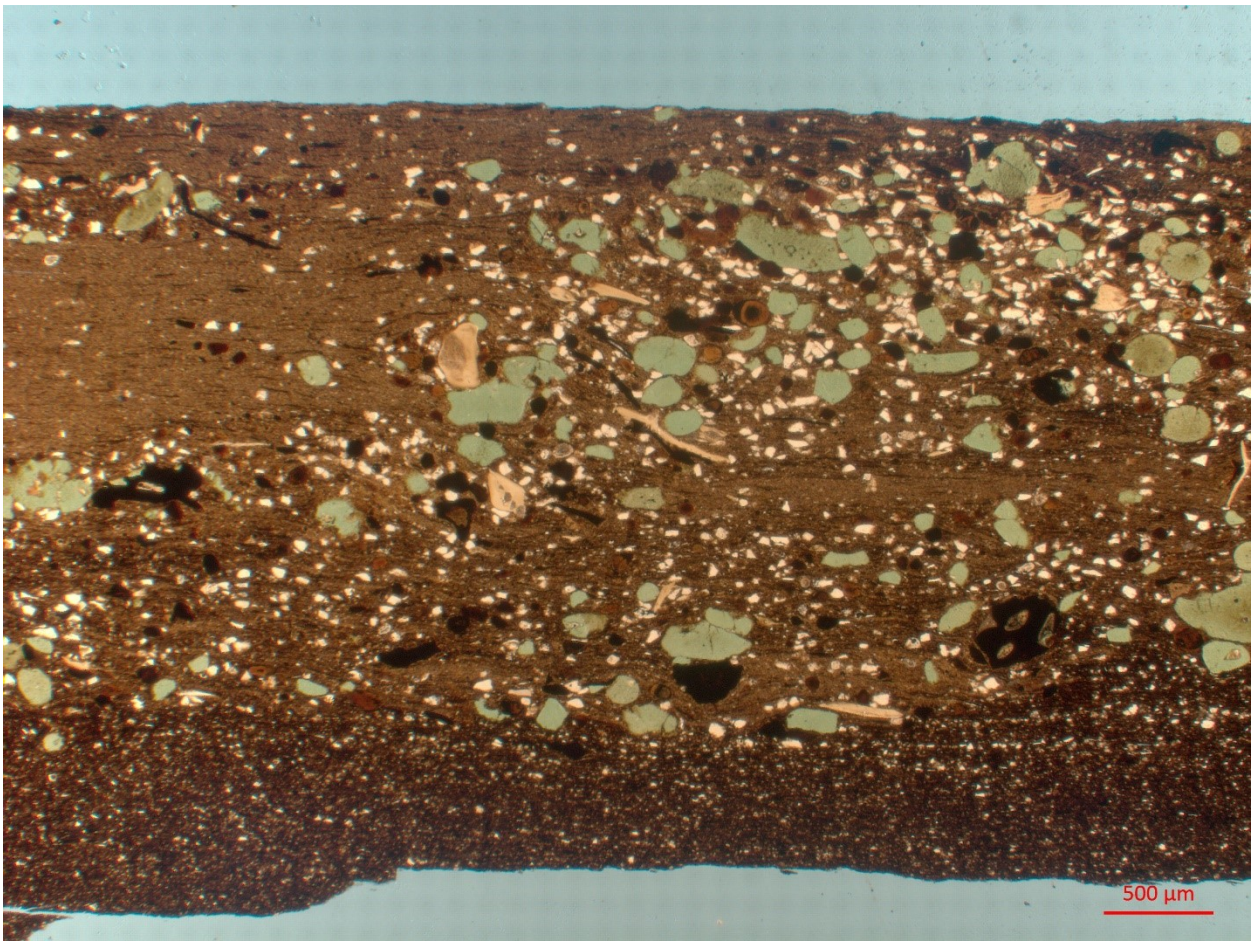

3304.04

- Wavy and discontinuous to possibly lenticular (slightly pyritized) laminated Ireton mud
- overlain by massive Ireton mud
    - ~10% vf-m sand grains
        - ~60% styliolinids
        - ~10% tentaculitids
        - ~20% conodont elements
        - ~10% phosphatic grains

Core 4 – SCL HZ Kaybob

<u>3122.74 m</u>

- Sedimentary structures:
    - Planar, continuous laminae
        - Up to ~500 um thick
        - Somewhat concentrated into more silty and less silty laminae
    - Discontinous, planar, whispy, thin pyrite laminae
        - Up to ~100 um thick
    - 1-2 mm diameter burrows
        - 2 Infilled by calcite and fossil fragments
            - Much skeletal fragments concentrated in infilled burrows
        - 2-3 possible pyritized 500-1000 um burrows
- Texture:
    - Subrounded to rounded
    - Well sorted
- Medium to Coarse Sand: (0%)
- V. Fine to Fine Sand: (~1%)
    - Non-Skeletal: (0%)
    - Skeletal: (100%)
        - Common calcispheres?
        - Common styliolinid fragments (concentrated in infilled burrows)
            - Cross sections and lengthwise fragments

        - Rare possible ostracod fragments
- Medium to Coarse Silt: (~10%)
    - Non-Skeletal: (~80%)
        - 90% Calcite grains
        - 10% quartz grains
    - Skeletal: (~20%)
        - Calcite - Very broken up, styliolinid fragments and possible small recrystallized rads
- V.Fine to Fine Silt: (~55%)
    - 60% calcite grains
    - 30% quartz/feldspar grains
    - 10% micas (bed parallel aligned)
- Matrix: (~35%)

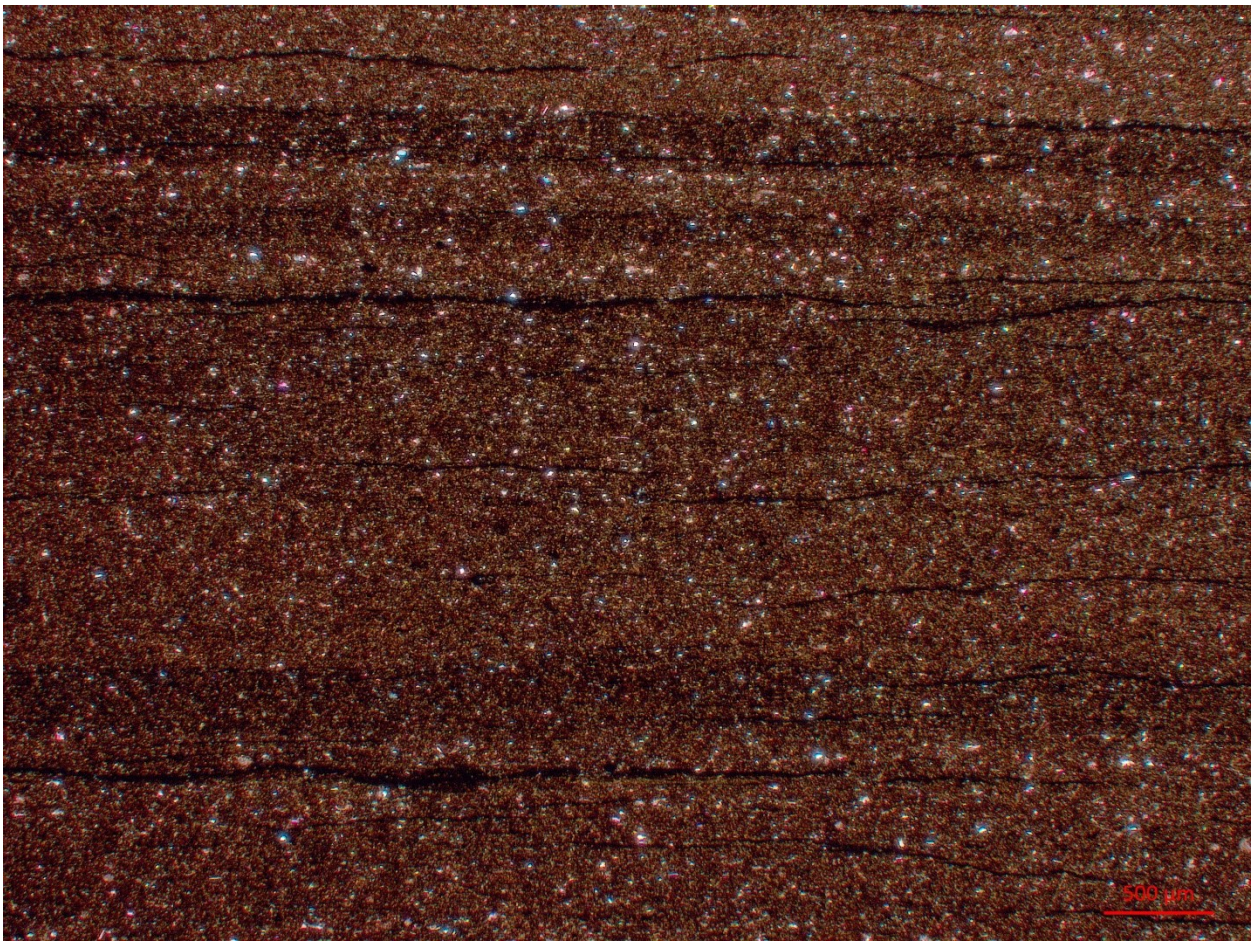

3122.5 m

- Sedimentary structures:
  - Up to 8 mm, subvertical to subhorizontal pyritized burrows (at least 3 visible)
  - Faint, Planar continuous laminae
    - Near bottom, fossil fragments concentrated into thicker (~1mm) laminae
  - Possible erosive surface with calcite infilled burrows
- Texture:
  - Subrounded to rounded
  - Well sorted
- Medium to Coarse Sand: (~2.5%)
  - Non-Skeletal: (0%)
  - Skeletal: (100%)
    - Styliolinids (mostly cross section or cut at angle)
      - Infilled by recrystallized calcite
      - Most concentrated in coarser laminae
- V. Fine to Fine Sand: (~2.5%)
  - Non-Skeletal: (50%)

        - Amorphous, round, calcite silt
    - Skeletal: (50%)
        - Styliolinids (small cross sections and fragments)
        - Calcitized radiolarians? Calcispheres?
        - Possible rare ostracod fragments
- Medium to Coarse Silt: (25%)
    - Non-Skeletal: (80%)
        - 65% Amorphous, round, calcite silt
        - 30% quartz/feldspar
        - 5% pyrite grains
    - Skeletal: (20%)
        - Calcitized rads? Calcispheres?
        - Styliolinid fragments
        - Possible rare ostracod fragments
- V.Fine to Fine Silt: (25%)
    - 70% Amorphous, round, calcite silt
    - 30% quartz/feldspar
- Matrix (Und.): (~45%)

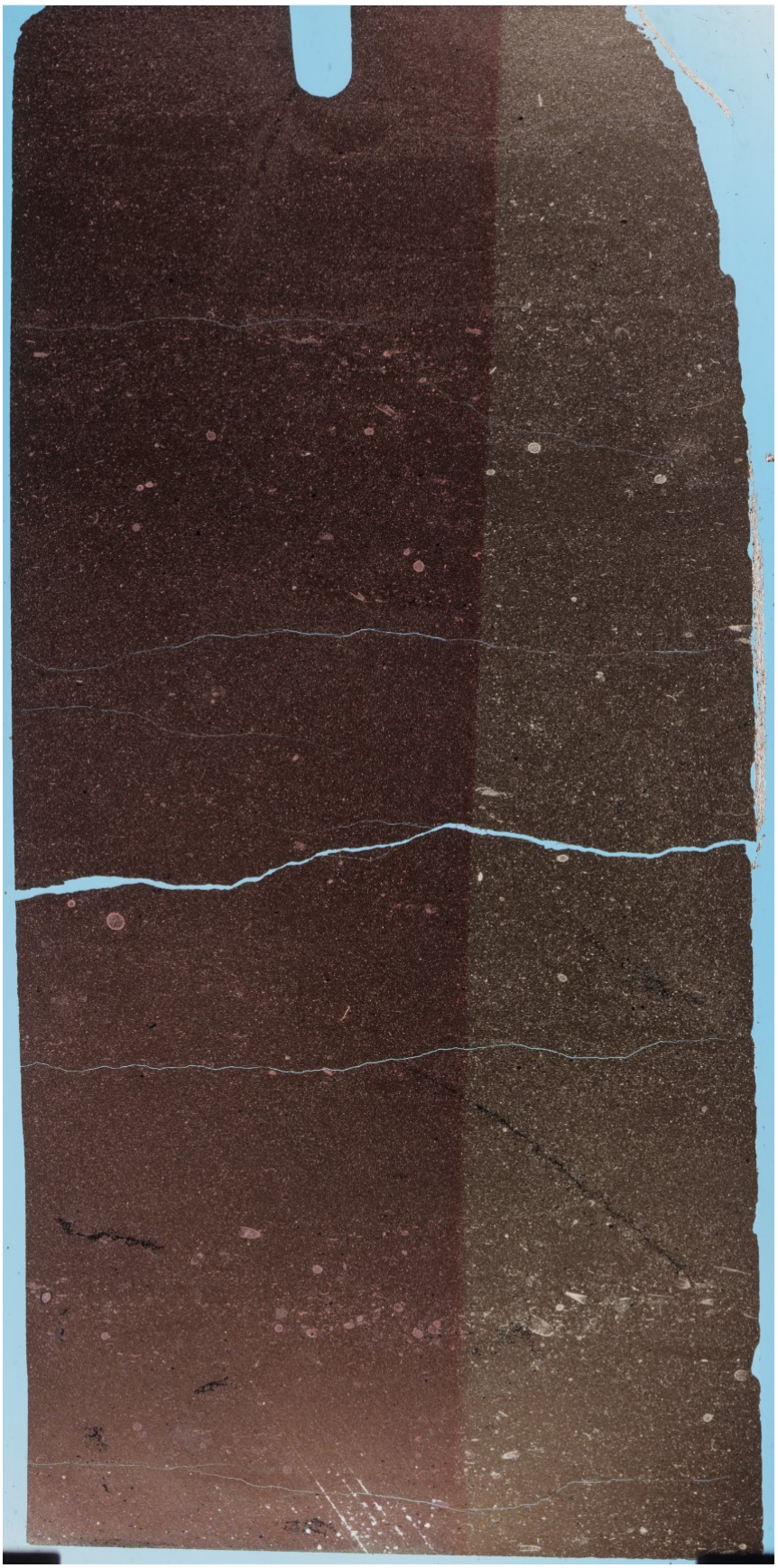

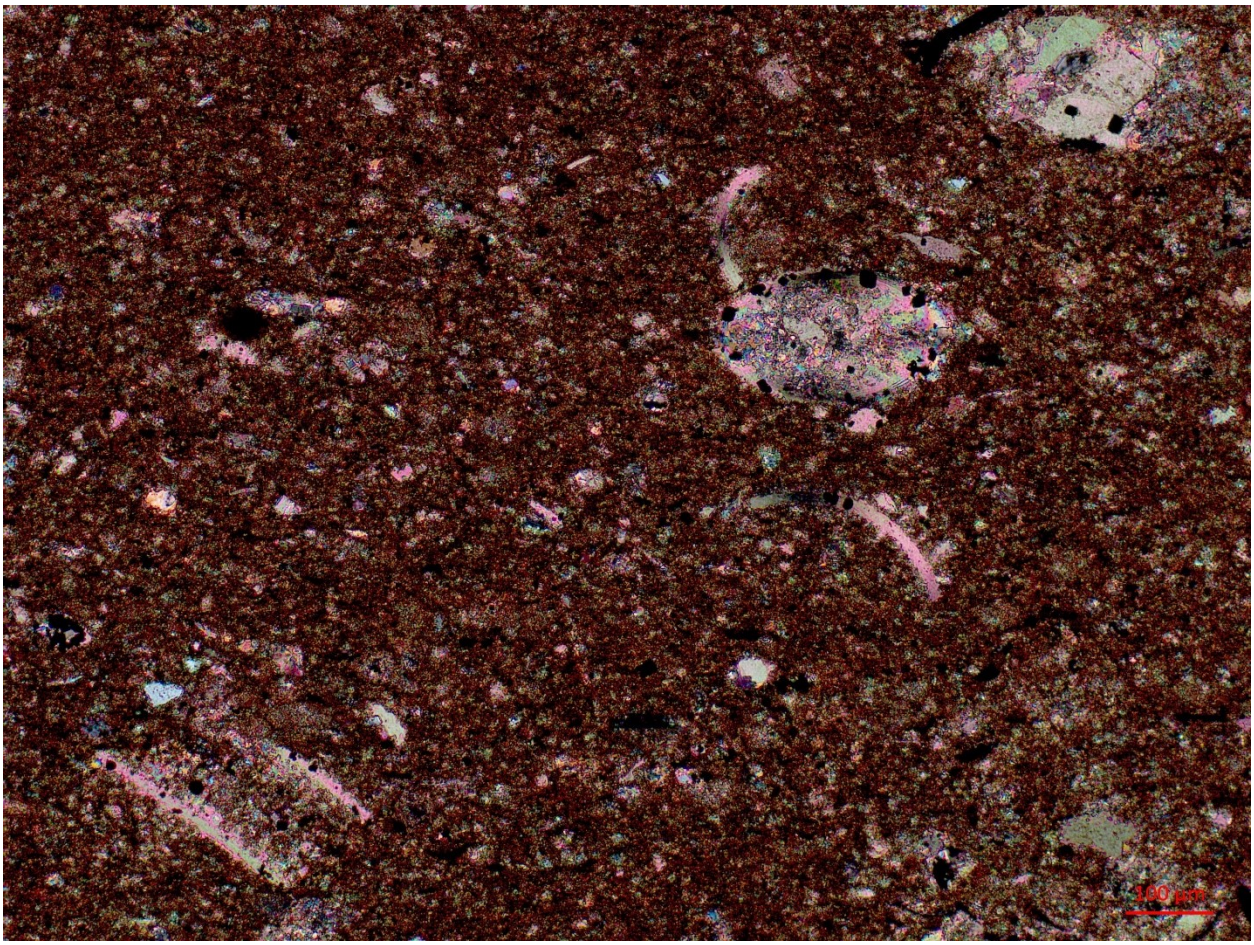

3121.6 m

- Sedimentary structures:
    - Slightly wavy, planar, continuous laminae
        - Some are pyrite cemented
        - 2mm thick pyrite cemented laminae at bottom of TS is quite wavy on bottom contact and may have been erosive
            - Burrow or dewatering structure going through laminae
    - 7mm thick fossil fragment and dolomitized silt grain lag deposit? Near bottom of thin section
- Texture:
    - Up to 2.5 mm long grains (longest = long brachiopod? fragments)
    - Moderately sorted
    - Angular to rounded
- Medium to Coarse Sand: (~5%) (~50% in coarse lag deposit)
    - Non-Skeletal: (30%)
        - Glauconite grains (in lag deposit)
            - Quite round or elongated sub-bed horizontal

                - Spongy-looking, smaller recrystallized dolomite infilling grains
        - Skeletal: (70%)
            - Styliolinids
                - Most abundant
                - Appear mostly bed-parallel
                - Infilled and slightly recrystallized interiors
            - Possible brachiopod fragments (in lag deposit)
                - Largest (longest) fragments
            - Conodont fragments (in lag deposit)
- V. Fine to Fine Sand: (5%)
    - Non-Skeletal: (30%)
        - Abundant glauconite grains (in lag deposit)
            - Quite round or elongated sub-bed horizontal
        - Sparse pyrite grains
    - Skeletal: (70%)
        - Styliolinids
            - Most abundant
            - Appear mostly bed-parallel
            - Infilled and slightly recrystallized interiors
        - Calcitized rads
        - Conodont fragments (in lag deposit)
        - Possible ostracod fragments
        - Possible brachiopod fragments (in lag deposit)
        - Tentaculitid fragment (outside lag deposit)
- Medium to Coarse Silt: (10%)
    - Non-Skeletal: (60%)
        - 60% quartz/feldspar (amorphous)
        - 15% mica (mostly sub-bed parallel orientation)
        - 15% calcite (amorphous)
        - 5% pyrite
    - Skeletal: (40%)
        - Styliolinid fragments
        - Possible ostracod/brachiopod fragments
        - Possible recrystallized very small rads
- V.Fine to Fine Silt: (25%)
    - ~65% quartz/feldspar
    - ~30% calcite
    - 5% pyrite
- Matrix (Und.): (55%)

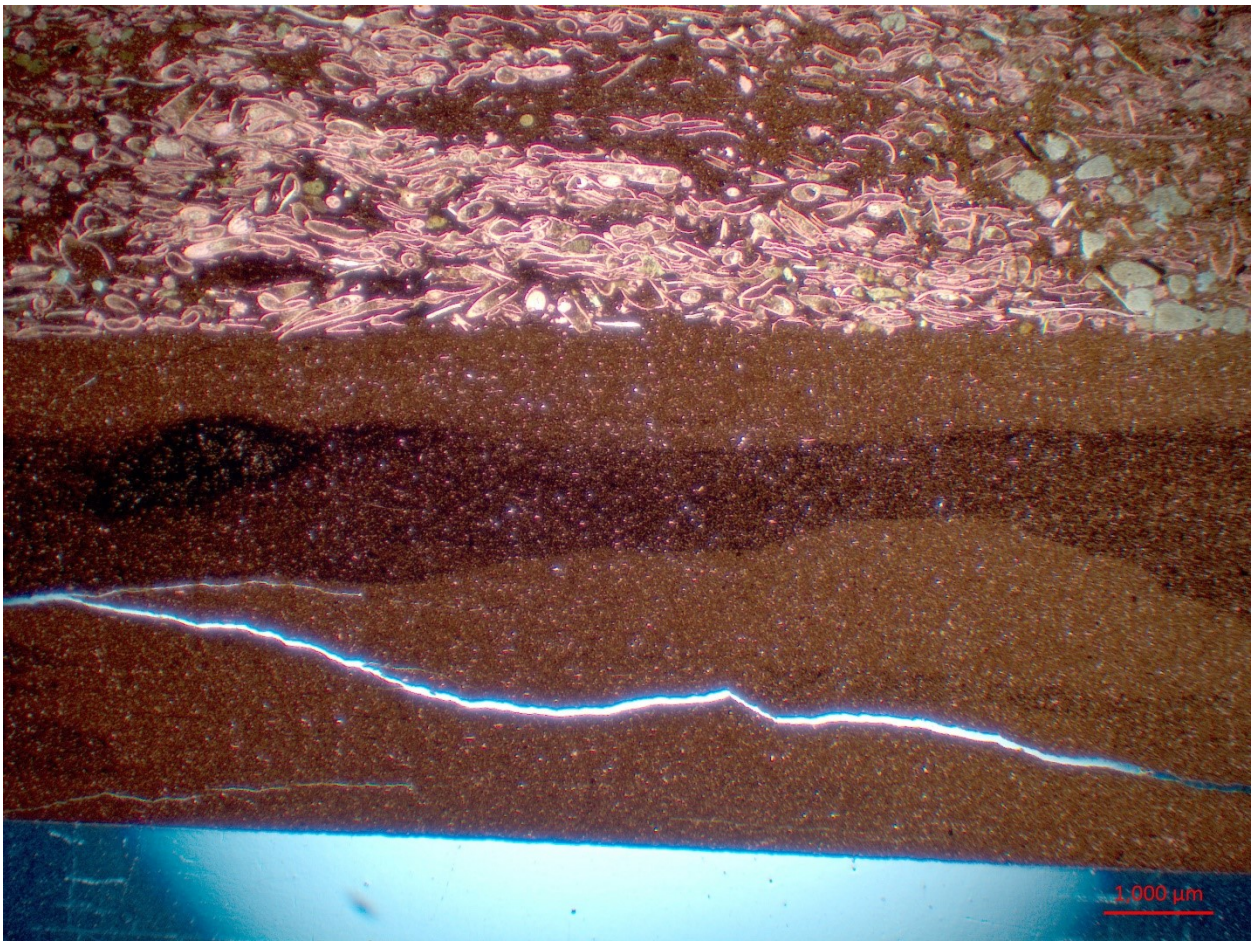
1.000 µm

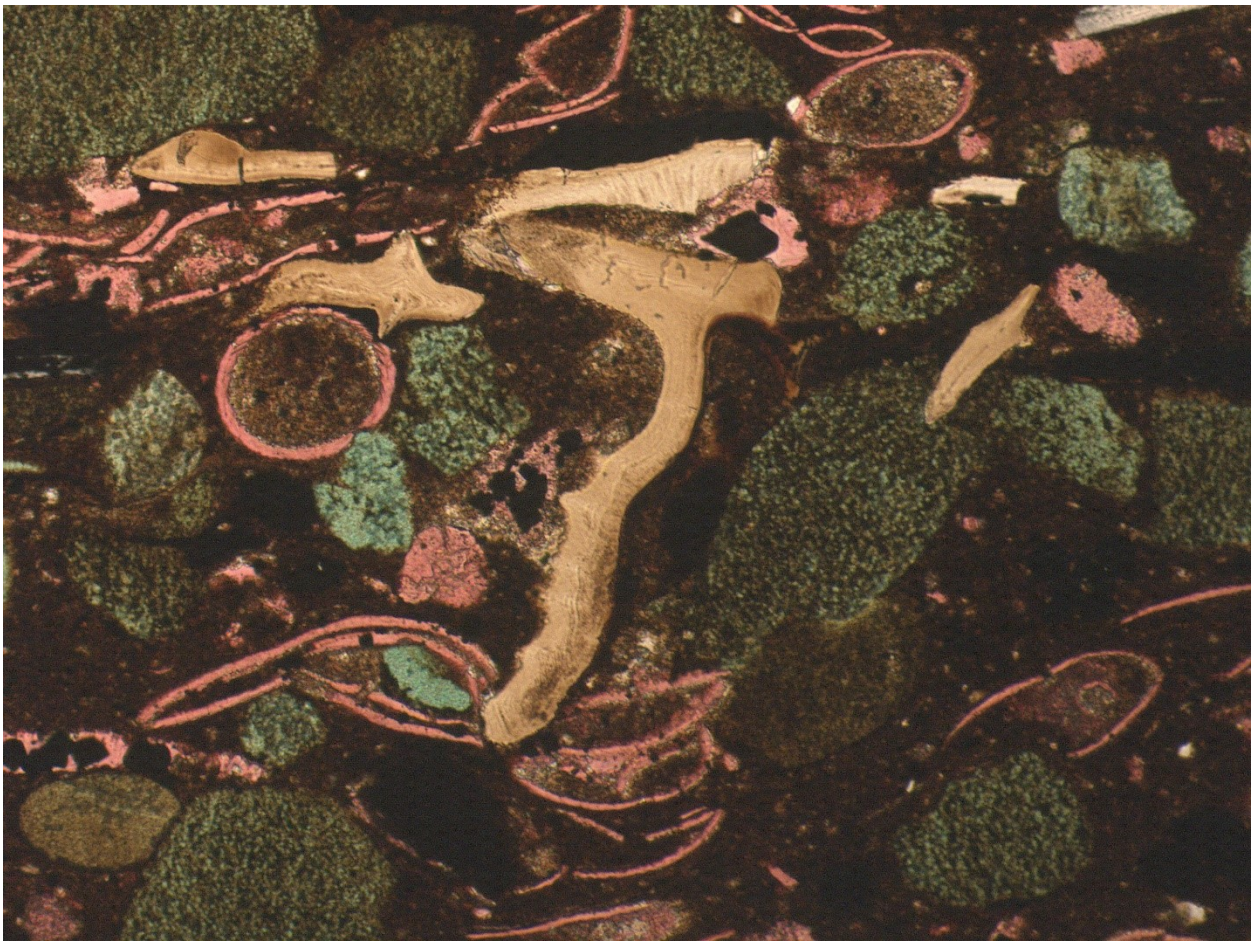

3121.5 m

- Sedimentary structures:
    - 1-5 mm thick planar, continuous laminae
        - Some slightly wavy
        - Differentiated by more pyrite and organic rich and more calcite rich
    - Laminated structures of organic material
        - Bed parallel, discontinuous laminae
        - Up to 400 x 20 um
        - Concentrated in more pyrite and OM rich laminae (~25% in those laminae)
- Texture:
    - Well sorted
    - Rounded
- Medium to Coarse Sand: (<1%)
    - Non-Skeletal: (0%)
    - Skeletal: (100%)
        - Styliolinid fragments
            - Appear bed parallel to sub-bed parallel

                - Infilled and calcite-recrystallized interiors
- V. Fine to Fine Sand: (~1%)
    - Non-Skeletal: (0%)
    - Skeletal: (100%)
        - Styliolinid fragments
            - Appear bed parallel to sub-bed parallel
            - Infilled and calcite-recrystallized interiors
        - Possible calcitized radiolarians
            - Calcite-recrystallized interiors
- Medium to Coarse Silt: (15%)
    - Non-Skeletal: (70%)
        - ~40% quartz/feldspar
        - ~30% pyrite
        - ~20% calcite
        - ~10% micas (quite bed-parallel)
    - Skeletal: (30%)
        - Styliolinid fragments
        - Possible calcitized rads
- V.Fine to Fine Silt: (20%)
    - 45% quartz/feldspar
    - 25% pyrite
    - 30% Calcite
- Matrix (Und.): (65%)

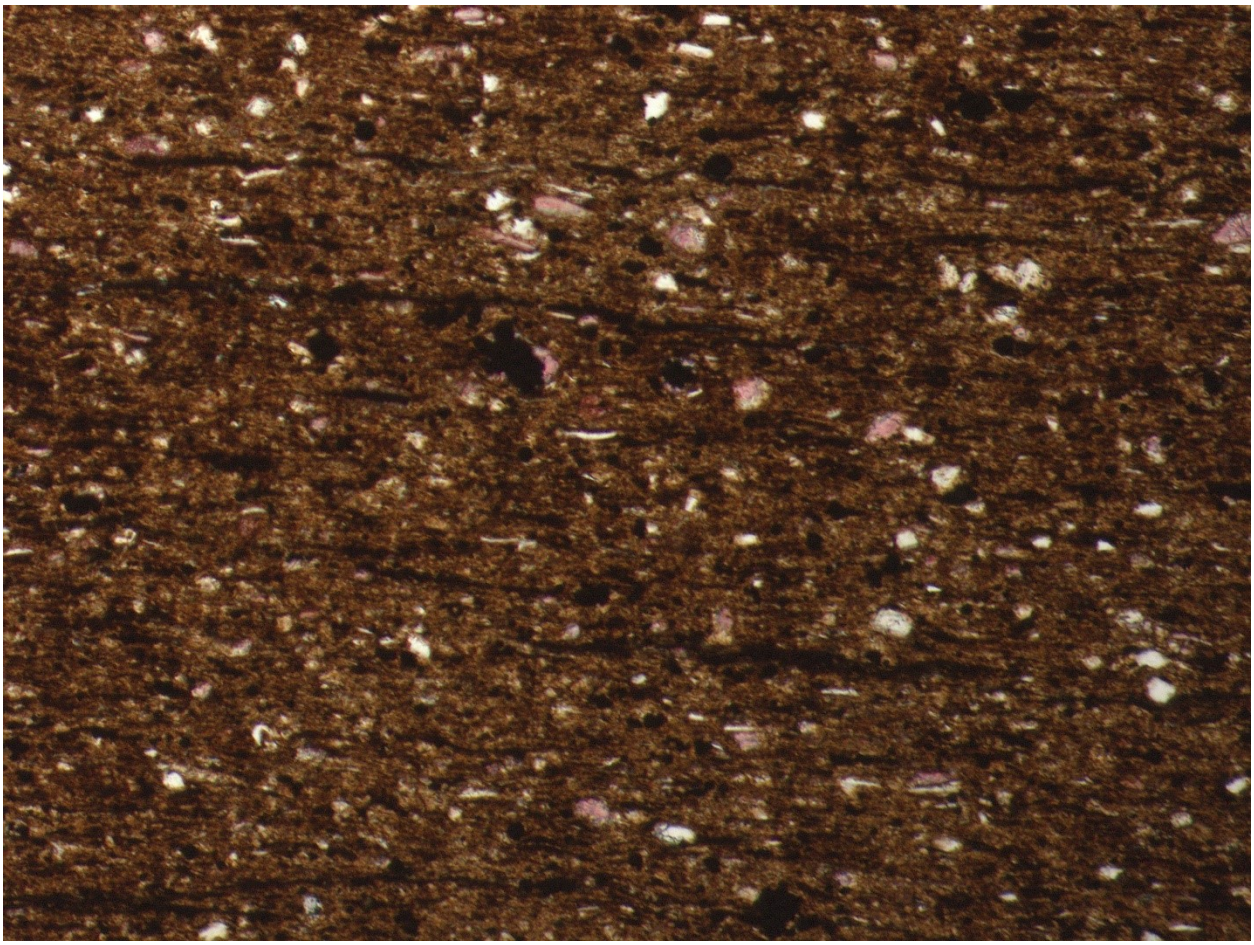

3118.5

- Sedimentary structures:
  - Very faint, planar, continuous, slightly wavy laminae
  - Many laminae contain concentrated calcitized rads
- Texture:
  - Well sorted
  - Rounded
- Medium to Coarse Sand: (0%)
- V. Fine to Fine Sand: (<1 to 20%) (20% in concentrated rad laminae)
  - Non-Skeletal: (0%)
  - Skeletal: (100%)
    - Calcitized radiolarians?
      - Round; quite massive (no visible rim); slightly irregular margins; very recrystallized interiors
- Medium to Coarse Silt: (~15%)
  - Non-Skeletal: (70%)
    - 50% quartz/feldspar

        - Subrounded, quite massive
    - 30% pyrite
        - Subangular to rounded
        - Partially replacing some larger calcite grains
    - 20% calcite
        - Subrounded, quite massive
  - Skeletal: (30%)
    - Possible styliolinid fragments
- V.Fine to Fine Silt: (~15%)
  - 50% quartz/feldspar
  - 30% pyrite
  - 20% calcite
- Matrix (Und.): (50%)

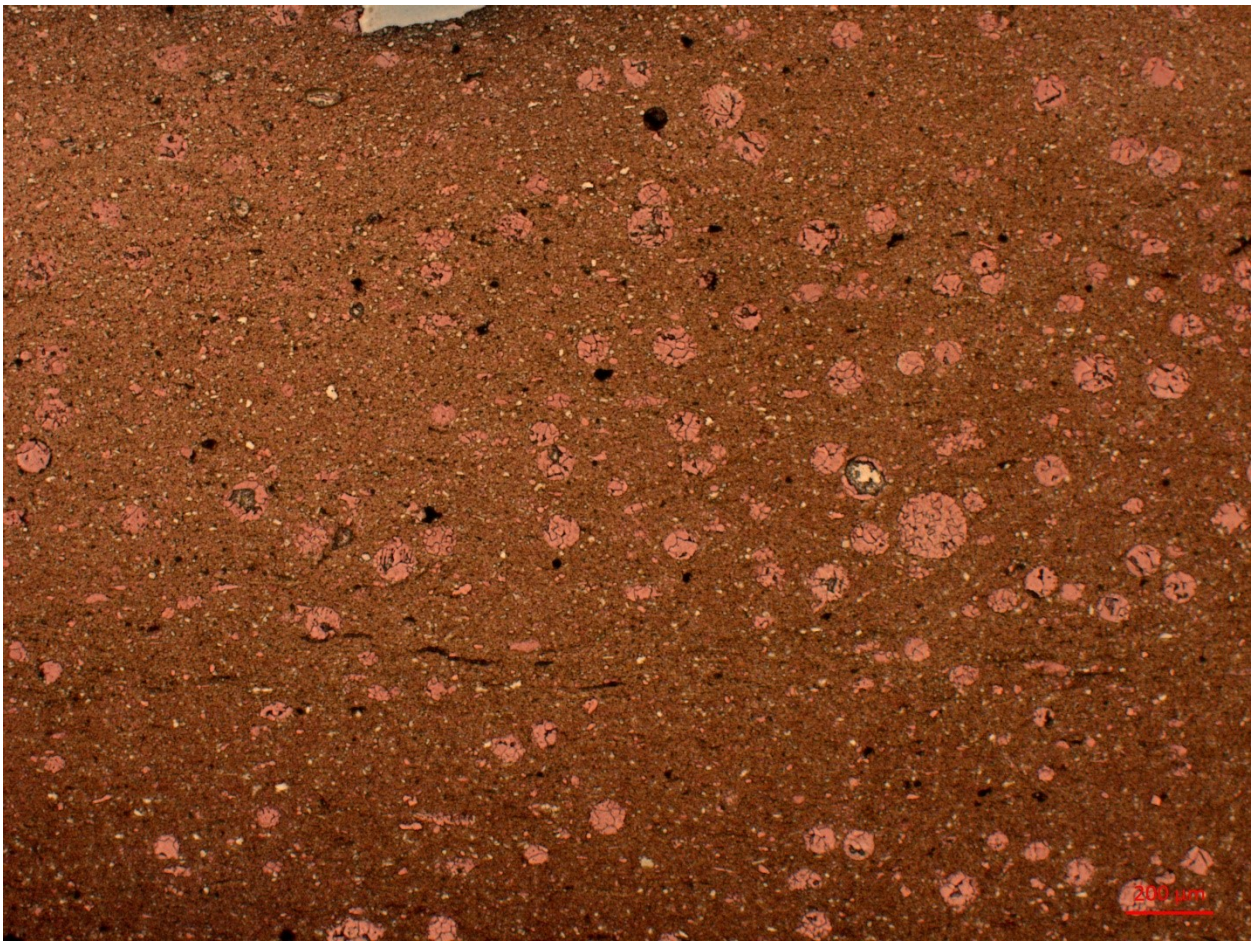

3116.5 m

- Sedimentary structures:
    - Coarsest grains at bottom and top of thin section, grading to finest grains in middle
    - Pyritized subhorizontal to subvertical burrows (~0.5x 4mm)
- Texture:
    - Well sorted
    - Subrounded
- Medium to Coarse Sand: (0%)
- V. Fine to Fine Sand: (20%)
    - Non-Skeletal: (100%)
        - Calcite grains
            - Likely recrystallized; semi rounded, somewhat amorphous
    - Skeletal: (0%)
- Medium to Coarse Silt: (25%)
    - Non-Skeletal: (100%)
        - 90% Calcite grains
            - Likely recrystallized; semi rounded, somewhat amorphous

        - 10% pyrite grains
            - Semi-round grains; often clustered
    - Skeletal: (0%)
- V.Fine to Fine Silt: (%)
    - 90% calcite
    - 10% pyrite
- Matrix (Und.): (~15%)

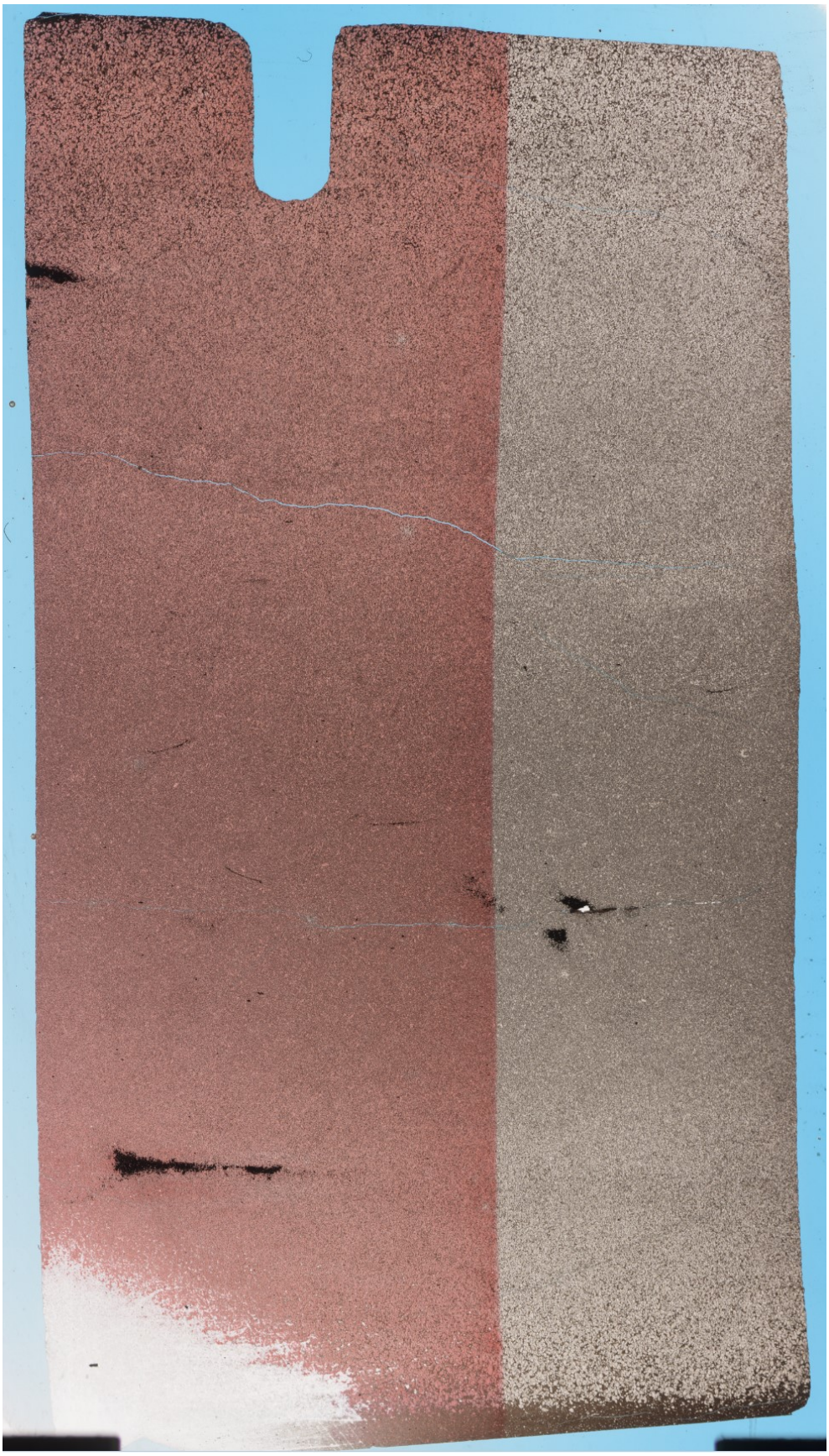

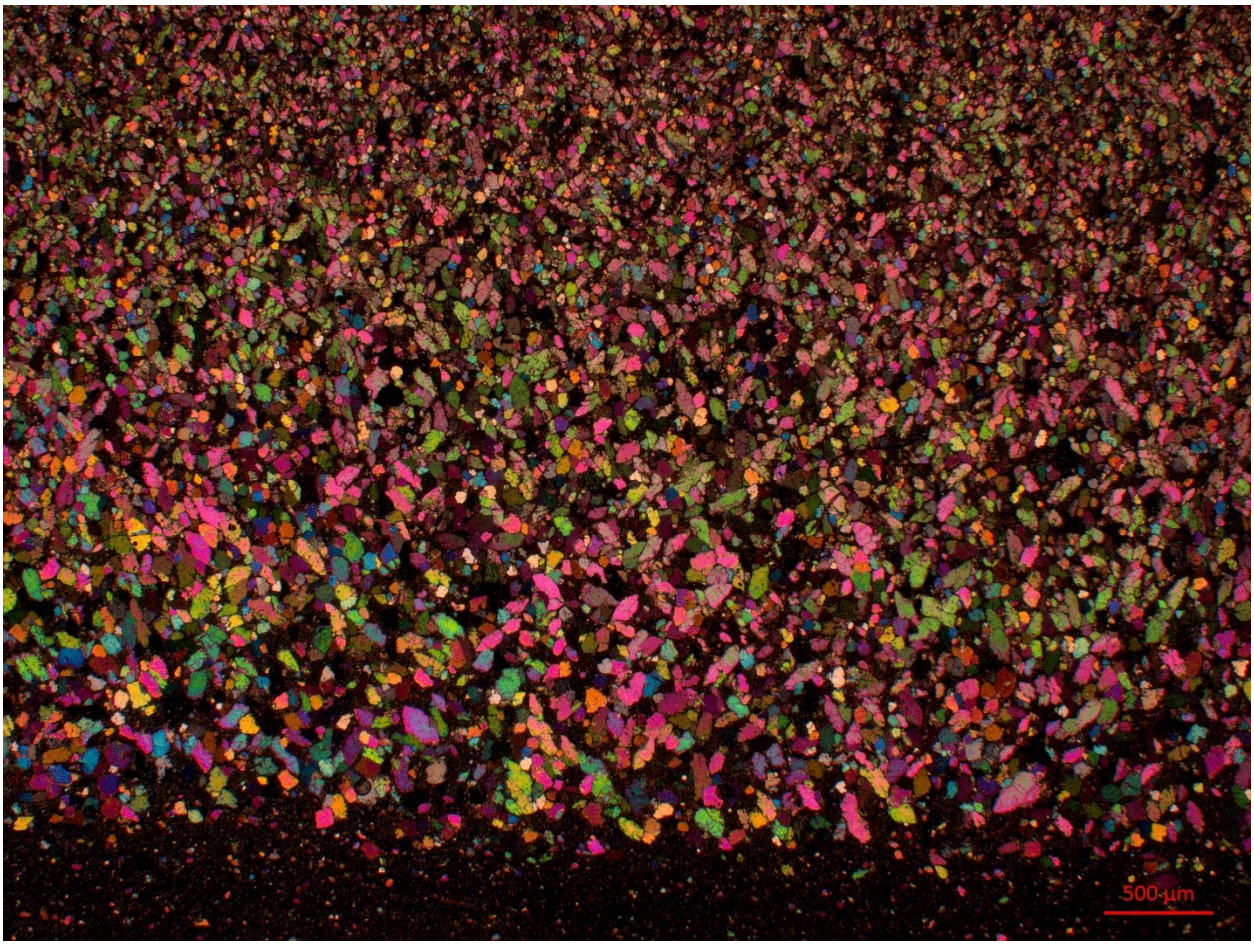

3115.4 m

- Sedimentary structures:
    - Up to 22 mm (visible), round calcite nodules in a more clay-rich matrix
        - Nodules contain more abundant, coarser, fossil fragment grains
    - Possible up to 6mm pyritized burrows
- Texture:
    - Moderately sorted
    - Subangular to subrounded
- Medium to Coarse Sand: (1%)
    - Non-Skeletal: (15%)
        - One large amorphous calcite grain
            - Subrounded, appears recrystallized
            - Partly replaced on edges by pyrite grains
    - Skeletal: (85%)
        - Styliolinid fragments (no clear orientation)
- V. Fine to Fine Sand: (20%)
    - Non-Skeletal: (25%)

        - Calcite - Quite rounded; amorphous
    - Skeletal: (75%)
        - Styliolinid fragments (no apparent orientation)
        - Possible calcitized rads
        - Possible rare ostracod fragments
- Medium to Coarse Silt: (30%)
    - Non-Skeletal: (60%)
        - 50% calcite
        - 40% quartz/feldspar
        - 10% pyrite
    - Skeletal: (40%)
        - Styliolinid fragments
        - Possible rare ostracod fragments
- V.Fine to Fine Silt: (20%)
    - 60% calcite
    - 35% quartz
    - 5% pyrite
- Matrix (Und.): (25%)

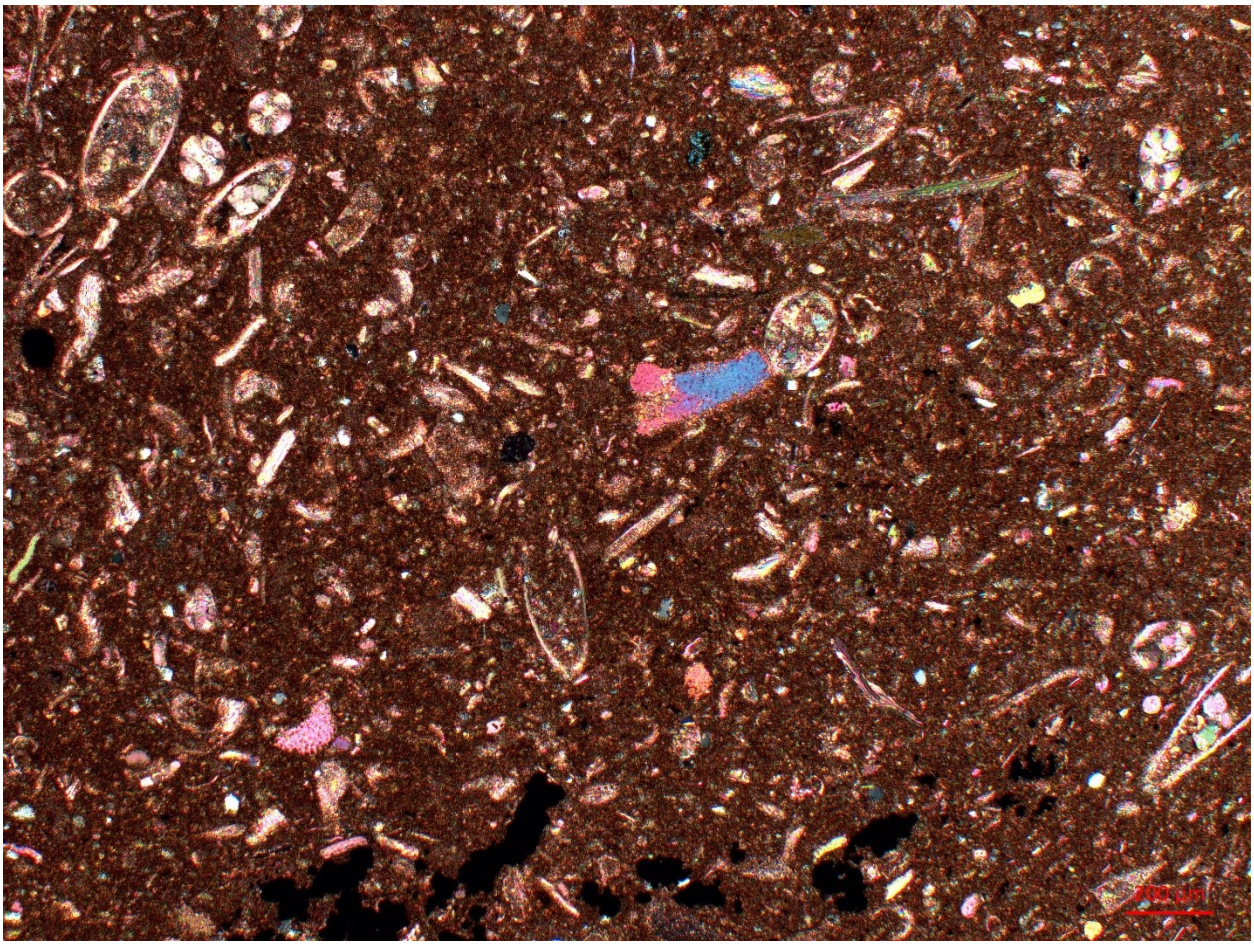

3114.5 m

- Sedimentary structures:
  - Nodular limestone with very minor matrix
  - Up to 1 x 10 mm calcite infilled fractures (subvertical)
  - Up to 1mm diameter pyritized burrows (quite round and horizontal)
- Texture:
  - Well sorted
  - Well rounded
- Medium to Coarse Sand: (~1%)
  - Non-Skeletal: (0%)
  - Skeletal: (100%)
    - Possible recrystallized styliolinid fragments and calcispheres?
- V. Fine to Fine Sand: (~1%)
  - Non-Skeletal: (0%)
  - Skeletal: (100%)
    - Styliolinid fragments
    - Possible calcispheres?

- Medium to Coarse Silt: (25%)
    - Non-Skeletal: (70%)
        - 65% calcite (round, amorphous, possibly recrystallized)
        - 30% quartz/feldspar (round, amorphous, possibly recrystallized)
        - 5% pyrite grains (most concentrated in burrows)
    - Skeletal: (30%)
        - Styliolinid fragments
        - Possible ostracod, brachiopod fragments?
- V.Fine to Fine Silt: (25%)
    - 60% calcite
    - 35% quartz/feldspar
    - 5% pyrite
- Matrix (Und.): (20%)
    - Appears to be calcite

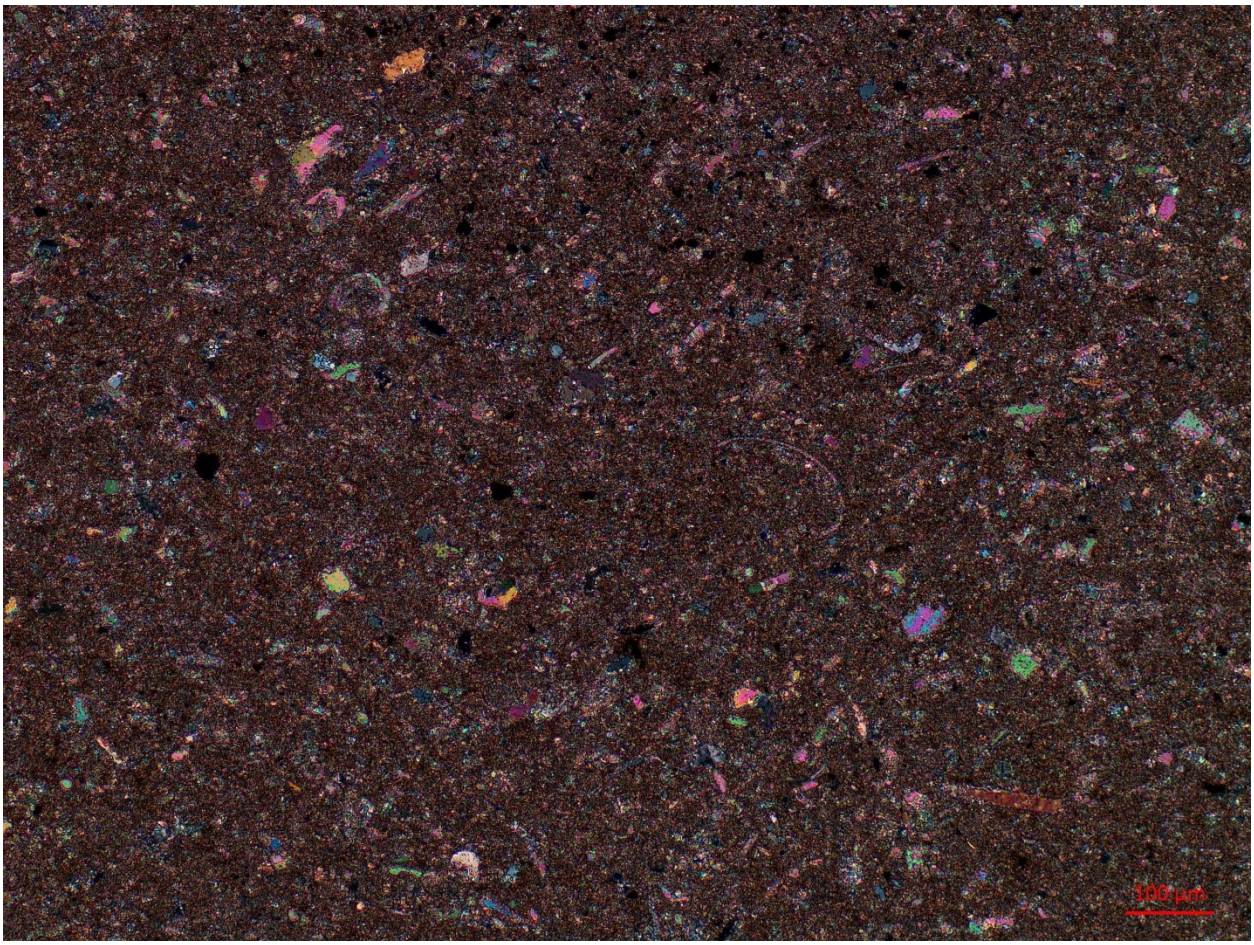

3113.5 m

- Sedimentary structures:
  - Nodular limestone in calcite-rich matrix
    - ~30% matrix in this thin section
    - Grains in nodules are larger, appear to be more recrystallized
    - Relatively even distribution of skeletal and non-skeletal grains inside and outside of nodules
  - 11 mm long, pyritized, subvertical burrow
- Texture:
  - Moderately sorted
  - Subangular to subrounded
- Medium to Coarse Sand: (~1%)
  - Non-Skeletal: (0%)
  - Skeletal: (100%)
    - Possibly recrystallized/infilled styliolinid fragment cross sections or calcispheres
      - Ring structure on exterior, infilled, sometimes recrystallized interior
- V. Fine to Fine Sand: (5%)

    - Non-Skeletal: (30%)
        - ~95% Round, amorphous, calcite grains
        - ~5% Round pyrite grains
    - Skeletal: (70%)
        - Likely calcispheres (or possibly calcitized radiolarians?)
- Medium to Coarse Silt: (30%)
    - Non-Skeletal: (85%)
        - ~70% round, amorphous calcite grains
        - ~25% quartz/feldspar
        - ~5% pyrite grains (round, often clumped)
    - Skeletal: (15%)
        - Likely styliolinid fragments (appear recrystallized)
- V.Fine to Fine Silt: (30%)
    - ~65% calcite
    - ~30% quartz/feldspar
    - 5% pyrite
- Matrix (Und.): (10%)

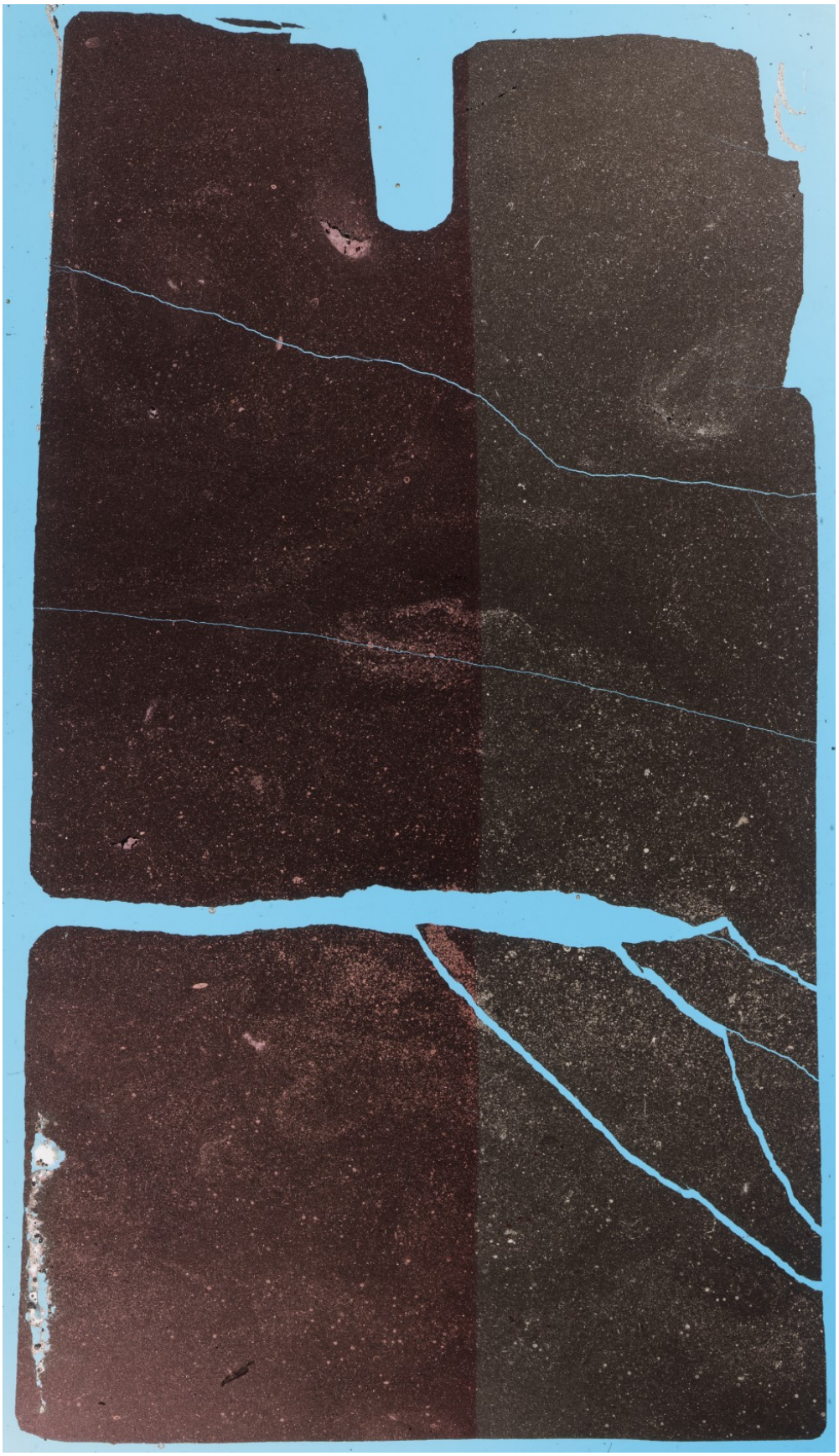

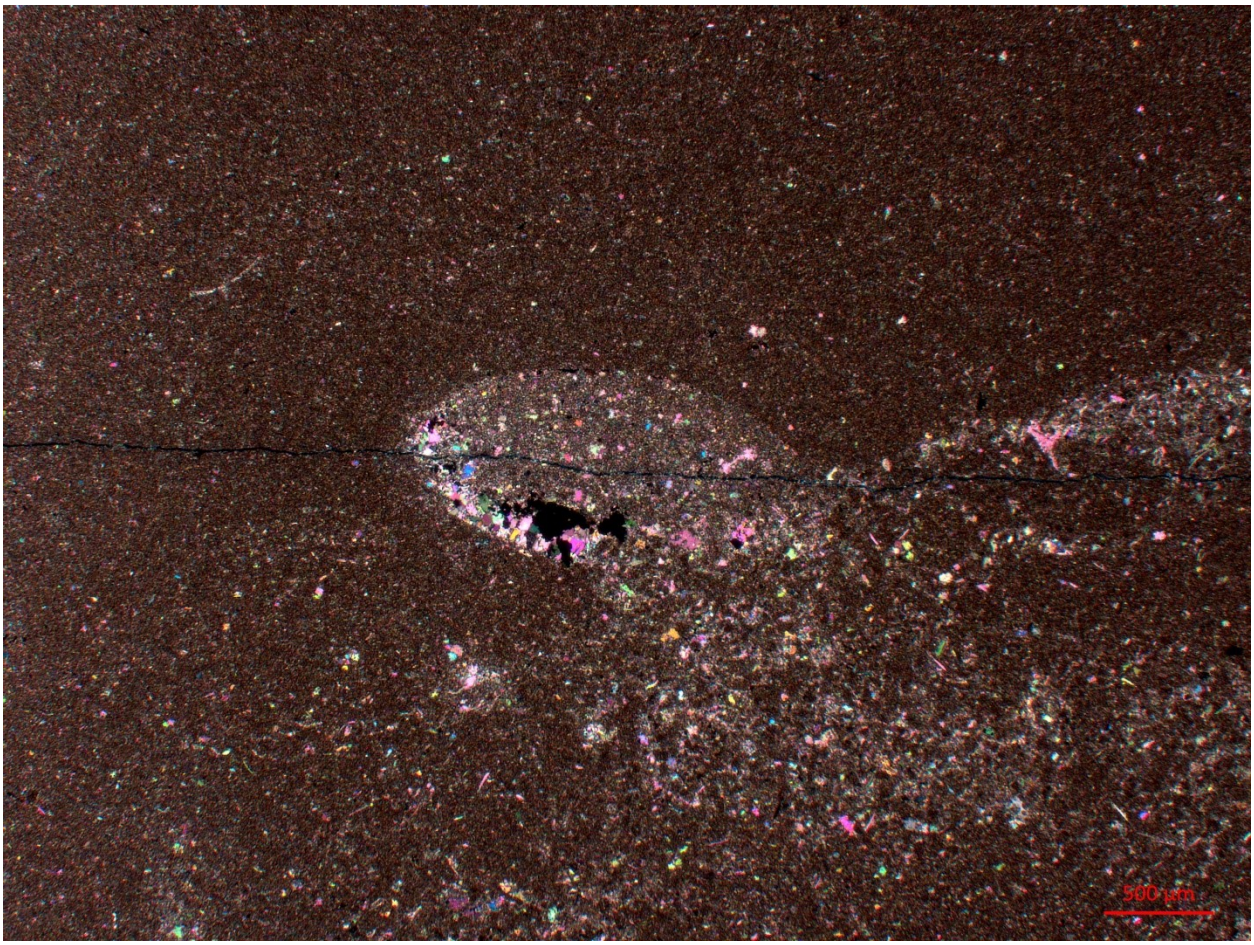

3113.3 m

- Sedimentary structures:
    - ~10% of rock is wispy, discontinuous, slightly wavy, pyritized laminae
        - Contain ~50% pyrite grains
    - Top 4mm of thin section has a ¼ mm thick fossiliferous (fining up) lag over the pyritized burrowed carbonate rich mud
        - Over lag is faintly planar laminated, coarser, more silt abundant mudstone
            - ~10% coarse silt
                - Calcitized rads?/calcispheres? and styliolinid fragments
            - ~50% fine silt
                - 60% quartz silt
                - 20% mica grains, sub-bed parallel
                - 10% calcite silt
                - 10% pyrite silt
            - ~40% matrix
        - Lag
            - Grains:

        - ~20% styliolinid fragments
        - ~20% calcitized rads?/calcispheres?
        - ~20% phosphatic grains (round to ovoid)
        - ~20% pyrite grains
        - ~20% Conodont fragments
    - Grain supported, very fine to coarse sand (skeletal grains)
    - Slightly bed parallel oriented
    - Undulating bottom (possibly soft sed def or erosive)
- Texture:
    - Well sorted
    - Subrounded to Rounded
- Medium to Coarse Sand: (1%) (~30% in lag deposit)
    - Non-Skeletal: (0%)
    - Skeletal: (100%)
        - Styliolinid fragments
            - Infilled and not recrystallized to fully recrystallized
- V. Fine to Fine Sand: (1%) (~30% in lag deposit)
    - Non-Skeletal: (0%)
    - Skeletal: (100%)
        - Styliolinid fragments (infilled and some recrystallized interiors)
        - Calcispheres?
- Medium to Coarse Silt: (15%)
    - Non-Skeletal: (30%)
        - ~45% quartz/feldspar
        - ~40% calcite
        - ~15% pyrite grains
    - Skeletal: (70%)
        - Styliolinid fragments
        - Possible calcitized rads?
- V.Fine to Fine Silt: (30%)
    - 45% quartz/feldspar
    - 40% calcite
    - 15% pyrite
- Matrix (Und.): (~55%)
- Surface:
    - Likely erosive
        - Possibly scour
        - Could be soft sed def but very hard to tell because underlying mud is very burrowed, recrystallized, and massive carbonate rich mud (no obvious distortion of laminae)
            - Some grains of lag sticking into underlying mud
            - Some possible distortion of laminae in underlying mud
        - Sharp boundary between underlying carbonate-rich OM poor mud and overlying siliceous, OM and pyrite-rich mud

- Lag:
    - Up to ~1mm thick
    - Quite massive
    - Possible decrease in coarse grains upwards
        - Visible in some spots
    - Sharp, possibly erosive base, slightly wavy
    - More gradational to possibly more sharp in parts top contact
    - Rough alignment of elongate grains horizontal to bedding
    - Composition:
        - Silt to vfs grains
        - Abundant calcite grains
            - Partially dissolved, commonly pyritized
                - Subrounded to subangular
        - Common styliolinid and possibly ostracod/small brach fragments
        - Common conodont elements/bone fragments
        - Common possible organo-phosphatic grains
            - Often partially pyritized
            - At least one looks like elongate bone fragment
        - Rare quartz grains
        - One possible lingulid brachiopod fragment??
            - Siliceous or similar to conodont elements optically
                - Very dark in XPL
        - Matrix more OM and pyrite-rich like above lithology
        - Appears pyrite cemented in spots
- Above:
    - Discontinuous pyrite laminae?
    - More siliceous
    - more OM and pyrite-rich
    - more planar laminated
        - discontinuous pyrite laminae
    - Common quartz, calcite, and mica silt
- Below:
    - Massive, bioturbated, pyritic, carbonate rich mud of M.Duv.

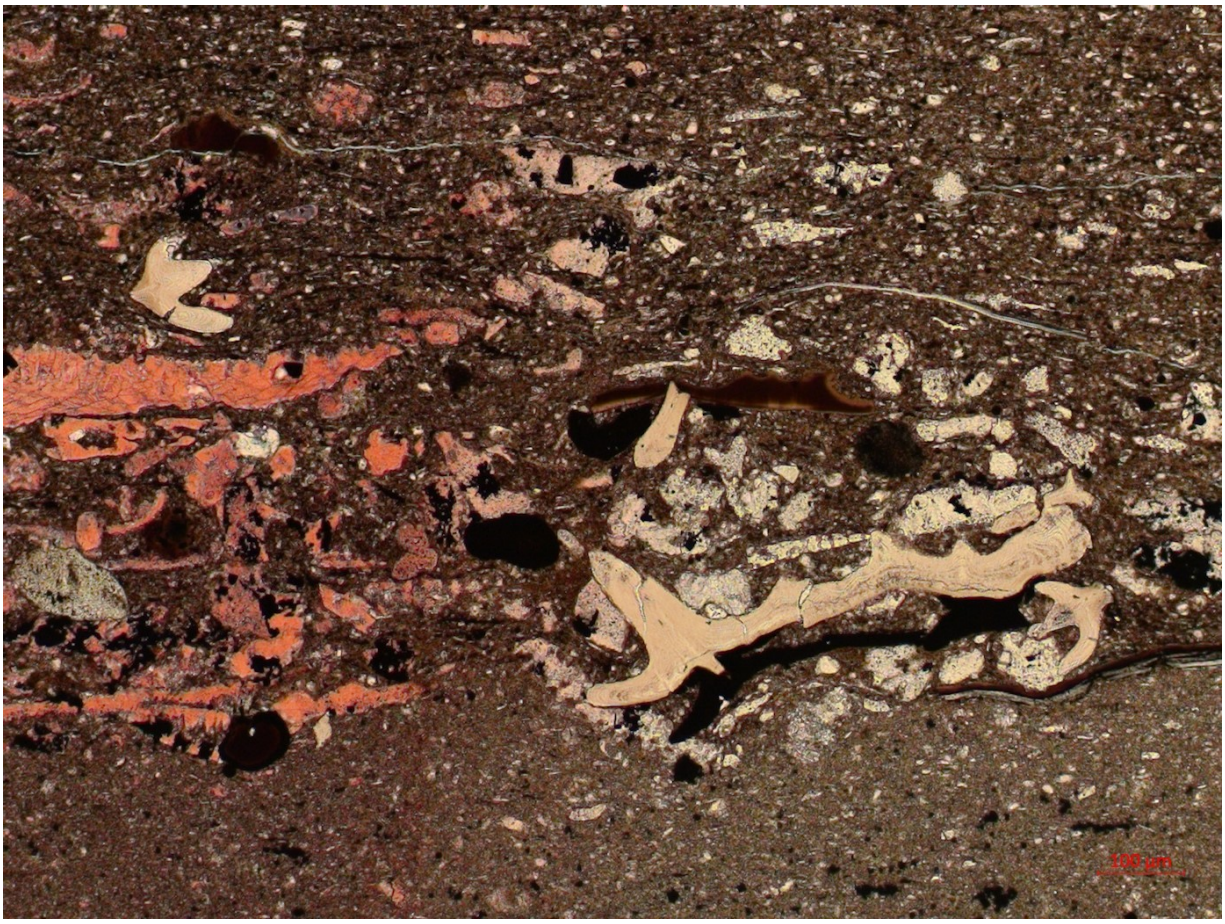

3111.37 m

- Sedimentary structures:
  - Very massive appearing texture
    - Squished and elongate grains still generally aligned with bedding
  - More pyrite and OM in bottom 4mm of TS
  - Coarse grains concentrated in laminae near top of TS
  - Up to 30x500 um? squished clay aggregates
    - Most abundant in bottom 4mm of TS
  - Abundant typically up to 4mm thick, subhorizontal to subvertical mud infilled (preferentially pyritized) very faint background burrows
    - Possibly Helminthopsis?
  - Up to ~15 um thick larger, scarcer bed horizontal to subhorizontal pyritized mud infilled burrows
- Texture:
  - Well sorted
  - Subrounded to rounded
- Medium to Coarse Sand: (~1%)
  - Non-Skeletal: (0%)

    - Skeletal: (100%)
        - Styliolinid fragments
        - Very rare conodont fragments
- V. Fine to Fine Sand: (~1%)
    - Non-Skeletal: (0%)
    - Skeletal: (%)
        - Styliolinid fragments (infilled and slightly recrystallized interiors)
- Medium to Coarse Silt: (25%)
    - Non-Skeletal: (50%)
        - 45% quartz/feldspar
        - 30% mica
        - 20% calcite grains
        - 5% pyrite grains
    - Skeletal: (50%)
        - Styliolinid fragments
        - Possibly some small brachiopod/ostracod fragments
- V.Fine to Fine Silt: (40%)
    - 45% quartz/feldspar
    - 35% calcite
    - 20% mica
- Matrix (Und.): (35%)

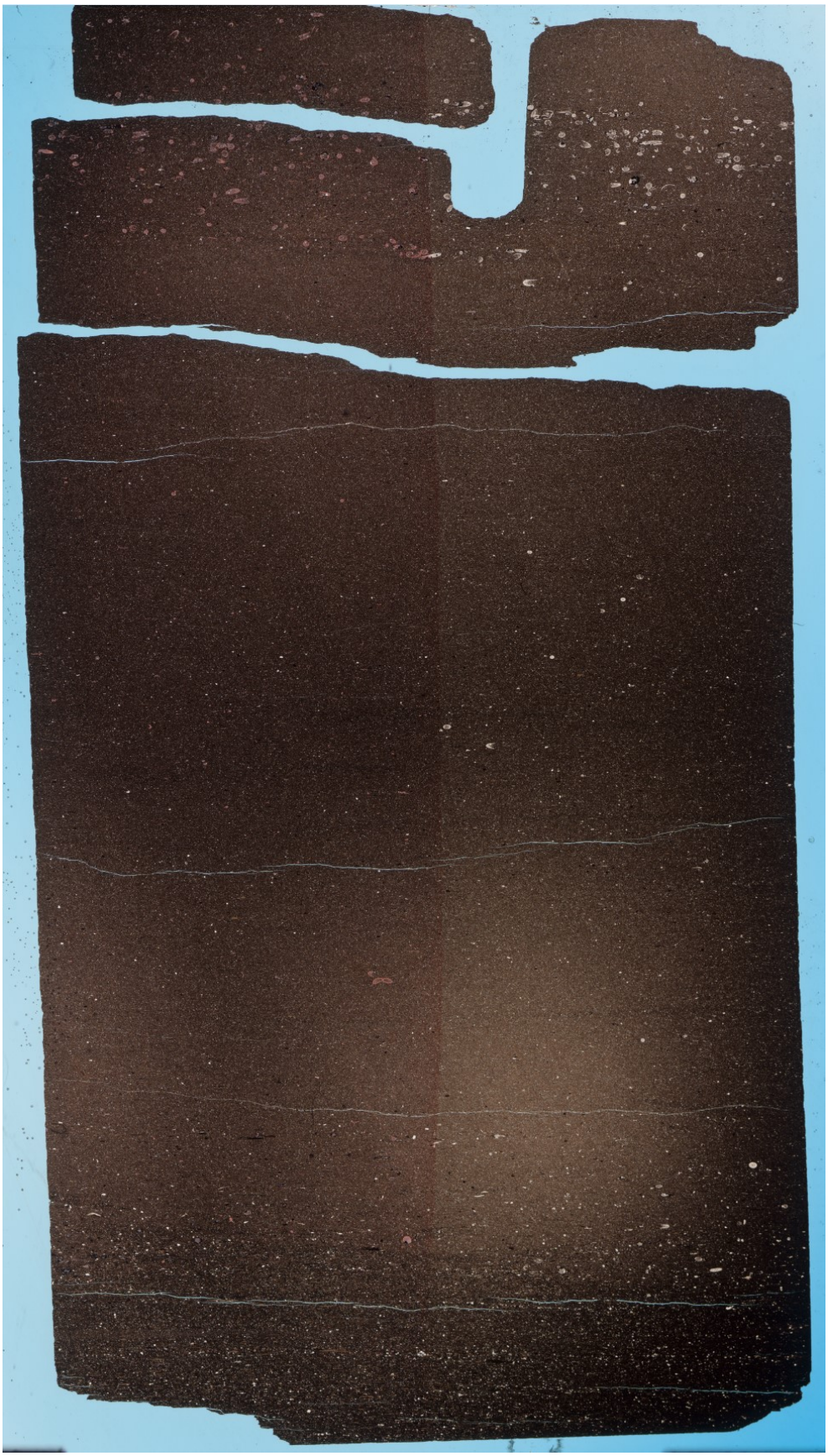

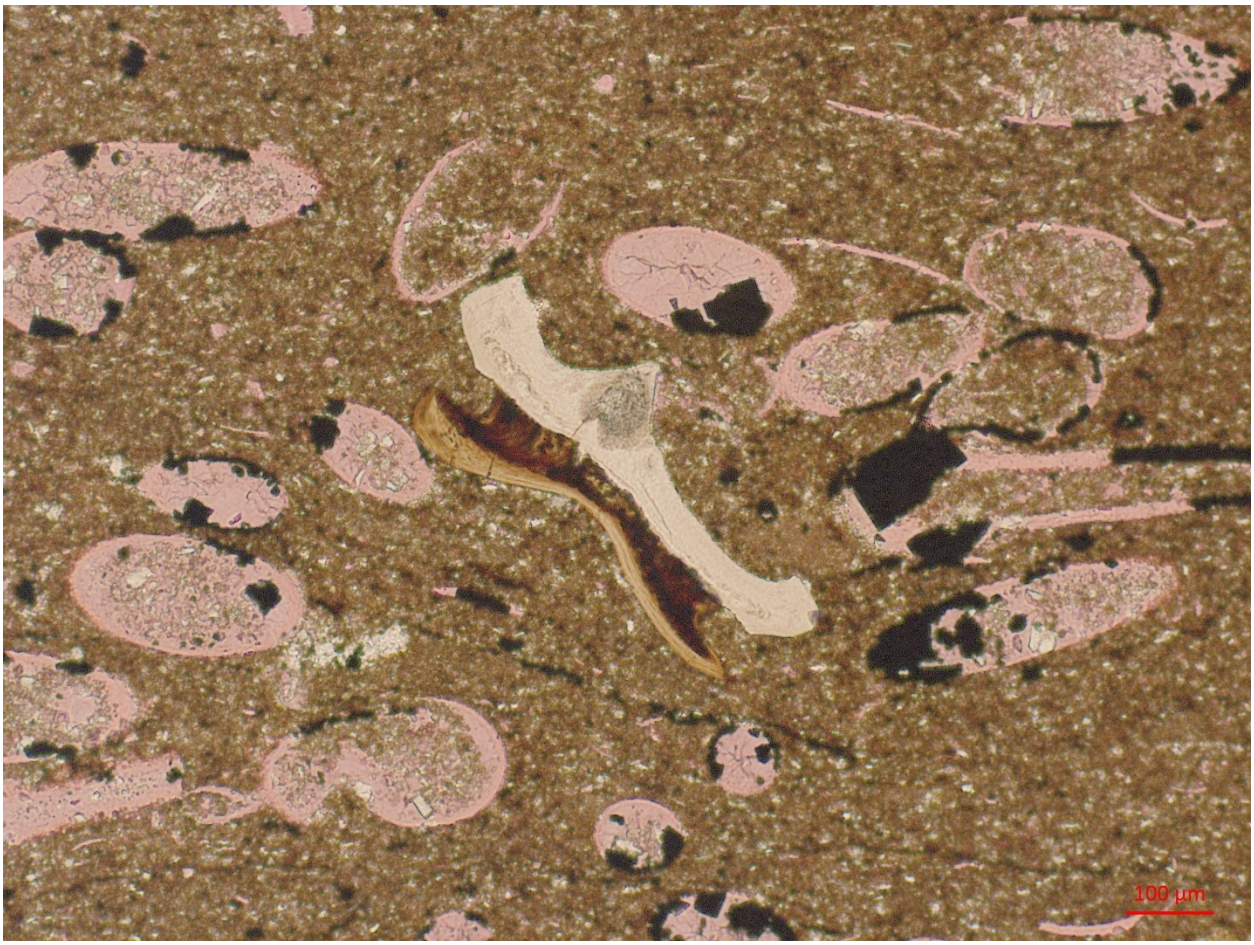

3110.5 m

- Sedimentary structures:
  - Very faint planar continuous laminae (in mud)
  - Very thin, discontinuous possible fractures likely filled with pyrite
    - Could be OM-rich structures but are very opaque
    - ~1% of rock
- Texture:
  - Well sorted
  - Subrounded to rounded
- Medium to Coarse Sand: (0%)
- V. Fine to Fine Sand: (<1%)
  - Non-Skeletal: (25%)
    - Pyrite grains (quite round)
  - Skeletal: (75%)
    - Calcitized rads? Calcispheres?
    - Possible single styliolinid fragment (infilled and slightly recrystallized)
- Medium to Coarse Silt: (15%)

    - Non-Skeletal: (100%)
        - ~50% quartz/feldspar
        - ~25% mica grains
        - ~15% pyrite grains
        - ~10% calcite grains
    - Skeletal: (0%)
- V.Fine to Fine Silt: (30%)
    - ~40% quartz/feldspar
    - ~30% calcite
    - ~20% mica
    - ~10% pyrite
- Matrix (Und.): (55%)

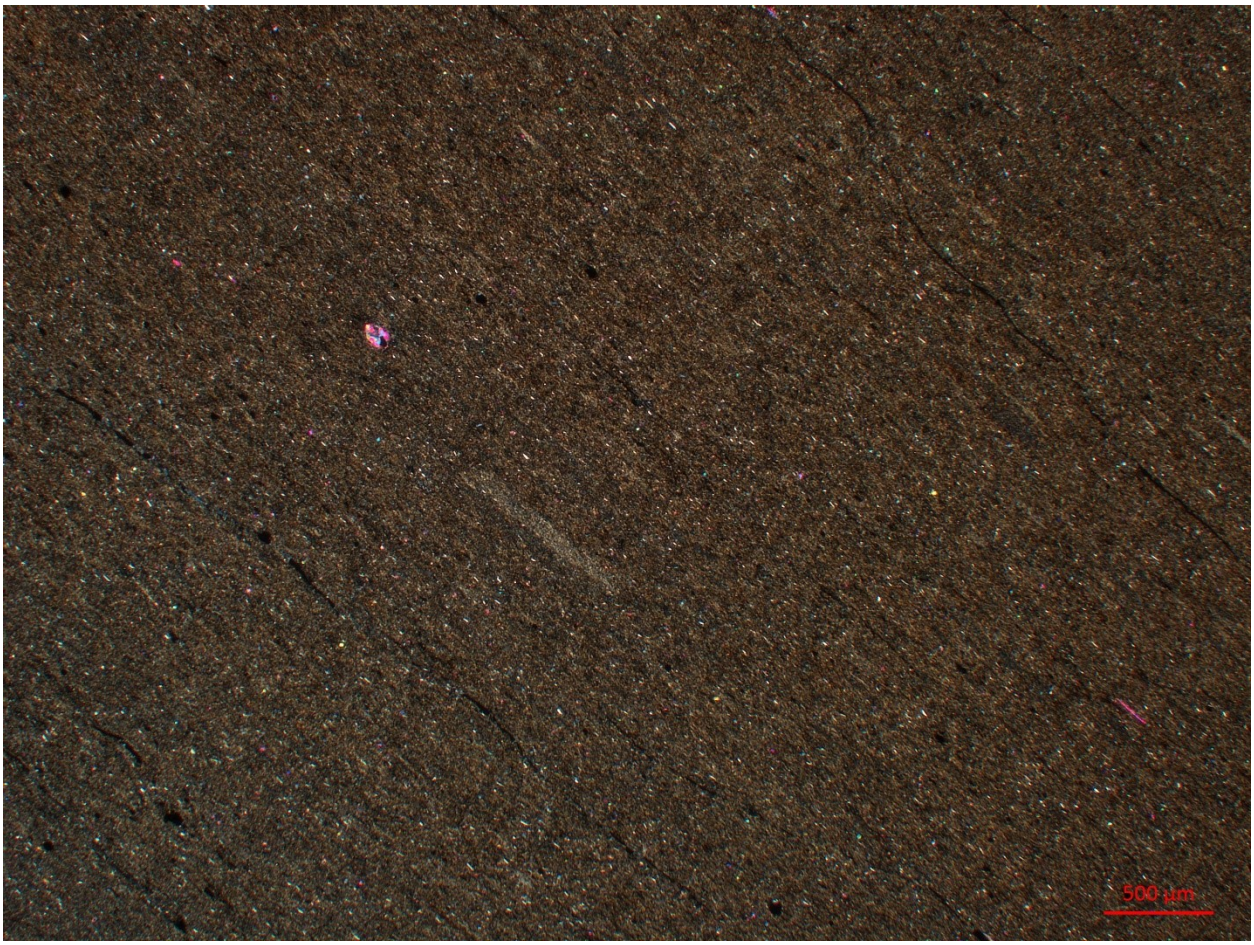

3109.6 m

- Sedimentary structures:
    - Planar continuous laminae
        - Distinguished by more silty and less silty laminae
        - Sometimes radiolarians concentrated into laminae
- Texture:
    - Moderately sorted
    - Subrounded
- Medium to Coarse Sand: (~1%)
    - Non-Skeletal: (0%)
    - Skeletal: (100%)
        - Styliolinid fragments (mostly cross sections, infilled and recrystallized interiors)
- V. Fine to Fine Sand: (~5%)
    - Non-Skeletal: (0%)
    - Skeletal: (100%)
        - Calcitized rads? Calcispheres? (round and quite recrystallized)
        - Sparse styliolinid fragments

- Medium to Coarse Silt: (30%)
    - Non-Skeletal: (90%)
        - ~40% calcite grains (somewhat amorphous)
        - ~30% quartz/feldspar grains (more rounded)
        - ~25% pyrite grains
        - ~5% mica grains (not particularly bed parallel)
    - Skeletal: (%)
        - Possible styliolinid fragments
- V.Fine to Fine Silt: (30%)
    - ~50% calcite
    - ~40% quartz/feldspar
    - ~10% pyrite
- Matrix (Und.): (35%)

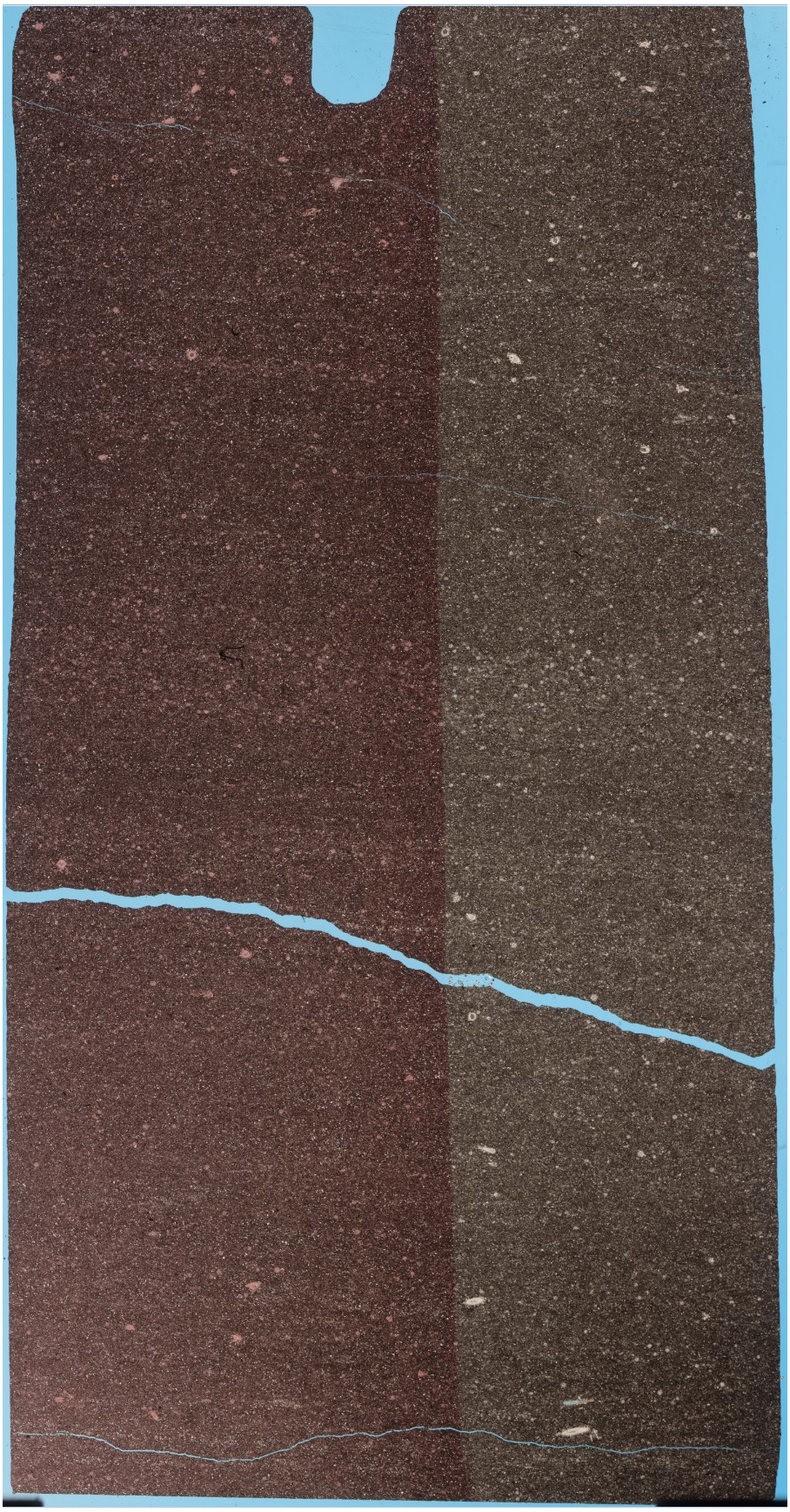

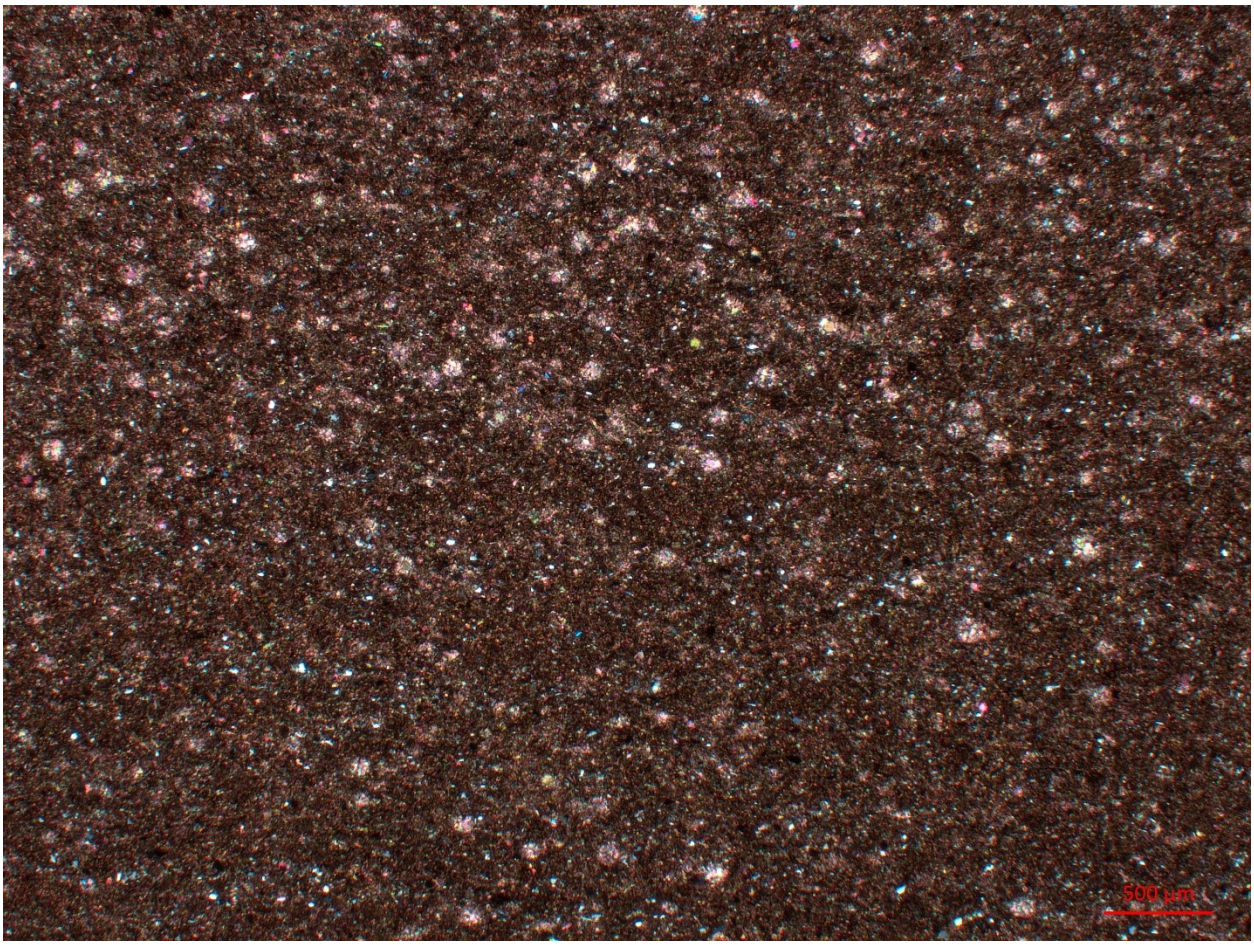

3106.5 m

- Sedimentary structures:
  - Quite massive appearance to rock
  - Slight bed-parallel orientation of styliolinid fragments
  - Sparse, small, likely pyritized burrows
- Texture:
  - Moderately sorted
  - Subrounded
- Medium to Coarse Sand: (~1%)
  - Non-Skeletal: (0%)
  - Skeletal: (100%)
    - Styliolinid fragments (infilled and partially recrystallized interiors)
      - Slightly bed oriented
      - Lots of lengthwise cross sections visible
- V. Fine to Fine Sand: (~10%)
  - Non-Skeletal: (0%)
  - Skeletal: (100%)

        - Styliolinid fragments
            - (many partially replaced by pyrite)
- Medium to Coarse Silt: (15%)
    - Non-Skeletal: (70%)
        - ~55% calcite
        - ~30% quartz/feldspar
        - ~15% pyrite
    - Skeletal: (30%)
        - Styliolinid fragments
        - Possible ostracod fragments and small brachiopods
- V.Fine to Fine Silt: (30%)
    - ~70% calcite
    - ~20% quartz/feldspar
    - ~10% pyrite
- Matrix (Und.): (45%)

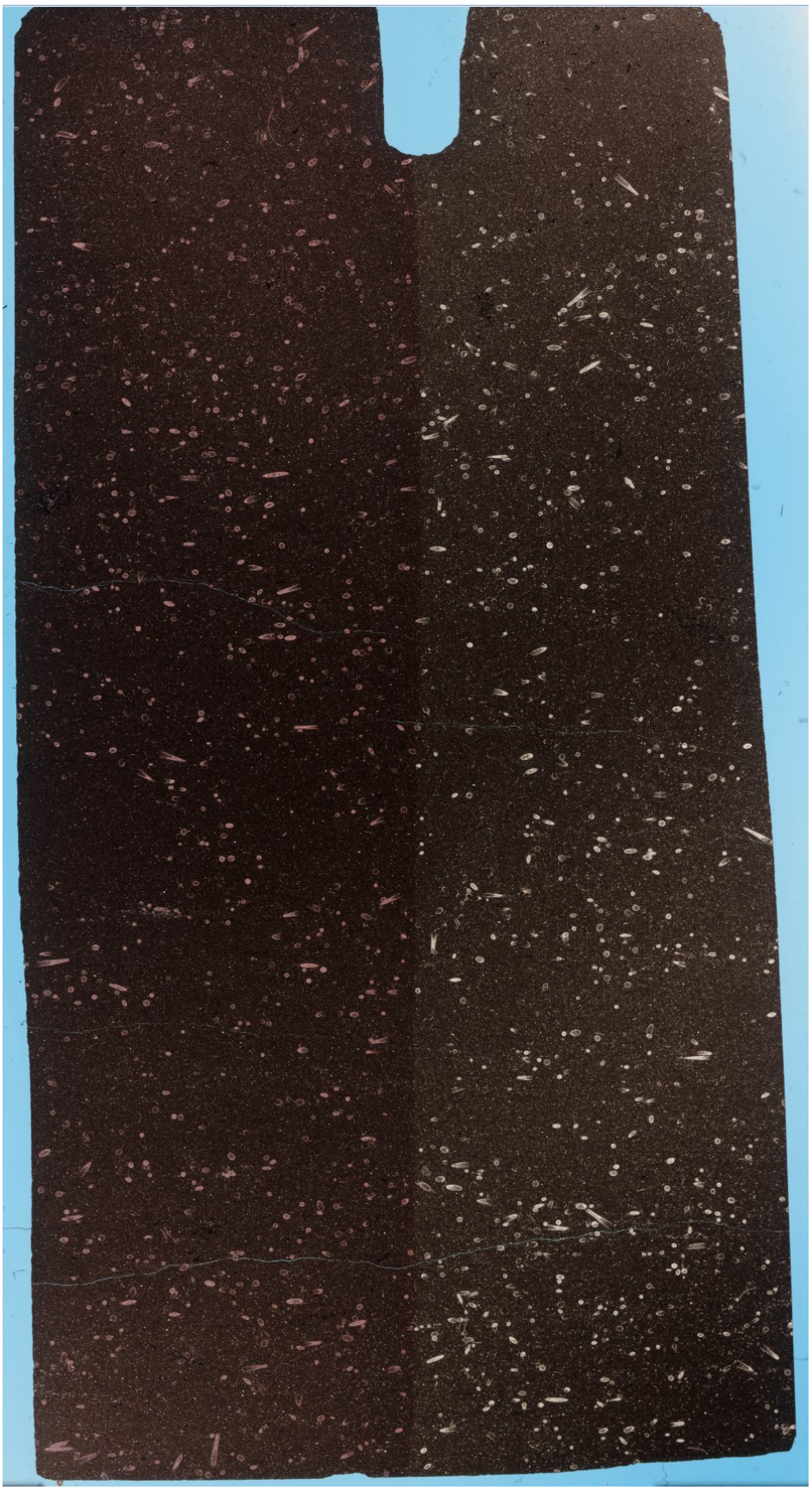

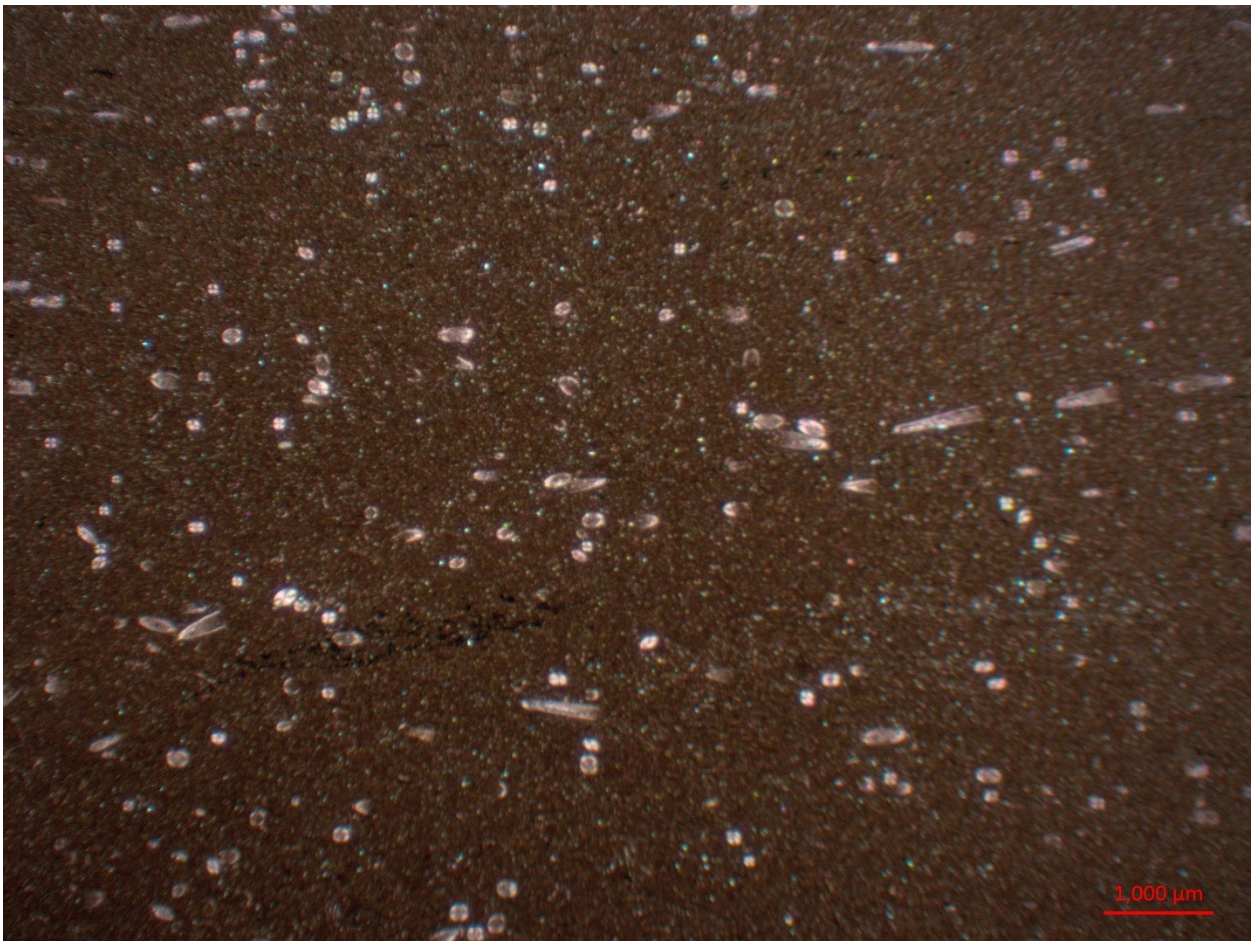

3106.39 m

- Sedimentary structures:
  - Quite massive structure
  - Abundant styliolinid fragments that may be slightly concentrated into coarser laminae (but quite massive)
    - Very slightly bed parallel oriented
  - Abundant pyritized burrows (subvertical to subhorizontal)
    - Up to 3mm diameter
    - Likely *Planolites* and *Arenicolites*
  - 3mm calcite infilled burrow
    - Rim is calcitized and partly pyritized
    - Round shape
- Texture:
  - Moderately sorted
  - Subrounded
- Medium to Coarse Sand: (10%)
  - Non-Skeletal: (10%)

        - Pyrite grains (round, likely clusters of small pyrite grains)
    - Skeletal: (90%)
        - Styliolinid fragments
            - Interiors infilled and lightly recrystallized by calcite
            - Many lengthwise cross sections
            - Very slightly bed parallel orientation
- V. Fine to Fine Sand: (20%)
    - Non-Skeletal: (20%)
        - Pyrite grains
    - Skeletal: (80%)
        - Styliolinid fragments
        - Calcitized rads
- Medium to Coarse Silt: (15%)
    - Non-Skeletal: (70%)
        - ~40% quartz/feldspar
        - ~30% pyrite
        - ~25% calcite
        - ~5% mica
    - Skeletal: (30%)
        - Styliolinid fragments
        - Possible sparse very small calcitized rads
- V.Fine to Fine Silt: (25%)
    - ~40% calcite
    - ~40% quartz/feldspar
    - ~10% pyrite
- Matrix (Und.): (30%)

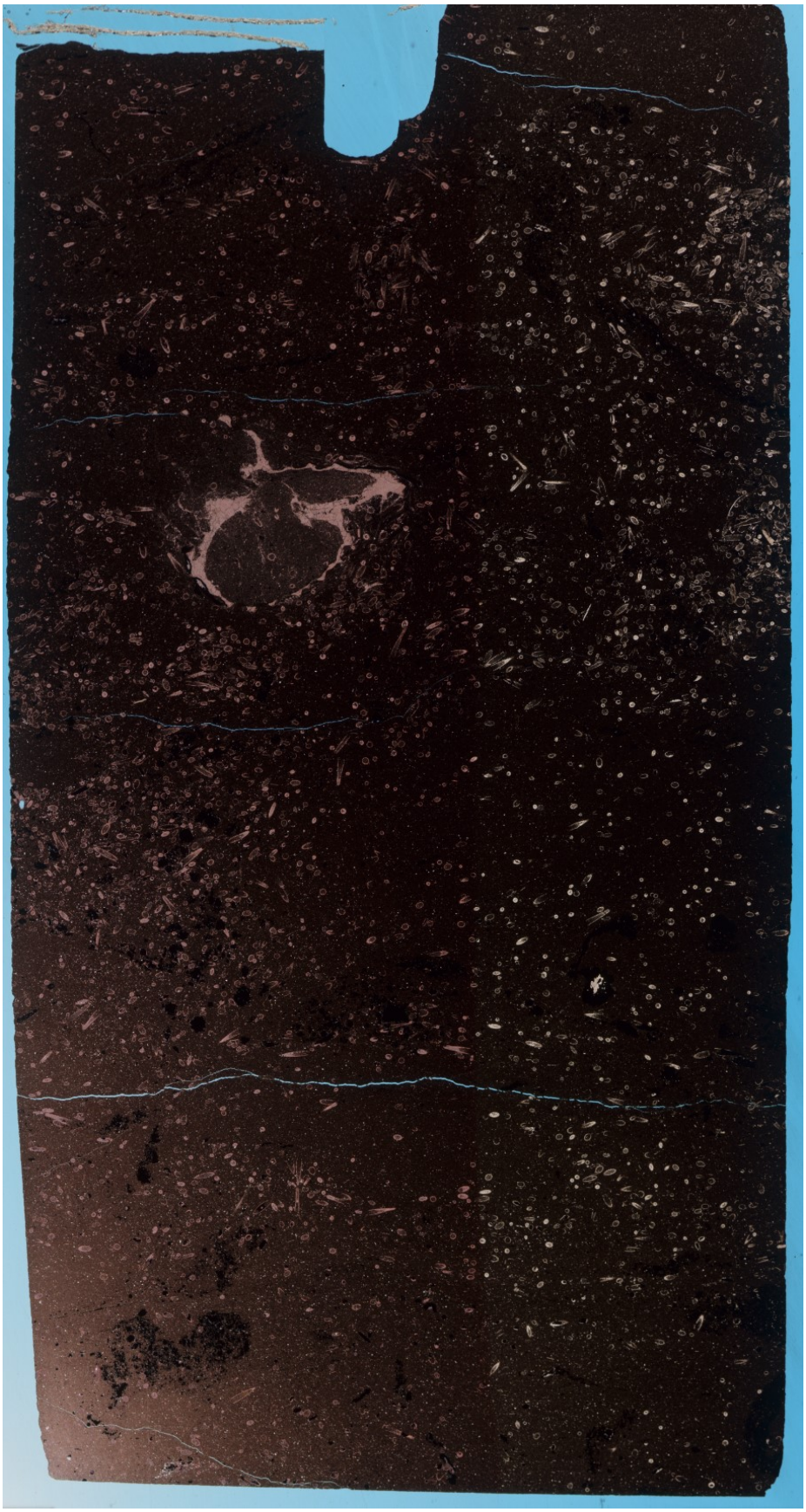

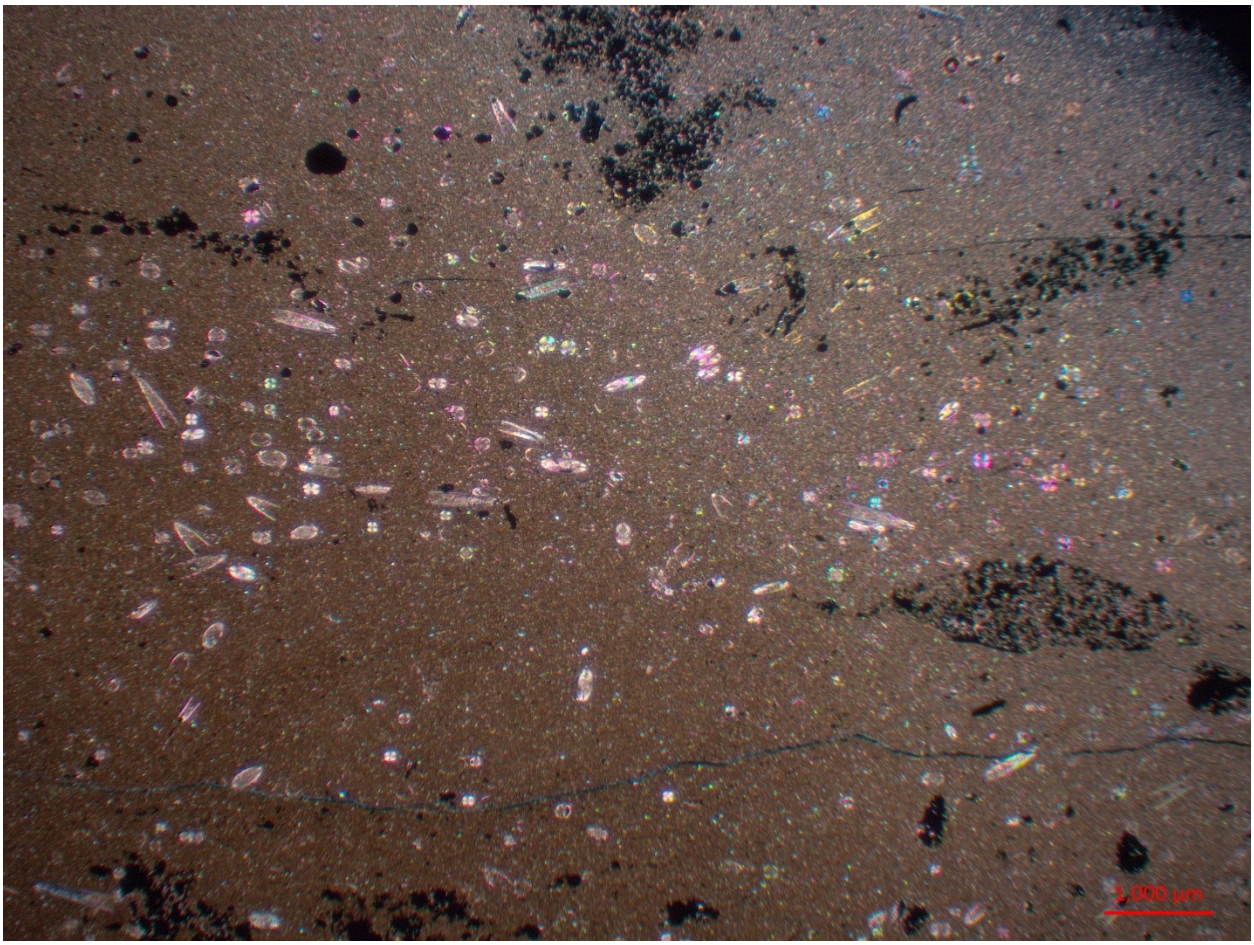

3104.0 m

- Sedimentary structures:
  - Quite massive structure
  - Very faint planar continuous laminae near bottom of thin section
    - From more concentrated coarser grains
- Texture:
  - Well sorted
  - Sub-rounded
- Medium to Coarse Sand: (<1%)
  - Non-Skeletal: (50%)
    - Calcite grains
  - Skeletal: (50%)
    - Styliolinid fragments
      - Infilled and partly recrystallized
    - Possible conodont fragment
- V. Fine to Fine Sand: (10%)
  - Non-Skeletal: (20%)

        - Calcite grains
    - Skeletal: (80%)
        - Common calcispheres or x-section styliolinids?
        - Sparse styliolinid fragments
        - Likely brachiopod/ostracod fragments?
- Medium to Coarse Silt: (25%)
    - Non-Skeletal: (100%)
        - ~45% calcite grains
        - ~35% quartz/feldspar grains
        - ~15% pyrite grains
        - ~5% mica grains (very faintly bed parallel oriented)
    - Skeletal: (0%)
- V.Fine to Fine Silt: (%)
    - ~45% calcite
    - ~35% quartz/feldspar
    - ~20% pyrite
- Matrix (Und.): (25%)

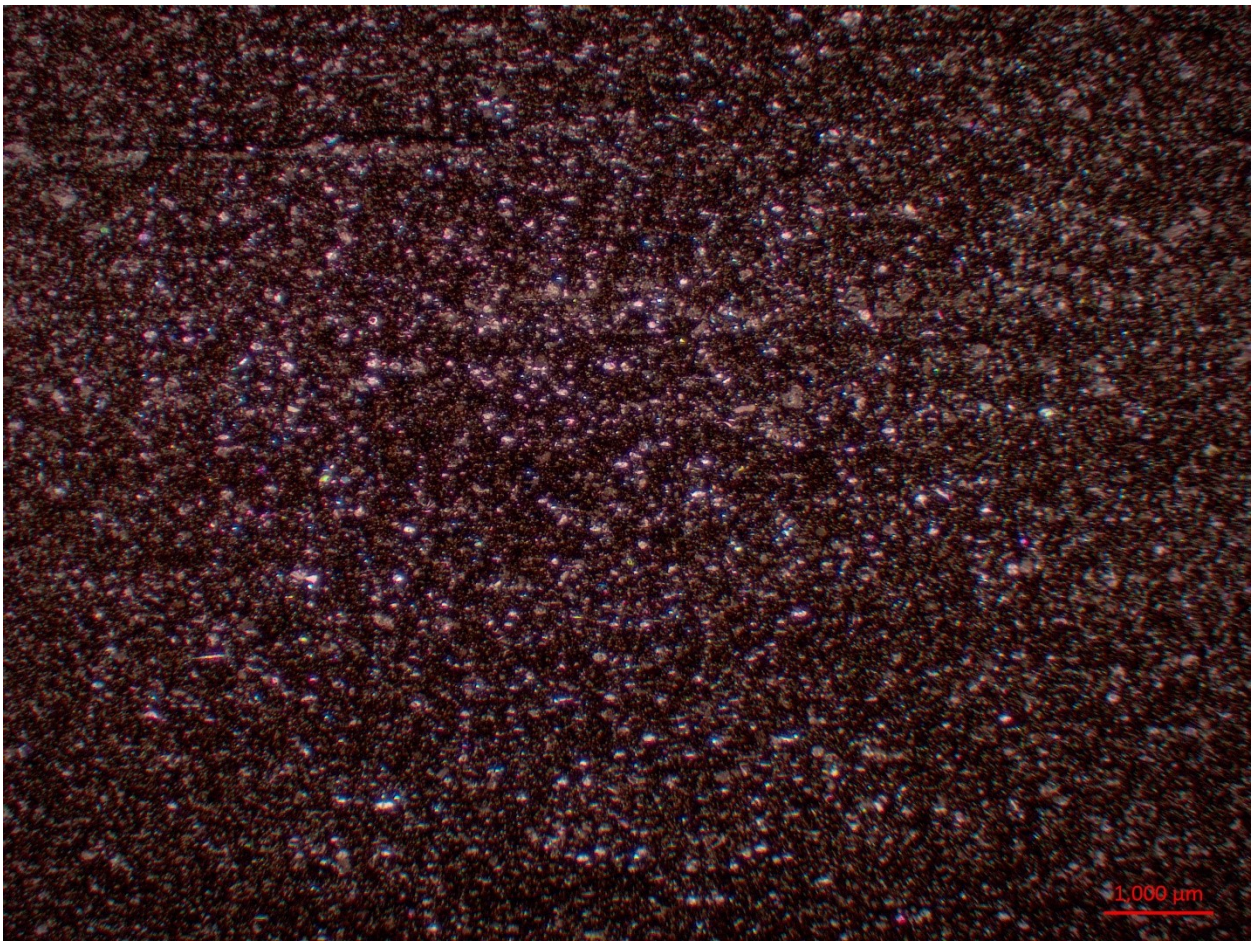

3102.5 m

- Sedimentary structures:
    - Planar, continuous laminae
        - Appears to be slightly coarser (and possibly more quartz/feldspar rich) and finer/more matrix laminae
- Texture:
    - Well sorted
    - Rounded
- Medium to Coarse Sand: (<1%)
    - Styliolinids (Flattened, bed parallel aligned)
- V. Fine to Fine Sand: (~1%)
    - Non-Skeletal: (90%)
        - ~ 40% quartz/feldspar grains
        - ~30% calcite grains
        - ~20% pyrite grains
        - ~10% mica grains
    - Skeletal: (10%)

        - Styliolinid fragments (infilled and partially recrystallized by calcite)
- Medium to Coarse Silt: (30%)
    - Non-Skeletal: (95%)
        - ~40% quartz/feldspar grains
        - ~30% calcite grains
        - ~20% pyrite grains
        - ~10% mica grains
    - Skeletal: (5%)
        - Styliolinid fragments (infilled and partially recrystallized calcite)
- V.Fine to Fine Silt: (40%)
    - ~40% quartz/feldspar
    - ~35% calcite
    - ~25% pyrite
- Matrix (Und.): (30%)

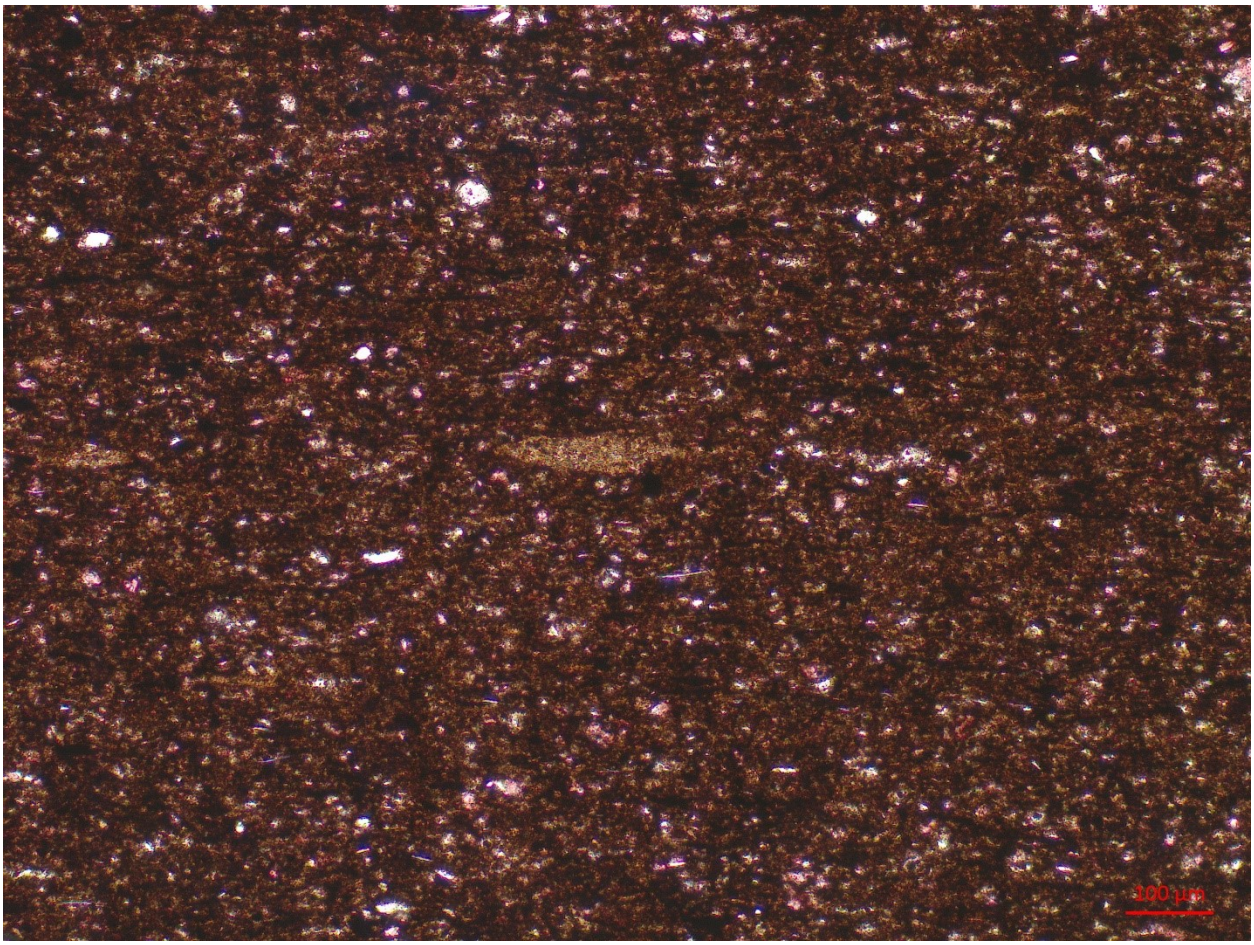

3098.5 m

- Sedimentary structures:
    - Planar, continuous laminae
        - Laminae distinguished by more silt-rich (mostly quartz silt) and silt poor laminae
- Texture:
    - Well sorted
    - Subrounded to rounded
- Medium to Coarse Sand: (0%)
- V. Fine to Fine Sand: (<1%)
    - Non-Skeletal: (0%)
    - Skeletal: (100%)
        - Likely styliolinid fragments
            - Crushed x-section (slightly recrystallized)
- Medium to Coarse Silt: (~20%)
    - Non-Skeletal: (~99%)
        - ~70% quartz/feldspar
        - ~10% calcite

        - ~10% mica (bed parallel oriented)
    - Skeletal: (~1%)
        - Styliolinid fragments (longer, thinner fragments only; oriented bed parallel)
        - Some possible very recrystallized calcitized radiolarians)
- V.Fine to Fine Silt: (35%)
    - ~40% quartz/feldspar
    - ~30% pyrite
    - ~20% calcite
    - ~10% mica
- Matrix (Und.): (~45%)

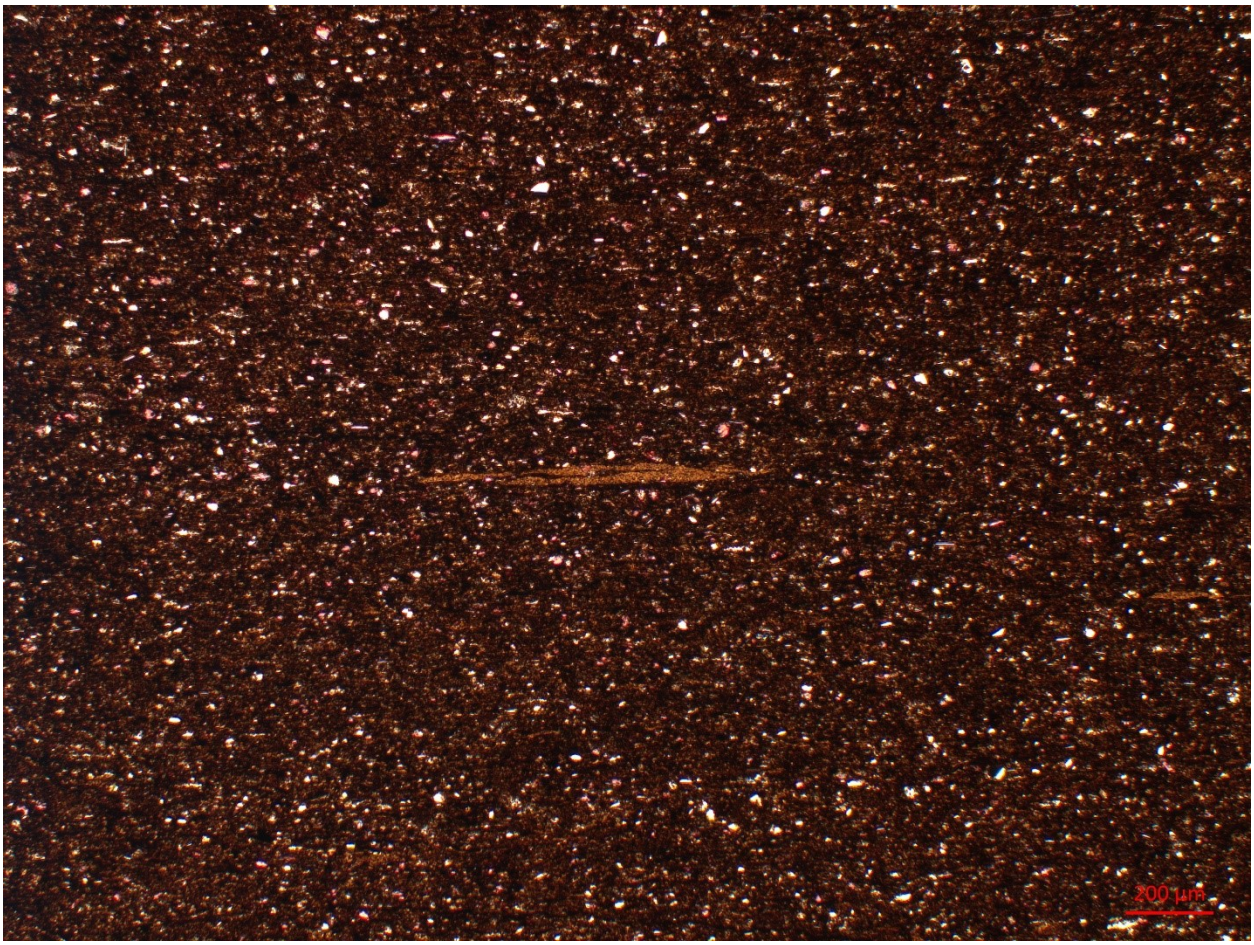

3095.9 m

- Sedimentary structures:
    - Planar, continuous, silty laminae (and silt poor laminae)
        - Quite quartz rich
        - Thicker (up to almost 2mm thick)
- Texture:
    - Well sorted
    - Subrounded to rounded
- Medium to Coarse Sand: (<1%)
    - Non-Skeletal: (0%)
    - Skeletal: (100%)
        - Styliolinid fragments
            - Lengthwise or cross sections
            - Oriented bed parallel
            - Appear vertically squished/crushed
            - Infilled but not very recrystallized interiors (some partially pyrite replaced)

- V. Fine to Fine Sand: (~1%)
    - Non-Skeletal: (50%)
        - Quartz/feldspar grains
    - Skeletal: (50%)
        - Styliolinid fragments (aligned bed parallel)
- Medium to Coarse Silt: (~30%)
    - Non-Skeletal: (75%)
        - ~55% quartz/feldspar
        - ~30% calcite
        - ~10% pyrite
        - ~5% mica
    - Skeletal: (25%)
        - Styliolinid fragments (aligned bed parallel)
        - Possible recrystallized calcitized rads
- V.Fine to Fine Silt: (35%)
    - ~50% quartz/feldspar
    - ~30% pyrite
    - ~20% calcite
- Matrix (Und.): (35%)

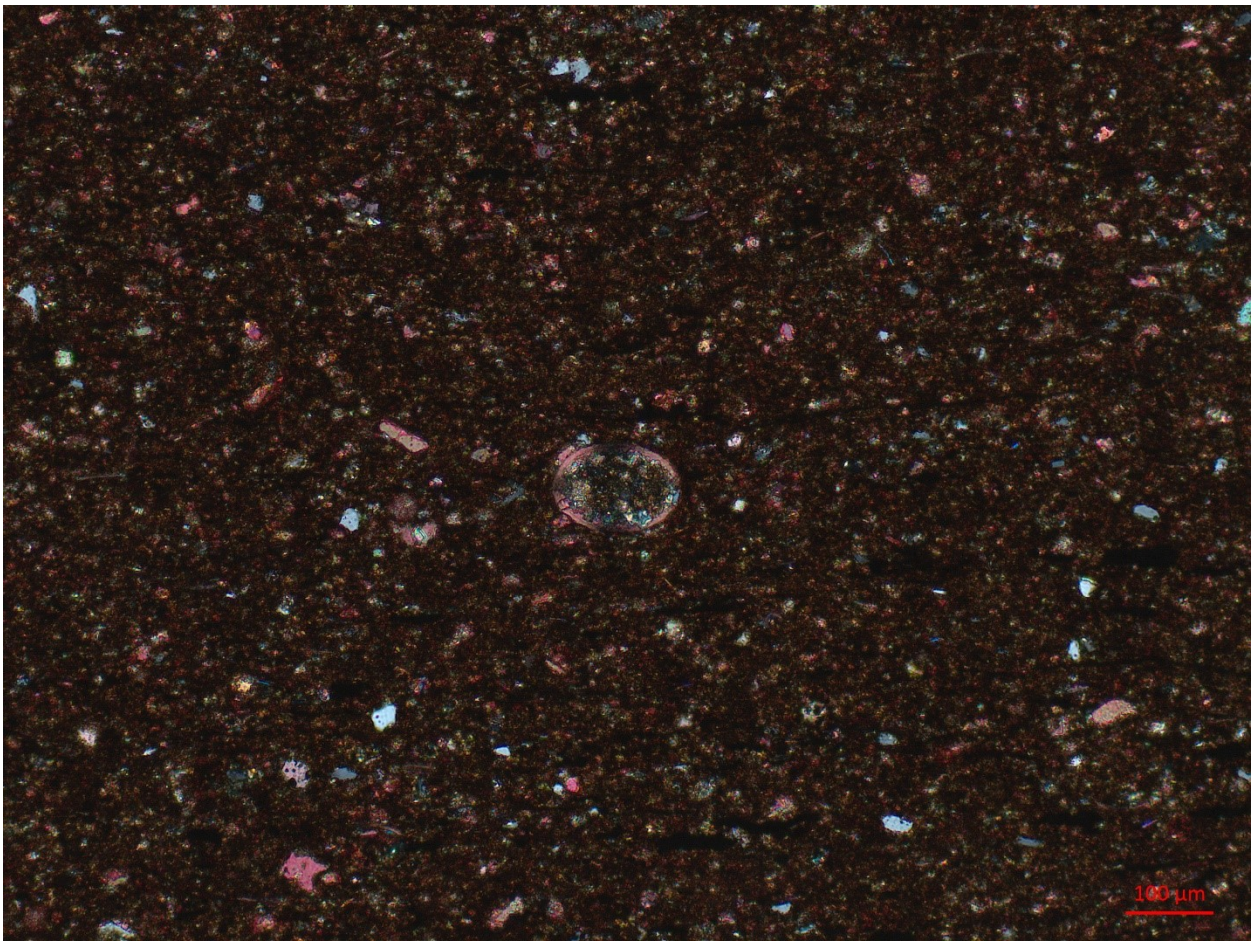

3095.5

- Sedimentary structures:
    - Planar, continuous laminae
        - Defined by siltier (mostly quartz/feldspar) and less silty laminae
        - Bottom half of thin section has sand-sized fossil fragments defining laminae
            - Styliolinid fragments (weakly bed aligned); possibly some calcispheres, rare conodont fragments; rare likely brachiopod fragments, (possibly some calcitized rads?
- Texture:
    - Moderately sorted
    - Subangular to subrounded
- Medium to Coarse Sand: (~10%)
    - Non-Skeletal: (0%)
    - Skeletal: (100%)
        - Styliolinid fragments (Vertically squished/crushed; infilled, slightly recrystallized interiors; quite bed-parallel aligned)
        - Possible calcitized rads
        - Possible brachiopod fragment
- V. Fine to Fine Sand: (~10%)
    - Non-Skeletal: (0%)
    - Skeletal: (100%)
        - Calcispheres??Calcitized rads??
        - Styliolinid fragments
        - Likely conodont fragments
- Medium to Coarse Silt: (20%)
    - Non-Skeletal: (80%)
        - ~40% quartz/feldspar
        - ~30% pyrite
        - ~20% calcite
        - ~10% mica (sub-bed parallel)
    - Skeletal: (20%)
        - Styliolinid fragments (sub-bed parallel)
        - Some possible calcitized rads
- V.Fine to Fine Silt: (30%)
    - ~40% quartz/feldspar (quite round)
    - ~30% pyrite
    - ~30% calcite
- Matrix (Und.): (30%)

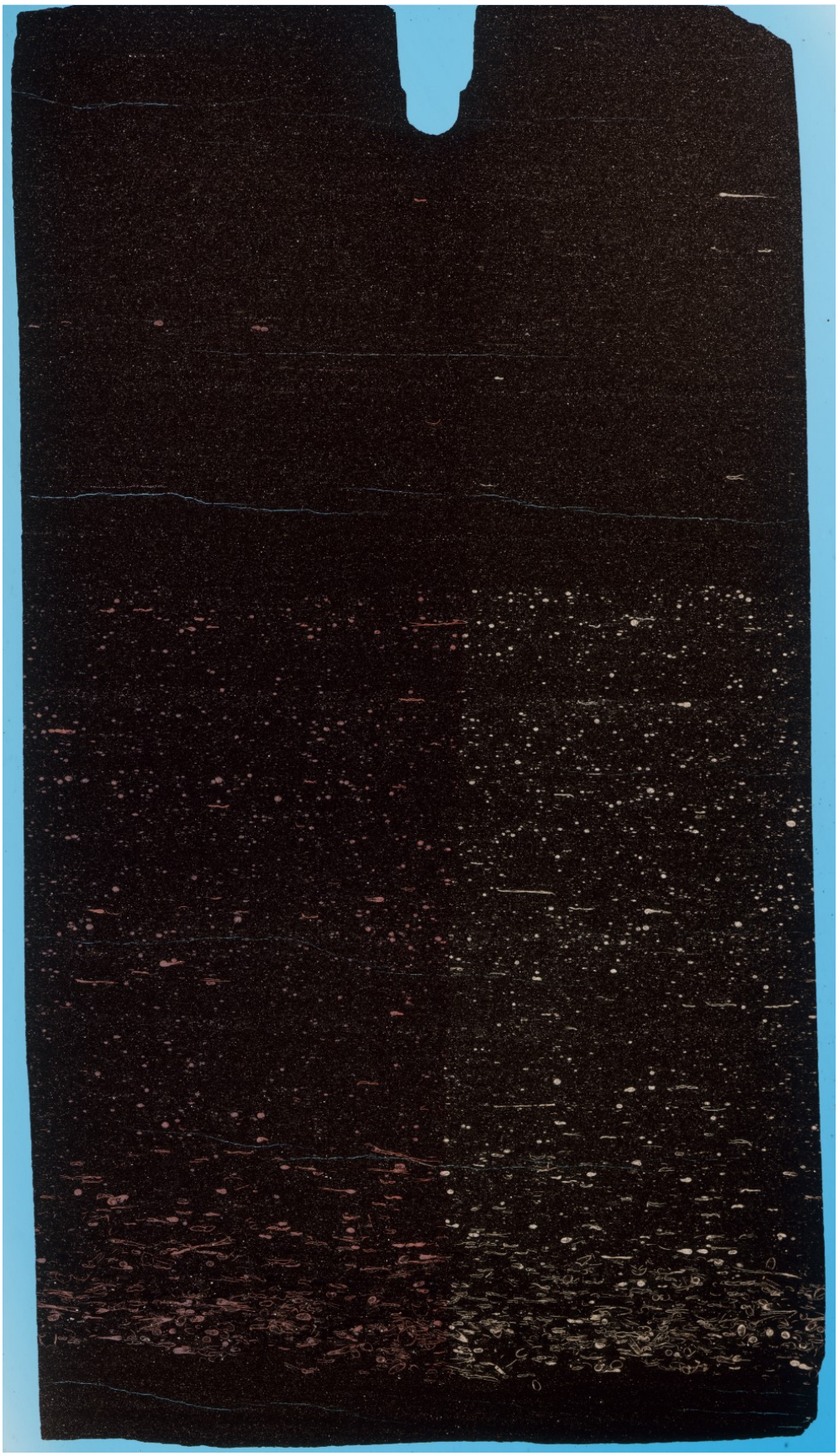

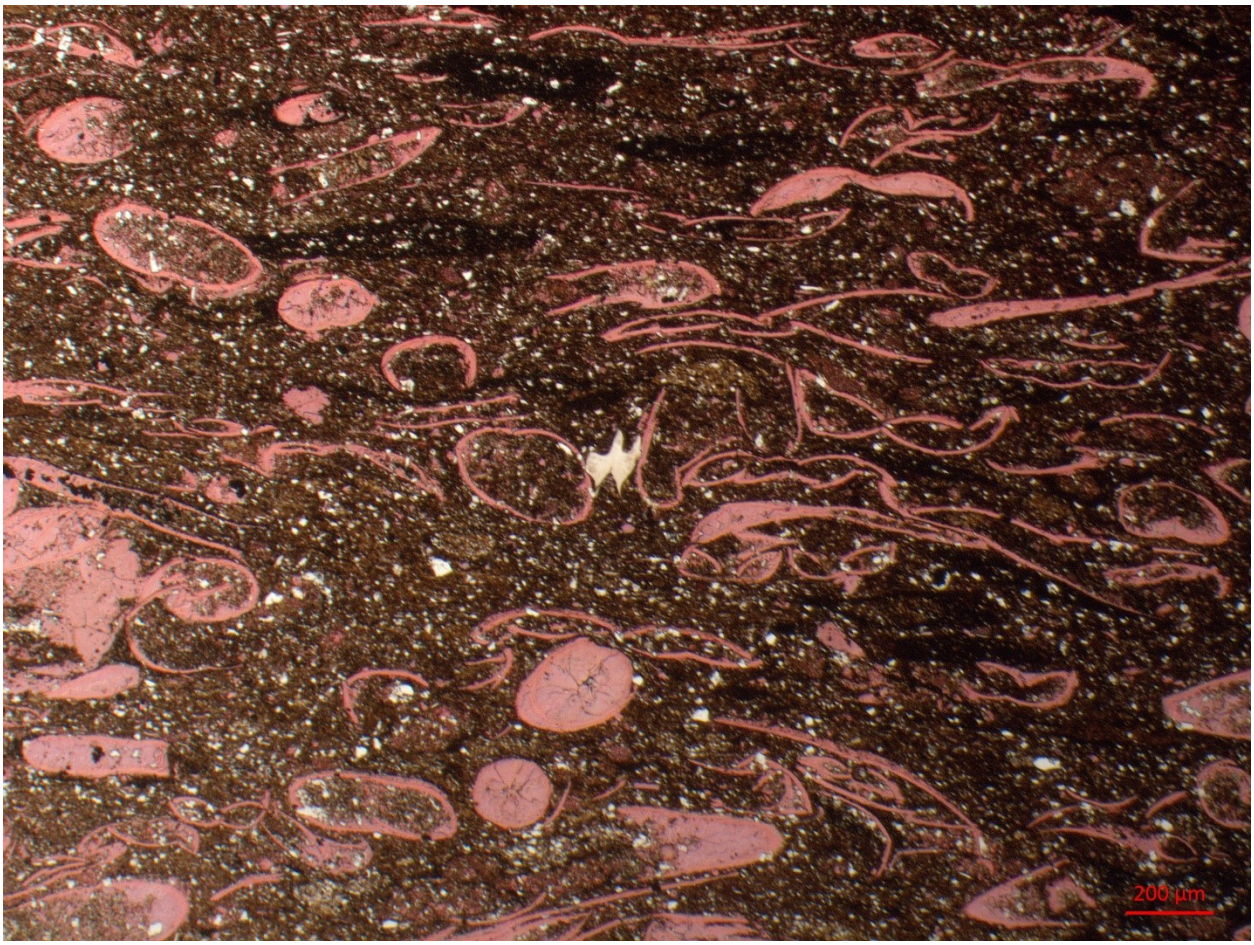

3094.75 m

- Sedimentary structures:
    - Planar, continuous laminae
        - Defined by siltier (mostly quartz/feldspar) and less silty laminae
        - Up to ~750 um thick
- Texture:
    - Moderately sorted
    - Subrounded to rounded
- Medium to Coarse Sand: (~1%)
    - Non-Skeletal: (~20%)
        - Quartz/feldspar grain (single grain; amorphous; appears pitted, possibly recrystallized siliceous grains)
    - Skeletal: (~80%)
        - Styliolinid fragments (mostly large, lengthwise cross sections; oriented bed parallel; infilled but not very recrystallized)
- V. Fine to Fine Sand: (~1%)
    - Non-Skeletal: (0%)

    - Skeletal: (100%)
        - Styliolinid fragments
- Medium to Coarse Silt: (~30%)
    - Non-Skeletal: (~80%)
        - ~50% quartz/feldspar grains
        - ~30% calcite grains (some partially replaced by pyrite)
        - ~20% mica grains (sub-bed parallel aligned)
    - Skeletal: (~20%)
        - Styliolinid fragments
        - Possible sparse ostracod fragments
- V.Fine to Fine Silt: (35%)
    - ~40% quartz/feldspar
    - ~30% calcite
    - ~30% pyrite
- Matrix (Und.): (35%)

3091.4 m

- Sedimentary structures:

    - Very obvious, wavy, continuous, silty (mostly quartz/feldspar) and not silty laminae
        - Very slight fining upward in some laminae
        - Sharp bottoms, more gradational tops
- Texture:
    - Moderately sorted
    - Sub-rounded to rounded
- Medium to Coarse Sand: (0%)
- V. Fine to Fine Sand: (~1%)
    - Non-Skeletal: (50%)
        - ~70% Quartz/feldspar grains
        - ~30% Calcite grains
    - Skeletal: (50%)
        - Styliolinid fragments (oriented bed parallel in silt-poor laminae and sub-bed parallel in silt-rich laminae)
- Medium to Coarse Silt: (~35%)
    - Non-Skeletal: (~80%)
        - ~70% quartz/feldspar grains
        - ~20% calcite grains
        - ~10% mica grains (oriented roughly bed parallel)
    - Skeletal: (~20%)
        - Styliolinid fragments (Oriented roughly bed parallel)
- V.Fine to Fine Silt: (35%)
    - ~40% quartz
    - ~30% calcite
    - ~30% pyrite
- Matrix (Und.): (30%)

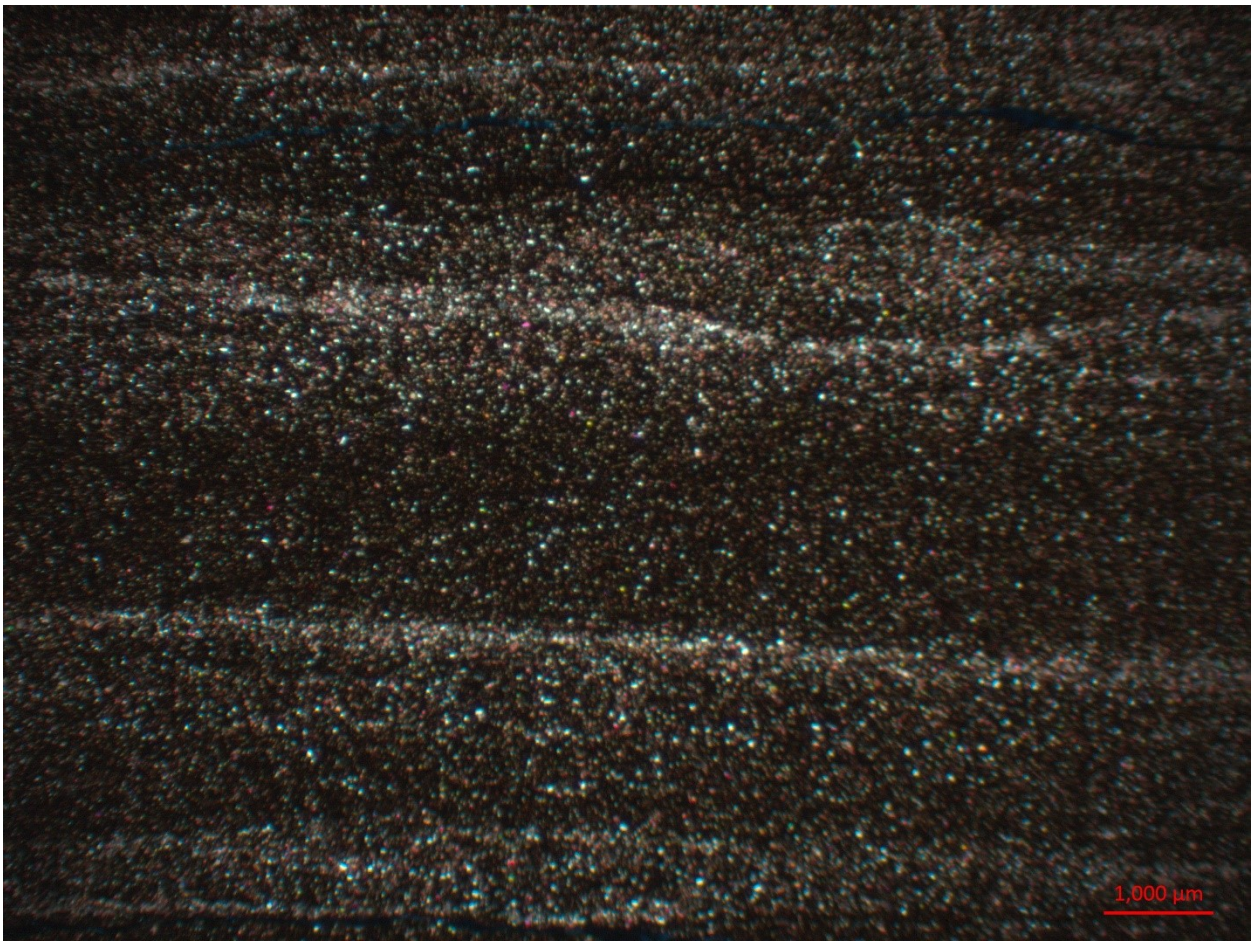

3089.97

- Surface
    - No visible surface
        - One possible laminae that may represent surface and lag
        - But not obvious at all
            - Whole section made up of silt laminae in mud (all quite similar in shape and composition)
- Lag
    - (and other silt laminae composition)
    - Quartz silt
    - Calcite silt (most dolomitized)
    - Some possible phosphatic grains
        - Some possible lingulid fragments (and maybe some skeletal/conodont fragments)
        - Some possible peloids
    - Lots of pyritized grains
    - Clay OM and pyrite rich matrix likely

3089.5

- Sedimentary structures:
  - Faint planar continuous laminae
    - Slightly disrupted
  - Large pyritized possible burrow overlain by pyritized surface (layer), overlain by pyritized dewatering structure
    - 18 mm tall by 11 mm wide
    - Laminae disrupted around structure
    - Pyrite in the form of quite round, recrystallized grains
      - V. fine silt to v. fine sand sized
      - (not included in rest of rock %'s)
  - Smaller, bed parallel, calcite and quartz/feldspar concentrated in burrows found below pyritized surface and large burrow
- Texture:
  - Well sorted
  - Subrounded to rounded
- Medium to Coarse Sand: (0%)
- V. Fine to Fine Sand: (<1%)

    - Non-Skeletal: (0%)
    - Skeletal: (100%)
        - Styliolinid fragments
        - Possible ostracod fragments
- Medium to Coarse Silt: (20%)
    - Non-Skeletal: (90%)
        - ~40% calcite grains
        - ~35% quartz/feldspar grains
        - ~20% mica grains
        - ~5% pyrite grains
    - Skeletal: (10%)
        - Styliolinid fragments
        - Possible ostracod fragments
        - Possible broken up conodont fragments
- V.Fine to Fine Silt: (35%)
    - ~35% calcite grains
    - ~35% quartz/feldspar grains
    - ~15% mica grains
    - ~15% pyrite grains
- Matrix (Und.): (45%)

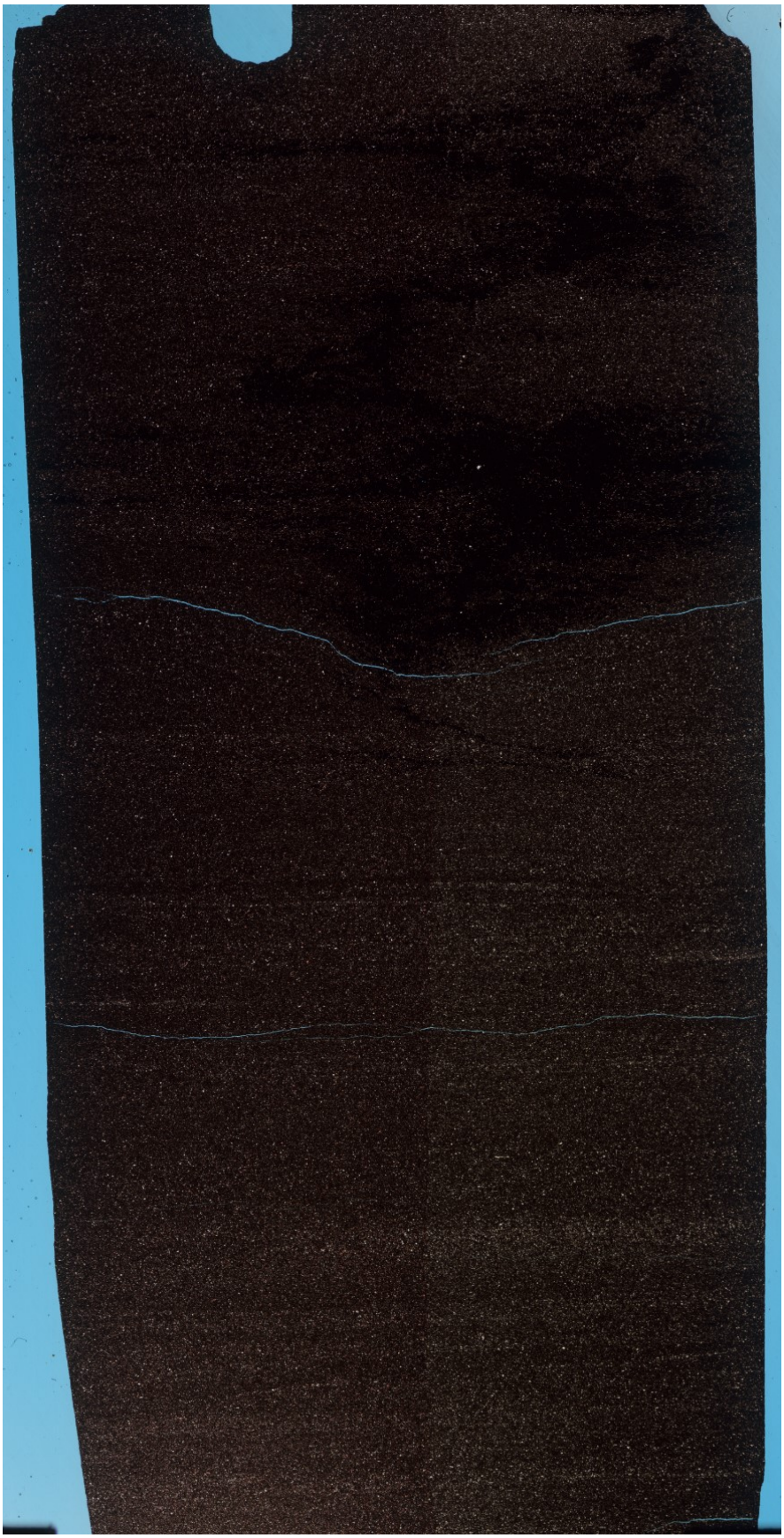

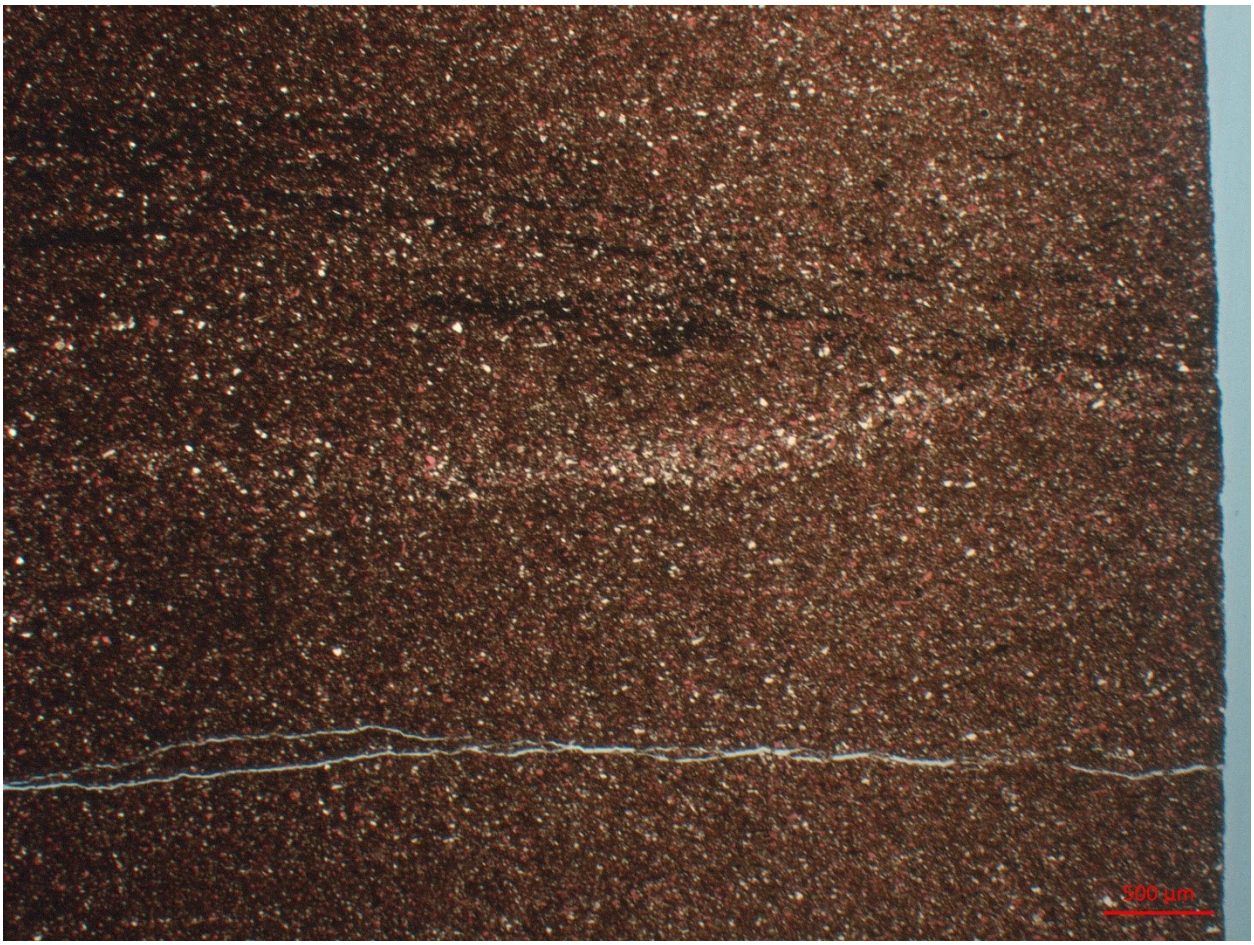

3088.5 m

- Sedimentary structures:
    - Faint planar continuous laminae
        - More silty and less silty laminae
        - Slight fining up in laminea
            - Possible coarsening up in some laminae
    - ~0.5 mm pyritized burrows (bed parallel)
- Texture:
    - Subrounded to well rounded
    - Well sorted
- Medium to Coarse Sand: (0%)
- V. Fine to Fine Sand: (0%)
- Medium to Coarse Silt: (~30%)
    - Non-Skeletal: (~90%)
        - 40% quartz/feldspar grains
        - 35% calcite grains
        - 15% pyrite grains

        - 10% muscovite
    - Skeletal: (~10%)
        - Calcitized rads?
        - Possible styliolinid fragments and possible ostracod fragments
        - Rare conodont fragments
- V.Fine to Fine Silt: (30%)
    - 40% quartz/feldspar grains
    - 35% calcite grains
    - 15% pyrite grains
    - 10% muscovite
- Matrix (Und.): (40%)

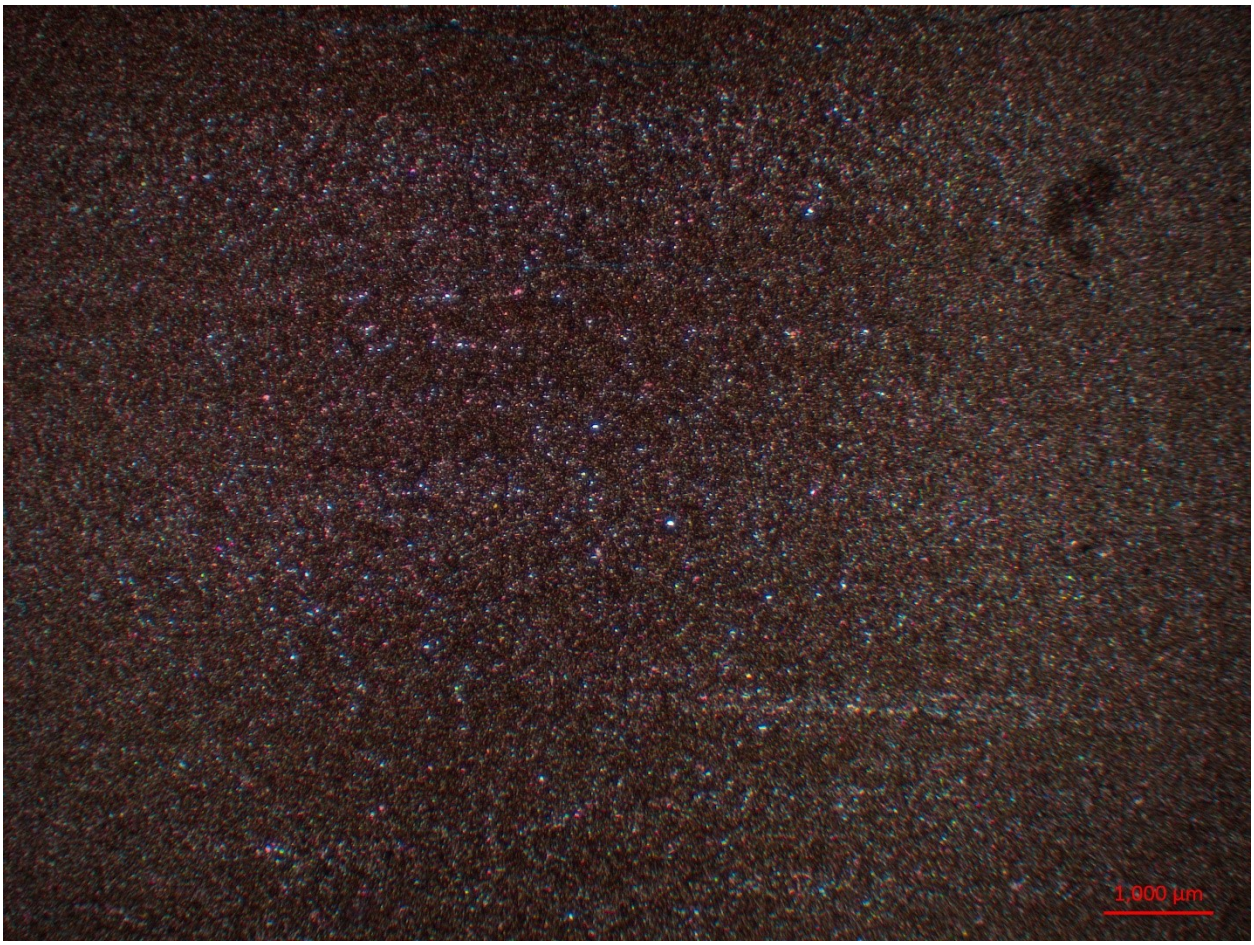

3085.5 m

- Sedimentary structures:
  - Slightly wavy, continuous silt laminae in mud
    - Big contrast between silt and mud laminae
    - Apparently coarsening up and fining up in laminae
    - Some sharp bases
  - Possible silt concentrated bed-parallel burrow in silt laminae
- Texture:
  - Moderately sorted
  - Subrounded to rounded
- Medium to Coarse Sand: (0%)
- V. Fine to Fine Sand: (~1%)
  - Non-Skeletal: (~80%)
    - ~60% Quartz/feldspar grains
    - ~40% Calcite grains
  - Skeletal: (~20%)
    - Possible rads

        - Styliolinid fragments
- Medium to Coarse Silt: (~30%)
    - Non-Skeletal: (~90%)
        - ~45% Quartz/feldspar grains
        - ~35% Calcite grains
        - ~15% pyrite grains
        - ~5% muscovite grains
    - Skeletal: (~10%)
        - Styliolinid fragments
        - Possible calcitized rads
- V.Fine to Fine Silt: (~25%)
    - ~45 Quartz/feldspar grains
    - ~35% calcite grains
    - ~15% pyrite grains
    - ~5% muscovite grains
- Matrix (Und.): (45%)

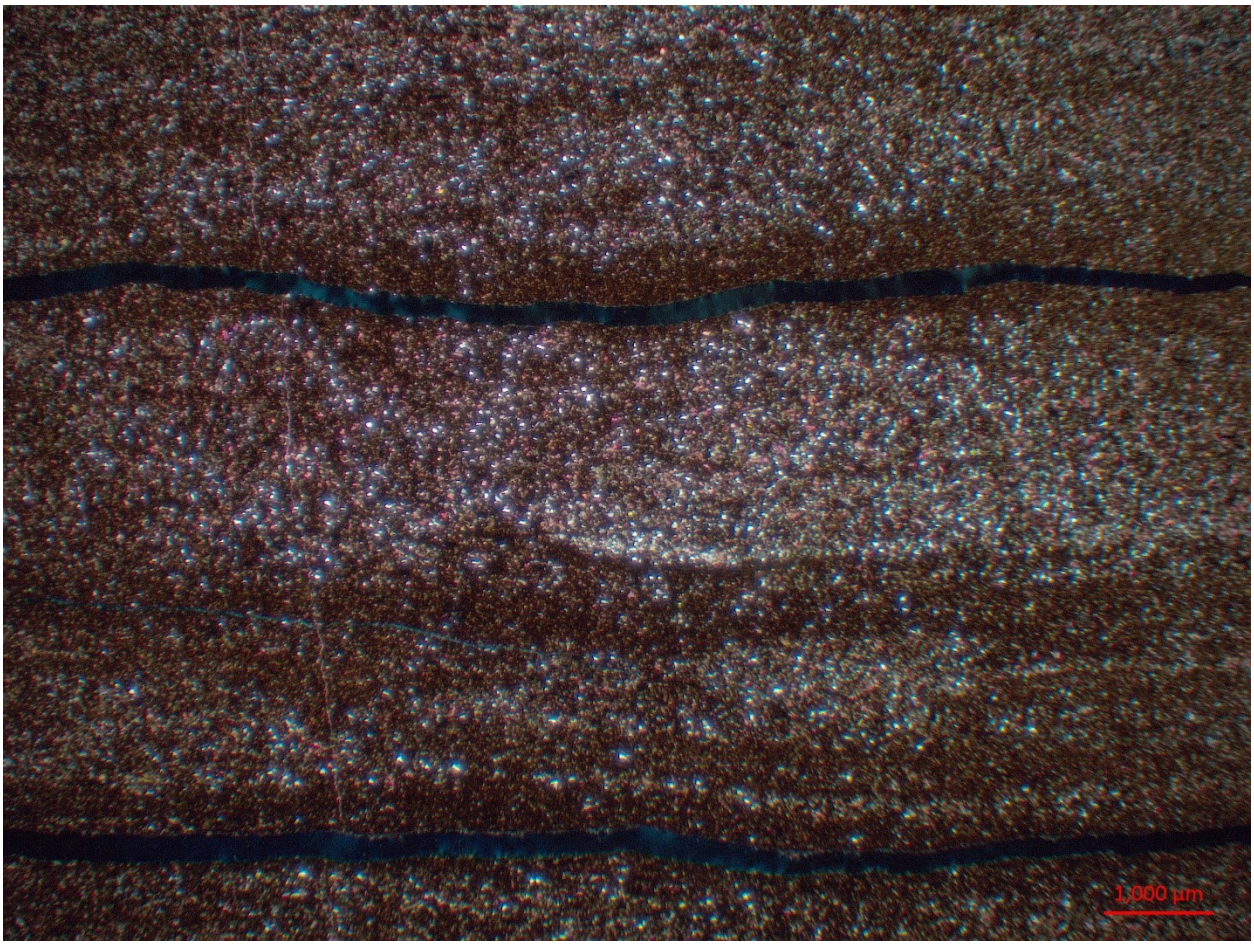

3084.5 m

- Sedimentary structures:
  - Faint planar continuous laminae
    - Slightly more silty and less silty laminae
  - Sparse pyrite nodules
    - ~0.5 mm
    - Preserved internal grains and structures
- Texture:
  - Well sorted
  - Sub to well rounded
- Medium to Coarse Sand: (0%)
- V. Fine to Fine Sand: (<1%)
  - Non-skeletal: (50%)
    - Quartz/feldspar
  - Skeletal: (50%)
    - Likely brachiopod fragment
- Medium to Coarse Silt: (15%)

    - Non-Skeletal: (~99%)
        - ~90% quartz/feldspar
        - ~5% Mica grains
        - ~5% calcite grains
    - Skeletal: (~1%)
        - Possible brachiopod fragments
        - Radiolarians?
- V.Fine to Fine Silt: (30%)
    - ~40% Quartz/feldspar
    - ~35% Pyrite
    - ~20% Mica
    - ~5% Calcite
- Matrix (Und.): (55%)

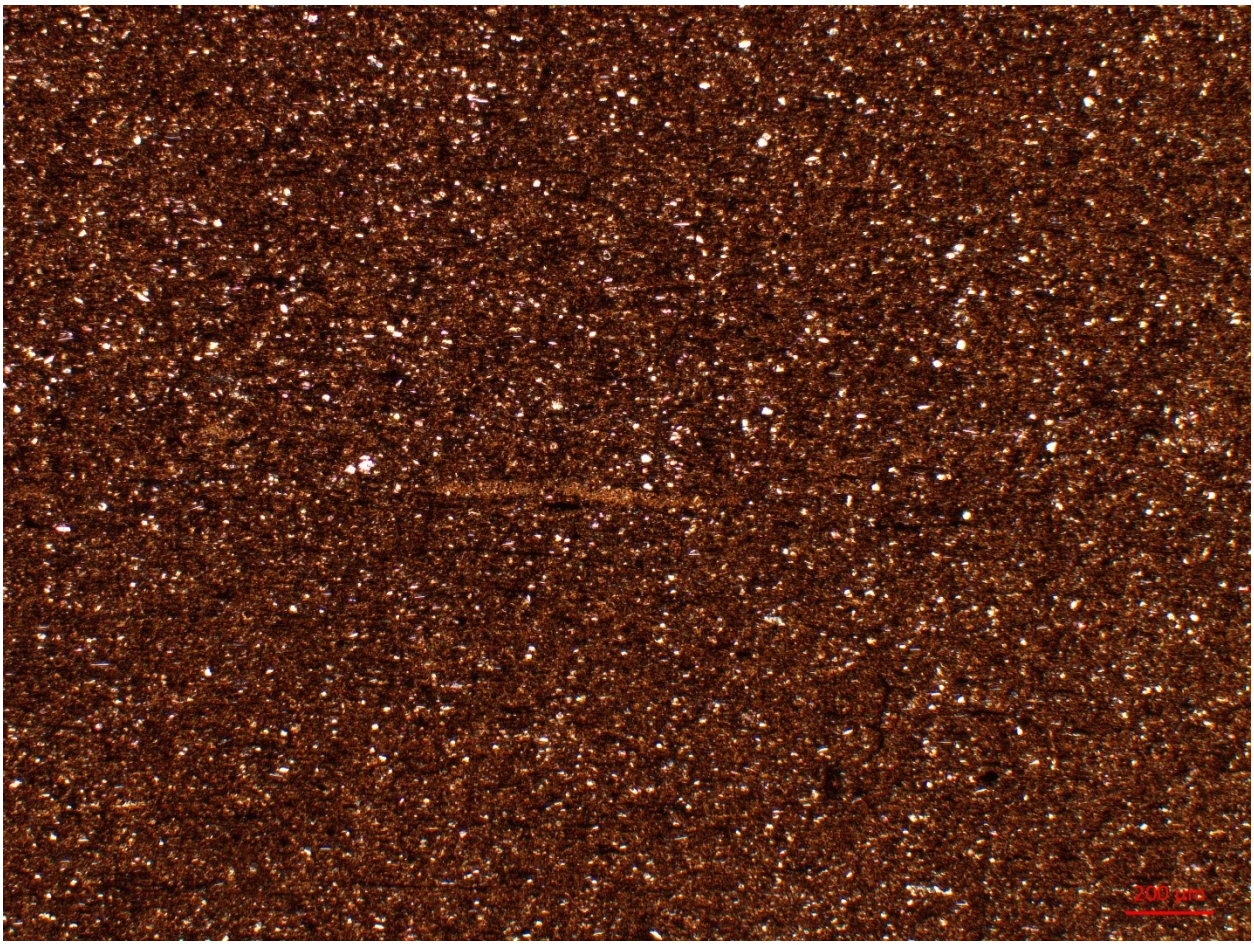

<u>3082.5 m</u>

- Sedimentary structures:
    - Planar, continuous coarser laminae
        - Composed of predominantly styliolinid fragments and calcitized radiolarians?

    - Botom of thin section has very little sand sized fossil fragments compared to top half
    - Calcitized and slightly pyritized planar layer
    - 1mm diameter pyritized burrow
- Texture:
    - Moderately sorted
    - Subrounded to rounded
- Medium to Coarse Sand: (~5%)
    - Non-Skeletal: (0%)
    - Skeletal: (100%)
        - Styliolinid fragments (Infilled; not very recrystallized; quite bed parallel oriented; slightly vertically crushed/squished)
- V. Fine to Fine Sand: (~10%)
    - Non-Skeletal: (0%)
    - Skeletal: (100%)
        - Calcitized rads
        - Styliolinid fragments
- Medium to Coarse Silt: (~20%)
    - Non-Skeletal: (~70%)
        - ~50% Calcite grains
        - ~25% Quartz/feldspar
        - ~15% pyrite grains
        - ~10% mica grains
    - Skeletal: (~30%)
        - Styliolinid fragments
        - Possible calcitized rads
- V.Fine to Fine Silt: (~20%)
    - ~40% Quartz/Feldspar
    - ~40% Calcite
    - ~20% pyrite grains
- Matrix (Und.): (~45%)

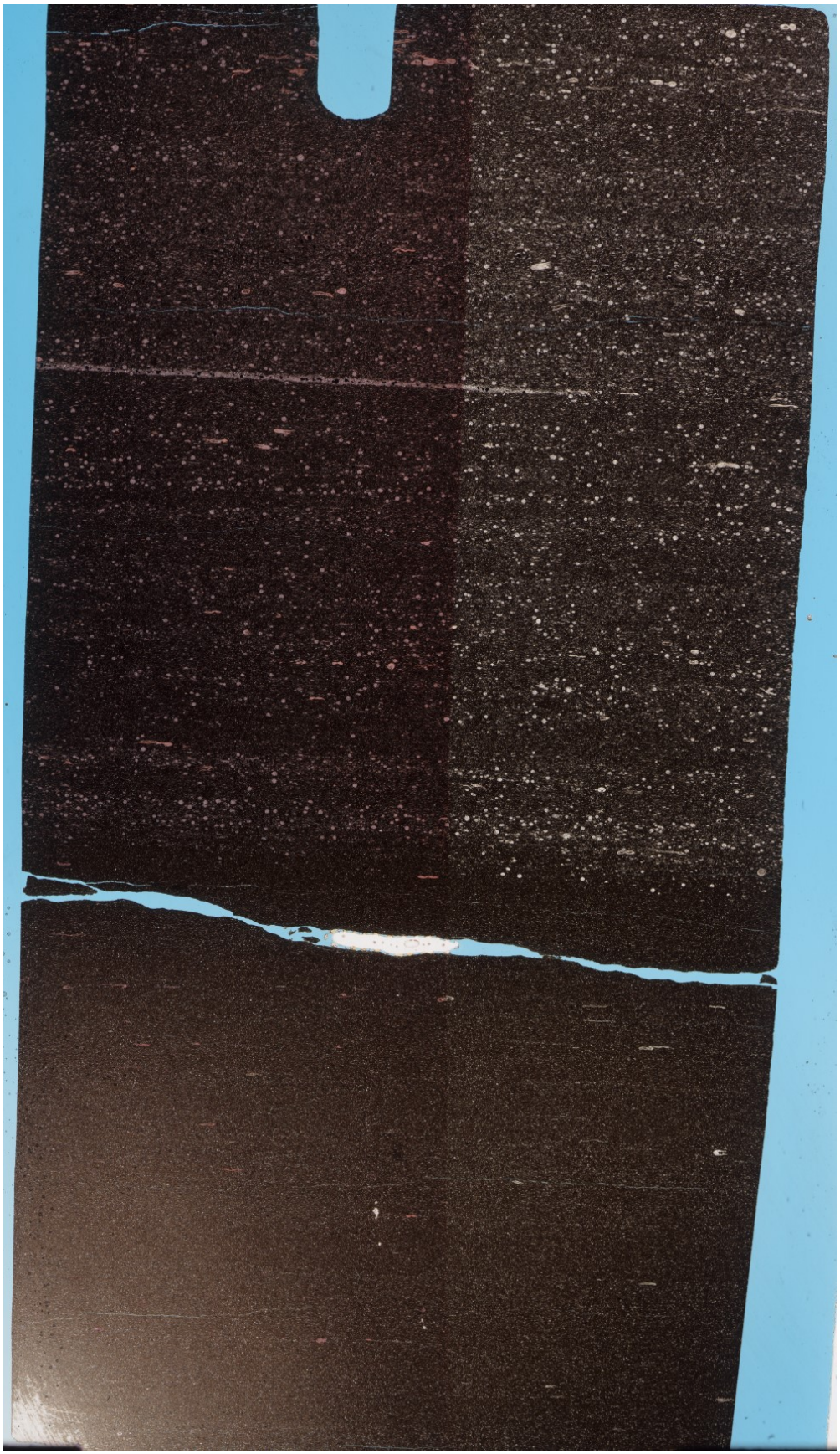

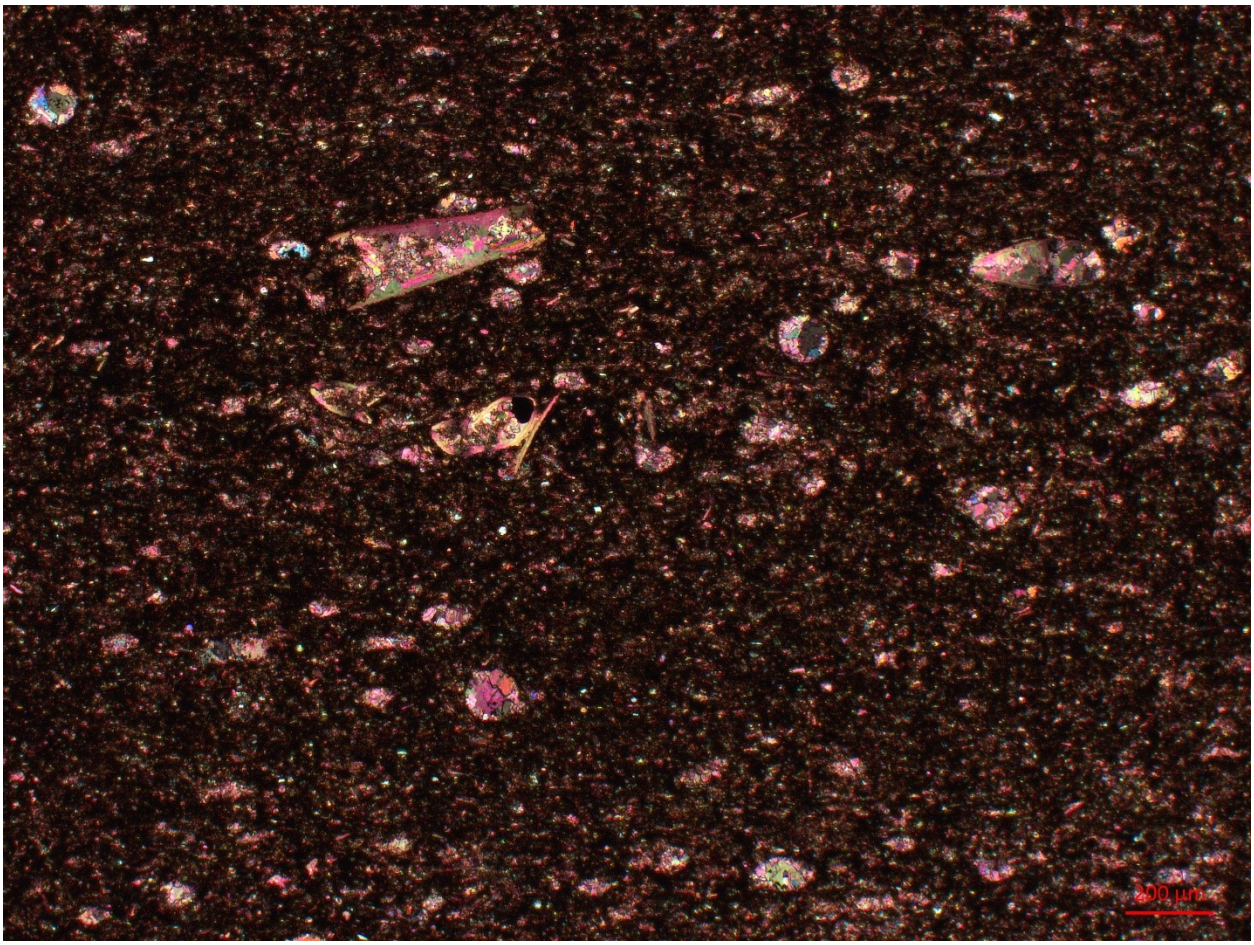

3080.4 m

- Sedimentary structures:
  - Very faint planar continuous laminae
    - Slightly more silty and less silty laminae
  - Top ¼ of thin section has common calcitized rads?, tentaculites, and styliolinids (much less than tentaculites)
    - Slightly concentrated into rough laminae
- Texture:
  - Subrounded to rounded
  - Moderately sorted
- Medium to Coarse Sand: (~1%)
  - Non-Skeletal: (0%)
  - Skeletal: (100%)
    - Tentaculitid fragments (oriented bed parallel, quite in-tact, vertically crushed)
    - Styliolinid fragments (oriented bed parallel, infilled (not very recrystallized), typically vertically crushed)
- V. Fine to Fine Sand: (~5%)

    - Non-Skeletal: (0%)
    - Skeletal: (100%)
        - Calcitized rads
        - Tentaculitid fragments
        - Styliolinid fragments
- Medium to Coarse Silt: (~20%)
    - Non-Skeletal: (~90%)
        - ~50% quartz/feldspar grains
        - ~25% pyrite grains
        - ~20% calcite grains
        - ~5% mica grains
    - Skeletal: (~10%)
        - Styliolinid fragments
        - Tentaculitid fragments
- V.Fine to Fine Silt: (25%)
    - ~50% Quartz/feldspar
    - ~25% pyrite grains
    - ~25% calcite grains
- Matrix (Und.): (~50%)

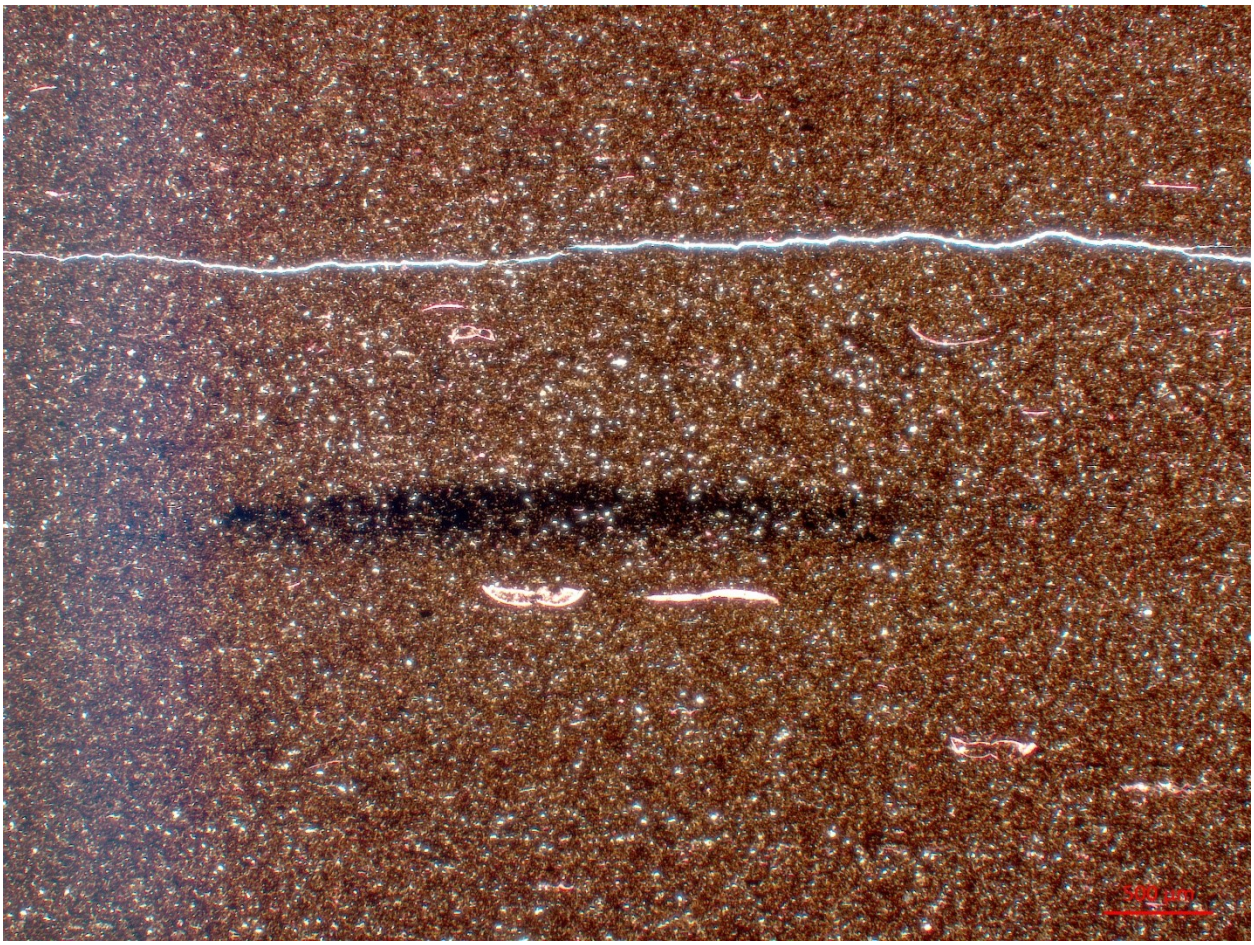

3077.22 m

- Sedimentary structures:
    - Abundant thick wavy silt laminae in mudstone
        - Made up of almost entirely quartz/feldspar and calcite silt grains with some pyrite grains
            - Cemented together with dolomite cement (sometimes up to 40% dolomite cement in laminae)
        - Generally sharp boundaries
        - Slight fining up and coarsening up laminae
    - Possible starved ripples or silt concentrated burrows in silt laminae
    - ~1mm thick vertical fracture through entire thin section
        - Infilled by almost entirely dolomite cement (some calcite cement or calcite grains)
- Texture:
    - Moderately sorted
    - Subrounded to rounded
- Medium to Coarse Sand: (0%)

- V. Fine to Fine Sand: (~5%)
    - Non-Skeletal: (~30%)
        - Quartz/feldspar grains subrounded to rounded
    - Skeletal: (~70%)
        - Likely Styliolinid fragments (oriented sub-bed parallel)
        - Likely brachiopod or conodont fragments
- Medium to Coarse Silt: (25%)
    - Non-Skeletal: (70%)
        - ~40% Quartz/feldspar grains
        - ~35% Calcite grains
        - ~10% pyrite grains
        - ~5% mica grains
    - Skeletal: (30%)
        - Styliolinid fragments?
            - Oriented bed parallel to sub-bed parallel
        - Likely brachiopod and or ostracod fragments?
- V.Fine to Fine Silt: (~25%)
    - ~45% Quartz/feldspar
    - ~35% calcite
    - ~20% pyrite grains
- Matrix (Und.): (~45%)
    - Appears to have significant dolomite cement component

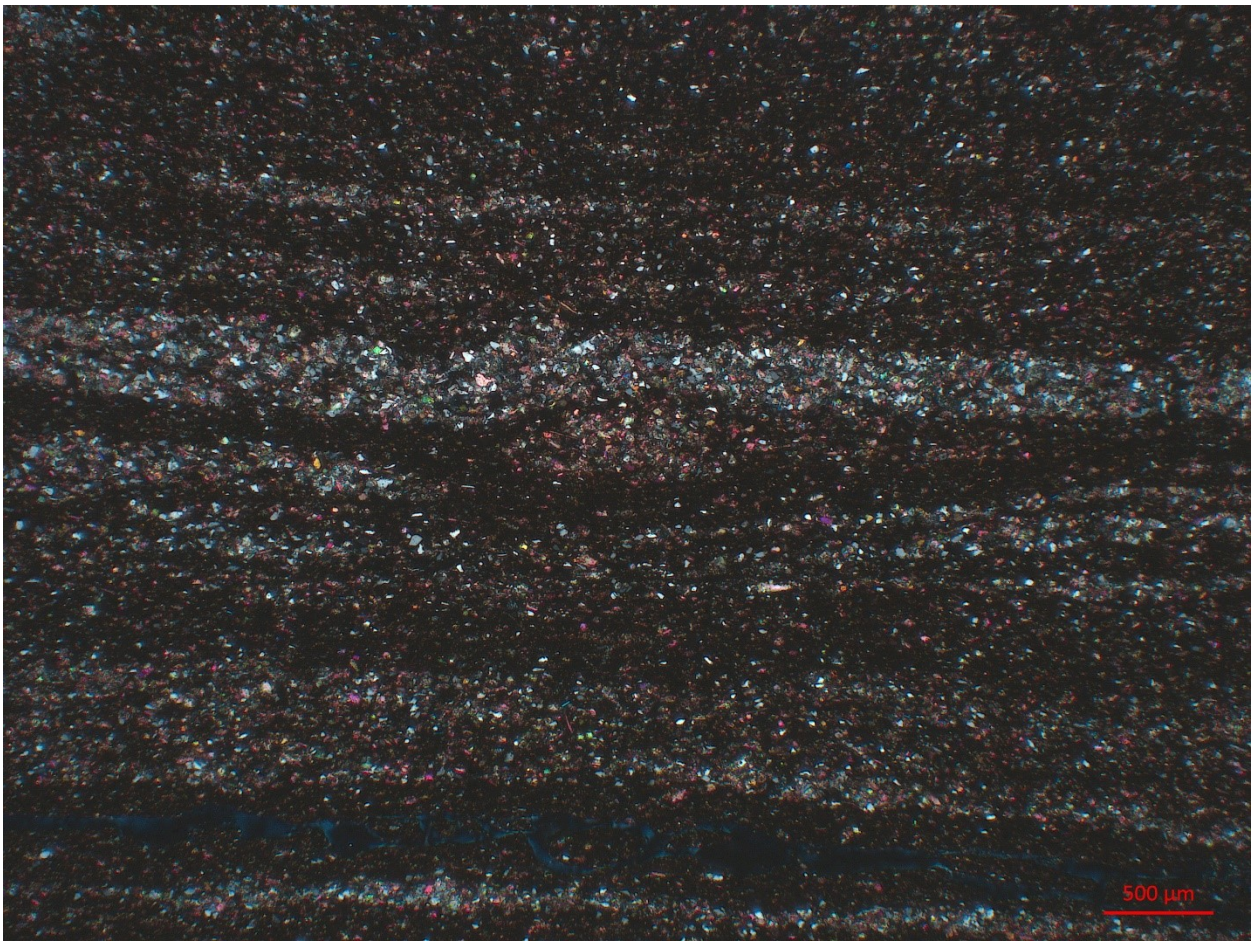

3075.85 m

- Sedimentary structures:
    - Faint planar continuous laminae
        - Slightly siltier and less silty laminae
    - 15x36mm (visible part) calcite nodule
        - Very fine recrystallized calcite
        - Sparse pyrite grains within
        - Reaction rim? (~1mm thick) of recrystallized calcite and dolomite
            - Coarser grained than inside nodule
            - Sparse pyrite grains inside
- Texture:
    - Well sorted
    - Subrounded to rounded
- Medium to Coarse Sand: (<1%)
    - Non-Skeletal: (0%)
    - Skeletal: (100%)
        - Likely styliolinid fragment

        - Infilled, slightly recrystallized
- V. Fine to Fine Sand: (~1%)
    - Non-Skeletal: (80%)
        - ~60% quartz/feldspar
        - ~40% calcite
    - Skeletal: (20%)
        - Styliolinid fragments (oriented roughly bed parallel)
- Medium to Coarse Silt: (~20%)
    - Non-Skeletal: (~95%)
        - ~60% quartz/feldspar grains
        - ~20% Calcite Grains (appear slightly recrystallized)
        - ~10% Pyrite grains
        - ~5% Mica
        - ~5% Dolomite? (sometimes rhombohedral, often recrystallized)
    - Skeletal: (~5%)
        - Styliolinid fragments (sub-bed parallel orientation)
- V.Fine to Fine Silt: (~30%)
    - ~60% Quartz/feldspar
    - ~20% calcite
    - ~10% pyrite grains
    - ~5% mica
    - ~5% dolomite?
- Matrix (Und.): (~49%)

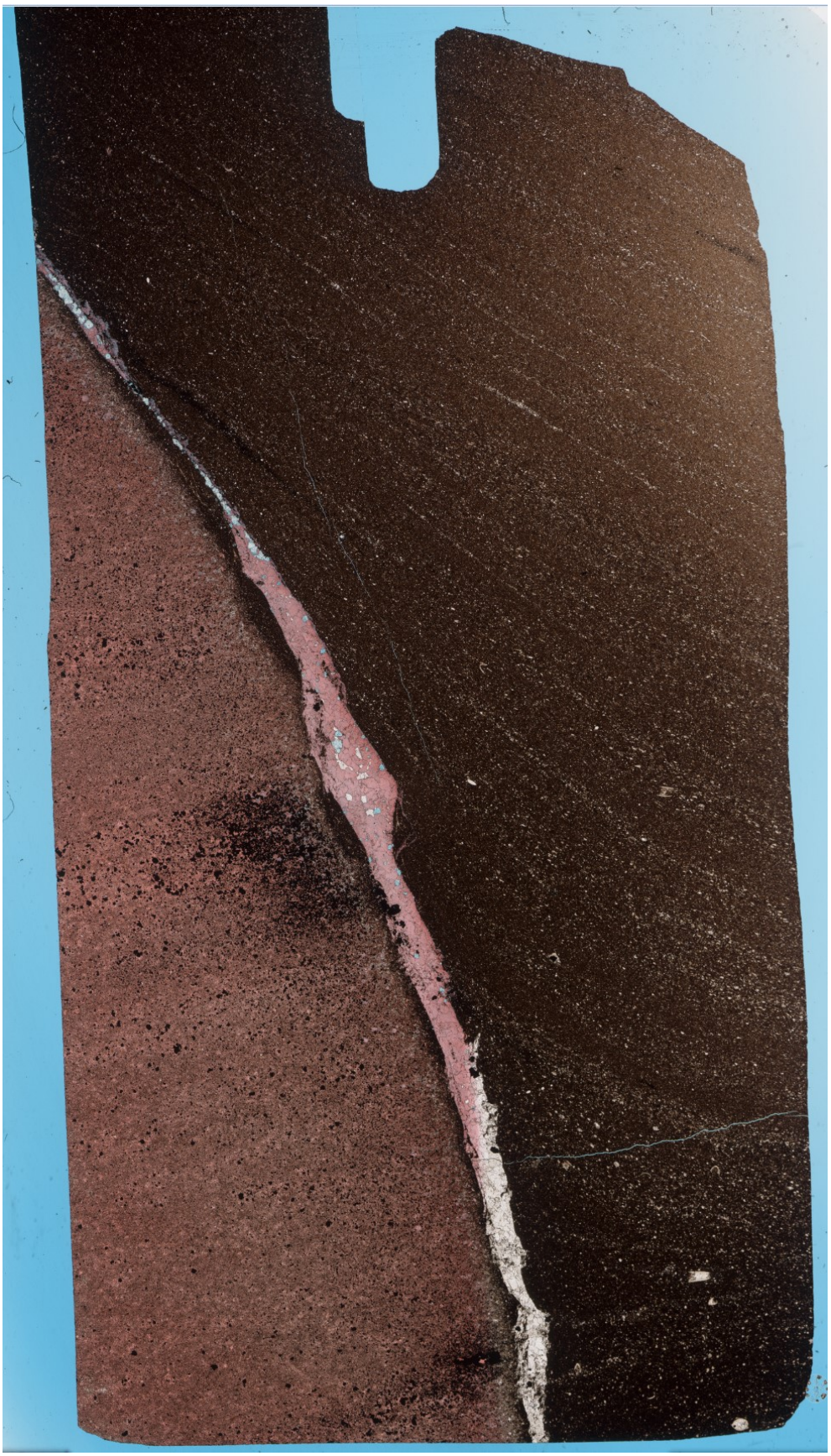

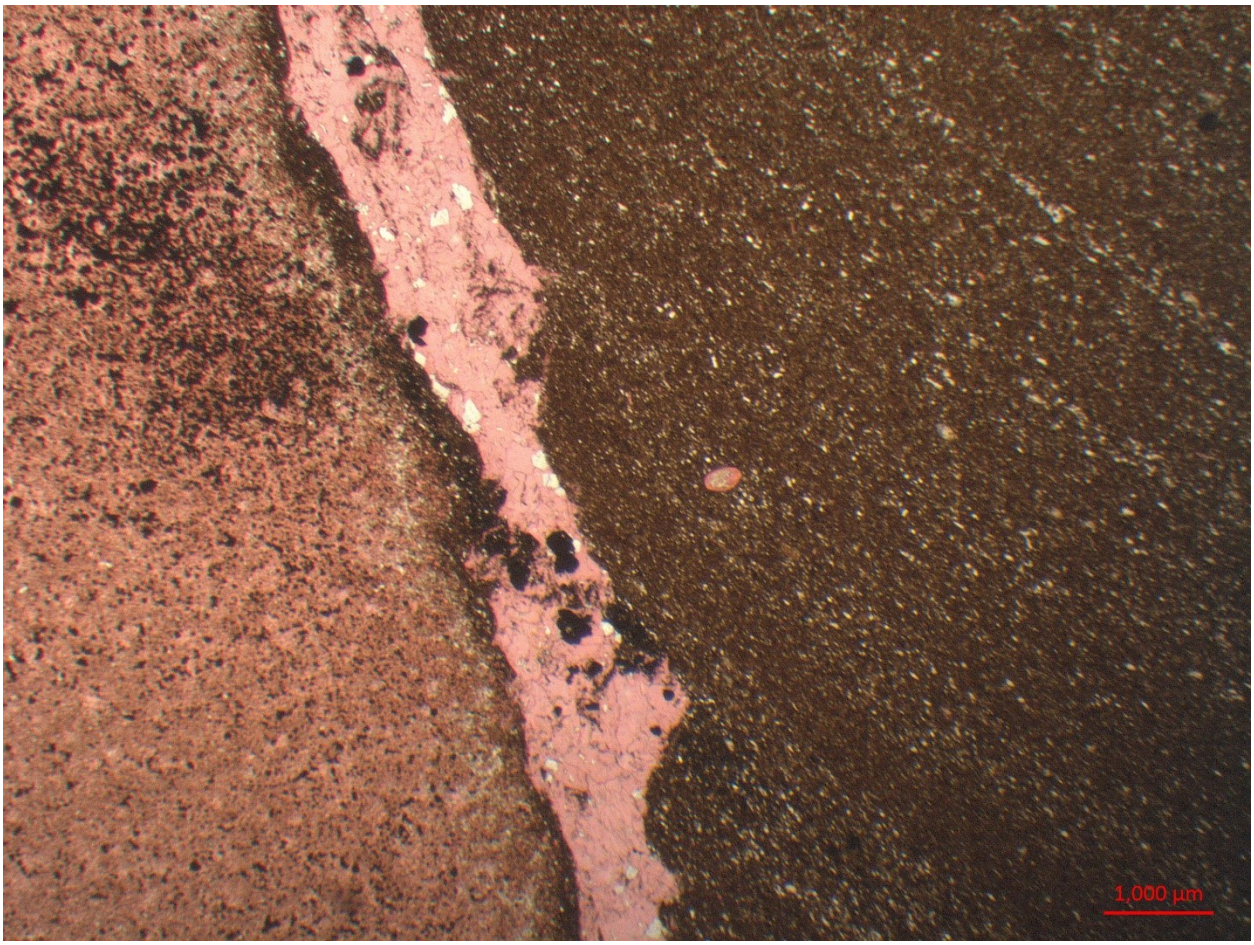

3068.1 m

- Sedimentary structures:
  - Very faint planar laminae in very calcite cemented, quite fine grained rock
    - Shown by pyrite grains and flat pyrite grains oriented bed parallel
  - Sparse calcitized radiolarians? in top and bottom ¼'s of TS
- Texture:
  - Well sorted
  - Rounded
- Medium to Coarse Sand: (0%)
- V. Fine to Fine Sand: (~1%)
  - Non-Skeletal: (0%)
  - Skeletal: (100%)
    - Calcitized radiolarians?
- Medium to Coarse Silt: (~3%)
  - Non-Skeletal: (~40%)
    - ~70% Pyrite grains
    - ~30% quartz/feldspar grains

    - Skeletal: (~60%)
        - Calcitized rads?
- V.Fine to Fine Silt: (~30%)
    - ~40% Calcite
    - ~30% Quartz/feldspar
    - ~30% Pyrite
- Matrix (Und.): (~66%)
    - Appears to be almost entirely recrystallized dolomite and some calcite

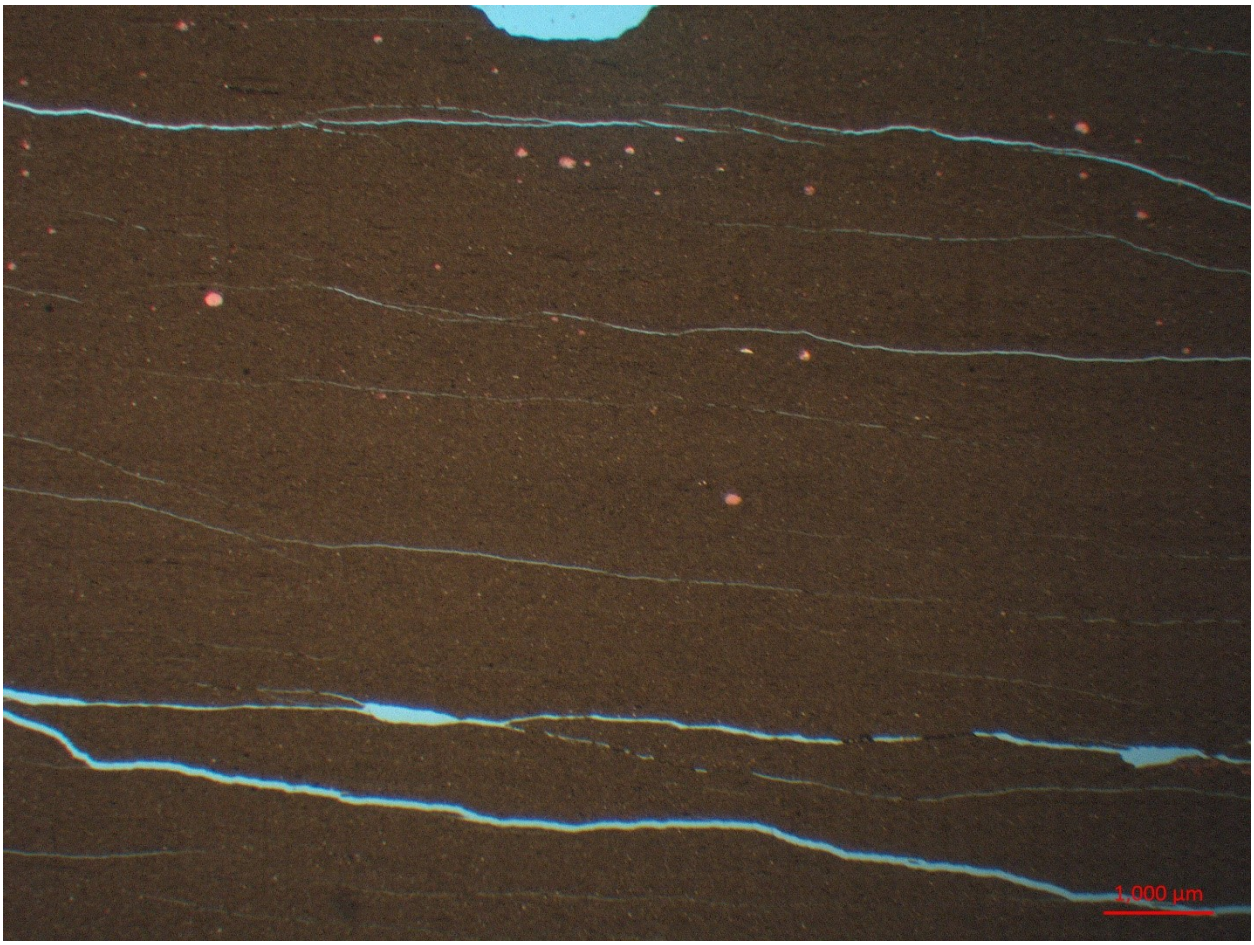

Core 5 – TQN FOXCK

<u>3101.65</u>

- Top part of thin section supposed to be at bottom (planar laminated mud)
- Surface
    - Likely ball and pillow structure soft sed def into underlying mud
        - Deformation of underlying mud laminae?
        - More diffuse than sharp edges to balls
        - Maybe smaller ones right below surface could be burrows but less likely
        - Infilled by overlying 'lag' material
        - Extend into underlying mud for ~14mm
        - 1-4mm thick
- Lag
    - Silt to vfs mostly
        - Some grains up to coarse (shell fragments)
    - Composition:
        - Abundant fossil fragments

            - Styliolinids
            - Tentaculitids
            - Ostracods/small brachiopods
        - Common Phosphatic grains
            - Peloids (massive internal structure)
            - Conodont elements/skeletal fragments
            - Possible lingulid shell fragments
        - Abundant quartz silt
        - Common calcite and dolomite silt
        - Fairly OM rich matrix
    - Very massive internal structure
    - Likely very bioturbated
        - Subhorizontal to subvertical mud infilled burrows
- Above
    - Likely continues
- Below
    - Silty planar laminated mud
        - Abundant calcite and quartz silt
        - OM and pyrite rich matrix
        - Styliolinid, ostracod/small brachiopod shell fragments
        - Rare very small phosphatic peloids

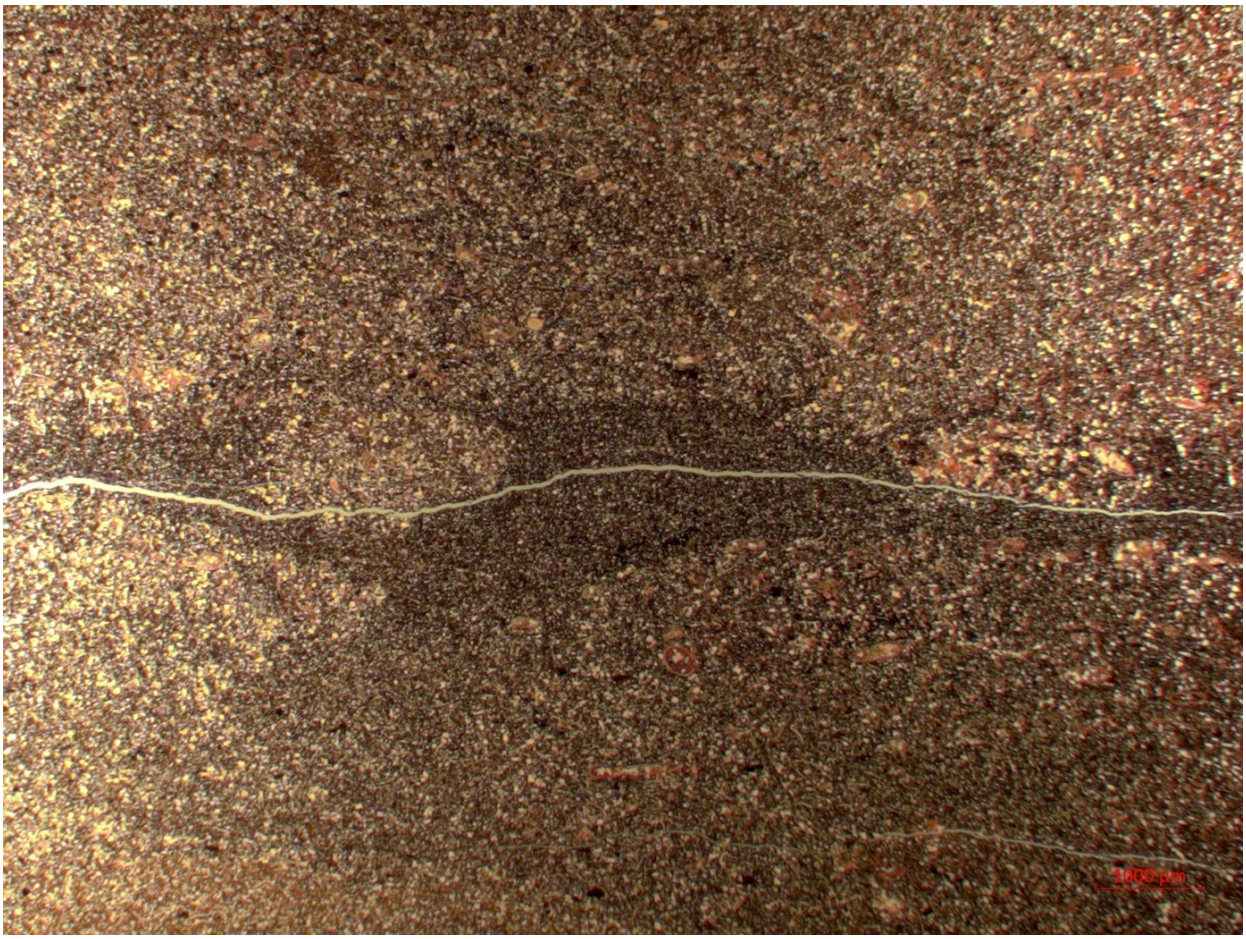

Core 6 – ROGCI HZ Kaybobs

<u>3397.85</u>

- Entire thin section very pyrite cemented (matrix) and dolomite cement (very recrystallized subrounded calcite grains (mostly vfs) that stain a purple colour?)
    - Calcite grains replaced by dolomite
        - Calcite grains likely concentric interiors
            - Possibly calcispheres
                - Possibly precipitated in-situ
                    - Not likely transported (or very short distance)
                        - Not sure if deposited there or precipitated in place
        - Dolomitized calcite grains have dolomite reaction rims
- Matrix possibly very pyrite cement and clay rich
- Surface
    - Actual surface probably not visible
        - Too cemented and recrystallized to see

        - Possibly just below first 'lag' of phosphate grains
            - Possibly at top of phosphatic section before change to planar mud??
- Lag
    - Likely multiple lag deposits above surface
        - Very recrystallized and hard to see
        - Mostly going off location of phosphate grains
        - Lags appear to deform around calcite nodule (nodule likely formed from below lags)
    - First lag:
        - ~1mm thick
        - Composition:
            - Lags have much less dolomite recrystallized calcite grains than rest of sample
            - Appears to have lots of pyrite cement and some dolomite cement
            - Common likely phosphatic grains
                - Likely peloids with likely halo of silica cement (possibly chert) (some dolomite cement too)
                    - Most appear structureless (possibly some internal concentric)
                    - Some partially pyritized
                - More rare conodont elements (possible skeletal fragments)
                - Some likely fish bone fragments
                - Possibly partially dissolved
                - Phosphate grains came first (likely transported in)
                    - Rims definitely came after (very irregular)
            - Sparse quartz grains
            - Dolomitized calcite grains
                - Subrounded
            - Dolomitized calcite silt
            - Some shell fragments
        - Quite massive appearing structure
        - Likely bioturbated
            - Subhorizontal to subvertical mud infilled burrows
    - Multiple possible phosphate lags to top of calcite rich section
        - Phosphate grains appear to increase in concentration to top of calcite rich section (beside calcite nodule)
        - Lags appear to become thicker upwards
        - Same composition as first lag
- Above
    - (above last phosphate-rich layer)
    - Phosphate disappears
    - Planar laminated mud
    - Quartz and calcite silt roughly concentrated into laminae
    - Appears quite bioturbated

        - Subhorizontal to subvertical mud infilled burrows
- Below
    - Similar to non lag sections but no visible phosphate grains
        - Calcispheres
        - Some shell fragments
        - Rare quartz grains
        - Some dolomite replaced grains
        - Lots of pyrite and OM matrix

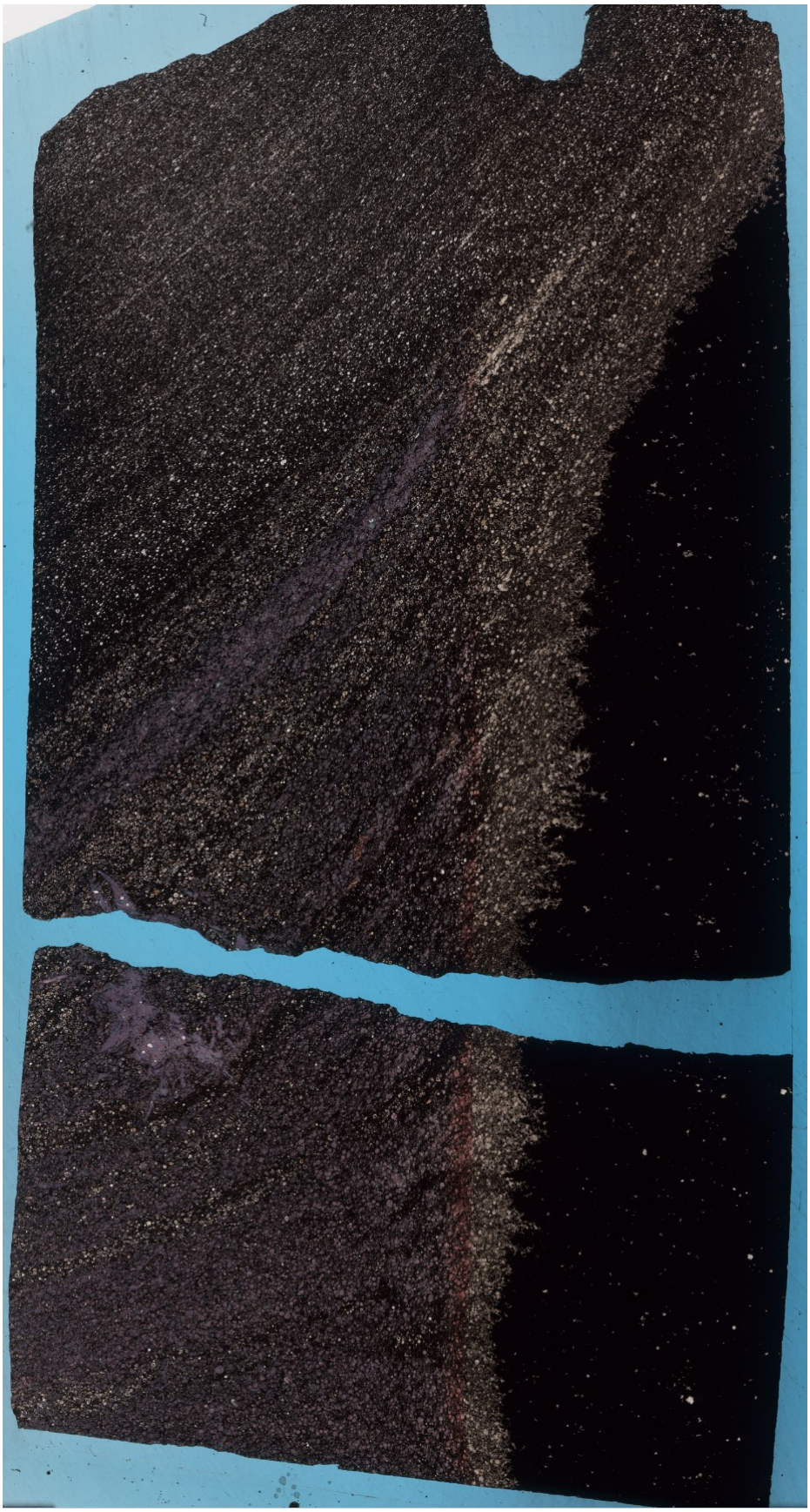

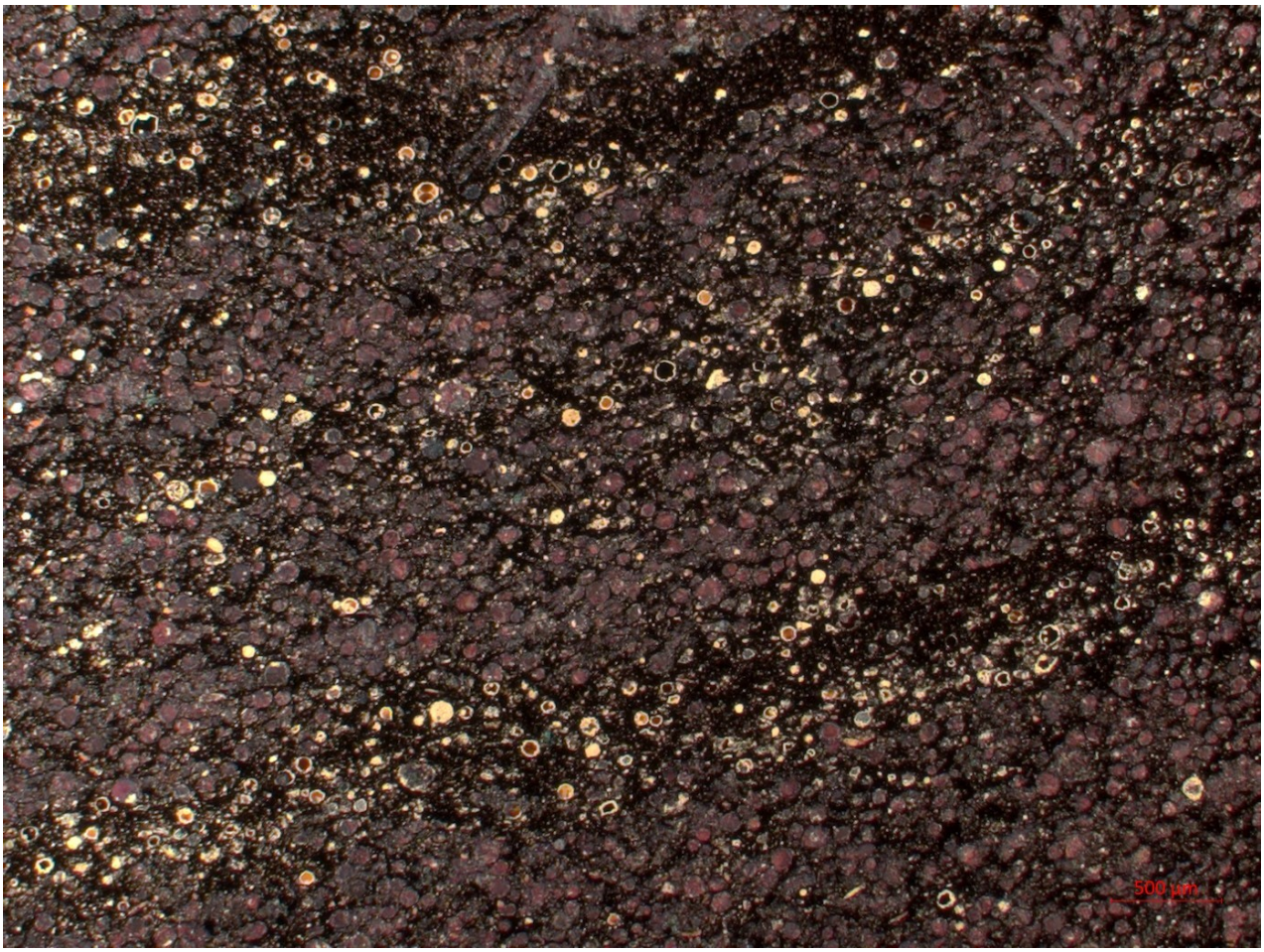

3370.48

- Surface
  - Likely soft sediment deformed
    - Ball and pillow structure into underlying mud
    - Deformation of underlying
- Lag
  - 22 mm thick
  - Mostly silt to vfs
  - Very calcite cemented
  - Lots of partial dolomitization of calcite grains and dolomite cement
    - Fossil fragments appear not to be dolomitized
  - Components:
    - Abundant calcite fossil fragments
      - Dominantly shell fragment (likely ostracod/small brachiopod)
      - Possibly some styliolinids
    - Calcite grains
      - Subangular to subrounded

            - Some partly or fully replaced by pyrite
            - Some partial replacement by dolomite
        - Rare phosphatic grains
            - Peloids (massive internal structure)
            - Rare siliceous halos
        - Pyrite grains
        - Sparse quartz silt grains
    - Very massive internal structure
    - Random orientation of grains
    - Sharp planar top
    - Possibly multiple depositional events that deposited overlying coarse ‘lag’ deposit
        - Could also just be soft sediment deformation
    - Possible Z structure in lag (slump?)
- Above
    - No phosphate grains
    - Very similar composition to the lag but finer grained, roughly planar laminated
    - Grains more aligned horizontal to bedding
- Below
    - Abundant dolomite and quartz silt in clay and OM matrix

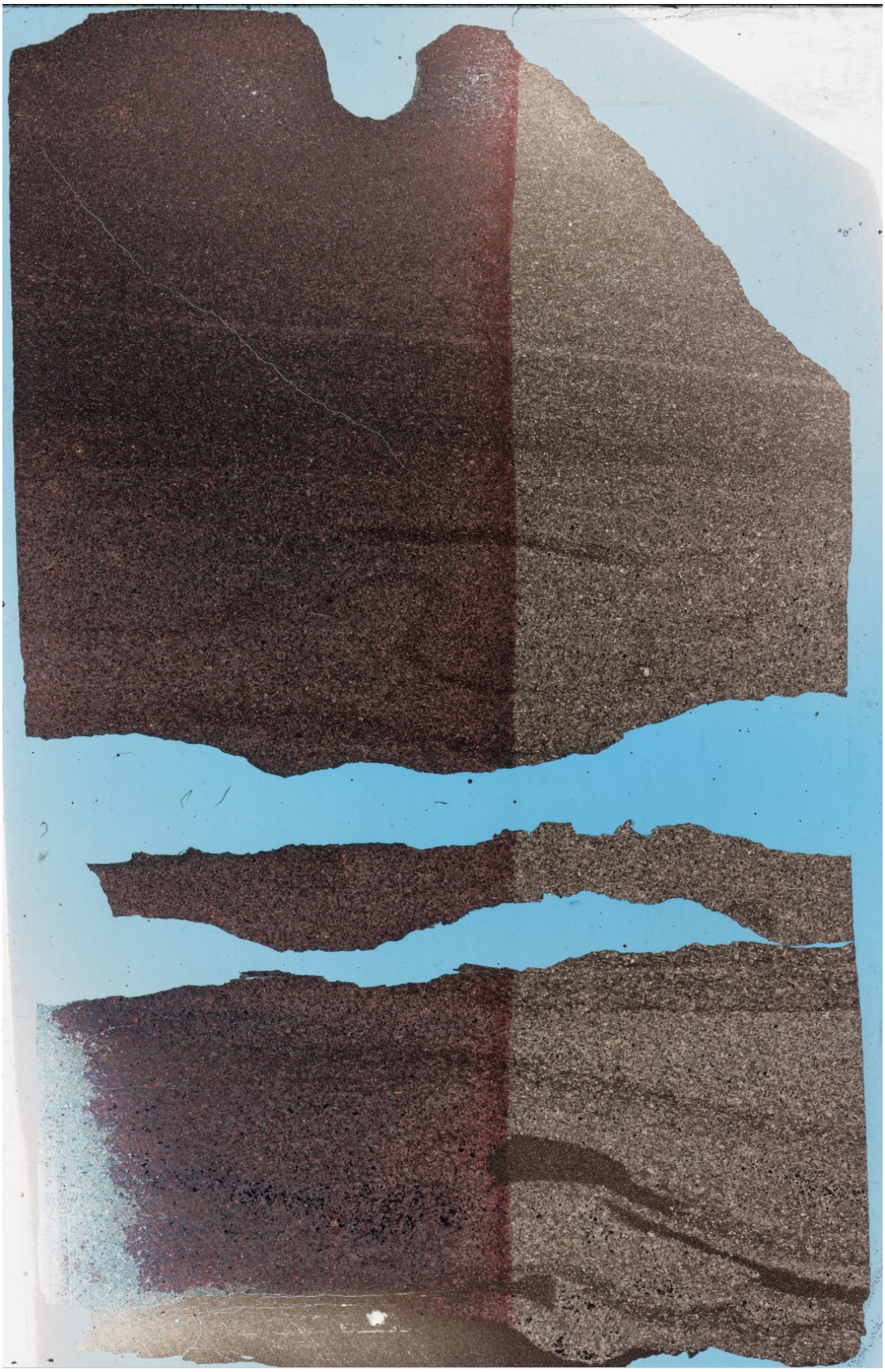

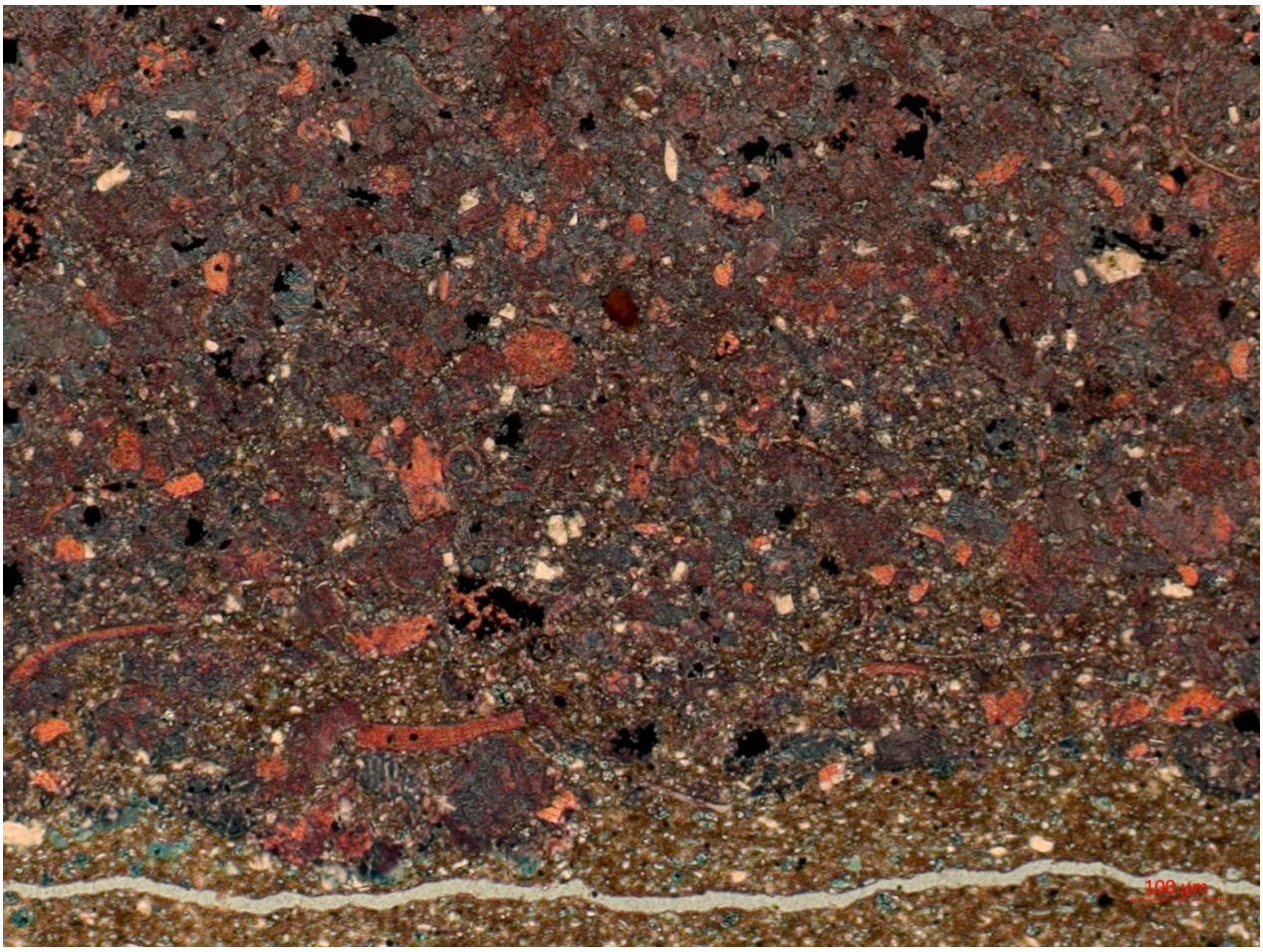

3349.08

- Surface:
  - Appears to be quite soft sediment deformed
    - Up to 5x11 mm thick ball structures into underlying mud
      - Up to 18 mm into underlying mud from present contact
      - Ball structures made up of more clay rich Ireton sediment
        - Also some styliolinid and ostracod/brachiopod shell fragments
      - Duvernay mud deformed around ball structures
  - May no longer actually have a definitive surface due to soft sed def
    - Actual surface likely just below main fossiliferous lag
- Lag:
  - Matrix to grain supported
  - Some pyritization of fossil fragments and some pyrite grains in lag
    - Grains possibly diagenetic/cement
  - Rough alignment bed horizontal of grains
  - Quite massive appearing
  - Some likely subvertical mud infilled bioturbation through lag but very hard to tell
  - Silt/Sand grains:

        - Very abundant styliolinid fragments
            - Typically very recrystallized
            - Some infilled by crystalline calcite
        - Likely also ostracod and brachiopod shell fragments
            - Typically very recrystallized
        - Rare possible cephalopod? Gastropod?? Fragments
        - Very rare conodont elements
        - Very rare small (~100um) phosphatic grains
- Above:
    - More clay rich Ireton
    - Quite massive
    - Appears to be quite bioturbated
        - Subvertical to subhorizontal mud infilled burrows throughout
        - <1mm
    - Styliolinids, ostracods/brachiopods continue into Ireton at least for extent of thin section
- Below:
    - More OM, Pyrite, siliceous rich Duvernay
    - Roughly planar laminated
        - Possibly the OM/pyrite rich and poor laminae
        - Very disturbed
            - Can see a bit of it closer to surface
    - Only very sparse and very small/broken up fossil fragments (likely small brachiopod/ostracod) in Duvernay other than in ball structures of Ireton
    - Appears to be quite bioturbated similar to overlying Ireton
        - At least where ball structures penetrate to
        - Abundant subvertical to subhorizontal <1mm thick mud infilled burrows

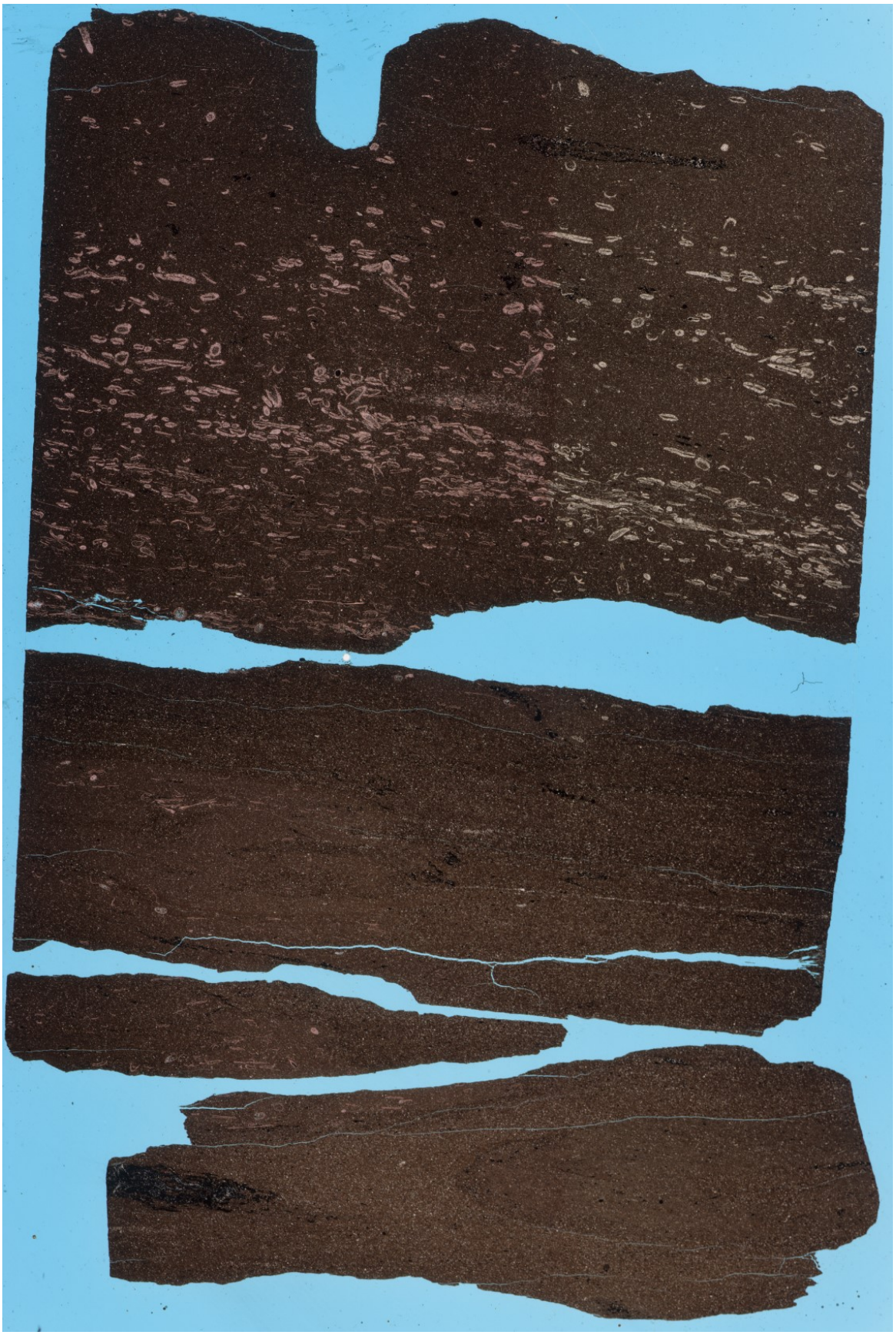

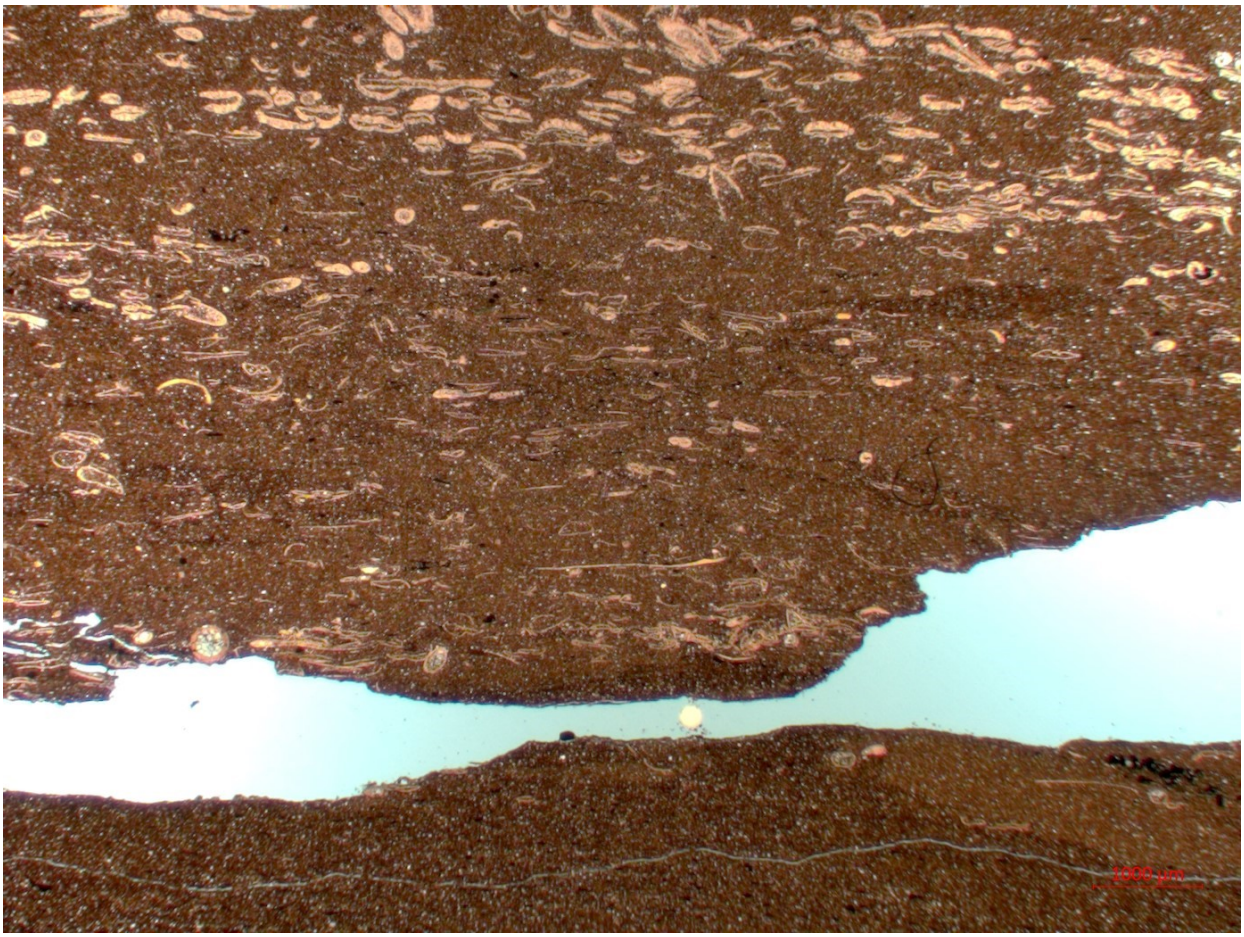

Core 7 – ATH HZ SAXON

3766.27

- Surface
  - Sharp, likely erosive surface
    - Cross cutting underlying mud laminae
    - Scour into underlying mud
  - Some possible large burrows into underlying mud
    - But only speculated from concentration of rhombohedral dolomite grains and pyrite
- Lag
  - Abundant rhombohedral dolomite grains
  - Mostly fine to medium sand components
  - Overlying lag ~3mm thick
  - Grains mostly composed of very recrystallized styliolinid fragments

    - Somewhat common (f-sand) possible glauconite grains
        - Typically quite round to subrounded
        - Most have pyritized? interiors
        - One is possible gastropod cast
    - Rare Phosphatic grains
        - one conodont element
        - couple phosphatic peloids
    - Very recrystallized by rhombohedral dolomite
    - Lag appears somewhat lenticular
        - Seems to pinch out to right
    - Possibly wavy base and top?
    - Quite massive
- Above
    - Very rhombohedral dolomite recrystallized
    - 15mm above main lag:
        - Very massive appearing
        - Glauconite grains continue to top of this section
        - More sparse more randomly oriented recrystallized styliolinid fragments
            - Slightly bed horizontal
        - Lots of pyrite and likely pyrite cement
    - To top of thin section:
        - No more glauconite or phosphatic grains
        - 2mm thick lag of more bed horizontal aligned styliolinid fragments
            - Possibly erosive or soft sed def (wavy base)
            - possibly sharp planar top
            - quite massive interior
        - Appears to be planar laminated with styliolinid fragments concentrated along laminae horizontal to bedding above lag
- Below
    - Very clay rich mud
        - Some rhombohedral dolomite

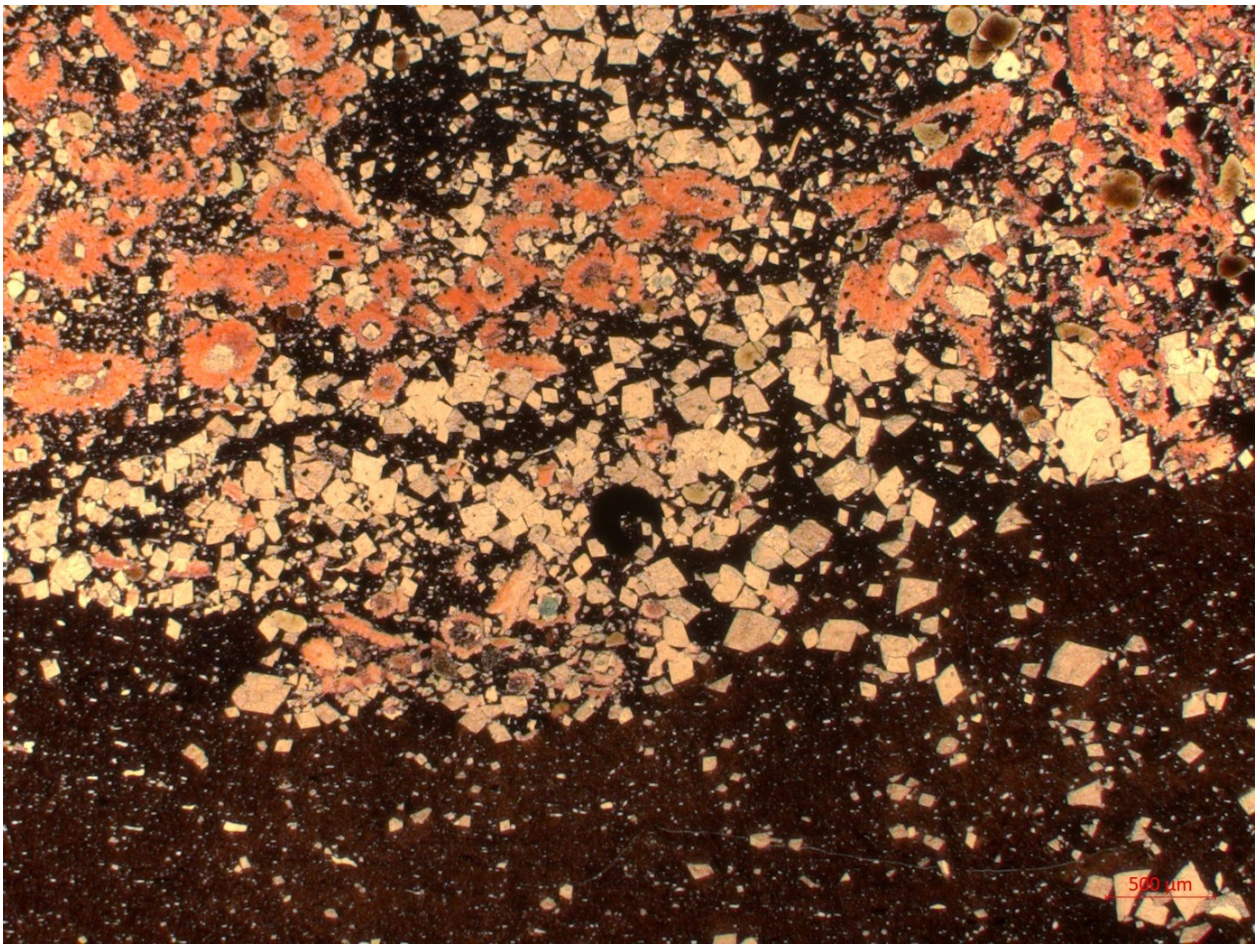

3717.55

- Surface:
  - No obvious erosive/scour or soft sed def or even very sharp surface below lag
  - Mud on mud contact
  - Does go from planar laminated below to massive mud in lag and above
  - Possibly sharp surface but very hard to tell
- Lag:
  - Matrix supported
    - Clay rich matrix
    - Rough planar fabric deformed around larger grains
  - Silt/sand grains
    - Common likely ostracods and brachiopod fragments
      - Possibly some styliolinid fragments
      - Commonly partially pyritized
    - A couple large possible stromatoporoid fragments
      - Up to ~1mm long
      - Pyritized (likely fully)

        - Common conodont jaw elements
        - Common phosphatic grains
            - Many small ones ~100 um
            - One very large one ~800 um
                - Quite concentric
                - Crystalline calcite growths within
                - Deformation of mud laminae around it
            - Appear to have at least somewhat concentric interiors
            - Commonly Partially pyritized
        - More sparse cephalopod shell fragments?
            - Possibly gastropods?
            - Have graptolite-like structure
        - One possible lingulid brachiopod shell fragment
            - ~50x800 um
            - Appears siliceous inside (possibly chitinous)
            - Has parallel banding within
        - One ~200 um quartz grain? (very hexagonal)
    - Rough planar horizontal structure to lag
- Underlain by discontinuous or possibly continuous pyrite laminated mud
    - Not clearly bioturbated
    - Quite mud rich
        - Lots of flattened clay aggregates
    - Not very different from overlying Ireton?
    - OM and pyrite appear to be more concentrated in laminae in the Duvernay
- Overlain by clay-rich ireton
    - Quite massive appearing
    - Lots of disseminated clay
    - More dolomite silt


200 µm

APPENDIX B: Additional Core Descriptions

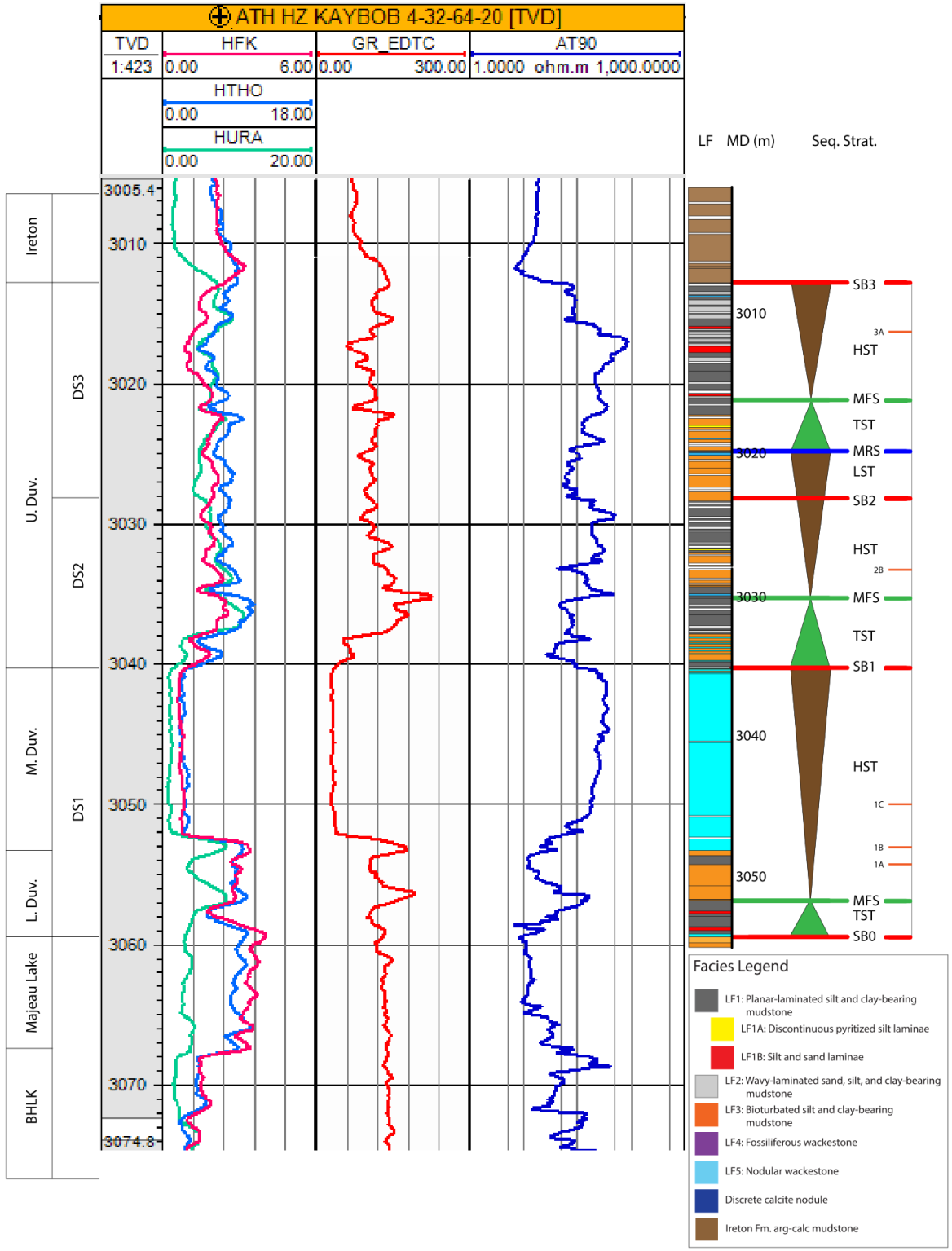

Spectral gamma, gamma, deep resistivity log, lithofacies interpretation, and sequence stratigraphic interpretation of core 2.

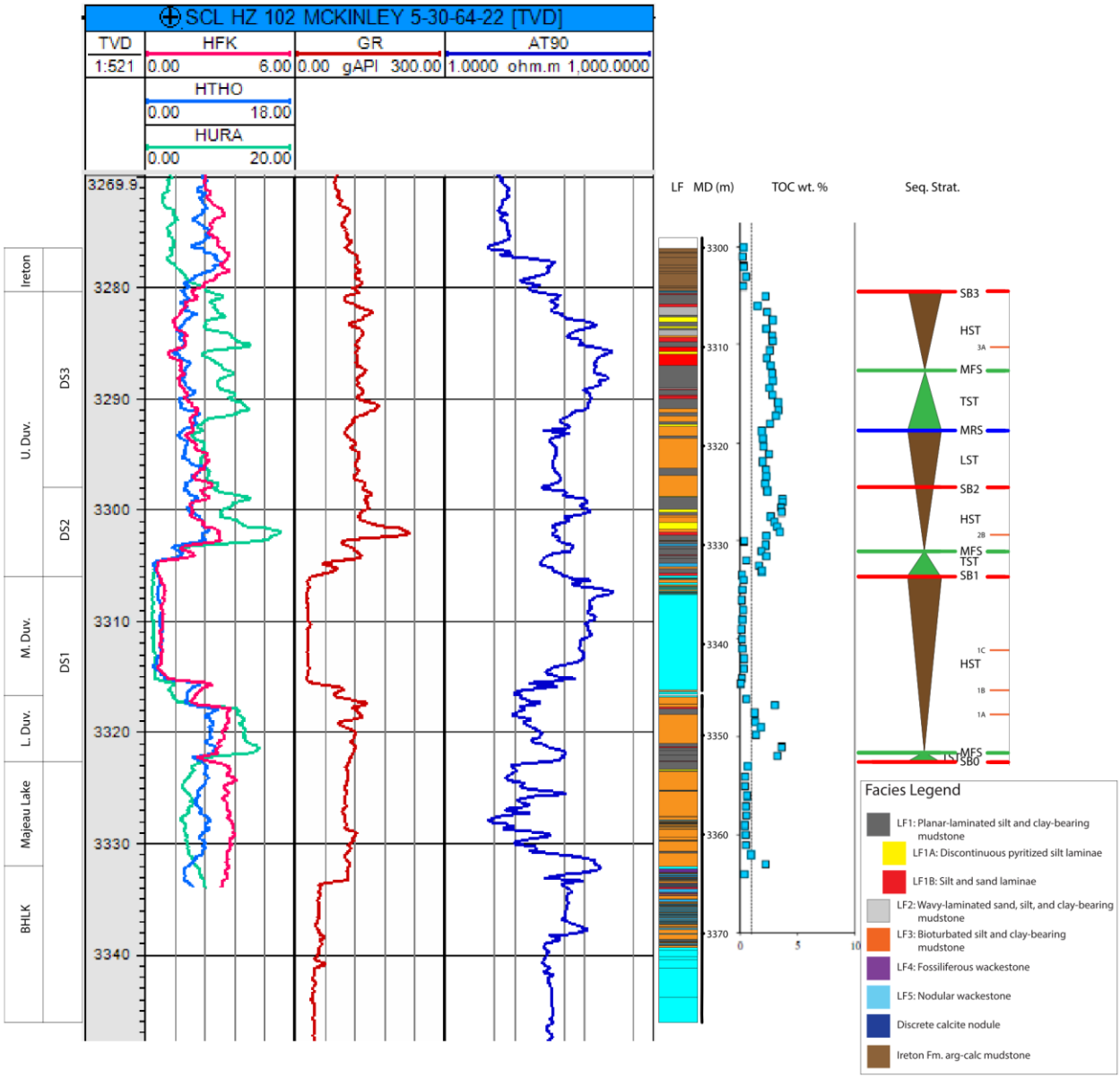

Spectral gamma, gamma, deep resistivity log, lithofacies interpretation, and sequence stratigraphic interpretation of core 3. TOC log by Weatherford Laboratories for Shell Canada Limited, accessed through the Alberta Energy Regulator.

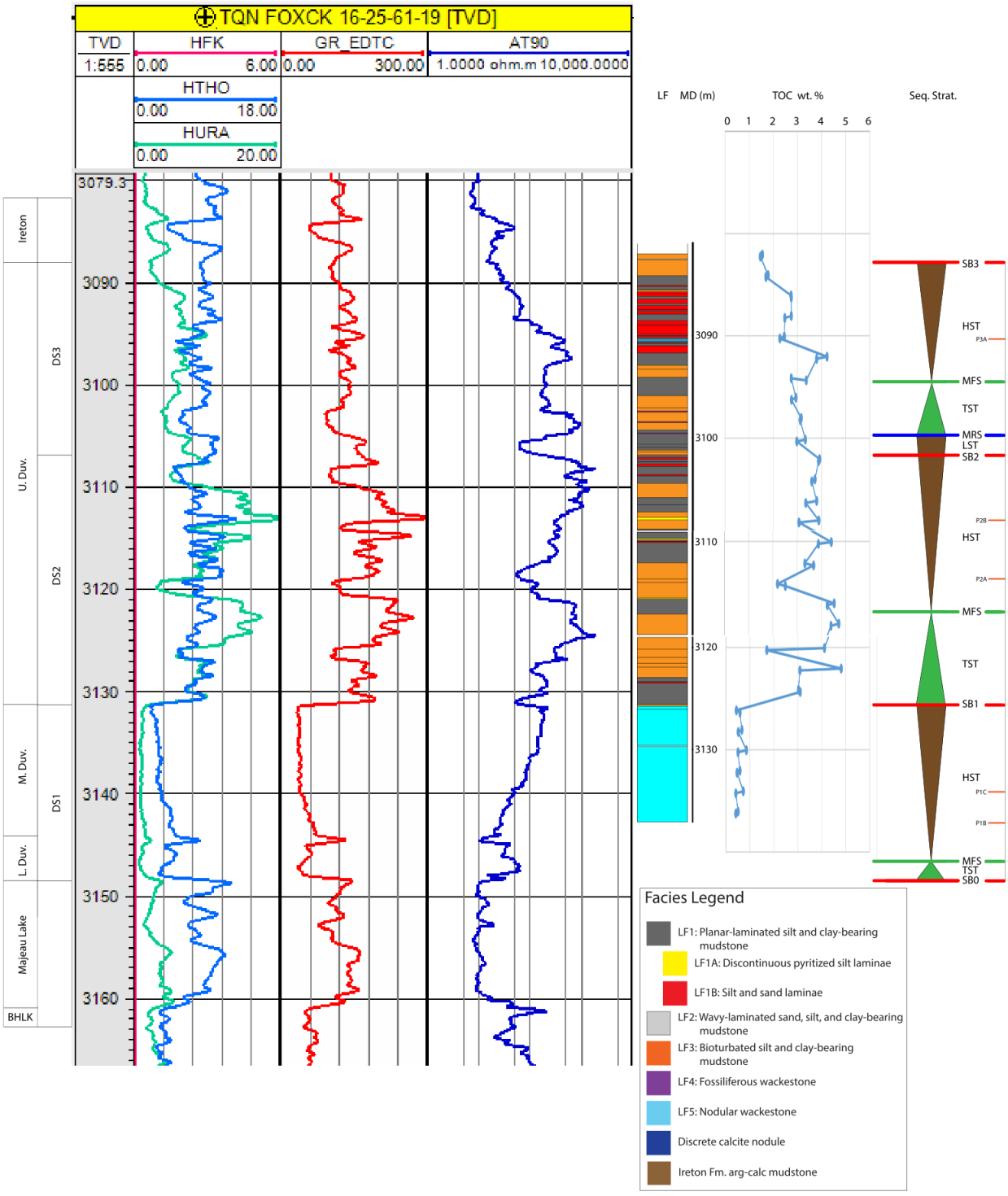

Spectral gamma, gamma, deep resistivity log, lithofacies interpretation, and sequence stratigraphic interpretation of core 5. TOC data by CBM Solutions for TAQA North Ltd., accessed through the Alberta Energy Regulator.

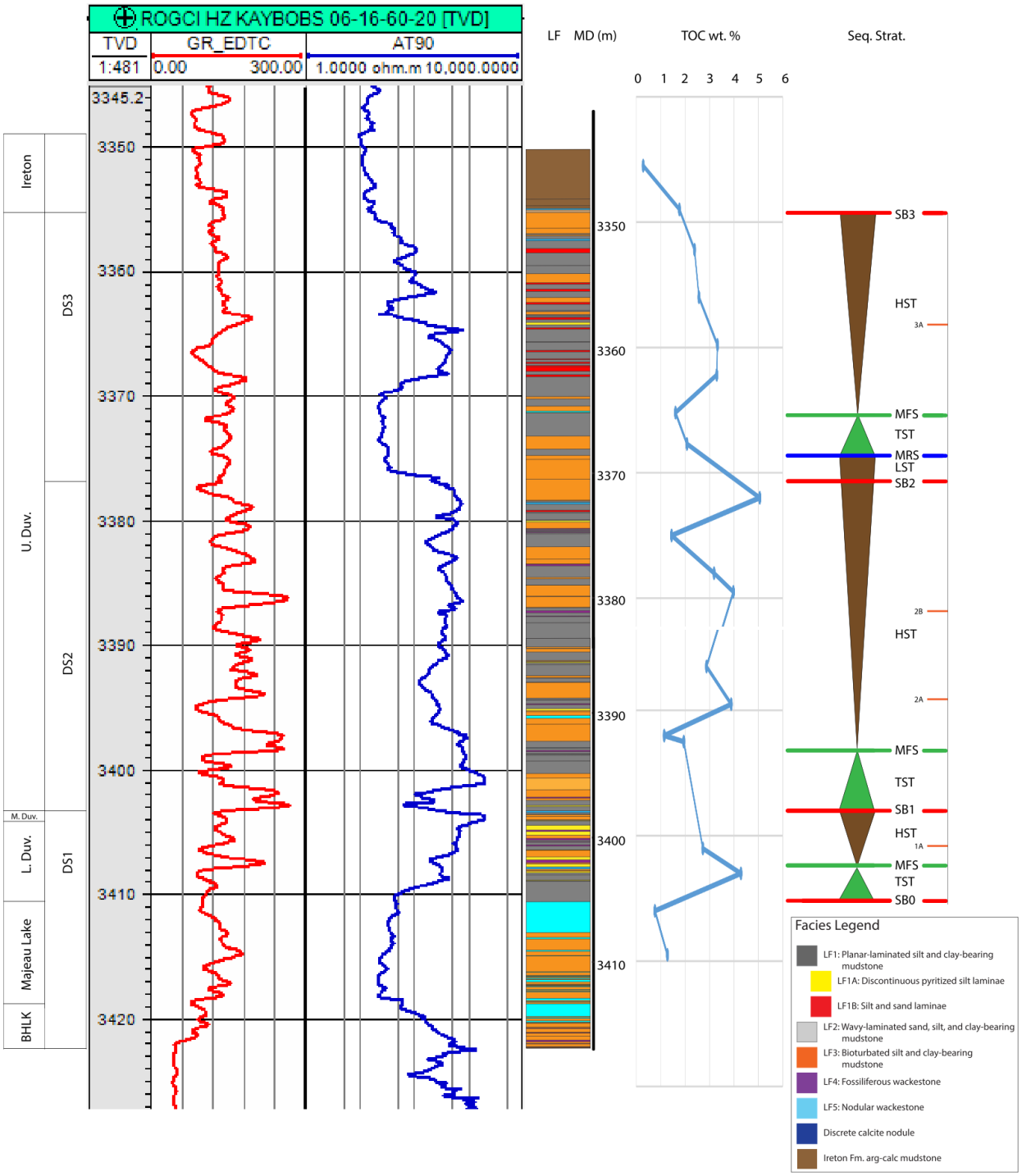

Gamma, deep resistivity log, lithofacies interpretation, and sequence stratigraphic interpretation of core 6. TOC data by Core Lab for Repsol Oil and Gas Canada LTD., accessed through the Alberta Energy Regulator.

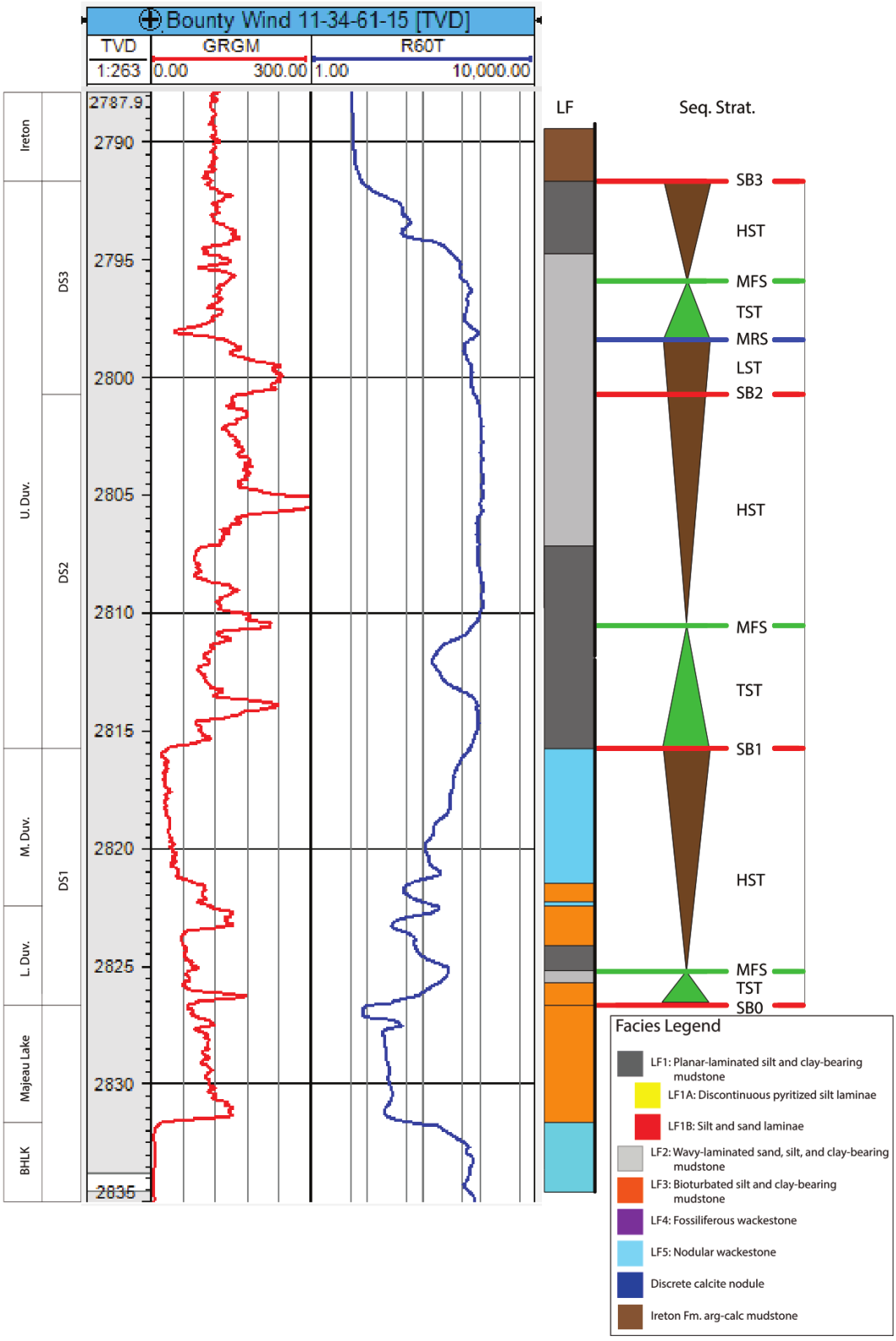

Gamma, deep resistivity log, lithofacies interpretation, and sequence stratigraphic interpretation of core 8.

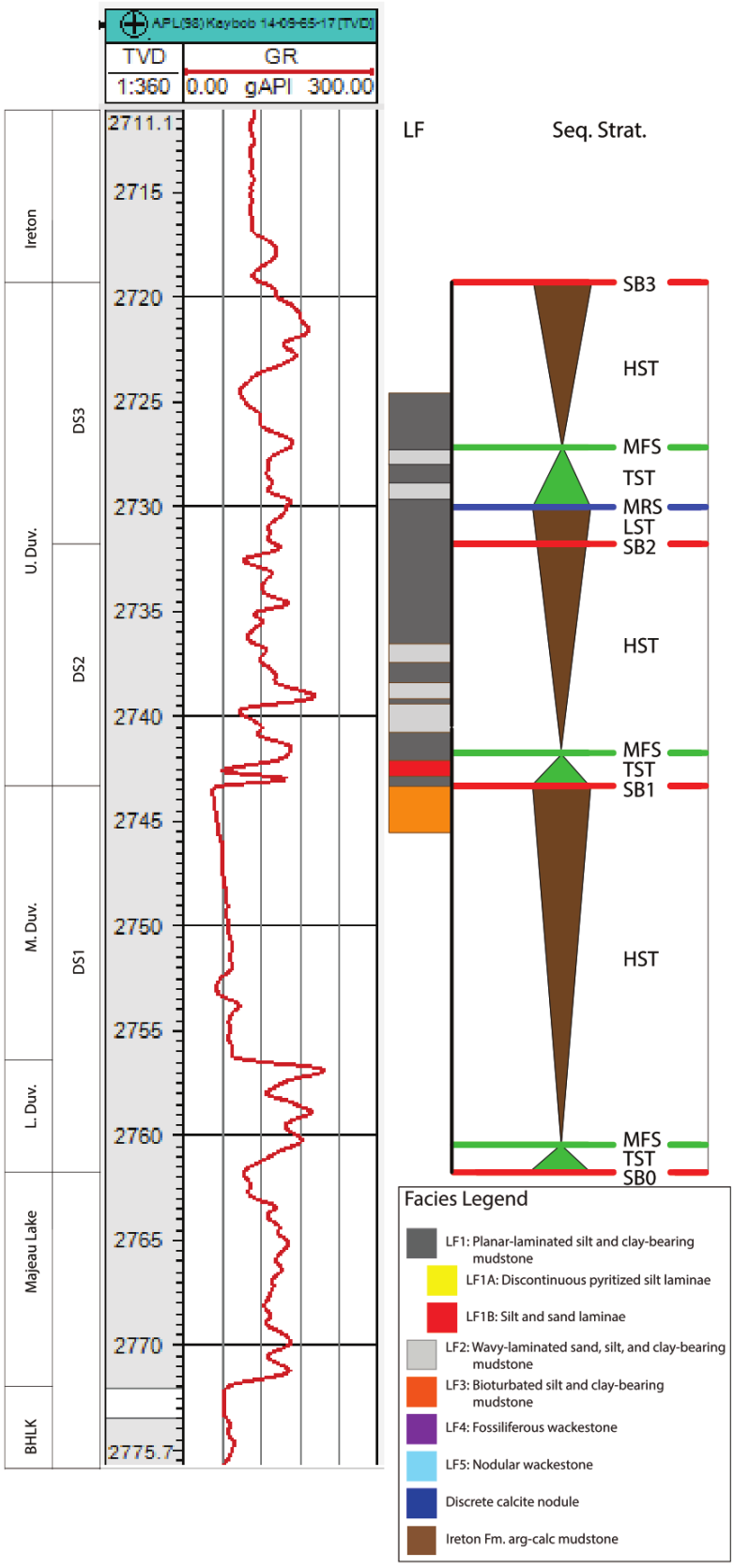

Gamma, lithofacies interpretation, and sequence stratigraphic interpretation of core 9.

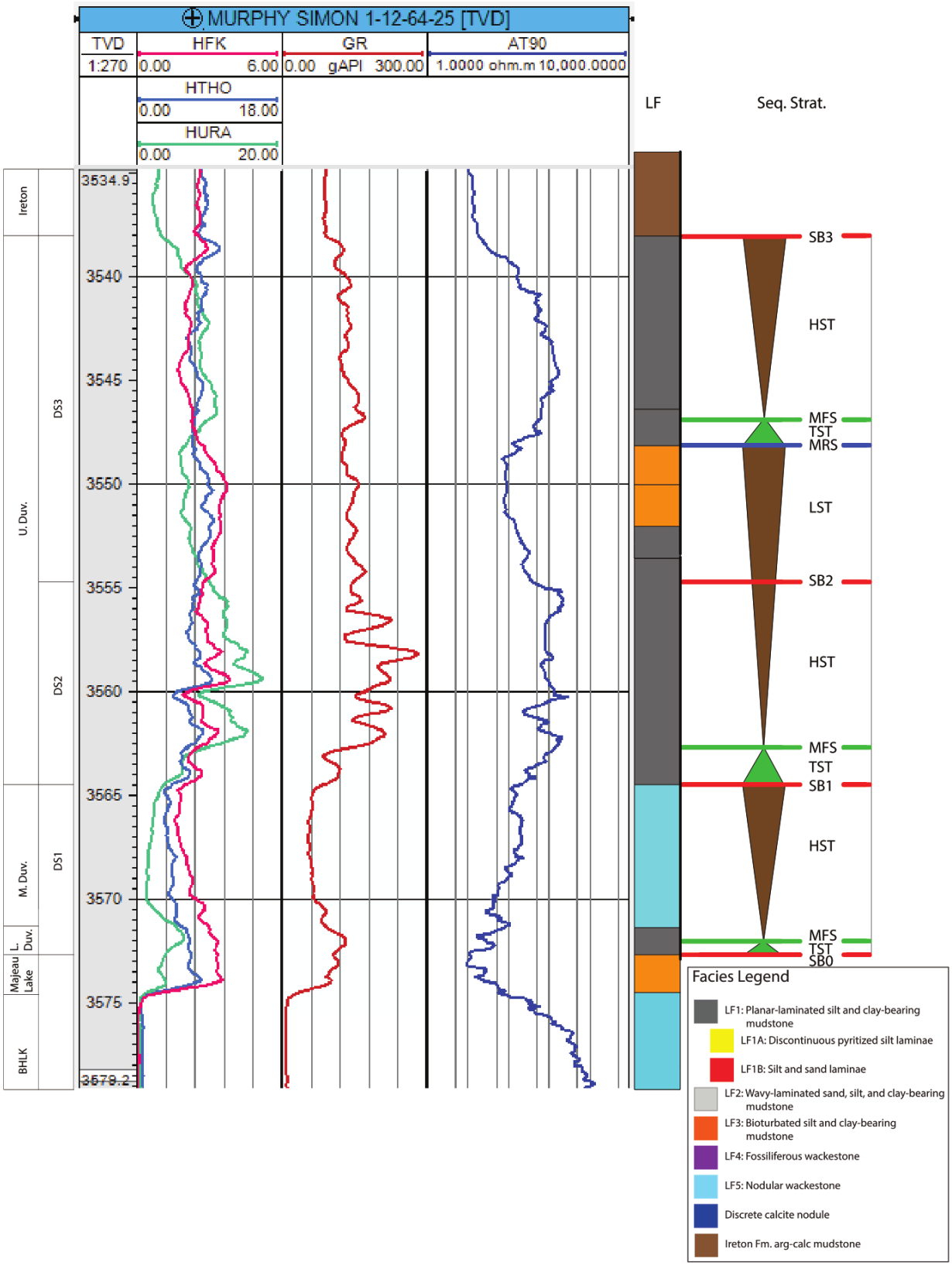

Spectral gamma, gamma, deep resistivity log, lithofacies interpretation, and sequence stratigraphic interpretation of core 10.

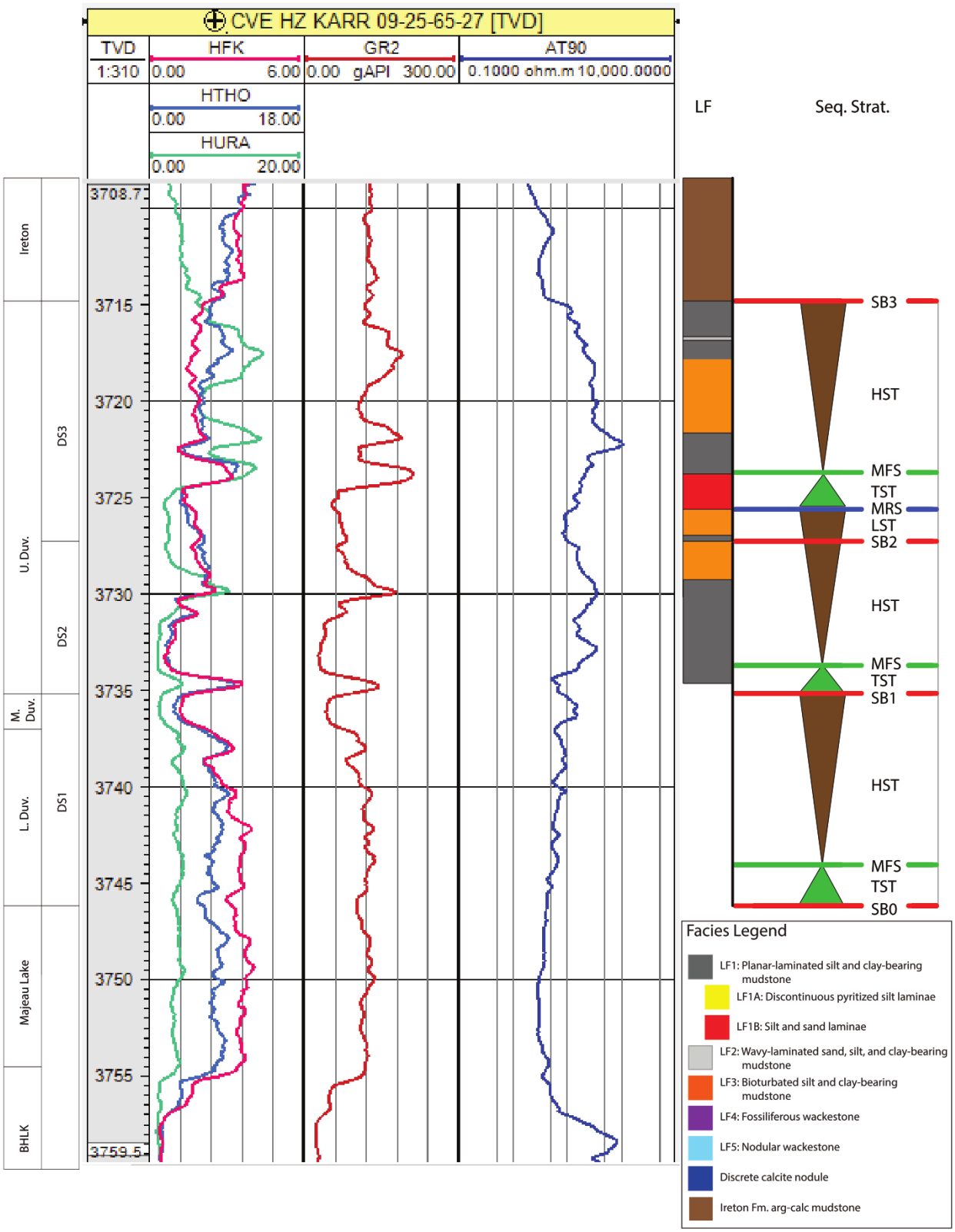

Spectral gamma, gamma, deep resistivity log, lithofacies interpretation, and sequence stratigraphic interpretation of core 11.

APPENDIX C: Organic Geochemical Data

Analysis by GeoMark Reseach LTD.

Source rock analyses: Leco TOC, Rock-Eval-2, and Maturity Testing

GeoMark

SOURCE ROCK ANALYSES

GeoMark Research, Ltd.

University of Alberta

102 McKinley 100/04-19-064-22W5/00,

Sample ID											Source Rock Analyses													
Project / Sample ID	Rock ID	Well Name	County	State	Formation Name	Upper Depth (m)	Lower Depth (m)	Median Depth (m)	Sample Type	Percent Carbonate (wt%)	Leco TOC (wt%)	Rock-Eval-2 S1 (mg HC/g)	Rock-Eval-2 S2 (mg HC/g)	Rock-Eval-2 S3 (mg CO2/g)	Rock-Eval-2 Tmax (°C)	Measured %Ro (Vitrinite Refl.)	Calculated %Ro (RE TMAX)	Hydrogen Index (S2x100/TOC)	Oxygen Index (S3x100/TOC)	S2/S3 Conc. (mg HC/mg CO2)	S1/TOC Norm. Oil Content	Production Index (S1/(S1+S2)	Experimental Notations
RALB-181101-001		102 McKinley 100/04-19-064-22W5/00					3,304.04	3,304.04	Core Chip	15.53	0.75	1.50	0.58	0.58	437		0.71	77	77	1	200	0.72	Low Temp S2 Shoulder
RALB-181101-002		102 McKinley 100/04-19-064-22W5/00					3,304.37	3,304.37	Core Chip	17.74	2.11	2.86	2.26	0.42	450		0.94	107	20	5	135	0.56	Low Temp S2 Shoulder
RALB-181101-003		102 McKinley 100/04-19-064-22W5/00					3,316.97	3,316.97	Core Chip	21.44	3.35	3.96	3.86	0.53	450		0.94	115	16	7	118	0.51	Low Temp S2 Shoulder
RALB-181101-004		102 McKinley 100/04-19-064-22W5/00					3,325.12	3,325.12	Core Chip	24.04	3.45	3.89	3.66	0.58	451		0.96	106	17	6	113	0.52	Low Temp S2 Shoulder
RALB-181101-005		102 McKinley 100/04-19-064-22W5/00					3,328.70	3,328.70	Core Chip	7.85	3.99	4.56	4.46	0.70	454		1.01	112	18	6	114	0.51	Low Temp S2 Shoulder
RALB-181101-006		102 McKinley 100/04-19-064-22W5/00					3,329.75	3,329.75	Core Chip	31.01	3.28	4.75	4.54	0.66	452		0.98	138	20	7	145	0.51	Low Temp S2 Shoulder
RALB-181101-007		102 McKinley 100/04-19-064-22W5/00					3,331.05	3,331.05	Core Chip	38.59	2.37	2.82	2.68	0.75	454		1.01	113	32	4	119	0.51	Low Temp S2 Shoulder
RALB-181101-008		102 McKinley 100/04-19-064-22W5/00					3,332.85	3,332.85	Core Chip	56.75	1.21	1.25	1.03	0.62	447		0.89	85	51	2	103	0.55	Low Temp S2 Shoulder
RALB-181101-009		102 McKinley 100/04-19-064-22W5/00					3,333.04	3,333.04	Core Chip	64.00	0.56	0.70	0.22	0.36	0		0.00	39	64	1	125	0.76	
RALB-181101-010		102 McKinley 100/04-19-064-22W5/00					3,346.35	3,346.35	Core Chip	22.68	3.13	4.83	3.33	0.51	452		0.98	106	16	7	129	0.55	Low Temp S2 Shoulder
RALB-181101-011		102 McKinley 100/04-19-064-22W5/00					3,346.87	3,346.87	Core Chip	31.75	1.96	2.49	2.12	0.57	450		0.94	108	29	4	127	0.54	Low Temp S2 Shoulder
RALB-181101-012		102 McKinley 100/04-19-064-22W5/00					3,347.26	3,347.26	Core Chip	30.60	1.51	2.25	1.76	0.60	449		0.92	117	40	3	149	0.56	Low Temp S2 Shoulder
RALB-181101-013		102 McKinley 100/04-19-064-22W5/00					3,347.26	3,347.26	Core Chip	33.55	1.74	2.56	1.96	0.66	450		0.94	113	38	3	147	0.57	Low Temp S2 Shoulder
RALB-181101-014		102 McKinley 100/04-19-064-22W5/00					3,352.64	3,352.64	Core Chip	25.92	2.09	2.39	1.94	0.63	449		0.92	93	30	3	114	0.55	Low Temp S2 Shoulder
RALB-181101-015		102 McKinley 100/04-19-064-22W5/00					3,353.85	3,353.85	Core Chip	27.68	0.86	1.03	0.61	0.48	441		0.78	71	56	1	120	0.63	Low Temp S2 Shoulder
RALB-181101-016		102 McKinley 100/04-19-064-22W5/00					3,353.92	3,353.92	Core Chip	29.22	0.79	1.04	0.67	0.43	442		0.80	85	54	2	132	0.61	Low Temp S2 Shoulder
RALB-181101-017		102 McKinley 100/04-19-064-22W5/00					3,358.17	3,358.17	Core Chip	16.48	0.89	0.92	0.54	0.42	450		0.94	60	47	1	103	0.63	
RALB-181101-018		102 McKinley 100/04-19-064-22W5/00					3,363.78	3,363.78	Core Chip	86.55	0.18	0.19	0.10	0.16	0		0.00	55	87	1	104	0.66	
RALB-181101-019		102 McKinley 100/04-19-064-22W5/00					3,365.30	3,365.30	Core Chip	87.27	0.58	0.56	0.45	0.30	450		0.94	77	52	2	96	0.55	
RALB-181101-020		102 McKinley 100/04-19-064-22W5/00					3,365.89	3,365.89	Core Chip	94.16	0.18	0.18	0.04	0.16	0		0.00	22	89	0	100	0.82	
RALB-181101-021		102 McKinley 100/04-19-064-22W5/00					3,366.15	3,366.15	Core Chip	78.54	1.06	1.20	0.78	0.42	448		0.90	74	40	2	113	0.61	

University of Alberta | 102 McKinley 100/04-19-064-22W5/00,

Total Organic Carbon

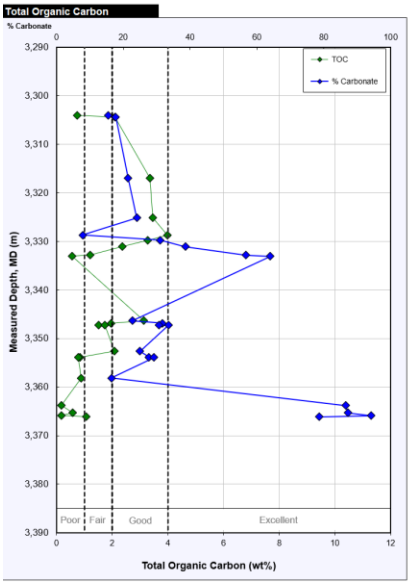

Oil Potential, S2

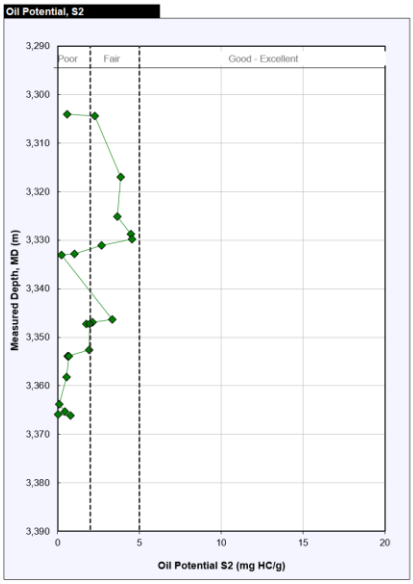

Hydrogen Index, S2/TOC

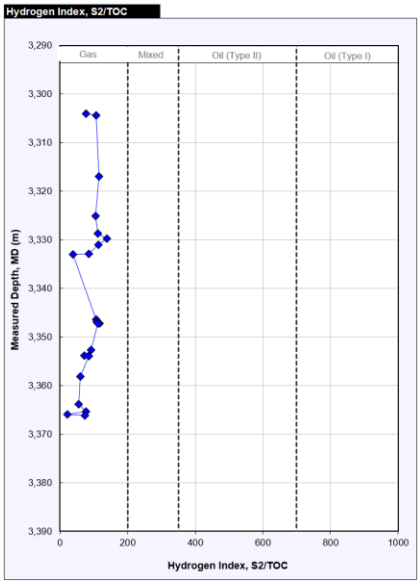

GeoMark
SOURCE ROCK ANALYSES
GeoMark Research, Ltd.

University of Alberta | 102 McKinley 100/04-19-064-22W5/00,

Norm. Oil Content, S1/TOC

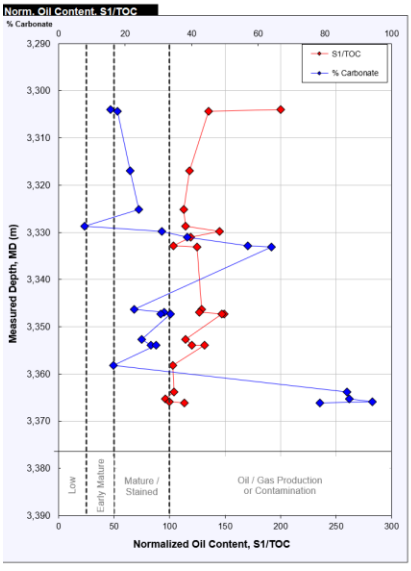

Production Index, S1/(S1+S2)

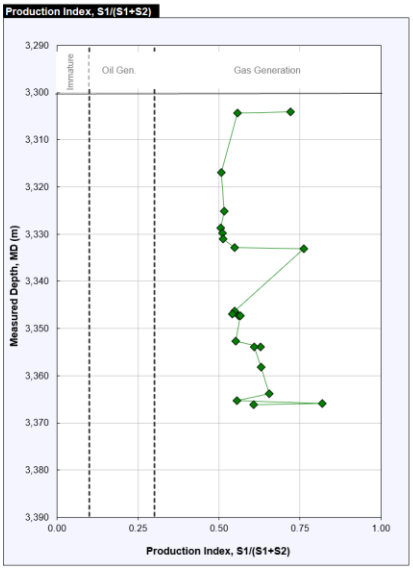

Maturity Indicators

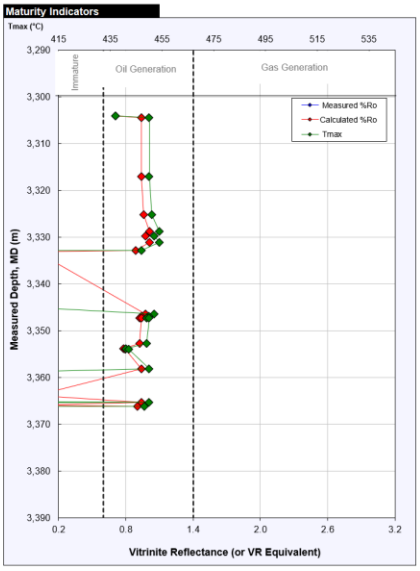

University of Alberta | 102 McKinley 100/04-19-064-22W5/00,

Pseudo Van Krevelen Plot

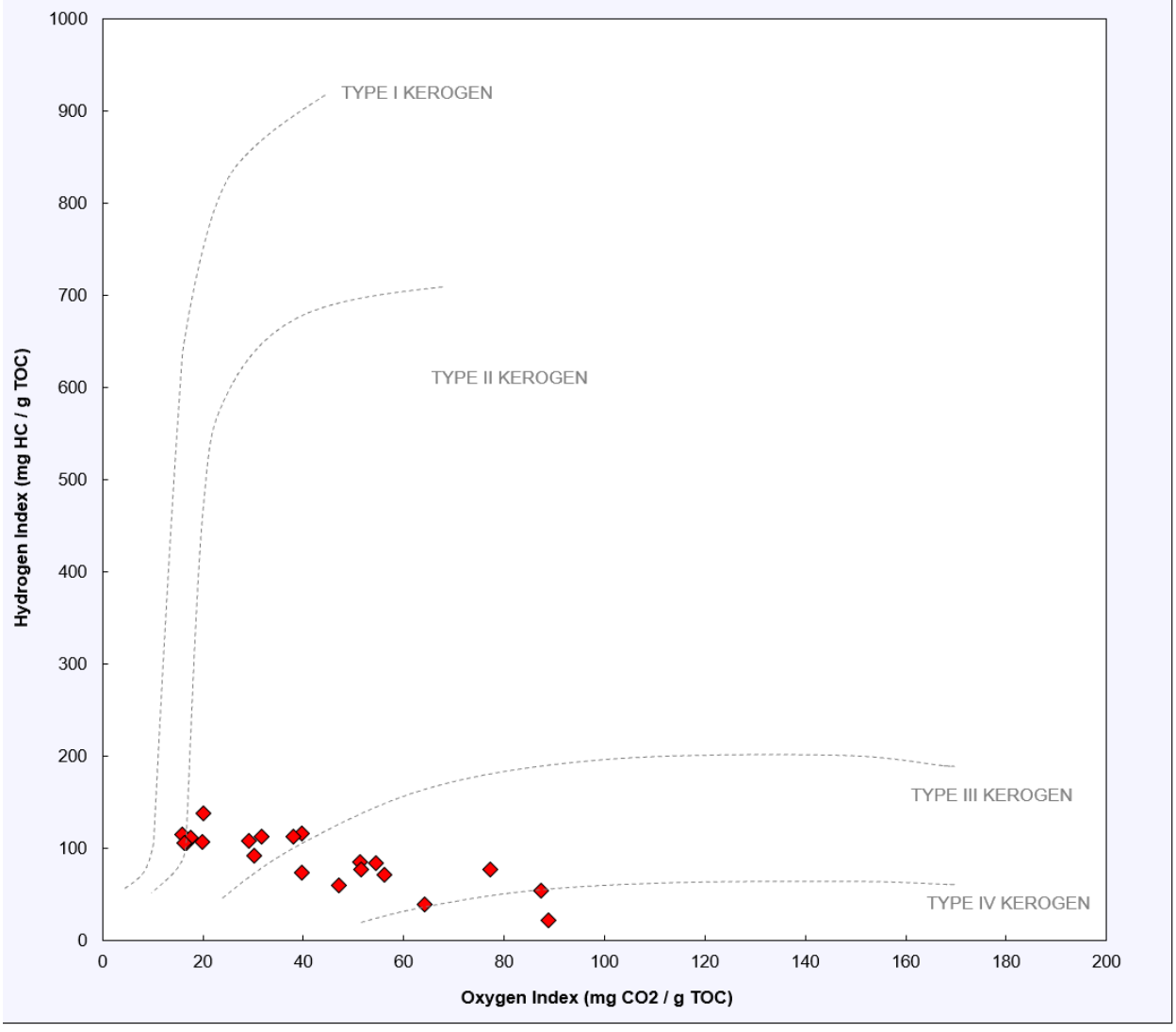

University of Alberta | 102 McKinley 100/04-19-064-22W5/00,

Kerogen Quality Plot

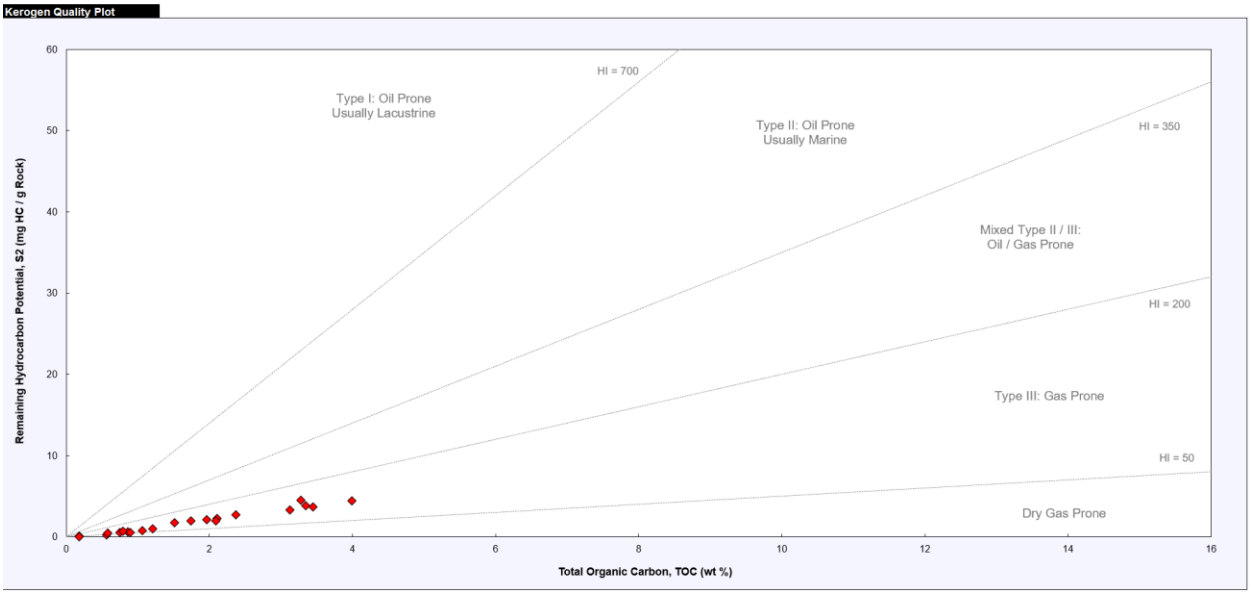

University of Alberta | 102 McKinley 100/04-19-064-22W5/00,

Kerogen Type and Maturity

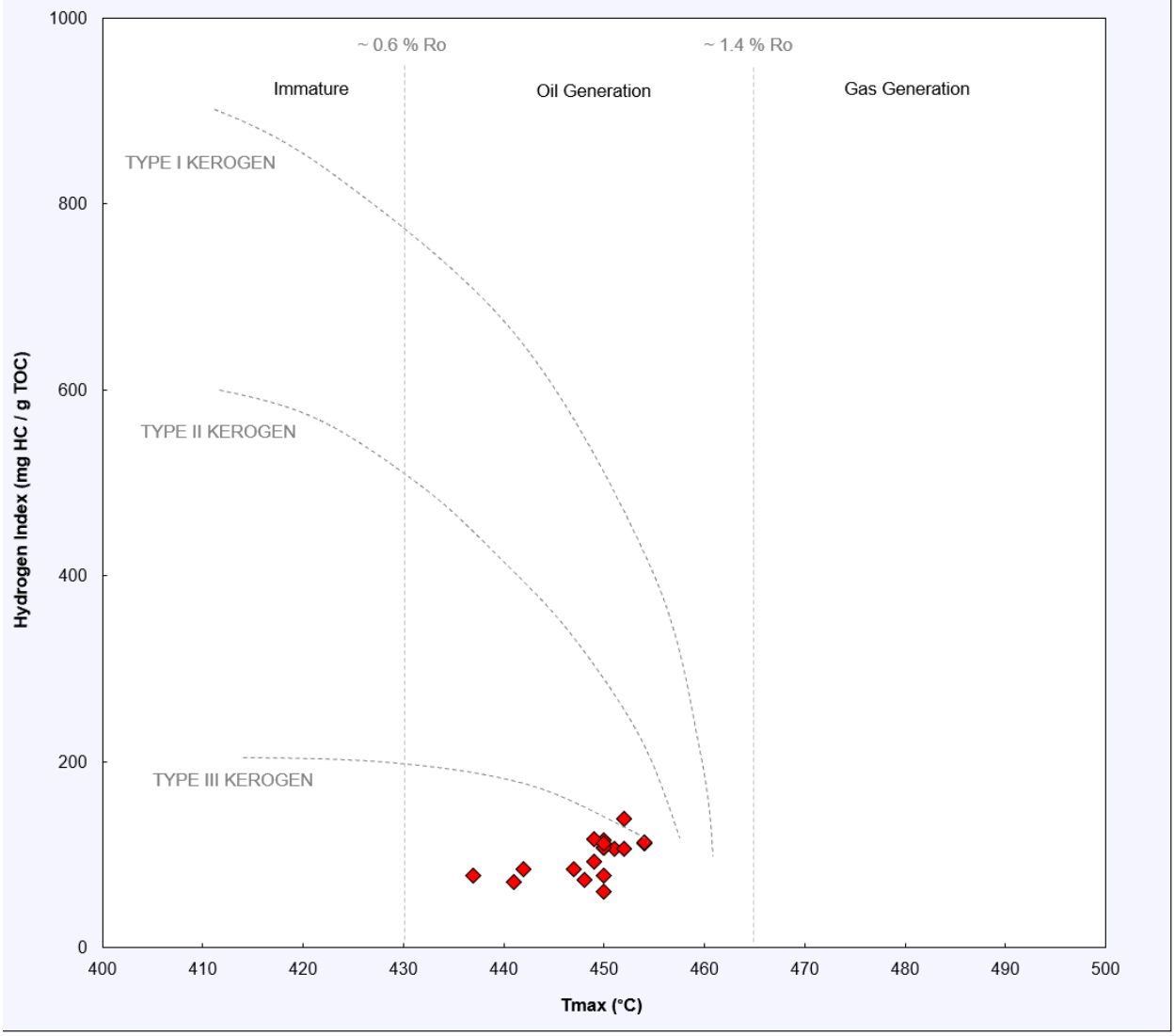

University of Alberta | 102 McKinley 100/04-19-064-22W5/00,

Kerogen Quality Plot

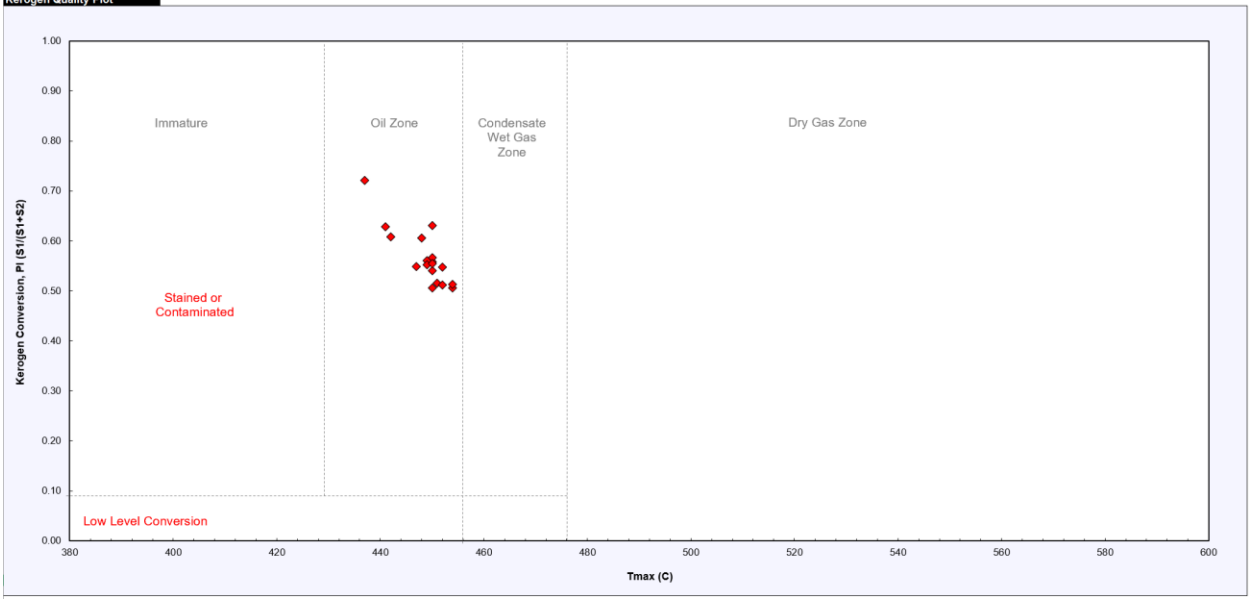

APPENDIX D: Inorganic Geochemical Data

Analysis by Bureau Veritas

XRF Whole Rock & ICP-MS Trace Elements

Bureau Veritas Commodities Canada Ltd. Final Report

Client: University of Alberta
File Created: 18-Feb-19
Job Number: VAN18003066
Number of: 47
Project: None Given
Shipment ID:
P.O. Number:
Received: 01-Nov-18

Method		WGHT	XF700	XF700	XF700	XF700	XF700	XF700	XF700	XF700	XF700	XF700	XF700	XF700	XF700	XF700	XF700	TC000	TC000
Analyte		Wgt	SiO2	Al2O3	Fe2O3	CaO	MgO	Na2O	K2O	MnO	TiO2	P2O5	Cr2O3	Ba	LOI	SO3	Sr	TOT/C	TOT/S
Unit		KG	%	%	%	%	%	%	%	%	%	%	%	%	%	%	%	%	%
MDL		0.01	0.01	0.01	0.01	0.01	0.01	0.01	0.01	0.01	0.01	0.01	0.01	0.01	-5.11	0.002	0.002	0.02	0.02
Sample	Type																		
102 McKinl	Drill Core	<0.01	31.9	9.49	7.95	21.1	2.51	0.21	3.03	0.08	0.35	0.63	0.01	0.06	17.85	8.09	0.038	5.86	3.61
102 McKinl	Drill Core	<0.01	42.3	11.8	4.43	17	2.06	0.29	3.74	0.05	0.47	0.08	0.02	0.03	17.07	2.15	0.021	4.78	0.97
102 McKinl	Drill Core	<0.01	41.6	11.6	4.85	16.8	2.05	0.29	3.63	0.05	0.45	0.29	0.01	0.03	16.36	3.21	0.027	4.81	1.5
102 McKinl	Drill Core	<0.01	48.3	10.4	9	10.1	1.84	0.37	3.14	0.05	0.43	0.15	0.01	0.03	13.05	>10.000	0.024	4.74	5.18
102 McKinl	Drill Core	<0.01	I.S.	I.S.	I.S.	I.S.	I.S.	I.S.	I.S.	I.S.	I.S.	I.S.	I.S.	I.S.	I.S.	I.S.	I.S.	5.9	2.18
102 McKinl	Drill Core	<0.01	39.7	10.8	5.4	17.5	2.07	0.35	3.23	0.04	0.43	0.17	0.01	0.03	18.43	5.46	0.034	5.72	2.46
102 McKinl	Drill Core	<0.01	45.2	10.5	7.81	11.8	1.98	0.39	3.32	0.03	0.4	0.52	0.01	0.03	15.33	9.78	0.03	5.41	4.39
102 McKinl	Drill Core	<0.01	41.6	8.43	5.81	17.7	1.87	0.36	2.53	0.03	0.34	0.63	0.01	0.02	18.95	7.51	0.035	6.09	3.31
102 McKinl	Drill Core	<0.01	25.6	6.2	2.53	32.3	1.59	0.38	1.71	0.05	0.26	0.07	<0.01	0.02	27.19	1.87	0.037	8.53	0.86
102 McKinl	Drill Core	<0.01	27.5	5.59	5.21	29	1.54	0.36	1.55	0.04	0.22	0.17	<0.01	0.02	24.28	6.94	0.044	8.67	3.13
102 McKinl	Drill Core	<0.01	46.5	7.11	2.88	18.4	1.3	0.4	2.05	0.03	0.35	0.13	0.01	0.04	19.25	2.61	0.024	7.31	1.24
102 McKinl	Drill Core	<0.01	45.6	7.18	4.09	17.4	1.41	0.47	2.12	0.04	0.36	0.17	0.01	0.02	17.96	3.49	0.02	7.51	1.66
102 McKinl	Drill Core	<0.01	59.4	10.9	7.94	2.53	1.68	0.58	3.42	0.02	0.53	0.38	0.01	0.04	10.86	>10.000	0.011	4.91	4.95
102 McKinl	Drill Core	<0.01	48.6	7.39	9.7	10.7	1.33	0.42	2.2	0.03	0.35	0.13	0.01	0.04	14.67	>10.000	0.018	6.53	6.73
102 McKinl	Drill Core	<0.01	I.S.	I.S.	I.S.	I.S.	I.S.	I.S.	I.S.	I.S.	I.S.	I.S.	I.S.	I.S.	I.S.	I.S.	I.S.	6.42	2.53
102 McKinl	Drill Core	<0.01	53.8	13.2	6.03	6.67	2.49	0.46	3.73	0.04	0.59	0.33	0.02	0.04	11.32	4.22	0.014	4.01	2.1
102 McKinl	Drill Core	<0.01	47.9	14.7	6.11	10.2	2.27	0.49	4.04	0.05	0.55	0.48	0.02	0.05	11.94	4.42	0.024	2.99	1.99
102 McKinl	Drill Core	<0.01	14.8	3.5	4.09	36.4	3.79	0.11	1.11	0.08	0.18	0.08	<0.01	<0.01	33.37	2.51	0.047	10.75	1.17
102 McKinl	Drill Core	<0.01	8.03	2.19	2.23	46.1	1.2	0.11	0.66	0.09	0.1	0.09	<0.01	0.02	36.96	2.64	0.041	11.19	1.24
102 McKinl	Drill Core	<0.01	9.06	2.09	1.47	46.9	0.82	0.08	0.63	0.08	0.08	0.05	<0.01	0.02	37.64	1.21	0.036	11.4	0.57
102 McKinl	Drill Core	<0.01	2.35	0.55	1.19	52.8	0.75	<0.01	0.16	0.09	0.03	0.08	<0.01	0.02	41.36	0.361	0.029	12.13	0.16
Gordondal	Drill Core	<0.01	53.1	19.3	7.57	1.28	1.91	0.82	3.11	0.03	0.76	0.11	0.02	0.09	11	>10.000	0.014	2.27	4.85
Gordondal	Drill Core	<0.01	67.8	4.11	3.07	5.27	1.17	0.26	0.66	0.03	0.21	0.25	<0.01	0.05	15.22	4.16	0.011	I.S.	I.S.
Gordondal	Drill Core	<0.01	17.9	4.39	1.91	38.9	0.69	0.31	0.61	0.07	0.17	0.96	<0.01	0.06	IS	2.24	0.038	10.64	0.95
Gordondal	Drill Core	<0.01	65.1	4.21	2.46	8.78	0.88	0.22	0.65	0.03	0.18	0.5	0.01	0.08	15.39	2.83	0.023	8.44	1.27
Gordondal	Drill Core	<0.01	69.9	4.8	3.83	4.96	1.06	0.35	0.87	0.03	0.22	0.55	0.01	0.07	IS	3.72	0.014	7.43	1.72
Gordondal	Drill Core	<0.01	22.6	6.58	1	35	1	1	0.47	0.06	0.1	0.05	<0.01	0.05	30.36	1.4	0.034	9.59	0.58
Gordondal	Drill Core	<0.01	52.3	7.14	5.02	7.3	1.31	0.49	1.67	0.03	0.35	0.4	0.01	0.13	21.5	7.08	0.017	12.73	3.58
Gordondal	Drill Core	<0.01	36	6.66	3.79	19.6	2.38	0.55	1.53	0.03	0.34	0.6	0.01	0.18	25	5.61	0.068	11.23	2.63
Gordondal	Drill Core	<0.01	31.3	4.3	3.38	25.8	1.14	0.55	0.93	0.03	0.22	0.14	0.01	0.13	IS	4.73	0.139	13.12	2.21
Gordondal	Drill Core	<0.01	15.5	3.1	2.32	37.5	0.92	0.27	0.68	0.02	0.16	0.33	<0.01	0.1	34.81	3.4	0.179	15.04	1.6
Gordondal	Drill Core	<0.01	20.8	4.44	3.22	31.5	1.21	0.26	1.02	0.02	0.21	0.36	<0.01	0.11	IS	4.71	0.197	14.6	2.14
Gordondal	Drill Core	<0.01	14.8	2.56	1.87	40	0.86	0.37	0.49	0.02	0.12	0.2	<0.01	0.09	34.77	2.86	0.15	13	1.24
Gordondal	Drill Core	<0.01	33	5.98	4.01	19.8	1.23	0.45	1.36	0.02	0.27	0.82	<0.01	0.09	28.56	7.17	0.112	16.68	3.47
Gordondal	Drill Core	<0.01	27.3	3.68	2.38	26.6	0.79	0.35	0.74	0.02	0.18	0.43	<0.01	0.05	31.96	5.51	0.154	18.43	2.56
Gordondal	Drill Core	<0.01	14.5	1.32	1.27	42.8	0.71	0.16	0.22	0.02	0.05	2.33	0.01	0.06	34.05	1.59	0.066	11.8	0.69
Gordondal	Drill Core	<0.01	I.S.	I.S.	I.S.	I.S.	I.S.	I.S.	I.S.	I.S.	I.S.	I.S.	I.S.	I.S.	I.S.	I.S.	I.S.	I.S.	I.S.
Gordondal	Drill Core	<0.01	17.2	2.31	1.17	42.2	0.5	1.11	0.07	0.02	0.05	0.2	<0.01	<0.01	34.01	1.14	0.048	10.53	0.52
Gordondal	Drill Core	<0.01	25.7	4.41	2.88	22.8	2.52	0.34	0.82	0.02	0.2	3.48	0.01	0.05	IS	6.41	0.056	18.9	2.96
Gordondal	Drill Core	<0.01	26.9	5.18	4.19	21.2	3.93	0.6	0.87	0.04	0.21	2.09	0.01	0.11	IS	5	0.041	I.S.	I.S.
Gordondal	Drill Core	<0.01	6.83	1.21	0.61	48.7	1.16	0.49	0.07	0.03	0.04	0.11	<0.01	<0.01	40.02	0.6	0.029	12.07	0.26
Gordondal	Drill Core	<0.01	6.36	1.04	1.31	48.9	0.91	0.21	0.17	0.04	0.06	0.13	<0.01	0.05	IS	0.858	0.064	12.22	0.35
Gordondal	Drill Core	<0.01	21.4	2.98	1.97	33.9	1.33	0.34	0.74	0.03	0.17	2.92	0.01	0.08	29.5	3.22	0.119	13.07	1.52
Gordondal	Drill Core	<0.01	14.1	2.8	1.92	36.4	0.93	0.23	0.69	0.02	0.17	0.47	<0.01	0.4	36.27	3.63	0.124	16.65	1.75
Gordondal	Drill Core	<0.01	29.9	3.82	2.58	22.3	0.98	0.3	1	0.02	0.2	0.25	0.03	0.02	IS	5.76	0.124	19.11	2.75
Gordondal	Drill Core	<0.01	42.1	12.1	4.58	4.5	2.26	0.6	3.22	0.03	0.52	0.25	0.04	0.03	27.57	8.68	0.015	18	3.98
Gordondal	Drill Core	<0.01	29	8.52	4.29	11.1	1.94	0.3	2.67	0.02	0.43	0.32	0.07	0.1	IS	9.62	0.034	24.05	4.38
Pulp Duplicates																			
102 McKinl	Drill Core	<0.01	I.S.	I.S.	I.S.	I.S.	I.S.	I.S.	I.S.	I.S.	I.S.	I.S.	I.S.	I.S.	I.S.	I.S.	I.S.	6.42	2.53
102 McKinl	REP																	6.25	2.49
Gordondal	Drill Core	<0.01	14.8	2.56	1.87	40	0.86	0.37	0.49	0.02	0.12	0.2	<0.01	0.09	34.77	2.86	0.15	13	1.24
Gordondal	REP																		
Gordondal	Drill Core	<0.01	6.36	1.04	1.31	48.9	0.91	0.21	0.17	0.04	0.06	0.13	<0.01	0.05	IS	0.858	0.064	12.22	0.35
Gordondal	REP																	12.22	0.36
102 McKinl	Drill Core	<0.01	41.6	11.6	4.85	16.8	2.05	0.29	3.63	0.05	0.45	0.29	0.01	0.03	16.36	3.21	0.027	4.81	1.5
102 McKinl	REP																		
102 McKinl	Drill Core	<0.01	39.7	10.8	5.4	17.5	2.07	0.35	3.23	0.04	0.43	0.17	0.01	0.03	18.43	5.46	0.034	5.72	2.46
102 McKinl	REP		39.6	10.8	5.38	17.5	2.05	0.34	3.21	0.04	0.43	0.17	0.01	0.03	18.43	5.47	0.032		
Gordondal	Drill Core	<0.01	33	5.98	4.01	19.8	1.23	0.45	1.36	0.02	0.27	0.82	<0.01	0.09	28.56	7.17	0.112	16.68	3.47
Gordondal	REP																		
102 McKinl	Drill Core	<0.01	I.S.	I.S.	I.S.	I.S.	I.S.	I.S.	I.S.	I.S.	I.S.	I.S.	I.S.	I.S.	I.S.	I.S.	I.S.	5.9	2.18
102 McKinl	REP																		
Reference Materials																			
STD GS311-	STD																	1.02	2.52
STD GS910-	STD																	2.71	8.2
STD SO-19	STD																		
STD SO-19	STD																		
STD GS311-	STD																	1.01	2.37
STD GS910-	STD																	2.67	7.99
STD SO-19	STD																		
STD OREAS	STD		42.1	4.6	39.3	0.21	3.03	<0.01	0.02	0.67	0.06	0.02	1.7	0.02	6.24	0.005	<0.002		
STD SY-4(D	STD		49.9	20.7	6.14	7.96	0.52	7.12	1.66	0.11	0.29	0.13	<0.01	0.04	4.56	0.055	0.111		
STD OREAS	STD		42.2	4.62	39.3	0.22	3.06	<0.01	0.01	0.67	0.06	0.02	1.72	0.03	6.24	0.003	0.005		
STD SY-4(D	STD		50	20.8	6.14	7.99	0.53	7.17	1.66	0.11	0.29	0.13	<0.01	0.03	4.56	0.054	0.116		
STD OREAS	STD																		
STD DS11	STD																		
STD OREAS	STD																		
STD OREAS	STD																		
STD DS11	STD																		
STD OREAS	STD																		
STD SO-19	STD																		
STD SO-19	STD																		
BLK	BLK																	<0.02	<0.02
BLK	BLK																		
BLK	BLK																	<0.02	<0.02
BLK	BLK																		
SI BLK	BLK		98.7	0.33	0.02	0.01	0.03	<0.01	0.03	<0.01	0.03	<0.01	<0.01	<0.01	0	<0.002	<0.002		
SI BLK	BLK		99.7	0.33	0.03	0.01	0.03	<0.01	0.02	<0.01	0.03	<0.01	<0.01	0.01	0	<0.002	<0.002		
BLK	BLK																		
BLK	BLK																		
BLK	BLK																		
Prep Wash																			
ROCK-VAN	Prep Blank		71.7	14.1	3.32	2.48	0.81	4.46	2.21	0.09	0.36	0.1	<0.01	0.09	0.72	0.007	0.021	0.05	<0.02
ROCK-VAN	Prep Blank		71.3	14.1	3.36	2.46	0.81	4.44	2.2	0.09	0.36	0.1	<0.01	0.09	0.77	0.009	0.019	0.05	<0.02

Method		LF100	LF100	LF100	LF100	LF100	LF100	LF100	LF100	LF100	LF100	LF100	LF100	LF100	LF100	LF100	LF100	LF100	LF100	LF100	LF100	LF100	LF100	LF100	LF100
Analyte		Ba	Be	Co	Cs	Ga	Hf	Nb	Rb	Sn	Sr	Ta	Th	U	V	W	Zr	Y	La	Ce	Pr	Nd	Sm	Eu	Gd
Unit		PPM	PPM	PPM	PPM	PPM	PPM	PPM	PPM	PPM	PPM	PPM	PPM	PPM	PPM	PPM	PPM	PPM	PPM	PPM	PPM	PPM	PPM	PPM	PPM
MDL		1	1	0.2	0.1	0.5	0.1	0.1	0.1	1	0.5	0.1	0.2	0.1	8	0.5	0.1	0.1	0.1	0.1	0.02	0.3	0.05	0.02	0.05
Sample	Type																								
102 McKinl	Drill Core	589	2	36.4	5.3	10.2	1.6	6	95.6	4	360.2	0.4	7.7	2.7	82	1.1	56.9	42.8	33.3	66.9	10.4	47.6	11.29	2.26	10.37
102 McKinl	Drill Core	281	3	12.8	6.3	13.7	2.1	7.3	131	4	199.8	0.5	7	2.8	101	0.9	72.3	26.1	30.1	51.3	7.13	26.6	4.59	0.97	4.09
102 McKinl	Drill Core	272	1	15.7	6.3	12.7	2	7.6	116.7	4	244	0.5	8.6	2.9	95	0.9	72.6	30.7	33.1	60.9	8.69	36.4	7.69	1.49	6.81
102 McKinl	Drill Core	284	1	22.9	6.1	11.5	2.1	7.5	103.5	10	218.3	0.4	6.8	3.5	141	1.5	74.3	18.3	25	44.7	6.07	23.3	4.38	0.92	3.93
102 McKinl	Drill Core	258	1	18	6.5	11.3	1.9	9.1	114.8	2	293.5	0.5	7.5	4.1	88	1.1	69.2	32.3	35.5	62.3	8.36	32.4	5.96	1.22	5.56
102 McKinl	Drill Core	245	2	14.9	6.9	11.7	1.9	8.5	114.8	2	296.1	0.5	7.6	3.6	96	1.2	69.6	29.5	33.7	54.7	7.68	29.1	5.26	1.15	5.05
102 McKinl	Drill Core	299	2	23.6	6.4	13.1	2.1	7.4	117	3	262	0.5	7.6	6.7	104	1.3	70	27.6	27.7	54.7	8.19	34.8	7.12	1.44	6.33
102 McKinl	Drill Core	210	<1	12.3	5.2	8.7	1.5	8.3	86.3	3	308.7	0.4	7.4	8.8	94	0.7	55.4	43.8	37.4	65.3	10.93	48.8	9.62	1.97	9
102 McKinl	Drill Core	253	3	6.5	2.8	5.9	1.1	4.5	56	3	350.4	0.2	3.8	2.4	49	<0.5	42.1	16.6	18.1	31.6	4.23	15.9	2.76	0.59	2.56
102 McKinl	Drill Core	241	<1	10.6	2.9	5.8	1	5.2	52.6	2	382.5	0.3	3.9	3.1	69	0.6	37.7	20.4	19.5	34.8	5.29	21.5	3.87	0.87	3.87
102 McKinl	Drill Core	358	2	8.1	3.9	7.3	1.6	10.8	68	5	247.2	0.8	6.4	7.4	107	0.6	59.8	28.8	30.7	49.8	6.86	26.9	4.75	1.08	4.59
102 McKinl	Drill Core	208	1	10.8	4.1	8.1	1.8	17.4	68.6	4	224.7	1.1	7.5	10.1	180	2.3	71.6	36.9	40.2	64.6	8.74	32.6	5.61	1.26	5.47
102 McKinl	Drill Core	331	3	33	5.9	12.1	3.7	27.2	106.5	3	113.6	1.6	11.5	17.7	169	1.6	147.4	32.4	39.7	70.2	11.03	43.5	8.08	1.68	7.16
102 McKinl	Drill Core	419	1	13.1	4.2	7.4	1.6	19	68.8	4	174.4	1	7.1	10.8	299	1.6	69.2	31	36.3	54.1	7.61	28.1	4.64	1.06	4.44
102 McKinl	Drill Core	1031	1	11.7	5.2	10.3	2.3	13.8	88.4	4	159.3	0.9	7.6	12.1	282	1.3	83.2	31.2	34.1	53	7.46	28.4	4.9	1.03	4.8
102 McKinl	Drill Core	387	3	16.8	7.7	15.2	3.3	12.3	133.9	5	140.6	0.9	10.3	8.9	344	1.4	122.7	36.1	35.6	63.6	9.3	39.2	8.44	1.68	7.77
102 McKinl	Drill Core	467	2	25.1	8.6	16.6	2.2	9.9	145.7	7	217.1	0.6	9.5	4.4	115	1.6	84.8	31.9	35	66.5	9.51	41.1	9.41	1.67	8.22
102 McKinl	Drill Core	164	<1	5.8	1.4	2.7	1.2	3.4	30	3	448.6	0.3	2.7	1.5	59	0.9	48.9	13.2	14.4	24.2	3.19	12.6	2.32	0.45	2.25
102 McKinl	Drill Core	329	<1	3.6	1	1	0.6	1.9	19	1	413.7	0.1	2.2	2.4	20	<0.5	21.3	10.4	12.4	20	2.56	9.9	1.91	0.37	1.75
102 McKinl	Drill Core	256	<1	3.4	1	0.8	0.4	1.5	18.3	3	366.6	0.1	1.5	0.9	25	0.7	16.9	10.3	13.8	20.2	2.74	10.8	1.72	0.43	1.85
102 McKinl	Drill Core	281	<1	1.1	0.3	<0.5	0.2	1.1	4.7	2	319.8	<0.1	0.6	0.7	8	<0.5	6.2	8.7	9.9	14.2	1.95	8	1.24	0.3	1.33
Gordondal	Drill Core	866	4	14.7	10	23.7	3.7	14.2	147.6	3	130	0.9	12.8	3.3	146	1.6	139.3	23	33.2	66.7	8.35	32.2	5.6	1.2	4.82
Gordondal	Drill Core	469	<1	4.8	1.2	4.8	1.9	4.9	24.2	2	107.5	0.2	3.1	10	157	0.6	76.4	20	12.9	17	3.56	14.8	3.31	0.75	3.27
Gordondal	Drill Core	599	1	2.4	1.6	3.9	1.3	3.1	24.9	<1	373.8	0.2	3.4	8	72	<0.5	58.1	66.8	38.1	45.2	8.89	37.4	7.32	1.83	8.67
Gordondal	Drill Core	742	<1	3	1.8	3.7	1.2	4.8	29.4	1	255.5	0.2	3.7	6.9	226	<0.5	48.5	35.6	21.3	26.3	5.43	23.1	4.65	1.03	4.81
Gordondal	Drill Core	668	<1	4.9	2	5.6	1.8	5.4	34.2	1	159.3	0.3	4.3	19.5	415	0.7	83.8	38.6	23.4	31.7	6.52	27	6.09	1.33	6.07
Gordondal	Drill Core	536	<1	1.2	0.4	4.2	1.4	5.2	11.9	<1	318.4	0.3	10.2	4.1	87	<0.5	56.2	4.4	16.1	26.8	2.59	8.4	1.17	0.27	0.87
Gordondal	Drill Core	1257	1	11.5	3.9	9.2	3	6.7	62.8	1	177	0.3	7.6	49.4	904	1.2	134.8	59.6	33.4	47.4	9.84	42.5	9.43	2.22	10.31
Gordondal	Drill Core	1755	1	5.9	3.8	7.3	2.8	6.9	60.2	1	604.5	0.3	6.1	21.1	741	0.7	119.6	35.2	24.6	37.9	6.25	26.1	5.02	1.16	5.4
Gordondal	Drill Core	1313	2	6.3	1.9	7.7	1.8	4.2	32.8	1	1190.6	0.2	4.1	23.8	499	<0.5	75.6	28.9	20	25.6	5.04	21.1	4.2	0.94	4.54
Gordondal	Drill Core	1024	1	5.1	1.5	4.5	1.3	3.6	25.3	1	1688.1	0.1	2.8	21.5	171	0.6	61.6	25	16.1	20.2	3.86	15.8	3.16	0.73	3.45
Gordondal	Drill Core	1200	1	7	2.7	6.6	1.5	4.3	40.1	1	1937.5	0.2	4.4	24.4	158	0.8	66.4	31.8	22.4	35	5.95	24.3	4.91	1.12	5.09
Gordondal	Drill Core	1029	<1	7.9	1.2	2.4	0.8	2.7	19.5	<1	1347.5	<0.1	2.1	10.3	58	<0.5	38.5	19.7	13.1	20.1	3.34	13.9	2.69	0.67	2.92
Gordondal	Drill Core	864	<1	23.8	3.2	7.5	2.1	5.7	51.6	1	1083.2	0.3	6.9	33.3	114	1.5	85.6	52.6	32.7	57.4	9.42	40.3	8.6	1.98	9.33
Gordondal	Drill Core	520	2	12	2	4.9	1.4	3.7	28.3	<1	1349.4	0.2	4.4	27.3	95	1.1	62.9	33.1	20.3	35.9	5.78	25.1	5.16	1.28	5.57
Gordondal	Drill Core	682	1	2.7	0.3	1.8	0.6	1.3	7.7	<1	600.2	0.1	5.1	44.2	110	<0.5	33.5	123.4	69.4	131.7	19.18	80.3	17.05	4.03	18.59
Gordondal	Drill Core	1992	<1	2.7	0.9	1.1	0.8	2.5	10	<1	400.5	0.1	0.3	2.7	236	<0.5	21.4	8	6.8	7.5	1.07	4.4	0.84	0.14	0.86
Gordondal	Drill Core	123	1	1.2	<0.1	1.1	0.5	1	2.1	<1	435	0.1	8.5	7	59	<0.5	16.2	17.8	13.2	20	3.11	12.5	2.48	0.62	2.72
Gordondal	Drill Core	576	<1	9.6	2.1	7.9	2.1	5.5	28.8	1	475.9	0.2	5.6	113.2	588	1.8	129.1	107.5	53	71.4	12.8	53.3	11.15	2.68	13.24
Gordondal	Drill Core	1138	1	9.3	2.4	7.2	2	6.9	32.9	1	385.3	0.2	5.2	71.6	490	2.2	102.7	70.3	37	49.5	9.18	38.8	8.16	1.94	9.26
Gordondal	Drill Core	170	<1	0.7	<0.1	<0.5	0.5	1.2	2.1	<1	244.5	<0.1	1.1	5.5	104	<0.5	33.1	7	4.6	7.3	1.08	4.1	0.76	0.19	0.82
Gordondal	Drill Core	598	<1	1.3	0.2	<0.5	0.6	1.6	5.7	<1	573.1	<0.1	1.1	8.3	131	0.8	29.9	10.2	6.3	8	1.31	5.1	1.04	0.27	1.15
Gordondal	Drill Core	871	<1	4.4	1.3	4.9	1.6	3.7	24.1	1	1044.9	0.2	2.8	109.6	637	0.6	101	129.6	57.3	67.2	14.06	59	12.21	3.18	15.57
Gordondal	Drill Core	4134	2	6.5	1.6	3.8	1.6	3.4	23.9	<1	1147.1	0.2	3	62.2	973	0.8	77.2	56.8	30.3	38.7	8.25	35.1	7.41	1.72	8.39
Gordondal	Drill Core	253	2	6.8	2.8	5.8	2.2	4.9	36.5	1	1135	0.2	4.3	32.3	1551	0.7	100.1	33.9	20.9	24.9	6.24	26.6	5.68	1.36	5.94
Gordondal	Drill Core	353	2	11.4	12.9	12.7	6.4	10.9	111.3	2	139.9	1.3	9	10.9	1238	1.1	210.3	32.2	22.5	32.4	6.28	25.3	5.55	1.23	5.58
Gordondal	Drill Core	1089	4	9.6	9.2	13.7	4.1	8.8	85.7	5	335	0.5	8.8	16.5	2148	1.6	219	42.2	24.7	32.6	7.71	31.2	7.12	1.61	7.04
Pulp Duplicates																									
102 McKinl	Drill Core	1031	1	11.7	5.2	10.3	2.3	13.8	88.4	4	159.3	0.9	7.6	12.1	282	1.3	83.2	31.2	34.1	53	7.46	28.4	4.9	1.03	4.8
102 McKinl	REP																								
Gordondal	Drill Core	1029	<1	7.9	1.2	2.4	0.8	2.7	19.5	<1	1347.5	<0.1	2.1	10.3	58	<0.5	38.5	19.7	13.1	20.1	3.34	13.9	2.69	0.67	2.92
Gordondal	REP	1023	<1	7.8	1.2	2.6	0.8	2.5	19.7	<1	1374.5	<0.1	2.2	10.4	60	<0.5	38.8	19.6	12.8	19.6	3.35	14.3	2.79	0.63	3.05
Gordondal	Drill Core	598	<1	1.3	0.2	<0.5	0.6	1.6	5.7	<1	573.1	<0.1	1.1	8.3	131	0.8	29.9	10.2	6.3	8	1.31	5.1	1.04	0.27	1.15
Gordondal	REP																								
102 McKinl	Drill Core	272	1	15.7	6.3	12.7	2	7.6	116.7	4	244	0.5	8.6	2.9	95	0.9	72.6	30.7	33.1	60.9	8.69	36.4	7.69	1.49	6.81
102 McKinl	REP	285	2	16.2	6.7	13.4	2	8.1	120.1	4	255.6	0.5	8.6	3.2	107	0.8	75.2	31.7	35.4	62.5	9.04	37.8	7.67	1.52	6.75
102 McKinl	Drill Core	245	2	14.9	6.9	11.7	1.9	8.5	114.8	2	296.1	0.5	7.6	3.6	96	1.2	69.6	29.5	33.7	54.7	7.68	29.1	5.26	1.15	5.05
102 McKinl	REP																								
Gordondal	Drill Core	864	<1	23.8	3.2	7.5	2.1	5.7	51.6	1	1083.2	0.3	6.9	33.3	114	1.5	85.6	52.6	32.7	57.4	9.42	40.3	8.6	1.98	9.33
Gordondal	REP																								
102 McKinl	Drill Core	258	1	18	6.5	11.3	1.9	9.1	114.8	2	293.5	0.5	7.5	4.1	88	1.1	69.2	32.3	35.5	62.3	8.36	32.4	5.96	1.22	5.56
102 McKinl	REP																								
Reference Materials																									
STD GS311-	STD																								
STD GS910-	STD																								
STD SO-19	STD	455	16	21.7	4.3	16.7	3.1	71.5	18.8	19	278	4.4	12.9	17.7	147	9.2	116.7	35.5	65.3	147.5	19.14	73.9	12.94	3.55	10.18
STD SO-19	STD	475	24	22.5	4.3	16.2	3	70.1	18.7	19	280.1	4.7	13.6	17.2	149	9.9	111.3	35.8	65.1	148.3	19.3	76.1	12.88	3.56	10.13
STD GS311-	STD																								
STD GS910-	STD																								
STD SO-19	STD	486	14	22.7	4.4	16.3	3.2	71.2	17.9	19	280.3	5.2	14	18.4	155	8.7	111.5	36.9	66.4	145.6	19.94	77.9	13.32	3.78	10.42
STD OREAS	STD																								
STD SY-4(D	STD																								
STD OREAS	STD																								
STD SY-4(D	STD																								
STD OREAS	STD																								
STD DS11	STD																								
STD OREAS	STD																								
STD OREAS	STD																								
STD DS11	STD																								
STD OREAS	STD																								
STD SO-19	STD	458	20	23.7	4.7	19.1	3.1	70.5	20.4	19	273.7	5	13.1	17.3	173	10.7	114.4	35.3	63.1	139.4	19.51	75.3	13	3.75	10.55
STD SO-19	STD	438	16	23.4	4.4	19.4	3.2	68.3	19.9	18	272	4.7	13.4	16.8	169	10.3	110	35.2	61.9	137.9	19.06	74.5	12.69	3.56	10.31
BLK	BLK																								
BLK	BLK	<1	<1	<0.2	<0.1	<0.5	<0.1	<0.1	<0.1	<1	<0.5	<0.1	<0.2	<0.1	<8	<0.5	0.1	<0.1	<0.1	<0.1	<0.02	<0.3	<0.05	<0.02	<0.05
BLK	BLK																								
BLK	BLK	<1	<1	0.2	<0.1	<0.5	<0.1	<0.1	<0.1	<1	<0.5	<0.1	<0.2	<0.1	<8	<0.5	<0.1	<0.1	<0.1	<0.1	0.09	<0.3	<0.05	<0.02	<0.05
SI BLK	BLK																								
SI BLK	BLK																								
BLK	BLK																								
BLK	BLK																								
BLK	BLK	2	<1	<0.2	<0.1	<0.5	<0.1	<0.1	<0.1	<1	<0.5	<0.1	<0.2	<0.1	<8	<0.5	0.2	<0.1	<0.1	<0.1	<0.02	<0.3	<0.05	<0.02	<0.05
Prep Wash																									
ROCK-VAN	Prep Blank	825	2	3.9	0.3	11.7	3.9	5.1	41.5	<1	179.6	0.4	3.1	1.1	34	<0.5	142.7	18.5	13.4	24.4	3.34	12.8	2.65	0.77	2.85
ROCK-VAN	Prep Blank	803	<1	4	0.3	11.8	3.4	5.2	40.4	<1	172.5	0.4	3.2	1.2	32	0.7	135.6	17.6	13.4	24.8	3.31	13.1	2.75	0.74	2.7

Method		LF100	LF100	LF100	LF100	LF100	LF100	LF100	AQ200	AQ200	AQ200	AQ200	AQ200	AQ200	AQ200	AQ200	AQ200	AQ200	AQ200	AQ200	AQ200	AQ200
Analyte		Tb	Dy	Ho	Er	Tm	Yb	Lu	Mo	Cu	Pb	Zn	Ni	As	Cd	Sb	Bi	Ag	Au	Hg	Tl	Se
Unit		PPM	PPM	PPM	PPM	PPM	PPM	PPM	PPM	PPM	PPM	PPM	PPM	PPM	PPM	PPM	PPM	PPM	PPB	PPM	PPM	PPM
MDL		0.01	0.05	0.02	0.03	0.01	0.05	0.01	0.1	0.1	0.1	1	0.1	0.5	0.1	0.1	0.1	0.1	0.5	0.01	0.1	0.5
Sample	Type																					
102 McKinl	Drill Core	1.31	6.72	1.22	2.97	0.36	2.15	0.29	6.1	63.5	35.6	25	134.6	20.9	<0.1	0.6	0.2	<0.1	5	0.07	0.3	1.1
102 McKinl	Drill Core	0.6	3.78	0.71	2.26	0.33	2.11	0.33	2.3	57.1	11.7	48	40	7.6	0.1	0.3	0.2	<0.1	<0.5	0.05	0.1	<0.5
102 McKinl	Drill Core	0.86	4.77	0.86	2.46	0.32	1.95	0.3	2.4	85.2	15.8	68	51.9	11.8	<0.1	0.4	0.2	<0.1	2.9	0.06	0.1	<0.5
102 McKinl	Drill Core	0.53	3.13	0.6	1.63	0.25	1.43	0.22	24.3	138.8	45.9	68	86.9	29.8	0.3	1.6	0.2	0.2	1.6	0.12	0.1	1.9
102 McKinl	Drill Core	0.76	4.42	0.93	2.67	0.34	2.17	0.33	7.7	63.2	18.6	85	52.7	20.7	0.6	0.3	0.2	<0.1	<0.5	0.08	<0.1	1.6
102 McKinl	Drill Core	0.7	4.15	0.89	2.47	0.33	2.04	0.3	5.2	56.7	20.1	32	45.6	15.7	0.1	0.2	0.2	0.1	2.3	0.07	<0.1	0.9
102 McKinl	Drill Core	0.83	4.34	0.81	2.12	0.28	1.84	0.25	11.8	90.3	29	19	62	38.2	<0.1	0.7	0.2	0.2	<0.5	0.19	0.1	1.8
102 McKinl	Drill Core	1.17	5.97	1.14	3.04	0.37	2.22	0.3	9.2	59	20.1	18	53.4	22.4	<0.1	0.6	0.1	0.1	0.9	0.11	0.2	2
102 McKinl	Drill Core	0.38	2.21	0.46	1.32	0.17	1.07	0.15	3.1	36.2	8.5	18	22.4	7.9	<0.1	0.4	<0.1	<0.1	<0.5	0.03	<0.1	<0.5
102 McKinl	Drill Core	0.5	2.71	0.55	1.56	0.18	1.15	0.18	5.9	72.6	20.7	11	38.5	14.1	<0.1	0.5	0.1	0.2	1	0.08	<0.1	1.9
102 McKinl	Drill Core	0.64	3.62	0.78	2.27	0.3	1.84	0.27	8.2	52.9	15.4	15	52.4	13.7	<0.1	0.8	0.2	0.1	1.8	0.1	0.1	2.7
102 McKinl	Drill Core	0.77	4.51	0.93	2.85	0.38	2.32	0.33	25.8	79.2	19.9	13	67.7	18.3	<0.1	1.2	0.2	0.3	<0.5	0.15	0.2	3.3
102 McKinl	Drill Core	0.92	4.82	0.88	2.34	0.31	1.91	0.27	49.2	87	43.4	327	153.9	53.6	2.9	2.5	0.5	0.6	2.3	0.55	2.3	7.7
102 McKinl	Drill Core	0.64	3.55	0.77	2.27	0.32	1.85	0.29	36.4	98.1	57.6	14	191.4	62	0.2	5	0.1	0.5	<0.5	0.25	0.4	11.7
102 McKinl	Drill Core	0.67	3.99	0.87	2.32	0.32	2.04	0.29	28.2	58.8	26.4	42	87.8	20.8	0.5	1.2	0.2	0.2	<0.5	0.18	0.3	7.1
102 McKinl	Drill Core	1.04	5.64	1.09	3	0.4	2.48	0.37	27	64.7	52.2	37	89.3	34.2	0.2	0.9	0.3	0.2	<0.5	0.14	0.4	5.9
102 McKinl	Drill Core	1.05	5.5	0.98	2.73	0.37	2.38	0.35	9.6	63.7	37.6	47	55.8	34	0.1	0.5	0.2	0.1	<0.5	0.07	0.4	1.2
102 McKinl	Drill Core	0.33	2.04	0.37	1.11	0.15	0.94	0.14	4.4	26.5	12.1	9	15	12.4	<0.1	0.6	0.1	<0.1	1.2	0.08	<0.1	0.8
102 McKinl	Drill Core	0.25	1.47	0.3	0.76	0.09	0.54	0.06	2.3	19	7.3	7	8.2	15.6	<0.1	0.5	<0.1	<0.1	<0.5	0.02	<0.1	0.7
102 McKinl	Drill Core	0.25	1.4	0.27	0.84	0.11	0.63	0.09	2.5	20	5.6	6	8	7.7	<0.1	0.9	<0.1	<0.1	<0.5	0.02	<0.1	<0.5
102 McKinl	Drill Core	0.18	1.03	0.2	0.59	0.07	0.4	0.06	7.3	14.8	1.9	5	0.5	4.8	<0.1	0.7	<0.1	<0.1	3.6	<0.01	<0.1	<0.5
Gordondal	Drill Core	0.73	4.25	0.82	2.46	0.36	2.39	0.36	25.2	36.4	17	119	85.9	18.6	1.1	<0.1	0.3	<0.1	2.3	0.04	0.5	1.5
Gordondal	Drill Core	0.48	2.86	0.62	1.81	0.26	1.5	0.24	132.6	88.3	6.7	205	126.5	31.2	5.7	1	0.2	0.4	0.9	0.05	1	3.6
Gordondal	Drill Core	1.24	8	1.69	5.04	0.73	4.61	0.71	22.5	16.6	3.8	26	16.7	12.9	0.4	0.3	<0.1	<0.1	<0.5	0.04	0.1	1.9
Gordondal	Drill Core	0.7	4.21	0.89	2.73	0.37	2.35	0.36	49.8	49.1	5.1	93	49.1	30	3.1	1.8	0.1	0.3	<0.5	0.06	0.3	5.2
Gordondal	Drill Core	0.91	5.47	1.19	3.44	0.45	2.72	0.4	179.3	78.8	10.3	831	208.1	32.6	14.6	2.5	0.2	0.6	2	0.08	1.6	11.2
Gordondal	Drill Core	0.13	0.74	0.14	0.54	0.08	0.67	0.11	15.2	7.3	8.2	31	6.8	19.3	0.3	0.2	<0.1	<0.1	2.2	0.04	0.7	2.5
Gordondal	Drill Core	1.52	9.42	1.91	5.5	0.73	4.77	0.76	396.5	187.6	18.8	1573	798.4	85.1	19.6	4.1	0.3	1.4	2	0.16	3	35.6
Gordondal	Drill Core	0.8	4.85	1.04	3.13	0.44	2.96	0.46	68.3	98.4	16.1	1267	149.8	37.4	18.1	1.9	0.2	1.1	1.3	0.12	1.7	20.8
Gordondal	Drill Core	0.66	4.15	0.89	2.53	0.35	2.42	0.36	132.1	105.1	12.7	1880	273.1	34.9	18.3	2.2	0.2	1	1.4	0.09	1.2	12.9
Gordondal	Drill Core	0.51	3.08	0.68	1.94	0.3	1.93	0.3	113.5	51	6.9	288	151.7	22.4	5.8	1.1	<0.1	0.4	1.1	0.06	0.3	5.4
Gordondal	Drill Core	0.76	4.47	0.92	2.71	0.36	2.26	0.34	113.6	61	11	362	179.9	24.1	4.9	1.2	0.1	0.3	0.8	0.06	0.4	6
Gordondal	Drill Core	0.44	2.69	0.53	1.66	0.23	1.5	0.22	20.5	34	5	52	35.4	15.8	0.9	0.6	<0.1	0.1	1	0.05	0.2	1.6
Gordondal	Drill Core	1.31	7.56	1.53	4.48	0.6	3.73	0.57	48.9	99.6	15.1	230	175.9	35.5	4.1	1.4	0.3	0.4	<0.5	0.12	0.3	5.4
Gordondal	Drill Core	0.83	4.74	0.98	2.92	0.41	2.58	0.41	40.1	83.8	9	103	150.1	22.1	2.3	0.9	0.2	0.3	<0.5	0.07	0.2	2.9
Gordondal	Drill Core	2.59	14.66	3.03	8.58	1.1	7.12	1.09	62.9	32.8	6.9	282	188.9	15.5	4.5	1.6	<0.1	0.3	<0.5	0.03	0.6	6.4
Gordondal	Drill Core	0.14	0.97	0.2	0.63	0.11	0.74	0.14	47.9	24.6	5.2	72	20.8	64.5	1.4	0.8	<0.1	0.7	1	0.08	0.9	8.2
Gordondal	Drill Core	0.41	2.31	0.49	1.5	0.22	1.49	0.28	43.5	13.1	4.7	103	66.1	8.3	1.5	1.4	<0.1	0.2	1	0.02	0.4	2.6
Gordondal	Drill Core	1.95	12.36	2.78	8.33	1.1	7.21	1.2	674.1	139.5	19.2	2479	1009.5	60.6	20.8	5.6	0.3	1.1	<0.5	0.11	0.5	20.7
Gordondal	Drill Core	1.33	8.23	1.85	5.53	0.74	4.93	0.79	462.4	108.1	14.2	686	596.7	47.8	11.2	3.5	0.2	0.6	0.7	0.09	0.5	11.2
Gordondal	Drill Core	0.13	0.76	0.18	0.5	0.08	0.53	0.1	35.8	9.6	1.3	69	31.9	5.6	0.9	0.7	<0.1	<0.1	0.5	0.02	0.2	1.4
Gordondal	Drill Core	0.18	1.11	0.26	0.84	0.12	0.85	0.15	53.2	21	2.7	177	41.9	7	4.2	0.8	<0.1	0.1	0.7	0.03	0.5	2.6
Gordondal	Drill Core	2.32	14.33	3.37	10.31	1.34	8.58	1.38	330.9	68.6	6.6	1998	472	19.8	22.8	4.4	<0.1	0.7	<0.5	0.11	1.3	16.2
Gordondal	Drill Core	1.24	7.66	1.61	4.75	0.63	3.93	0.64	432.7	65.3	5.2	1144	632.1	22.7	14.1	3.1	<0.1	0.4	<0.5	0.1	1.8	28.3
Gordondal	Drill Core	0.84	5.16	0.98	3	0.42	2.65	0.43	807.3	228.3	8.6	4105	687.7	44.7	59.2	9	0.2	2	<0.5	0.22	2.8	38.9
Gordondal	Drill Core	0.83	4.81	1	2.98	0.42	2.83	0.48	625.5	279.1	16.5	362	546.8	65.2	12.6	2.5	0.4	1.2	<0.5	0.31	0.9	27.6
Gordondal	Drill Core	1.04	6.51	1.23	3.65	0.52	3.72	0.58	1050.4	572.8	19.7	7796	1226.6	86.5	195	9.8	0.5	4.2	<0.5	0.82	2.5	55.4
Pulp Duplicates																						
102 McKinl	Drill Core	0.67	3.99	0.87	2.32	0.32	2.04	0.29	28.2	58.8	26.4	42	87.8	20.8	0.5	1.2	0.2	0.2	<0.5	0.18	0.3	7.1
102 McKinl	REP																					
Gordondal	Drill Core	0.44	2.69	0.53	1.66	0.23	1.5	0.22	20.5	34	5	52	35.4	15.8	0.9	0.6	<0.1	0.1	1	0.05	0.2	1.6
Gordondal	REP	0.44	2.58	0.58	1.7	0.23	1.5	0.22														
Gordondal	Drill Core	0.18	1.11	0.26	0.84	0.12	0.85	0.15	53.2	21	2.7	177	41.9	7	4.2	0.8	<0.1	0.1	0.7	0.03	0.5	2.6
Gordondal	REP																					
102 McKinl	Drill Core	0.86	4.77	0.86	2.46	0.32	1.95	0.3	2.4	85.2	15.8	68	51.9	11.8	<0.1	0.4	0.2	<0.1	2.9	0.06	0.1	<0.5
102 McKinl	REP	0.87	4.74	0.91	2.57	0.36	2.16	0.32														
102 McKinl	Drill Core	0.7	4.15	0.89	2.47	0.33	2.04	0.3	5.2	56.7	20.1	32	45.6	15.7	0.1	0.2	0.2	0.1	2.3	0.07	<0.1	0.9
102 McKinl	REP																					
Gordondal	Drill Core	1.31	7.56	1.53	4.48	0.6	3.73	0.57	48.9	99.6	15.1	230	175.9	35.5	4.1	1.4	0.3	0.4	<0.5	0.12	0.3	5.4
Gordondal	REP								48.7	98.4	15.4	224	172.9	35.6	4.2	1.5	0.3	0.4	<0.5	0.14	0.4	5.5
102 McKinl	Drill Core	0.76	4.42	0.93	2.67	0.34	2.17	0.33	7.7	63.2	18.6	85	52.7	20.7	0.6	0.3	0.2	<0.1	<0.5	0.08	<0.1	1.6
102 McKinl	REP								6.9	61	18.5	82	51.3	19.9	0.5	0.4	0.2	0.1	1.1	0.09	0.1	1.7
Reference Materials																						
STD GS311-	STD																					
STD GS910-	STD																					
STD SO-19	STD	1.32	6.8	1.3	3.57	0.51	3.17	0.5														
STD SO-19	STD	1.33	7.09	1.33	3.73	0.49	3.27	0.49														
STD GS311-	STD																					
STD GS910-	STD																					
STD SO-19	STD	1.42	7.59	1.43	3.78	0.51	3.41	0.52														
STD OREAS	STD																					
STD SY-4(D	STD																					
STD OREAS	STD																					
STD SY-4(D	STD																					
STD OREAS	STD								1.5	722.2	12.3	30	401.8	11.2	<0.1	0.2	0.2	0.3	58.1	<0.01	<0.1	1.2
STD DS11	STD								15.2	147.9	137.3	350	81.3	45.4	2.4	5.7	11.3	1.8	113.4	0.32	5.6	1.8
STD OREAS	STD								0.7	115	52	147	64.3	36.9	0.6	2	0.9	0.5	62.6	0.17	0.5	<0.5
STD OREAS	STD								1.5	714.9	14.4	32	420.4	11.6	<0.1	0.2	0.3	0.3	55.6	0.02	<0.1	1.3
STD DS11	STD								14.2	146.2	137.1	342	77.3	43.5	2.4	5.8	10.8	1.6	160.7	0.25	5.2	1.9
STD OREAS	STD								0.6	116	61	151	64.8	37.1	0.7	1.9	1.1	0.5	61	0.18	0.5	<0.5
STD SO-19	STD	1.36	7.1	1.34	3.74	0.54	3.31	0.5														
STD SO-19	STD	1.34	7.17	1.38	3.75	0.5	3.44	0.51														
BLK	BLK																					
BLK	BLK	<0.01	<0.05	<0.02	<0.03	<0.01	<0.05	<0.01														
BLK	BLK																					
BLK	BLK	<0.01	<0.05	<0.02	<0.03	<0.01	<0.05	<0.01														
SI BLK	BLK																					
SI BLK	BLK																					
BLK	BLK								<0.1	<0.1	<0.1	<1	<0.1	<0.5	<0.1	<0.1	<0.1	<0.1	<0.5	<0.01	<0.1	<0.5
BLK	BLK								<0.1	<0.1	<0.1	<1	<0.1	<0.5	<0.1	<0.1	<0.1	<0.1	<0.5	<0.01	<0.1	<0.5
BLK	BLK	<0.01	<0.05	<0.02	<0.03	<0.01	<0.05	<0.01														
Prep Wash																						
ROCK-VAN	Prep Blank	0.45	2.73	0.6	1.9	0.31	2.12	0.36	0.7	2	1.4	27	1	1.1	<0.1	<0.1	<0.1	<0.1	0.8	<0.01	<0.1	<0.5
ROCK-VAN	Prep Blank	0.43	2.77	0.61	1.91	0.31	2.02	0.35	0.6	1.8	1.4	27	1.2	0.9	<0.1	<0.1	<0.1	<0.1	0.8	<0.01	<0.1	<0.5